Evaluating the effects of radio-frequency treatment of rocks: Textural changes and implications for rock comminution

Arthur James Swart (MTech: Eng: Elec)

9557512

A thesis submitted in fulfilment of the requirements for the

Doctoris Technologiae: Engineering: Electrical

Department: Electronic Engineering

Faculty of Engineering and Technology

Vaal University of Technology

Vanderbijlpark

Promoter: Professor HC vZ Pienaar

Co-Promoter: Professor P Mendonidis

Date: December 2010

Declaration

I, Arthur James Swart, hereby declare that the following research is solely my own work. This thesis is submitted for the requirements for the Doctoris Technologiae: Engineering: Electrical to the Department: Electronic Engineering at the Vaal University of Technology, Vanderbijlpark. This thesis has never before been submitted for evaluation to any educational institute. See Annexure 26 for the TURNITIN originality report.

Arthur James Swart

5 December 2010

Acknowledgements

I hereby acknowledge Prof. Christo Pienaar for his specific guidance relating to the methodology employed in this research. His continued encouragement and interest helped me surge ahead, continuing to search for answers to the relevant questions at hand. I also would like to acknowledge Prof. Peter Mendonidis for explaining difficult terms and principles relating to rock comminution. He took time to demonstrate to me the operation of rock cutting and particle screening. I further acknowledge my colleague, Ruaan Schoeman, who often provided a listening ear to my concerns and battles regarding this research. At times his advice provided insight and direction.

Dedication

For Charmain

Abstract

Ore, from a mining operation, goes through a process that separates the valuable minerals from the gangue (waste material). This process usually involves crushing, milling, separation and extraction where the gangue is usually discarded in tailings piles. Current physical methods used for crushing of rocks in the mineral processing industry result in erratic breakages that do not efficiently liberate the economically valuable minerals. Research studies have found that the rock comminution and mineral liberation can be enhanced through various electrical treatment techniques, including pulsed power, ultrasound and microwave. These electrical treatment techniques each have their own advantages and disadvantages which are discussed in this dissertation. However, this research proposes a new technique in an attempt to improve the rock comminution process.

The main purpose of this research is to evaluate the effect that RF power exerts on rock samples, with particular focus on textural changes. **Four valuable scientific contributions** to the fields of metallurgical and electrical engineering were made in this regard. Firstly, **a new technique for the treatment** of rock samples using RF heating is substantiated. The effect of RF power on textural changes of the rocks is evident in their surface temperature rise, where the RF heating of dolerite (JSA) and marble (JSB, JS1 and JS2) resulted in surface temperatures of approximately 100 °C within two minutes of treatment.

A particle screening analysis of particles obtained form a swing-pot mill of both the untreated (not exposed to RF power) and treated (exposed to RF power) rock samples were performed to ascertain if the treated samples' size had changed. Two samples (JSA and JSD) revealed a notable change in their particle size distribution. The fact that the percentage of larger sized particles increased (from 38 μm to 90 μm as seen in Chapter 6) suggests that the rock was **strengthened** rather than weakened.

Secondly, an **innovative coupling technique** (using a parallel-plate capacitor with dimensions of 28 x 47 mm) to connect rock samples to high powered RF electronic equipment is described. The feasibility of this technique is confirmed by repeated correlated measurements taken on a vector voltmeter and network analyser. Low SWR readings obtained from an inline RF Wattmeter in a practical setup also proves the viability of the matching network used in the coupling technique.

Thirdly, an **original coupling coefficient** (81.58×10^{-3}) for the parallel-plate capacitor is presented. This value may be used in similar sized capacitors to determine the specific heat capacity of dielectric materials. However, the value of the coupling coefficient was only verified for seven (relatively dark in surface colour) out of the ten rock samples. Therefore, this coupling coefficient may hold true for all dark coloured rock samples, as it represents the coupling of energy between the parallel-plate capacitor and the rock sample.

Finally, this research defines the **mathematical models** for 10 rock samples for the VHF range of frequencies (30 – 300 MHz), providing unique phase angle to resonance equations for each sample. These equations can be used with each specific rock to determine the resonating frequency where the maximum current flows and the minimum resistance is present.

Evaluating the effects of RF power treatment on rocks has brought to light that mineral grain boundaries within specified rock samples are not significantly weakened by RF treatment. This was firstly confirmed by the similar electrical properties of the untreated and treated samples, where consistent values for the resonating frequency were obtained from the network analyser. Secondly, the SEM analysis of the untreated and treated rock samples revealed no significant changes in the form of fractures or breakages along the mineral grain boundaries. Photomicrographs of the thin sections of all ten rock samples were used in this analysis. The particle size distribution of both samples further revealed no weakening or softening of the rock, as the percentage of smaller sized particles did not increase in the treated samples. It may therefore be stated that treating rock samples with

RF power within the VHF range will not significantly improve rock comminution and mineral liberation.

TABLE OF CONTENTS

LIST OF FIGURES

LIST OF TABLES

LIST OF ANNEXURES

GLOSSARY OF ABBREVIATIONS AND SYMBOLS

A

A - Ampere

B

C

C - Coulomb

C - Specific heat capacity in Joules / kg/ °C

D

DUT - Device under test

E

E - the electric field intensity in V/m

F

f - frequency in Hz

G

H

Hz - Hertz

I

J

J - Joule

JSA - Dolerite rock sample

JSB - Marble rock sample

JSC - Granite rock sample

JSD - Sandstone rock sample

JSE - Mudstone rock sample

JS1 - Marble rock sample

JS2 - Marble rock sample

JS3 - Marble rock sample

JS4 - Granite rock sample

JS5 - Marble rock sample

K

kg - kilogram

k - coupling coefficient

L

M

m - sample mass in kg

MPT - maximum power transfer

MHz - Megahertz

N

O

P

P - power in W

PPC - Parallel-plate capacitor

Q

R

RF - Radio-frequency

S

s - seconds

SEM - Scanning electron microscope

T

U

μ - micro

V

V/m - Voltage per meter

W

W - Watt

X, Y, Z

Symbols

Ω - Ohm

°C - Degrees Celsius

ε - permittivity of a material

ΔT - temperature rise in °C

Δt - RF heating time in s

σ - conductivity in Siemens per meter

ω - angular frequency in s^{-1}

ρ - resistivity in Ohm meters

E - electric field in Voltage per meter

Chapter 1 Introduction

1.1 Background

"You find remedy in the thorniest tree". This Arabic proverb well illustrates that scientific solutions to well defined engineering problems are often hard to find, resulting in much frustration and anguish. This has also proved true in the mineral processing industry were numerous exigent scientific endeavours have sought to improve rock comminution. Comminution may be divided into two steps; the reduction of large materials to a size suitable for grinding (termed crushing) and the reduction of crushed material into powder (termed grinding). Comminution efficiency is currently low and is based on the absolute ratio of energy required to generate new surface area relative to the total mechanical energy input (Tromans 2008). Current comminution techniques need to be enhanced if a higher efficiency is to be realized.

Mineral liberation efficiency subsequently relates to the amount of energy required to release a certain percentage of valuable minerals from the gangue through rock comminution methods. The major source of this energy generation is fossil fuels, coal, natural gas and oil, which are still expected to meet about 84% of energy demand in 2030 (Shafiee and Topal 2009). However, concerns continue to be raised regarding the burning of fossil fuels as a contributor to rising atmospheric concentrations of carbon dioxide (CO2) which contributes to global warming (Wolde-Rufael 2010). Subsequently, the importance of coal in energy generation and as a possible source of global warming necessitates the use of alternative methods to reduce the amount of energy used by mining industries while at the same time recovering the same (or higher) percentage of valuable minerals. This thorny dilemma continues to frustrate researchers around the globe within the fields of Metallurgical, Mechanical and Electrical Engineering.

Current research studies have found that the mineral liberation process can be enhanced through the use of pulsed power, ultrasound pre-treatment and microwave pre-treatment of run of mine ore (Haque 1999; Gaete-Garretón et al. 2000; Andres et al. 2001; Wilson et al. 2006; Jones et al. 2007; Wang and Forssberg 2007). Ore, from the mining operation, goes through a process that separates the valuable minerals from the gangue (waste material). This process usually involves crushing, milling, separation and extraction where the gangue is usually discarded in tailings piles (Perkins 1998:159). These electrical methods used to enhance the mineral liberation process, each have their own advantages and disadvantages which are discussed in this dissertation. However, this research proposes a technique which may have positive implications for rock comminution and mineral liberation.

1.2 Research activities

The international mining industry needs to enhance its mineral liberation process and reduce its enormous amount of power consumption (increase power efficiency) (Wang and Forssberg 2007). An example of a mineral processing line is demonstrated in Figure 1.1.

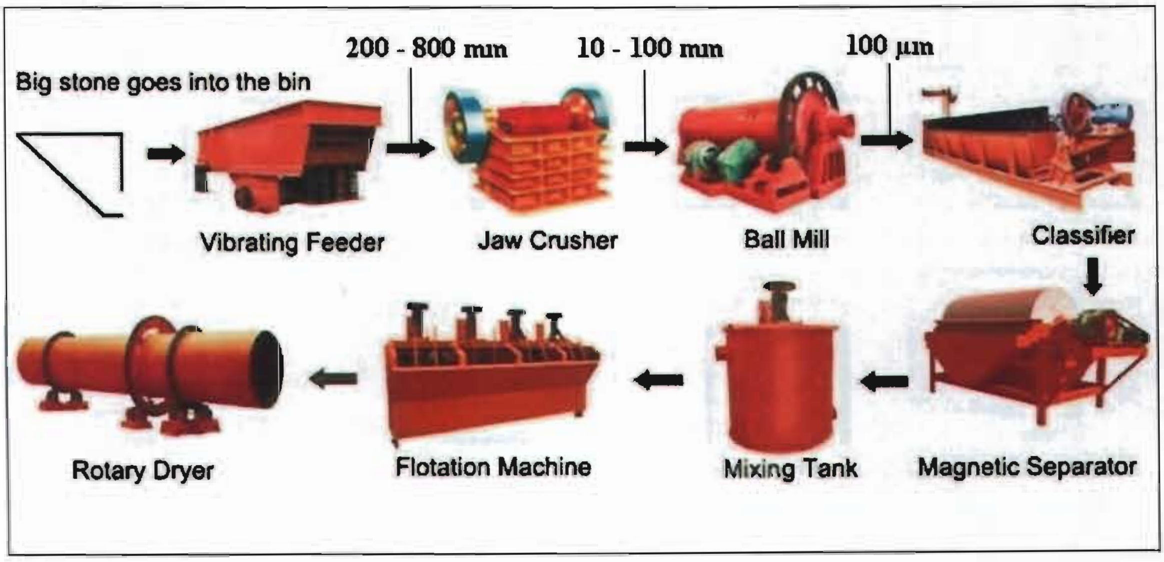

Figure 1.1: Mineral processing line (Henan Chuangxin Building-material Equipment Co 2009)

In this example, a vibrating feeder serves the purpose of making coarse separations of mining ores (200 – 800 mm in diameter) and providing a consistent, even supply of rock material to the jaw crusher. The jaw crusher breaks this material down to a particle size of approximately 10 – 100 mm. The next stage, the ball mill, is used for grinding various ore and other materials down to particle sizes of around 100 μm. The stages which follow (classifier to rotary dryer) are used to separate the valuable minerals from the gangue. It is estimated that in a mining-intensive country the minerals processing industry accounts for approximately 18% of the national energy consumption. This process is currently inherently inefficient, with less than 3% of the energy input directly involved in rock breakage and liberation (Moran 2009). Industry, therefore, aims to achieve a higher throughput of valuable minerals and increased power efficiency.

1.3 Problem statement

Current physical methods used for crushing of rocks in the mineral processing industry result in erratic breakages that do not efficiently liberate the economically valuable minerals.

1.4 Purpose and aims

The purpose of this research is to evaluate the effect that radio-frequency (RF) power exerts on rock samples with particular focus on textural changes. This evaluation aims to determine if RF power weakens mineral grain boundaries, subsequently leading to improved rock comminution and mineral liberation. This may result in significant reductions of energy consumption of current comminution and mineral liberation equipment.

The primary aim of this research is to design and develop a suitable innovative coupling device to connect relevant electronic equipment (test instruments and amplifiers) to various rock samples. This will contribute to new knowledge regarding the electrical properties of rocks and provide an improved understanding of RF treatment of dielectric materials.

A secondary aim is to ensure maximum power transfer between a RF amplifier and the rock sample at a specified frequency of operation. Rock samples exposed to RF power at this frequency will be referred to as treated samples.

Finally, this research aims to strengthen interdisciplinary research between electrical and metallurgical engineers, which is one of the objectives of the Competitive Support for Unrated Researchers Programme offered by the National Research Foundation (NRF).

1.5 Outline of the thesis and the research methodology

The following methodology is followed in this research. First, a detailed description of the physical and electrical properties of minerals and specified rocks are presented (Chapter 2). This theoretical study is based on authoritative literature in the field of Mineralogy.

Second, a theoretical study of different electrical methods used in enhancing the mineral liberation process is discussed (Chapter 3). Disadvantages of these techniques are reviewed. A new electrical technique using RF power in the treatment of rock samples is then introduced. The principle and significance of dielectric heating of materials is further explained.

Third, Chapter 4 introduces two notable coupling methods, with primary focus directed to the parallel-plate capacitor. The practical setup used to ascertain the electrical properties of dielectric samples is presented. This setup involves the use of a vector voltmeter and network analyser. Construction of the parallel-plate capacitor and novel wooden jig also forms part of this chapter. Initial network analyser results are evaluated. Mathematical modelling of the frequency to phase angle curve for each rock samples is considered.

Fourth, the design and implementation of a suitable matching network to connect the parallel-plate capacitor to specific RF equipment is given (Chapter 5). This includes a comparison of the mathematical, simulation and practical results of the matching network. This chapter further presents an examination of the coupling coefficient of the parallel-plate capacitor using the specific heat capacity of each rock sample.

Finally, Chapter 6 introduces the analysis and evaluation of the untreated rock samples, which include dolerite, marble, granite, sandstone and mudstone. This includes the physical properties of the sample (photomicrographs, SEM analysis and grain distribution) together with the particle screening analysis and colour of the powered rocks (samples ground to less than 250 μm). The analysis and evaluation of the treated samples regarding power consumption, surface temperature fluctuations, colour changes and particle screening analysis of the powered rocks (samples ground to less than 250 μm) are also expounded. The power consumption comparison involves measuring the amount of energy consumed in the crushing and milling of specified treated and untreated samples.

Chapter 7 closes with succinct conclusions and apposite recommendations.

1.6 Delimitations

The design and development of a high power RF amplifier does not form part of this research. The design and construction of the power supply unit (PSU) for use in conjunction with the RF amplifier will also not be considered. A further delimitation will be the evaluation and analysis of stray capacitances in the vicinity of the coupling device, as variable capacitors will be used for fine-tuning. This research will further be limited to the Very-High frequency range (VHF) due to the availability of relatively inexpensive ($350) commercially available VHF amplifiers.

1.7 Definition of important terms as used in this research

Dielectric material:	A non-conductive, insulating material in which an electrical field can be sustained with a minimum amount of power dissipation.

Maximum power transfer:	The maximum amount of available power which is transferred from a RF amplifier to a rock sample.
Parallel-plate capacitor:	A coupling device using two copper conducting plates sandwiching a dielectric material.
Radio-frequency power:	Radio-frequency (RF) power, as used in this research, refers to the product of an alternating voltage and current generated in the VHF range between 30 and 300 MHz.
Resonating frequency:	A resonating frequency results when the capacitive and inductive reactances in a circuit are equal, thereby cancelling each other and leaving only the resistive component in a series based circuit. At this point, maximum alternating current flows through the series circuit.
Rock comminution:	The crushing and grinding of rocks down to powder form.
Treated samples:	Rock samples of specific size which have been exposed to a known amount of RF power at a given frequency.
Untreated samples:	Rock samples of specific size which have not been exposed to RF power.

1.8 Importance of the research

This research makes the following novel scientific contributions to the fields of metallurgical and electrical engineering:

- Introduces a electrical technique using RF power in the treatment of rock samples;

- Describes a innovative coupling technique to connect rock samples to high powered RF electronic equipment;
- Defines the mathematical models for 10 rock samples for the VHF range; and
- Presents an original coupling coefficient for the parallel-plate capacitor.

1.9 Summary

The background to the possible use of RF power in assisting with rock comminution has been discussed. The mining industry aims to achieve a higher throughput of valuable minerals and increased power efficiency by means of various techniques including pre-treatment of run-of-mine ore. The methodology and overview of the dissertation has been reviewed as well as the delimitations of the project. Definitions of important terms were presented together with the importance of the research which highlighted significant contributions to the scientific community. The following chapter will consider the physical properties of minerals and the process of rock comminution.

Chapter 2 Minerals, rocks and comminution

2.1 Introduction

This chapter aims to provide a broad introduction into the description and classification of minerals and rocks and their physical properties, followed by a more detailed description and characterization of the rock samples used in the experimental investigations in this research. These physical properties are initially used in identifying the mineral composition of the rock samples used in this research. Secondly, they are used to indicate significant textural changes between the treated and untreated rock sample results presented in Chapter 6. The principles of rock comminution and mineral liberation are also introduced, as the objective of this research is to develop an alternative, non-conventional method to aid the comminution process.

2.2 Mineral definition and classification

A mineral is defined as a naturally occurring solid chemical compound of more or less fixed chemical composition (Skinner and Porter 1992:44; Wenk and Bulakh 2004:3, 255). Classification of minerals is based mainly in terms of chemical composition according to the anionic component of the molecular formula (Dana 1963:389). Some of the chemical groupings are further subdivided according to the atomic structures of the minerals (Trefil and Hazen 2007:162). Table 2.1 lists the major chemical groups of minerals.

The silicate minerals are by far the most abundant because of the prevalence of the elements of silicon and oxygen in the Earth's crust (Table 2.2) and mantle as well as the stable chemical affiliation of these elements (Dana 1963:389; Read 1984:348; Skinner and Porter 1992:57; Walther 2005:155; Thompson and Turk 2007:237). However, the other groups of minerals, although less abundant, are of major economic importance because some of them contain useful metals (e.g. iron in the oxide mineral haematite

(Fe_20_3)) and others have useful properties (e.g. the hardness of diamond finds use as an abrasive material).

Table 2.1: Chemical classification of minerals following the system of Dana (1963:222)

Mineral Class	Defining Anion	Example
Carbonates	$(CO_3)^{--}$	$CaCO_3$, calcite
Sulphates	$(SO_4)^{--}$	$BaSO_4$, barite
Phosphates	$(PO_4)^{---}$	Ca_5FPO_4, apatite
Oxides	O^{--}	Fe_2O_3, hematite
Hydroxides	OH^-	$Mg(OH)_2$, brucite
Halides	I^-, F^-, Cl^-	CaF_2, fluorite
Sulphides	S^{--}	PbS, galena
Native elements	None	Gold, graphite

Table 2.2: Average composition of the earth's crust (Skinner and Porter 1992:57; Klein 2002:40)

Element	Mass %
Oxygen	46.60
Silicon	27.72
Aluminium	8.13
Iron	5.00
Calcium	3.63
Sodium	2.83
Magnesium	2.09
Potassium	1.84
Titanium	0.44
Hydrogen	0.14
Phosphorous	0.12
Total	98.77

The physical properties of minerals are listed in Table 2.3, along with short definitions for each property. Many of these properties are used in the identification of minerals in hand specimen and under microscopes.

Table 2.3: A list of some physical properties of minerals and their explanations (Chernicoff and Fox 1997:30-33; Amethyst Galleries 2000; McGeary et al. 2001:230-236; Klein 2002:17,32,201; Thompson and Turk 2007:29-31; Trefil and Hazen 2007:A24)

Physical property	Definition
Cleavage	Cleavage is defined as the tendency of some minerals to break along certain crystallographic planes.
Colour	Colour is the most obvious property of a mineral, but can be unreliable for identification purposes due to the colour-altering effect of small amounts of chemical impurities and imperfections in the crystal structure.
Common form	The general outward appearance of the mineral. This depends on the atomic structure, chemical composition, cleavage panes and conditions of growth/origin of the mineral. Many minerals have more than one characteristic common form.
Crystal form	A crystal form consists of a group of crystal faces, all of which have the same relation to the elements of symmetry and display the same chemical and physical properties. The crystal form is the external manifestation of the internal atomic structure of the mineral.
Density	The density of a material is usually given in units of grams/cubic centimetre and refers to the quantity of matter per unit volume.
Electrical properties	Measured in terms of a mineral's ability to conduct or resist the flow of electrons.
Fracture	Fracture may be defined as the manner in which minerals break, other than along planes of cleavage.
Fluorescence	Fluorescence may be defined as the emission of visible light by a substance, such as a mineral, while it is exposed to ultraviolet light and absorbs radiation from it.
Hardness	Hardness is defined as the degree of resistance of a given mineral to scratching, indicating the strength of the bonds that hold the mineral's atoms together.
Lustre	Lustre describes the manner in which a mineral's surface reflects light and may be classified as either a metallic, glassy or earthy.
Magnetism	Magnetism derives from a property of electrons called magnetic moment that results from their spinning and orbiting motions.
Phosphorescence	Phosphorescence occurs with emission of visible light by a substance, such as a mineral, that has been exposed to ultraviolet light and absorbs radiation from it.
Refractive index	The index of refraction is defined as the ratio of the velocity of light in a vacuum to the velocity of light in a crystal, glass, liquid or other medium.
Specific gravity	The specific gravity of a mineral is the ratio of its mass to that of an equal volume of water.
Streak	Streak may be defined as the colour of a fine powder of a mineral, usually obtained by rubbing the material on an unglazed porcelain streak plate.
Tenacity	Tenacity may be defined as the resistance that a mineral offers to breaking, crushing, bending, or tearing – in short its cohesiveness.
Transparency	Transparency describes a mineral that is capable of transmitting light and through which an object may be seen. A mineral is said to be translucent when it is capable of transmitting light diffusely, not showing a sharp outline of an object seen through it. A mineral that does not transmit light at all is called opaque.

The physical properties that have the most influence on the comminution process (i.e. size reduction by way of crushing and grinding) are hardness, tenacity, fracture, cleavage and common form. Further automated mineral beneficiation, which essentially involves the separation of specific desired minerals from a crushed/milled mixture of minerals, usually exploits properties such as differences in densities, magnetic susceptibility, electrical conductivity, surface reactivity, refractive index, and fluorescence (Wills 1992).

Since this research is focused on the effects of RF power on rocks and minerals with a view to facilitating the comminution process, the electrical properties of minerals will be discussed briefly. Other properties that will be discussed in detail are those that may also affect the efficiency of comminution, such as hardness, cleavage, fracture, common form and tenacity.

2.2.1 Electrical properties of rocks

There are numerous uses for knowledge of the electrical properties of rocks. These include, among others:

- borehole radar technology development (Rutschlin et al. 2006);
- crustal, lunar and planetary soundings (Dyal and Parkin 1973; Hutton 1976; Nover 2005); and
- mineral exploration methods that exploit induced polarization, resistivity and electromagnetism (Collet and Katsube 1973; Daniels and Dyck 1984; Philips 1984).

Resistivity surveying involves the investigation of variations of electrical resistance or conductivity by causing an electrical current to flow through the ground, using wires connected to it (Philips 1984). These techniques exploit the differences of various electrical properties of rocks and minerals. The main uses of resistivity surveying are for mapping the presence of rocks of differing porosities, particularly in connection with hydrogeology for detecting aquifers and contamination, and for mineral prospecting, but other uses include investigating salinity and other types of pollution, archaeological surveying and detecting hot rocks. The amounts of positive and negative charges within a material are usually equal, resulting in electrical neutrality. When an imbalance occurs, the material becomes charged and its electrical properties become apparent. It is not so much the imbalance, but rather the flow of charge through rocks which is of primary concern. The amount of charge flowing through the rock is often referred to as an electric current caused by the application of a potential difference across the rock that is termed voltage. A relationship exists between the electrical current and voltage that is referred to as resistance (Musset & Khan 2000:181-182). This relationship is further discussed in Chapter 3. Many electromagnetic methods of surveying are used for the same purposes as resistivity methods because both methods respond to variations in the resistivity or conductivity of the subsurface. The main distinction between the two methods is that in the electromagnetic method the induced current usually flows in the subsurface without the use of electrodes.

Upper crustal rocks exhibit pores and fractures that may be partially or totally filled with fluid electrolytes (Nover 2005). Electrical charge transported within these rocks is an electrolytic process controlled by the geometry of the pore system. One objective of laboratory experiments is to measure the physical properties of minerals and rocks under simulated conditions ranging from the Earth's surface down through the mantle to even the core. This requires the use of High-Pressure High-Temperature devices that are designed to allow measurements within certain pressure and temperature ranges. Electrical properties are generally measured as frequency dependent complex impedances. Physical and chemical parameters that may constrain the transport of electrical charges thus are accessible when frequency dependent complex electrical conductivity measurements are performed instead of fixed frequency measurements. This technique allows an interpretation of electrical data in terms of charge carrier transport models and thus makes conductivity data much more reliable.

The use of any radar technology underground is completely dependent on knowledge of how the electromagnetic wave will be altered by the rock through which it propagates

(Rutschlin et al. 2006). In particular, a propagating signal loses energy as it travels, and will be partially reflected from interfaces between materials with differing properties. The range of detection of such a contrast in rock types is determined by the energy lost during transit and thus the loss tangent of the material, while an accurate calculation of the distance to a target is made possible by knowledge of the signal's propagation velocity, which is directly related to the rock's relative permittivity. Accurate knowledge of the frequency characteristics of attenuation and signal velocity is critical for interpretation of radar data, and even potentially for the design of the radar components themselves. If the attenuation changes with frequency, the dominant frequency of a propagating pulse will change with distance, as will the pulse shape, envelope and phase velocity. All measurement techniques have in common the desire to relate some measurable quantity to a complex dielectric constant. A variety of techniques, both destructive and nondestructive, have been developed to determine the permittivity and loss tangent of dielectric materials (Ku et al. 1999; Chen et al. 2003; Butkewitsch and Scheinbeim 2006; Kandala and Nelson 2007).

2.2.2 Hardness

Hardness is defined as the degree of resistance of a given mineral to scratching, indicating the strength of the bonds that hold the mineral's atoms together (Skinner and Porter 1992:55; Chernicoff and Fox 1997:G-3; Klein 2002:31; Thompson and Turk 2007:29). The hardness of a mineral (five shown in Table 2.4) is tested by scratching the unknown mineral with a series of minerals or substances with known hardness and is one of the most useful diagnostic properties of minerals (Tarbuck and Lutgens 1999:41).

Table 2.4: Mohs hardness scale (Klein 2002:32)

Mineral	Hardness	Common objects
Gypsum	2	Human finger nail
Calcite	3	Copper penny
Feldspar	6	Steel blade
Quartz	7	Streak plate
Diamond	10	Wedding ring

The Mohs hardness scale assigns relative hardnesses to several common and a few rare minerals (Chernicoff and Fox 1997:31-32). Table 2.4 illustrates selected values from the Mohs hardness scale.

2.2.3 Cleavage

Certain minerals fracture with an uneven surface when broken while others split or cleave along distinctive crystallographic planes. Cleavages occur when some crystals break in one or more smooth plane surfaces whose orientation is determined by the regular atomic structure of the crystal (Klein 2002:29; Wenk and Bulakh 2004:269). Cleavage is thus the ability of a mineral to break, when struck, along preferred directions (Skinner and Porter 1992:52; McGeary et al. 2001:233). Figure 2.1 illustrates seven possible types of mineral cleavage which are:

- A – One direction of cleavage;
- B – Two directions of cleavage at 90°;
- C – Two directions of cleavage not at 90°;
- D – Three directions of cleavage at 90°;
- E – Three directions of cleavage not at 90°;
- F – Four directions of cleavage; and
- G – Six directions of cleavage.

Cleavage is tested by striking or hammering a mineral, and is classified by the number of surfaces it produces and the angles between adjacent surfaces (Chernicoff and Fox 1997:G-4). A mineral tends to break along certain planes because the bonding between atoms is weaker there. For example, quartz has equally strong bonds in all directions and would thus have no cleavage whereas micas are easily split apart into sheets due to the fact the bonding between adjacent atomic sheets is weak. Cleavage is one of the most useful diagnostic tools because it is identical for a given mineral from one sample to another. It is especially useful for identifying minerals when they appear as small grains in rocks (McGeary et al. 2001:233).

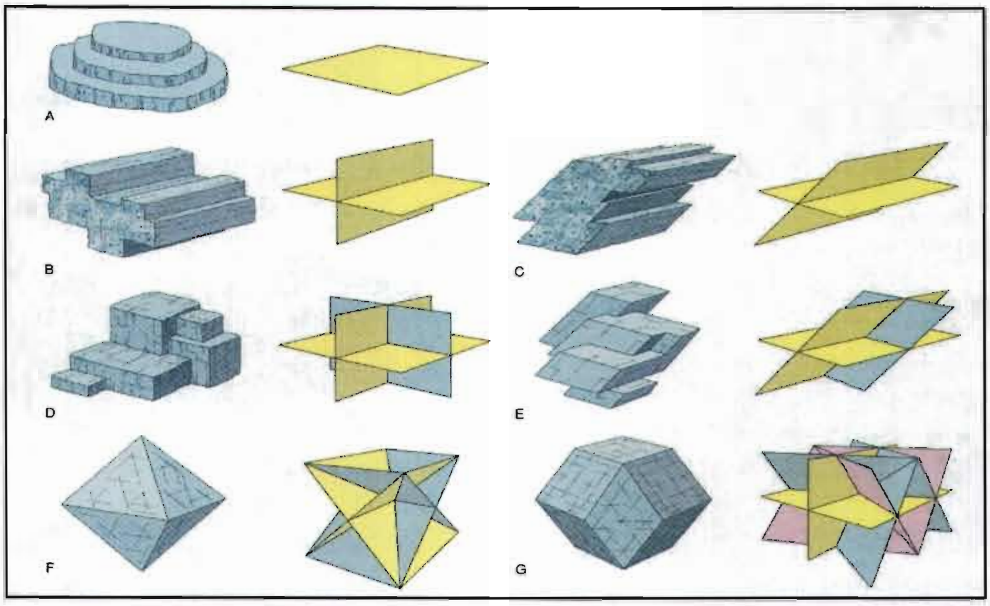

Figure 2.1: Seven possible types of mineral cleavage (Wenk and Bulakh 2004:217)

2.2.4 Fracture

Some minerals have poorly defined cleavages while others may not even show any at all. When broken, these minerals cause fractures in that they break on generally irregularly oriented, curved surfaces decided more by stress distribution in the crystal at the time of rupture than by the atomic structure of the mineral (Klein 2002:30; Wenk and Bulakh 2004:270). Fracture is thus the way a substance breaks when not controlled by cleavage and is the most common type of fracture for minerals (McGeary et al. 2001:235; Thompson and Turk 2007:29). Fracture may appear as a jagged, irregular or rough surface or as a curved, shell-shaped (conchoidal) surface (Chernicoff and Fox 1997:33). Minerals may further be identified by their common form.

2.2.5 Common form

The term form is often used to indicate general outward appearance (Klein 2002:201). In crystallography, external shape is denoted by the word habit, whereas the term form is used in a special and restricted sense. Thus a form consists of a group of crystal faces, all of which have the same relation to the elements of symmetry and display the same chemical and physical properties. The term common form is used synonymously to the term habit and refers to the external shape in which a mineral commonly occurs. Figure 2.2 illustrates selected photomicrographs of six mineral textures.

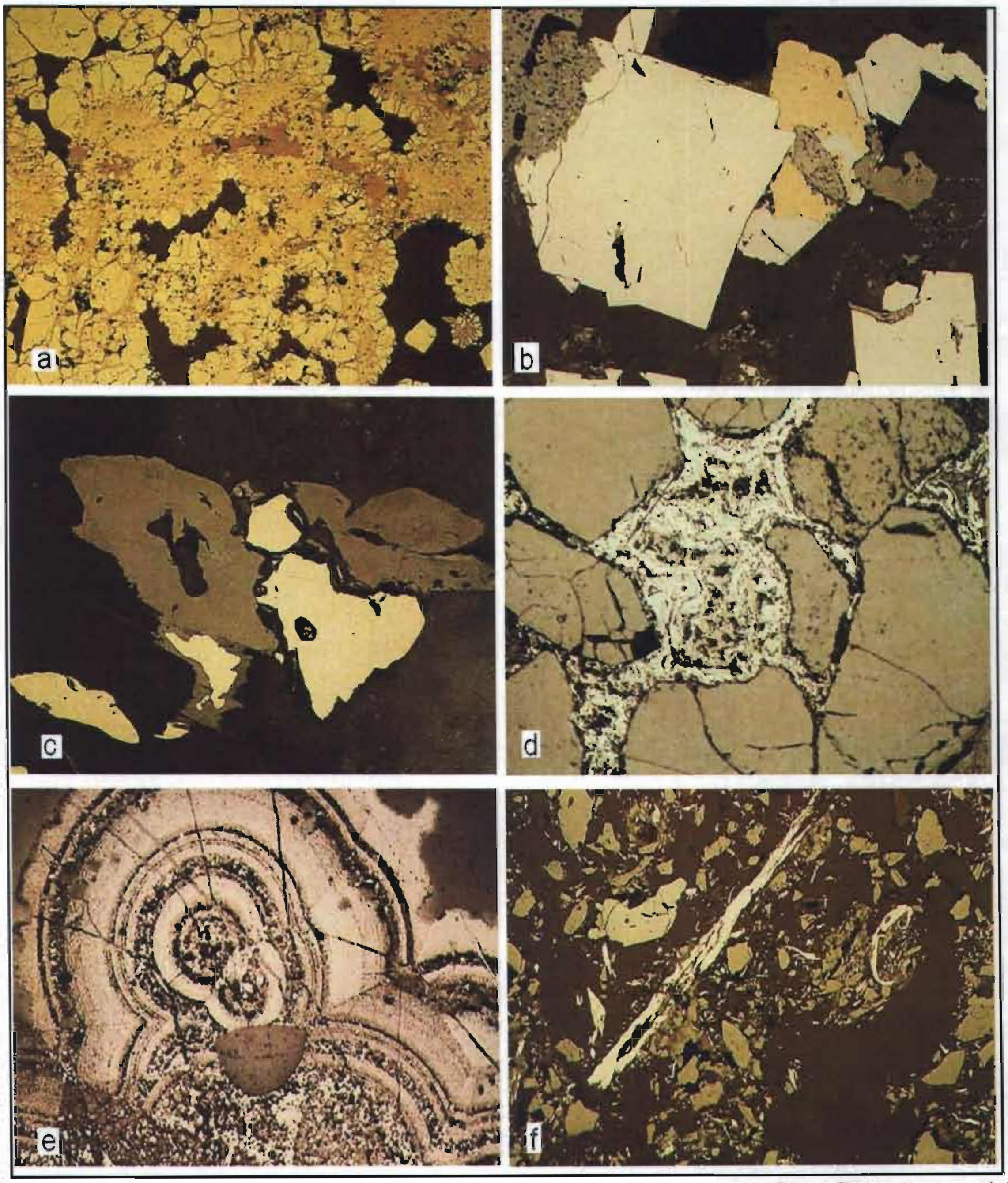

Figure 2.2: Photomicrographs showing some examples of mineral textures: (a) Granular texture; (b) euhedral crystals; (c) Angedral grains; (d) banding; (e) Botryoidal texture; (f) flaky (Ixer and Duller 1998)

Some minerals are commonly found as well-developed crystals, but others only occur in fine-grained masses. The terms used to describe the form of a mineral are (Klein 2002:20, 171):

- Crystallised or euhedral (well developed crystals);
- Crystalline (intergrown crystals);
- Microcrystalline (microscopic crystals);
- Cryptocrystalline (sub-microscopic crystals); and
- Irregular or anhedral (no evidence of the crystal structure).

In addition some of the following descriptive terms are used for mineral aggregates (Klein 2002:23):

- Acicular (needle like);
- Bladed (resembles flattened blades);
- Botriodal (similar to a bunch of grapes);
- Dendritic (tree like);
- Lamellar (like leaves in a book);
- Oolitic (resembling the roe of fish);
- Reniform (kidney shaped); and
- Stellate (star shaped).

2.2.6 Tenacity

Tenacity is a mineral's physical reaction to stress such as crushing, bending, breaking, or tearing (Klein 2002:32). Certain minerals react differently to each type of stress. Since tenacity is composed of several reactions to various stresses, it is possible for a mineral to have more than one form of tenacity. The different forms of tenacity are:

- **Brittle** - If a mineral is hammered and the result is a powder or small crumbs, it is considered brittle. Brittle minerals leave a fine powder if scratched, which is the way to test a mineral to see if it is brittle. Majority of all minerals are brittle. Minerals that are not brittle may be referred to as non-brittle minerals.

- **Sectile -** Sectile minerals can be separated with a knife into thin slices, much like wax (e.g. gold).
- **Malleable -** If a mineral can be flattened out into thin sheets by pounding it with a hammer, it is malleable. All true metals are malleable (e.g. gold).
- **Ductile -** A mineral that can be stretched into a wire is ductile. All true metals are ductile.
- **Flexible but inelastic -** Any minerals that can be bent, but remains in the new position after it is bent are flexible but inelastic. If the term flexible is singularly used, it implies flexible but inelastic (e.g. chlorite).
- **Flexible and elastic -** When flexible and elastic minerals are bent, they spring back to their original position. All fibrous minerals and some acicular and flaky minerals belong in this category (e.g. mica).

2.3 Rocks and ores

Rocks are composed of minerals (Chernicoff and Fox 1997:11). A rock composed of only one mineral is called monomineralic (Best and Christiansen 2001:27). Ores are essentially rocks that contain one or more type of mineral coveted for its metal content or its physical properties for industrial use (Wills 1992:6). The coveted minerals in the ores are called ore minerals (if they contain useful metals) or industrial minerals (if they have useful physical properties). Woollacot and Eric (1994) classify mined material into three categories:

- Mined material consisting of useful rock or soil, where the rock/soil has value in its natural form, e.g. as aggregate or filler material.
- Mined material containing industrial minerals, where the value lies in one or more minerals within the rock that must be liberated and separated from the rock, e.g. diamond in kimberlite, crysotile in greenstones, wollastonite in skarn, etc.
- Mined material containing value-bearing minerals, where the value lies in constituents of one or more minerals within the rock (ore) and the constituent (metal) needs to be extracted from the mineral after the latter has been liberated and separated from the rock (ore), e.g. extraction of copper from copper-bearing

minerals such as chalcopyrite ($CuFeS_2$) and bornite (Cu_5FeS_4) occurring as minerals in copper ore.

Ores, therefore, contain coveted minerals (called ore minerals) as well as unwanted minerals (called gangue minerals) (Wills 1992:12).

Rocks are broadly classified into three groups based on their mode of formation. These are:

- **Igneous rocks:** formed by the solidification/crystallization of molten silicate (mainly) material called magma or lava (Chernicoff and Fox 1997:11; Walther 2005:255). These rocks consist of tightly interlocked crystals. The size of the crystals range from <0.06 mm as in the case of those crystallized from lava at the surface of the earth, through to ± 10 mm as in the case of those crystallized from slow cooling magma deep in the earth's crust. In addition, there are very coarse-grained igneous rocks (pegmatites) which crystallized from magma containing high proportions of volatile material.
- **Sedimentary rocks:** formed by the solidification of loose material on the earth's surface (Skinner and Porter 1992:211; Chernicoff and Fox 1997:11). The loose material accumulates through the processes weathering, erosion and deposition/sedimentation. The solidification takes place by a process called lithification/diagenesis which involves the compaction, cementation and recrystallisation of sediments that are deeply buried (± 3 km). Sedimentary rocks are also formed by the lithification of chemical precipitates that accumulate as layers of microcrystals on lake floors or subterranean cavities (Kehew 1995:87; Thompson and Turk 2007:247; Carlson et al. 2008:427).
- **Metamorphic rocks:** formed by the exposure of rocks to high temperature and/or pressures during magmatic and/or tectonic events (Chernicoff and Fox 1997:11). Heat from nearby magmatic intrusions and pressure induced by mountain-building and other tectonic processes causes reactions and recrystallisation of minerals resulting in new sets of minerals within metamorphosed rocks. The process of

recrystallisation occurs in the solid state, or in extreme cases, in a partially molten state.

The relationship that exists between rocks is termed "the rock cycle" and is depicted in Figure 2.3 (Chernicoff and Fox 1997:11; McGeary et al. 2001:238).

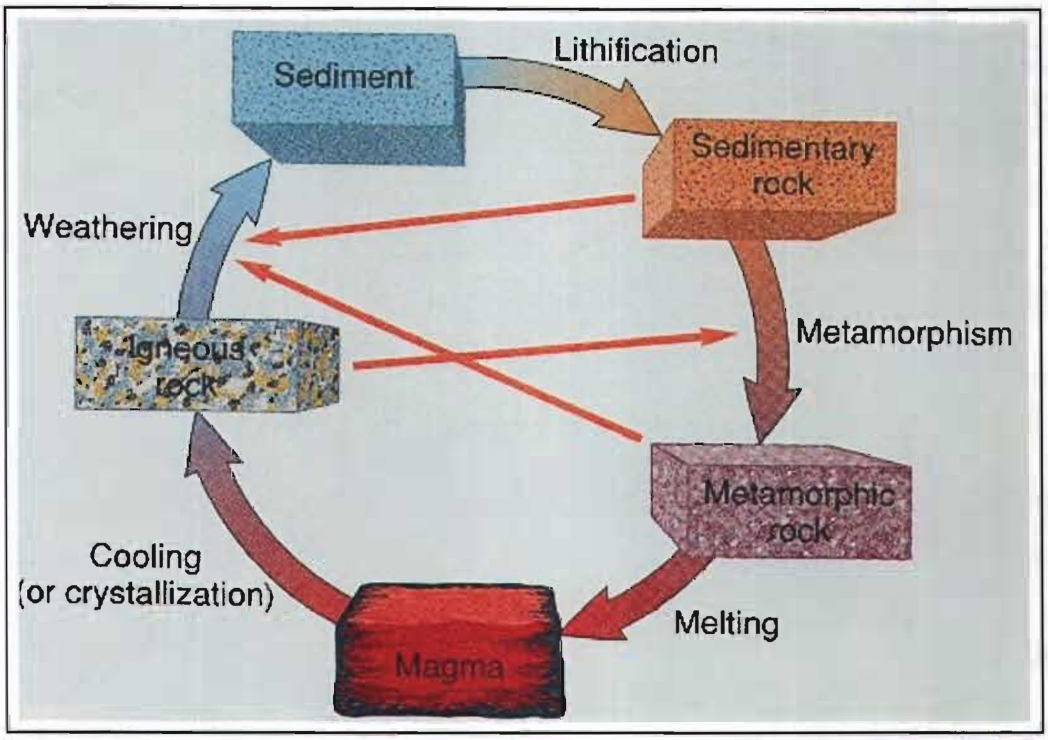

Figure 2.3: The rock cycle (Chernicoff and Fox 1997:12)

The three rock groups are characterised by important differences in the types of minerals and their textural relationships. These differences are manifest in the physical properties of the rocks, such as strength and elasticity ratios, that affect their behaviour during comminution. Consequently, the physical properties of minerals are not the only controlling factors on the effectiveness of comminution, but more importantly, the mineral assemblage and texture of the rock, which is the reason why five different rock types have been selected for trial in this research as described in more detail below. The same is true for different types of ores where the textures ultimately determine the grain-size to which an ore needs to be milled before liberation is properly effected.

2.3.1 Characteristics of granite and dolerite

Granite and dolerite are examples of igneous rocks. Granites have quartz contents of around 20 - 60%, are medium to coarse-grained and are relatively light in colour (Dietrich and Skinner 1979:113). They are composed predominately of feldspar and quartz and are the most abundant intrusive rock type found in the continents today. Table 2.5 highlights selected characteristics of granite and dolerite.

Table 2.5: Selected characteristics of granite and dolerite

Characteristic	Granite	Dolerite
Rock type	Igneous (plutonic)	Igneous (hypabysal)
Texture	Coarse grained and rough	Medium grained and smooth
Principal minerals	Feldspar and Quartz	Plagioclase and Pyroxene
Principal mineral hardness	Feldspar: 6 Quartz: 7	Plagioclase: 6 Pyroxene: 6
Principal mineral breakage	Two cleavages: Feldspar Concoidal fracture: Quartz	Two good cleavages at 90° for both pyroxene and feldspar
Specific gravity	2.40 – 2.70	3.00 – 3.05
Resistivity (Ω.m)	5 000 – 5 000 000	20 – 200
Colour	Mostly light coloured	Dark bluish, weathers to brown
Porosity	0.5 – 1.5%	0.1 – 0.5%

2.3.2 Characteristics of sandstone and mudstone

Sandstones and mudstones are types of sedimentary rocks. Table 2.6 outlines selected characteristics of sandstone and mudstone. Sandstones in particular consist of mineral grains, deposited in parallel layers, which have subsequently been cemented together. Sandstones are mostly white, light grey, buff, reddish or yellowish brown in colour.

Quartz is the predominant mineral found in most sandstones being chemically stable and physically durable under most weathering and transporting processes (Evans 1972:18; Dietrich and Skinner 1979:193-195).

Table 2.6: Selected characteristics of sandstone and mudstone

Characteristic	Sandstone	Mudstone
Rock type	Sedimentary	Sedimentary
Texture	Medium grained and rough	Fine grained and very smooth
Principal mineral	Quartz	Clays and quartz
Principal mineral hardness	7	< 2
Principal mineral breakage	Fracture	Fracture
Specific gravity	2.00 – 2.60	2.71
Resistivity (Ω.m)	8 – 4 000	8 – 4 000
Colour	White, light grey, buff, reddish or yellowish brown	Grey, greenish, bluish, reddish, brownish or blotchy combination
Porosity	5.0 – 25.0%	30.0%

Sedimentary rocks formed by the deposition of mineral grains are classified on the basis of grain-size. Mudstones have grain-sizes of < 0.002 mm and are composed mainly of clay material. Siltstones have grain-sizes ranging from 0.002 mm to 0.0625 mm and are composed mainly of quartz and clay. Sandstones have grain-sizes ranging from 0.0625 mm to 2 mm and generally comprise quartz with or without feldspar and other mineral fragments. In addition, sandstones may also have interstitial finer-grained material such as clay or cementing material which can vary in amount as a percentage of the total rock (< 5 - 25 %) (McGeary et al. 2001:339-341). Clay converted into a solid rock can become either a mudstone which shows no tendency to split into layers but has lost its plasticity, or a shale which splits readily along its bedding planes (Evans

1972:25). The most common colours found in mudstones are grey, greenish, bluish, reddish, or some blotchy combination of two or more of these colours. Most mudstones exhibit blocky breakage and feel gritty because they contain higher percentages of irregularly shaped fragments than shales do (Dietrich and Skinner 1979:200-202).

2.3.3 Characteristics of marble

Marble is an example of a metamorphic rock consisting primarily of calcite and/or dolomite. Table 2.7 presents selected characteristics of marble.

Table 2.7: Selected characteristics of marble

Characteristic	Marble
Rock type	Metamorphic
Texture	Coarse grained
Principal minerals	Calcite and dolomite
Principal mineral hardness	3
Principal mineral breakage	Three good cleavages at 75°/105°
Specific gravity	2.6 – 2.86
Resistivity (Ω.m)	100 – 250 000 000
Colour	White, grey, black, buff, yellowish, chocolate, pink, mahogany-red, bluish, lavender or greenish
Porosity	0.5 – 2.0%

Marble may be snow white, grey, black, buff, yellowish, chocolate, pink, mahogany-red, bluish, lavender or greenish in colour. The grains within marble tend to be of a rather uniform size (Dietrich and Skinner 1979:253). Marble forms by the metamorphism of limestone, during which recrystallisation of calcite occurs (Evans 1972:49). Completely recrystallised limestone can result in a rock with interlocking calcite crystals and the obliteration of the stratification and other textural characteristics of the parent limestone.

Impure parent limestone produces marble that contains other minerals in addition to calcite, with the most common being quartz, anorthite, serpentine, tremolite, diopside, and forsterite. The minerals present depend on the nature of the impurities and the grade of metamorphism.

The rocks shown in Table 2.8 were selected for this research from among the three main rock types discussed above. They were labelled with the text JS (representing James Swart) followed by either an alphabetical or numerical label.

Table 2.8: Rock samples chosen for this research

Sample code	Rock family	Rock type
JSA	Igneous	Dolerite
JSB	Metamorphic	Marble
JSC	Igneous	Granite
JSD	Sedimentary	Sandstone
JSE	Sedimentary	Mudstone
JS1	Metamorphic	Marble
JS2	Metamorphic	Marble
JS3	Metamorphic	Marble
JS4	Igneous	Granite
JS5	Metamorphic	Marble

2.4 Rock comminution and mineral liberation

As described above, an ore is a rock that consists of valuable ore minerals and useless gangue minerals. The aim of mineral beneficiation is to separate the ore minerals from the gangue minerals to produce an as pure as possible concentrate of ore minerals and a discard product called tailings comprising the gangue material with as little as possible of unrecovered ore minerals. The process is undertaken in steps where the run of mine ore first undergoes comminution followed by separation/concentration.

The aim of comminution is to liberate the ore minerals from the gangue by breaking the rock up into smaller particles until there are loose particles of ore mineral (Yarar and Dogan 1987:3; Wills 1992:13). This is to facilitate separation of the ore mineral from the gangue. The latter is done by exploiting the differences in physical properties of the ore and gangue minerals, and the most common processes include (Wills 1992:7-13):

- Gravity separation - This method exploits the density differences between minerals, and their response to gravity and resistance to motion in a fluid such as water. Typical apparatus includes jigs, Humphries spirals, Reichert cones, sluices, and shaking tables.
- Dense medium separation - Also exploits density differences. Here minerals are introduced to a dense liquid or suspension in which some minerals will float and others sink, thus effecting separation. A wide variety of separation vessels are employed in industry including some that incorporate a centrifugal aspect to expedite the process.
- Froth flotation - Exploits difference in the surface properties of different types of minerals. Here minerals are exposed to a solution which renders some of the minerals hydrophobic and other hydrophilic. Air is bubbled through the solution in which the minerals are suspended, resulting in separation because the hydrophilic ones settle to the bottom of the solution whereas the hydrophobic minerals can be skimmed off with the soapy froth at the surface.
- Magnetic separation - This process exploits the differences in magnetic susceptibility of minerals through the use of strong magnetic forces that can be adjusted to separate minerals of differing susceptibility.
- Electrostatic/high tension separation - Here the differences in electrical conductivity of minerals are exploited. Charge builds up in non-conductive minerals causing them to stick to charged surfaces, whereas conductive particles do not stick to such surfaces.

Before any of the above separation process can be effective, proper liberation of the ore minerals is essential. Incomplete liberation means that particles will comprise both ore and gangue material and their response to any of the separation techniques will be equivocal (see Figure 2.4). The degree of liberation can be described using the following terms:

- A completely liberated particle is one that consists of only one type of mineral, either ore mineral or gangue mineral.
- A middling is a particle that consists of two or more different types of minerals, i.e. it is incompletely liberated.
- Middlings can be further classified into attached mineral (binary, ternary, etc) or enclosed minerals.
- The degree of liberation can also described in terms of what is called particle grade. For example, a liberated particle comprising 100% ore mineral will have a particle grade of 100%, whereas a middling particle consisting of 25% ore mineral and 75% gangue mineral will have a particle grade of 25%.

Figure 2.4: Photomicrograph of a concentrated lead-zinc ore, consisting of particles/fragments of the minerals galena and sphalerite - the degree of liberation in this sample is very variable with few liberated particles, but mostly middlings. The few liberated particles may only appear so in this particular section since the third dimension is not observable, and hence the term apparently liberated is used (Ixer and Duller 1998)

Comminution is essentially the size reduction of the fragments of rock/ore (Wills 1992:110). Comminution is effected by compression, impact and abrasion, through crushing or grinding/milling. The process usually involves several steps each comprising a small reduction ratio of three to six. Fracture of the particles results from tensile forces arising perpendicular to the direction of compression on the particles. For a fracture to occur, the tensile force has to exceed the inter-atomic bond strengths within the rock material/minerals. Stress is not evenly distributed within a rock fragment because of the irregular shapes of the grains and the variety of minerals present. The presence of fractures, cracks, flaws and pores in the material has a profound effect. Stress is concentrated at the tips of cracks and if they have the correct orientation relative to the stress field will propagate and lengthen under a given amount of stress once they have reached a critical length (Inglis 1913). The energy released in relieving the stress through fracture has to exceed the surface energy generated by the creation of new surfaces by the fracture (Griffith 1921). Other constraints on the fracturing of materials include:

- The resilience or elastic properties of the materials that determine the amount of energy the material can store under stress and release again after the stress has been removed without fracturing.
- The toughness or ductility of the materials that determines to what extent the material can deform without fracturing.
- The presence of water or other fluid that can reduce the surface energy generated through fracturing.

In addition to the fractures formed perpendicular to the compressive stress directions, compressive failure occurs at the point of loading where the crusher is in contact with the rock fragment, producing very fine-grained material. The latter can be avoided by the use of impact crushing where rapid overloading of the particles results in tensile fracturing alone. Very fine-grained material is also produced by abrasion/attrition between particles within the crushing vessel. This can be avoided by reducing the feed rate of material into the crushing vessel.

The energy consumed by the comminution process is, however, not easily correlated to the amount size reduction effected because of the many factors affecting comminution, as discussed above, and the fact that the crushing/milling machines themselves and the heat generated in the process consume more than 75% of the input energy (Wills 1992:112; Somasundaran and Shroti 1995:49). All the theories of comminution assume that the material is brittle, so that no energy is absorbed in process such as elongation or contraction which is not finally utilized in breakage. Since the probability for particle breakage within a comminution vessel diminishes with particle size, a three tier approach to the prediction of energy consumption during comminution exists (Wills 1992:112-113):

- For particle sizes in the range of one cm, energy consumption (E) can be calculated using Kick's Theory:

$$E = \frac{Log\frac{f}{p}}{Log 2} \qquad \text{J} \tag{2.1}$$

Where

$f \equiv$ feed particles size in mm

$p \equiv$ product particle size in mm

- For particle sizes between 5 – 0.01 mm, energy consumption can be calculated using Bond's Theory:

$$E = 10 \times \mathrm{W_i} \times \left(\frac{1}{\sqrt{p}} - \frac{1}{\sqrt{f}}\right) \qquad \text{J} \tag{2.2}$$

Where

$\mathrm{W_i} \equiv$ work index which is a constant for each type of material and reflects its grindability or resistance to grinding

- For particles in the range of 10 – 1000 μm, energy consumption can be calculated using Rittinger's Theory:

$$E = \mathrm{k} \times (\frac{1}{D_2} - \frac{1}{D_1}) \qquad \mathrm{J} \qquad (2.3)$$

Where

k $\equiv$ coupling coefficient

D_1 $\equiv$ initial particle size in μm

D_2 $\equiv$ final particle size in μm

The grindability of an ore is a measure of the ease with which it can be comminuted and is a function of many factors including the elasticity, ductility, porosity, hardness and consistency of the material. The grindability or work index of a material is determined by the Bond standard grindability test described by Deister (1987). Levin (1989) described a grindability test for fine materials, Smith and Lee (1968) a batch-type grindability test method, and Berry and Bruce (1966) a comparative method for determining grindability of ores.

The successful liberation of valuable minerals from the waste gangue minerals at the coarsest possible particle size results in a considerable reduction of cost and energy. Complete liberation is seldom achieved in practice (Wills 1992:26; King 2001:45). Moreover, the adhesion between mineral and gangue particles is usually very strong resulting in a low degree of liberation. There are three main factors that affect the surface area of the interlocking bond forces at mineral grain contacts. These three factors are porosity, grain size, and grain shape which also contribute significantly to a rock's tenacity. Grain size and shape relates to the rocks texture while porosity indicates the percentage of the total volume of rock or sediment that consists of pore spaces (Tarbuck and Lutgens 1999:270). In most rocks the higher the surface area of mineral grain to grain contact the harder the rock becomes, for example (Solenhofen 2003):

- Decreasing porosity in rocks increases the surface area of grain contacts;

- Decreasing the size of mineral grains in the rock increases surface area of grain contacts; and
- The surface area of equant or irregular grains is greater than that of angular grains.

Therefore, the texture of a particular ore will have a profound effect on the ease of liberation. This is intuitively apparent in the textures depicted in Figure 2.5.

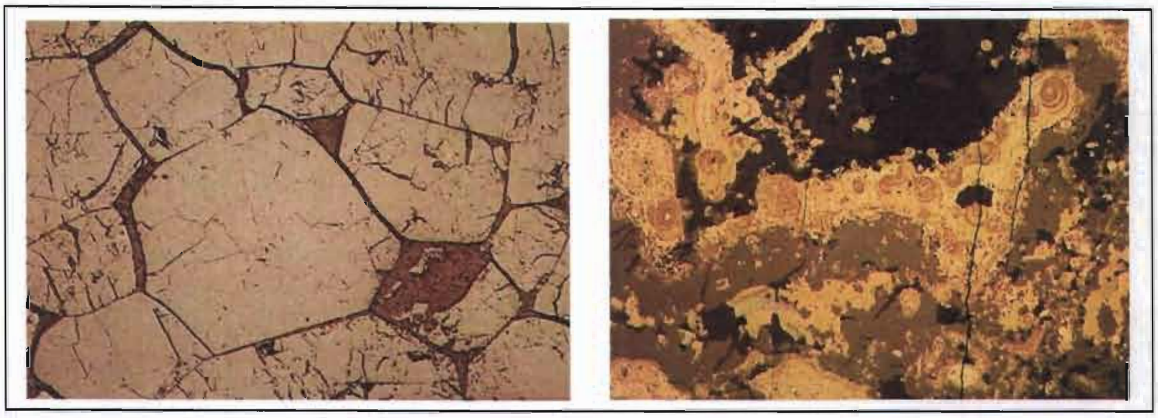

Figure 2.5: The photomicrograph on the left depicts euhedral chromite crystals in a silicate matix (darker areas) while on the right a finely intergrown texture of various copper minerals along with galena, sphalerite and silicate gangue is shown. It is intuitively clear that it will be easier to liberate the chromite grains from the ore depicted in the left hand photomicrograph than liberating the various ore minerals in that on the right (Ixer and Duller 1998)

There are diminishing returns on progressive energy consumption in comminution because the probability of particle breakage diminishes with particle size (see Figure 2.6). The implication is that achieving liberation in fine-grained ores with interlocking and inter-grown minerals is much more expensive. New approaches to increasing the degree of liberation involve directing the breaking stresses at the mineral crustal boundaries, so that the rock can be broken without breaking the mineral grains (Wills 1992:26). One of the objectives of this research is to investigate whether the use of RF power can increase the grindability of the material so as to reduce energy consumption, thereby promoting grain boundary fracturing to increase the degree of liberation at larger particle sizes.

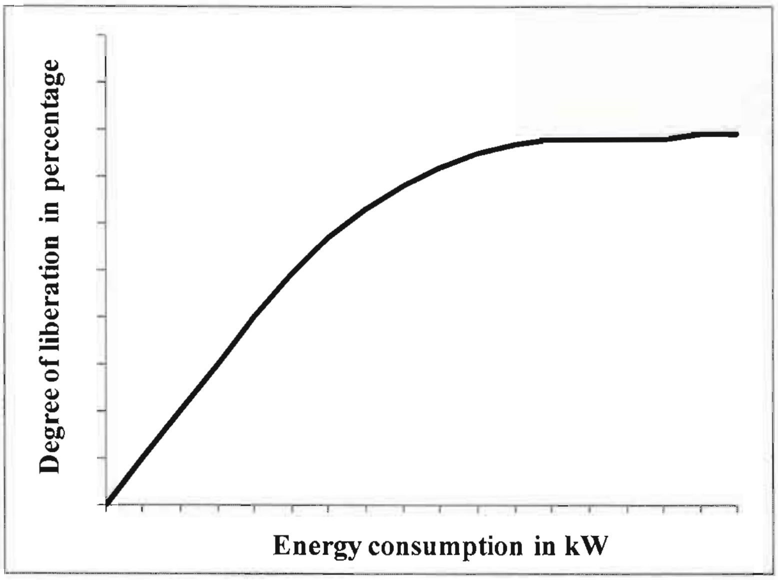

Figure 2.6: Hypothetical graph illustrating the diminishing returns on energy consumption in terms of degree of liberation

2.5 Summary

Chapter 2 gave an account of the classification of minerals as well as their physical and electrical properties. The three major rock types were introduced along with a brief description of the rock samples to be used in this research. Important factors relating to mineral liberation and rock comminution were also presented. The main characteristics of rocks such as structure, texture and mineral composition and their implications on comminution and liberation were also reviewed. These characteristics were used to determine significant textural changes between the treated and untreated rock samples, as described in Chapter 6.

Chapter 3 presents an overview of various electrical treatment techniques used in rock comminution, as well as the rationale behind a proposed new electrical treatment involving RF power.

Chapter 3 Electrical treatment techniques

3.1 Introduction

This chapter presents an overview of the theory of four techniques currently used in the electrical treatment of various materials, specimens and liquids. The rationale for using RF power in dielectric heating of rock materials is then established and a new electrical treatment technique for rocks at VHF frequencies is proposed.

3.2 Current electrical treatment techniques

Electrical treatment techniques refer to the use of electrical energy in specific ways to achieve desired changes in certain solid and liquid materials. Four specific electrical techniques currently employed include:

- Microwave pre-treatment;
- Ultrasound pre-treatment;
- High voltage electrical pulses; and
- Radio-frequency power.

3.2.1 Microwave pre-treatment

Numerous studies have shown that microwave pre-treatment is beneficial for:

- Drying of raisins (Kostaropoulos and Saravacos 1995);
- Accelerating enzymatic hydrolysis of chitin (Roy et al. 2003);
- Improved grindability and gold liberation (Amankwah et al. 2005);
- Improving the moisture diffusion coefficient of wood (Li et al. 2005);
- Enhancement of phosphorus release from dairy manure (Pan et al. 2006);
- Strength reduction in ore samples (Jones et al. 2007);
- Enhancing enzymatic digestibility of switchgrass (Hu and Wen 2008);

- A higher extractive yield of vegetable oil from Chilean hazelnuts (Uquiche et al. 2008); and
- The liberation of copper carbonatite ore after milling (Scott et al. 2008).

Microwave pre-treatment is found in many other applications where microwaves induce transient motions of free or bound charges, such as electrons or ions or charge complexes such as permanent dipoles. The resistance to these motions causes losses, which result in attenuation of the electric field and increased dissipation of energy in the material (Amankwah et al. 2005).

The most important early work on microwave pre-treatment was that of Chen et al. (1984), who investigated the reaction of 40 minerals to microwave exposure in a waveguide applicator which allowed the mineral samples to be inserted in an area of known high electric field strength. This study showed that microwave heating is dependent on the composition of the minerals.

Walkiewicz et al. (1988) later published data on microwave heating of a number of minerals and speculated on the potential reduction in grinding energy required for minerals with stress fractures induced by microwave heating.

Kingman et al. (2004) published an article stating that for the first time microwave-assisted comminution may have the potential to become economically viable. This conclusion was based on significant reductions in strength, coupled with major improvements in liberation of valuable minerals.

The microwave heating system is made up of four basic components: power supply, magnetron, cavity for the heating of the target material and waveguide for transporting microwaves from the generator to the cavity as depicted in Figure 3.1. Commonly, an industrial size microwave heating system is set to a frequency of 915 MHz with a magnetron as high as 75 kW power and an average working life of 6000 hours (Smith 1993).

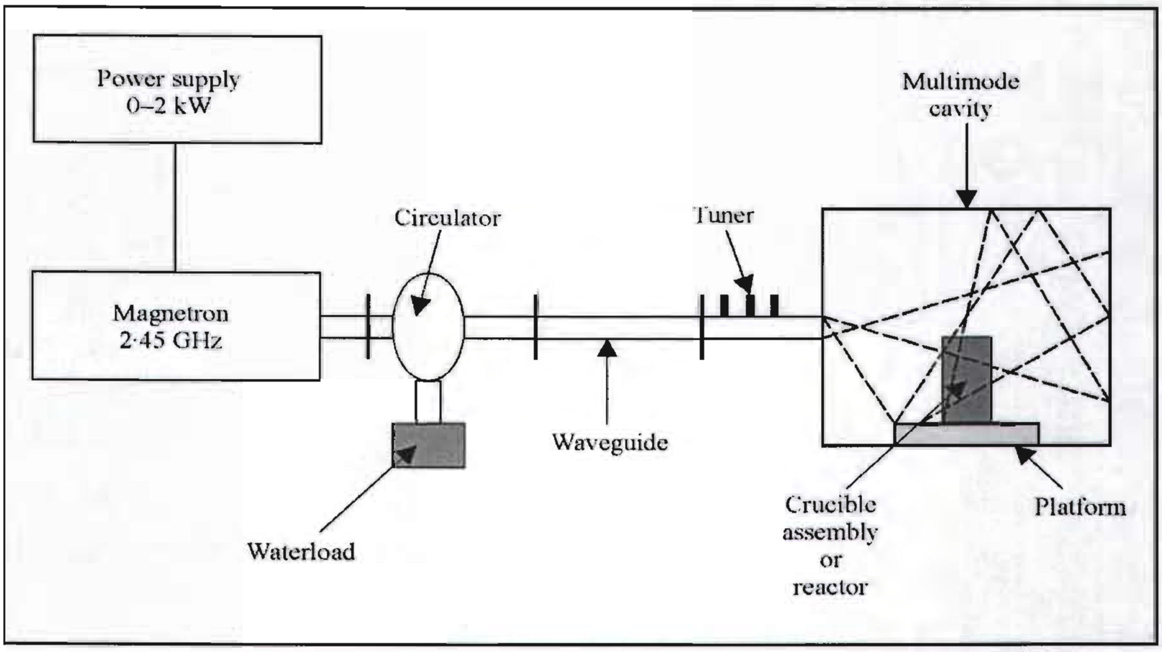

Figure 3.1: An industrial microwave heating system (Amankwah et al. 2005)

Microwave heating is a sophisticated electroheat technology requiring specialist knowledge and expensive equipment if meaningful results are to be obtained (Bradshaw et al. 1998). Included in this is the precision involved in the design and construction of the magnetron and cavity.

3.2.2 Ultrasound pre-treatment

The use of ultrasound pre-treatment has been applied to:

- Accelerate the anaerobic digestion of sewage sludge (Tiehm et al. 1997);
- Comminution (Gaete-Garretón et al. 2000);
- Titanium tanning of leather (Peng et al. 2007);
- Ammonia steeped switchgrass for enzymatic hydrolysis (Montalbo-Lomboy et al. 2007);
- Two-Minute skin anesthesia (Spierings et al. 2008); and
- Cassava chip slurry to enhance sugar release for subsequent ethanol production (Nitayavardhana et al. 2008).

The feasibility of the application of ultrasound energy to the grinding process as a viable avenue of study was stated at a meeting of the International Comminution Research Association in Warsaw, 1993 (Gaete-Garretón et al. 2000). One of the most significant reasons for this proposition originated in the accepted fact that inside any material there are a number of inherent cracks and ultrasonic energy has the capacity to produce crack propagation from within the particle to its outer surface, in spite of the very low energy producing an efficient fracture. An ultrasonic grinding machine can be designed in the form of a roller mill constructed over a specially designed ultrasonic transducer, as is shown schematically in Figure 3.2 (Gaete-Garretón et al. 2003).

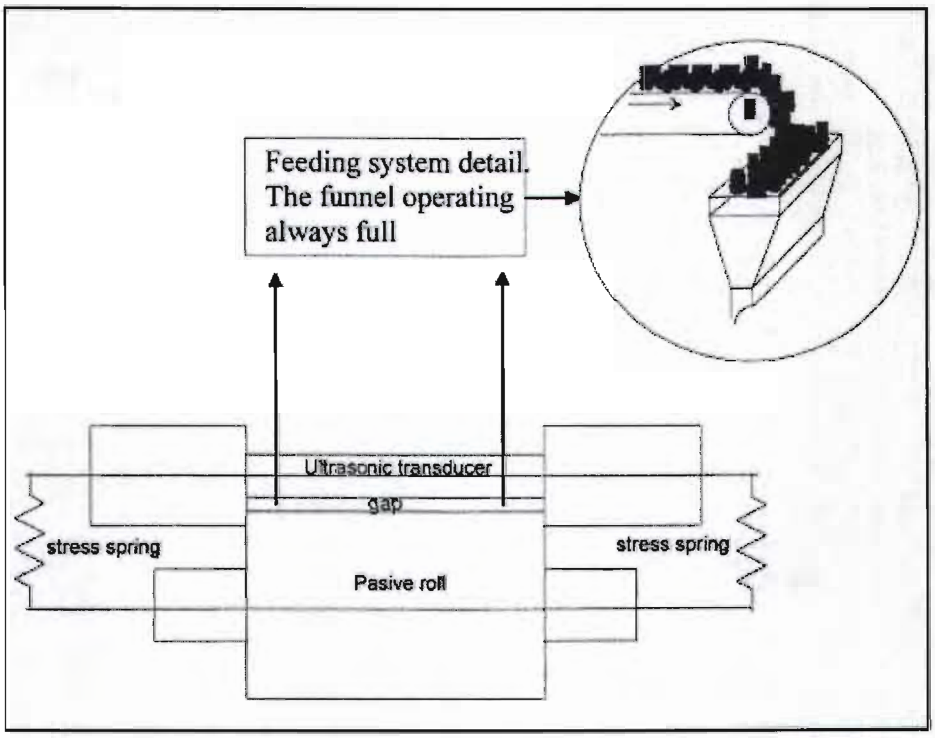

Figure 3.2: Schematic view of the ultrasound-assisted roller mill (Gaete-Garretón et al. 2003)

Gärtner (1953) was probably the first researcher to have attempted using ultrasonic waves in the fragmentation of particles, obtaining poor results. Leach and Rubin (1988) studied the fragmentation of resonant rocks samples fixed to the tip of an ultrasonic transducer, observing a preferred fracture at the nodes. Yerkovic et al. (1993) made grinding tests comparing standard copper ore with ultrasonic pre-treated samples in a ball mill. The pre-treated ore exhibited a 32% higher grinding rate.

An active roll, which is itself an ultrasonic transducer, is located in front of a passive roll. The vibration in extensional mode combines compression and shear action of the active roll on the mill feed. A funnel feeds the material in the gap by gravity which are then nipped by the rolls. A spring system furnishes the stress applied to the ore and the stress level can be varied by adjusting the spring tension. The rotation of the roll is produced by a variable speed electric motor. The ground ore is collected under the rolls in an iron receiver fed by gravity.

It is evident from the above description of the ultrasound mill that many different parts have to work together in the application of an ultrasonic field in the stressing zone of the material. This setup proves to be very precise and time consuming.

3.2.3 High voltage pulsed power

High voltage pulsed power has been applied to:

- Enhance coal comminution and beneficiation (Touryan and Benze 1991);
- Mineral liberation (Andres et al. 2001);
- Metal peening (Zhang and Yao 2002);
- Rock fragmentation (Hammon et al. 2000; Cho et al. 2006);
- Recover ferrous and non-ferrous metals from slag waste (Wilson et al. 2006); and
- Convective drying of raisins (Dev et al. 2008).

The history of high voltage pulsed power can be traced back to 1752 when Benjamin Franklin discovered that lightning was a discharge of static electricity (Staszewski 2010). It was reported that he raised a kite (with a key attached to his end of the string) which was tied to a post with a silk thread. As time passed, Franklin noticed the loose fibers on the string stretching out; he then brought his hand close to the key and a spark jumped the gap. This electrical discharge across a gap would prove significant in the research of high voltage pulsed power techniques.

In 1924 Erwin Marx described an apparatus, which produced high voltage pulses, and became known as the Marx-Generator (Fontana 2004). It is a clever technique for generating high-voltage short-duration waveforms by charging a number of capacitors in parallel, then quickly discharging them in series. While originally based upon the use of air-dielectric spark gaps to provide the switching mechanism, solid-state variants utilizing avalanche diodes or other solid-state switching devices have been used to generate nanosecond duration pulses having amplitudes exceeding several thousand volts of direct current (Baker and Johnson 1993).

There has been intense interest for the last several decades in the use of high-voltage pulse technology for rocks disintegration (Cho et al. 2006). The methods of electric pulse disintegration are mainly electrohydraulics and internal breakdown inside bulk solid dielectrics (Budenstein 1980; Owada et al. 2003). The first method refers to the generation of an intense shock wave in water from the passage of electrical current through water and the crushing and subsequent constituent separation by the impact of that shock wave on the sample. The second method refers to the passage of electrical current through the rock and the separation of the mineral contents from the rock matrix by preferential current flow along the mineral/rock boundary interface. Rock disintegration using the second method consumes substantially less energy than that using the first method and enhanced effect of liberation of mineral constituents of rock aggregates. The schematic of a test chamber using high voltage pulsed power in shown in Figure 3.3.

A major limiting factor to spark-gap switches used in high voltage pulsed power applications was their short lifetime (Winands et al. 2005). Other shortcomings with spark gaps are related to their limited pulse repetition rate, strong electrode erosion, insulator degradation, high arc inductance, limited hold-off voltage, and costly triggering.

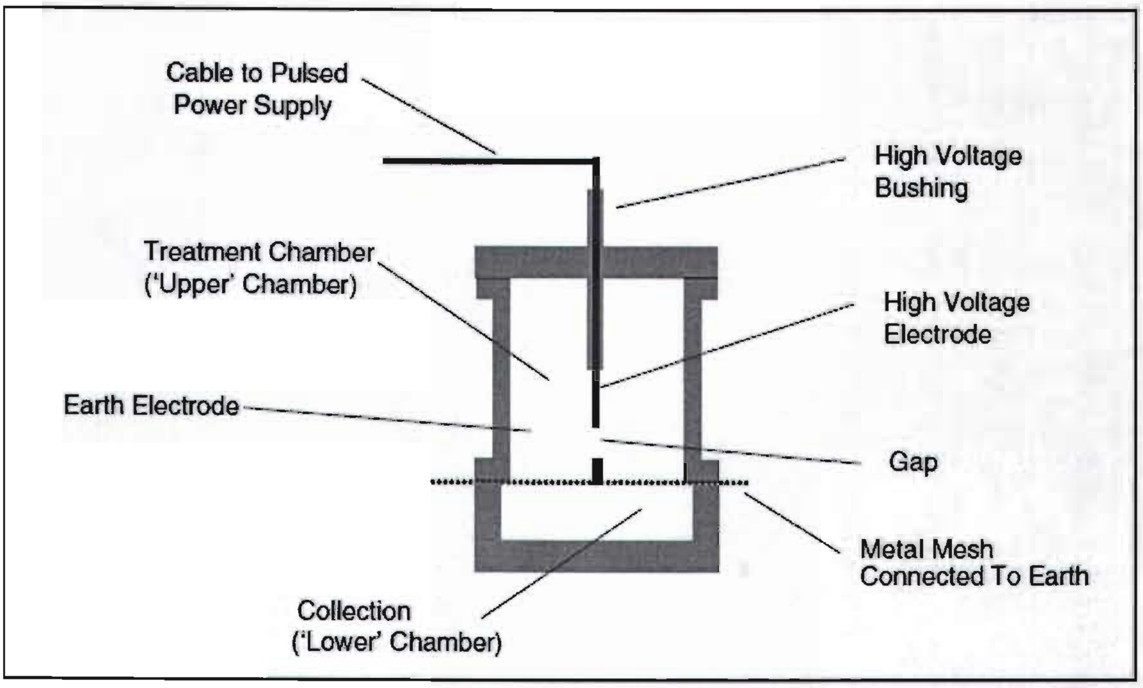

Figure 3.3: Schematic of a test chamber using high voltage pulses (Wilson et al. 2006)

3.2.4 Radio-frequency power

The application of electrical energy in the RF heating of various materials has been successfully employed in the following:

- Electrical heating along with radio frequency (RF) heating was used in the 1970s for the recovery of bitumen from tar sand deposits (Kawala and Atamanczuk 1998);
- RF treatments can potentially provide an effective and rapid quarantine security protocol against codling moth larvae in walnuts as an alternative to methyl bromide fumigation (Wang et al. 2001);
- RF heating was successfully used to increase the temperature of human blood without incurring cell destruction (Pienaar 2002);
- Treating fruit in immersion water of selected salt concentration and RF power may be used to develop an effective alternative quarantine method for fruit (Ikediala et al. 2002);

- RF power in conjunction with conventional hot water treatment can be used to develop feasible heat treatments to combat codling moths in apples (Wang et al. 2006);
- RF-based dielectric heating was used in the alkali pre-treatment of switchgrass to enhance its enzymatic digestibility (Hu et al. 2008); and
- Dielectric heating of soil using radio waves (RW) can be applied to support various remediation techniques, namely biodegradation and soil vapor extraction, under in situ or ex situ conditions (Roland et al. 2008).

Dielectrics have two important properties (Oespchuck 1984; Jones et al. 2002):

- They have very few free charge carriers. When an external electrical field is applied there is very little charge carried through the material matrix.
- The molecules or atoms comprising the dielectric exhibit a dipole movement.

The principle of dielectric heating basically involves the absorption of energy by dipoles (Chee et al. 2005). A dipole is essentially two equal and opposite charges separated by a finite distance. An example of this is the stereochemistry of covalent bonds in a water molecule, giving the water molecule a dipole movement. Water is the typical case of a non-symmetric molecule. Dipoles may be a natural feature of the dielectric or they may be induced (Kelly and Rowson 1995). Distortion of the electron cloud around non-polar molecules or atoms through the presence of an external electric field can induce a temporary dipole movement. This movement generates friction inside the dielectric and the power is dissipated subsequently as heat. The interaction of dielectric materials with electromagnetic radiation in a given frequency band results in energy absorbance (Wang et al. 2001; Jones et al. 2002). The power coupled into a sample is nearly constant when the electric field intensity and dielectric loss factor do not vary at a given frequency. The heat generated per unit volume (P in W / m^3) in a dielectric material when exposed to RF power can be expressed as (Nelson 1996):

$$P = 5.56 \times 10^{-11} \times f \times E^2 \times \varepsilon \qquad \text{W/m}^3 \qquad (3.1)$$

Where

f ≡ frequency of radiation in Hertz (Hz)

E ≡ the electric field intensity in Voltage per meter (V/m)

ε ≡ the permittivity of the material

Moreover, the amount of heat (Q) required to change the temperature of a given material is proportional to the mass of the material and to the temperature change as given by Giancoli (2005:387):

$$Q = C \times m \times \Delta T \qquad \text{J} \tag{3.2}$$

Where

ΔT ≡ temperature change in Degrees Celsius (°C)

m ≡ the sample mass in kilogram (kg)

C ≡ is the specific heat capacity of the sample in Joules per kilogram per degrees Celsius (J/kg/°C)

Subsequently, temperature rise within the sample due to absorbed electromagnetic energy is really a function of the heating time. The temperature increase can be estimated by assuming that the electric field is uniform and the dielectric properties are relatively constant. The temperature increase (ΔT in °C) of the sample during RF heating can furthermore be expressed as (Halverson et al. 1996):

$$\Delta T = \frac{\mathrm{k} \times P}{C \times m} \times \Delta t \qquad {}^{\circ}\text{C} \tag{3.3}$$

Where

k ≡ coupling coefficient

P ≡ input power (W)

Δt ≡ RF heating time in seconds (s)

The practical setup used to achieve the transfer of RF power to a dielectric sample is shown below in Figure 3.4. RF system consisted of a transformer, rectifier, oscillator, an inductance-capacitance pair commonly referred to as the 'tank circuit', and the work circuit (Wang et al. 2001). The transformer raises the voltage to 9 kV and the rectifier provides a direct current which is then converted by the oscillator into RF power at 27 MHz. This frequency is determined by the values of the inductance and capacitor in the tank circuit. The parallel-plate electrodes, with sample in-between, acted as the capacitor in the work circuit. The gap of the electrode plates can be changed to adjust RF power coupled to the sample between the two plates.

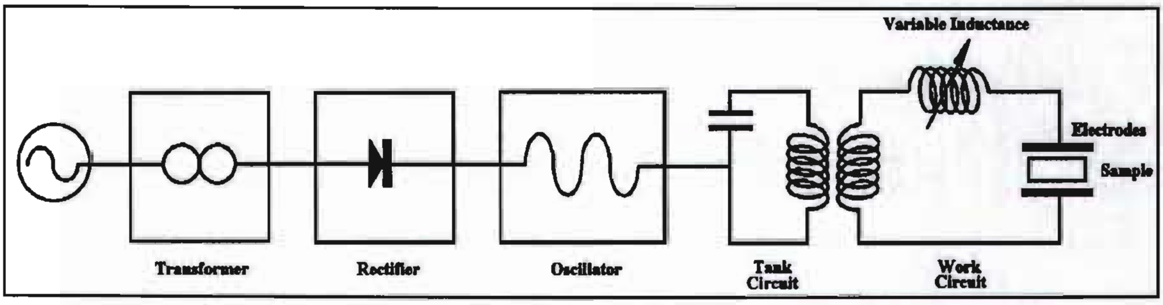

Figure 3.4: Practical setup used in the dielectric heating of a material (Wang et al. 2001)

Three (microwave, ultrasound and high voltage pulsed power) of the four electrical treatment techniques noted above have been successful in weakening the mineral grain boundaries of rocks, thereby enhancing mineral liberation within the rock comminution process. This is accomplished by the generation of stress within the material which gives rise to fractures and breakages. The weakening of mineral grain boundaries may yet be achieved by using RF power.

3.3 New proposed electrical treatment of rocks: RF power

Emanating from the above scientific literature on the use of electrical energy in various treatment techniques and in the dielectric heating of materials, the following hypotheses are made:

- The successful transfer of RF power to specific rocks through dielectric heating may exhibit positive effects on the textural characteristics of these samples; and
- These textural changes may further contribute to enhancing the rock comminution process, thereby increasing the percentage of valuable liberated minerals.

As far as could be established, no current literature exists substantiating these hypothesise. A novel electrical treatment technique of rock samples involving RF power is subsequently presented.

A high power RF amplifier may be connected to a rock sample (acting as a dielectric material) by means of a suitable coupling device. RF power is transferred from the amplifier to the rock sample at the resonating frequency. Confirmation of power transfer may be determined through the following results:

- Temperature increase on the surface of the rock sample and subsequently its specific heat capacity;
- Surface colour change of the sample;
- Screening of particles from pre-treated and non-treated sample;
- Scanning electron microscope (SEM) analysis of pre-treated and non-treated samples; and
- Power consumption analysis of pre-treated and non-treated samples in a ball mill.

The practical setup of this experiment is shown in Figure 3.5. A commercial RF transceiver (ICOM IC-V8000) may be used in conjunction with two RF amplifiers (MIRAGE PAC30-130B) to generate the power required at the resonating frequency. However, the output impedance of the RF amplifiers is 50 Ω while the input impedance of the rock samples may vary dramatically from a few hundred Ohm to a few thousand Ohm (Chapter 4 presents a more detailed description of these impedances). This necessitates the design and use of a matching network which will be presented in Chapter 5. The results (in terms of the five listed above) of this new proposed electrical technique are presented in Chapter 6.

The rock sample acts as a dielectric material within a coupling device, as shown in Figure 3.5. Suitable coupling devices along with RF electrical properties associated with dielectric materials are presented in Chapter 4.

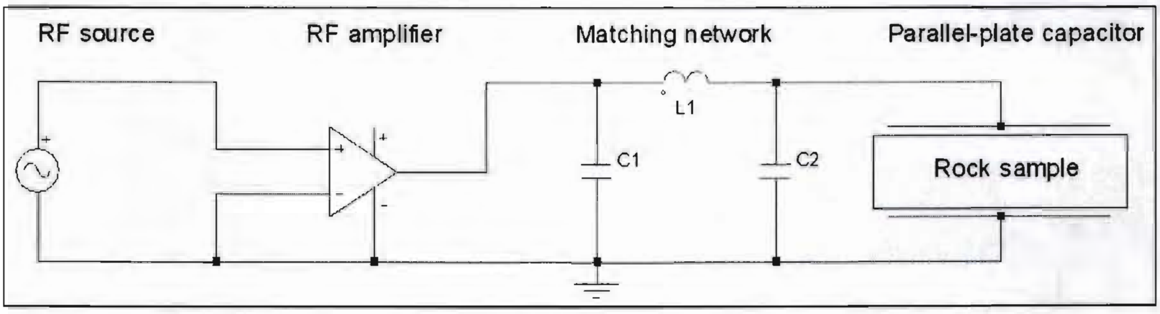

Figure 3.5: Practical setup of the experiment (Swart et al. 2009b)

3.4 Summary

Four treatment techniques (microwave pre-treatment, ultrasound pre-treatment, high voltage electrical pulses and RF power) currently used to achieve certain goals with regard to specified materials, specimens or liquids have been discussed. Rationale for using RF power in the dielectric heating of materials was presented. The practical setup of the equipment used in the transfer of RF power to a dielectric material was given. Chapter 4 will present various RF electrical properties associated with dielectric materials. It will also introduce two coupling techniques which have been substantiated by scientific literature in this field of dielectric heating.

Chapter 4 Electrical measurements of dielectric materials and subsequent findings

4.1 Introduction

This chapter presents various RF electrical properties associated with dielectric materials. Two RF methods currently used in connecting dielectric materials to electrical test equipment are reviewed together with the advantages and disadvantages of each method. The construction of a unique coupling device based on one of these proven scientific methods is described along with the practical setup to determine the RF electrical properties of ten different rock samples. As this research was limited to the VHF range, only readings between 30 and 300 MHz were recorded. These electrical properties were then used in the mathematical modelling of the phase angle to frequency equations for all ten rock samples. Resonance, resistivity and conductivity graphs are included as examples for the JSA sample, which may also be sketched for the other rock samples.

4.2 RF electrical properties associated with dielectric materials

The RF electrical properties of a dielectric material can be obtained by measuring its impedance (magnitude (|Z|) and phase angle (θ)) at various frequencies. Impedance may be represented as a complex quantity which is graphically shown on a vector plane illustrated in Figure 4.1. The well known unit of impedance is Ohm (Ω) and may be expressed in rectangular form as $Z = R \pm jX$ or in polar form as $Z = |Z| \angle \theta$. These impedance values are then used in conjunction with specified equations to obtain the following RF electrical characteristics of dielectric samples:

- R ≡ Resistance measured in Ohm (Ω);
- X ≡ Reactance measured in Ohm (Ω);
- C ≡ Capacitance measured in Farad (F);
- L ≡ Inductance measured in Henry (H);
- ρ ≡ Resistivity measured in Ohm meters (Ωm); and

- σ ≡ Conductivity in Siemens per meter (S/m).

The $+jX$ value in Figure 4.1 indicates an inductive reactance while the $-jX$ value indicates a capacitive reactance. The R value indicates a pure resistor. The following equations indicate that the frequency of operation (f) influences the value of reactance. For capacitive reactance the following equation is used:

$$Xc = \frac{1}{2 \times \pi \times f \times C} \quad \Omega \qquad (4.1)$$

For inductive reactance the following equation is used:

$$Xl = 2 \times \pi \times f \times L \quad \Omega \qquad (4.2)$$

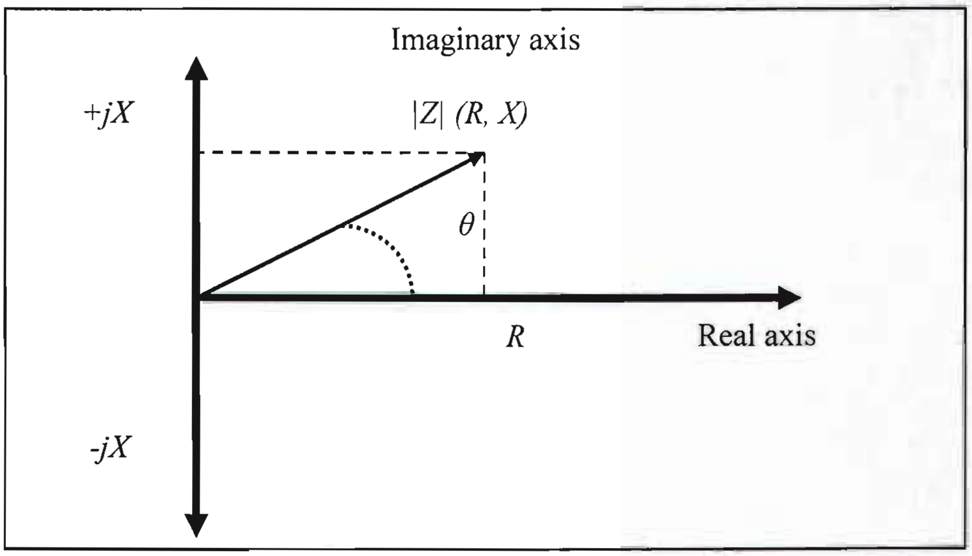

Figure 4.1: Impedance consists of a real and imaginary part

Beasley and Miller (2008:36) define resonance as a circuit condition whereby the inductive and capacitive reactance have been balanced; Xl and Xc tend to cancel each other leaving only the resistive component with maximum current flowing through the series circuit (see Figure 4.2). At this point a dielectric material acts purely as a resistive component, facilitating the maximum absorption of electrical energy. Increasing or decreasing the resonating frequency will introduce a reactive component which will modify the impedance of the circuit and subsequently negatively affect energy transfer. The following resonance equation results:

$$f_o = \frac{1}{2 \times \pi \times \sqrt{L \times C}} \quad \text{Hz} \qquad (4.3)$$

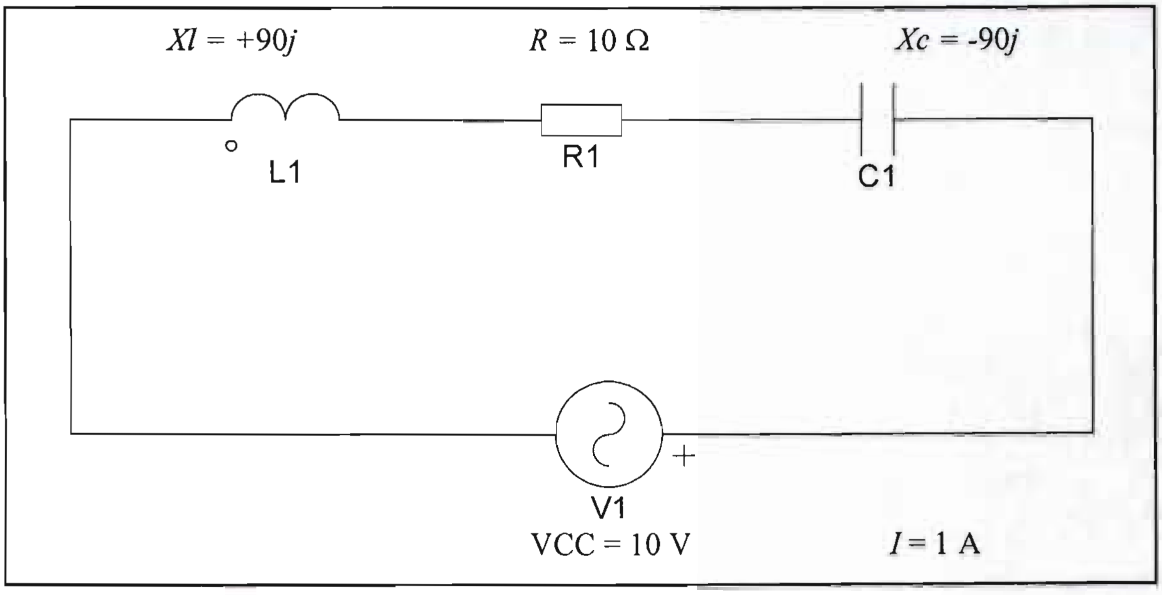

Figure 4.2: Series resonant circuit indicating a maximum current flow for *Xl* = *Xc*

Electrical resistivity is a measure indicating how strongly a material opposes the flow of electric current while electrical conductivity is just the reciprocal. Equations for resistivity and conductivity are:

$$\rho = \frac{R \times A}{l} \quad \Omega\text{m} \qquad (4.4)$$

$$\sigma = \frac{1}{\rho} \quad \text{S/m} \qquad (4.5)$$

Where

A ≡ the cross sectional area of the material in square meters (m^2)

l ≡ the thickness of the material specimen in meters (m)

4.3 Relative permittivity of materials

This research uses the characteristics of relative dielectric permittivity of materials to obtain maximum RF power transfer. The relative dielectric permittivity, or dielectric constant, (ε_r) of a material is generally described as a complex quantity by (Kasap 2006:605):

$$\varepsilon_r = \varepsilon'_r - j\varepsilon''_r \tag{4.6}$$

Where

ε'_r ≡ relative dielectric permittivity relating to the real part of the material

ε''_r ≡ relative dielectric permittivity relating to the imaginary part of the material

The real part (ε'_r) represents the relative permittivity which is used in calculating the capacitance, while the imaginary part (ε''_r) represents the energy lost in the dielectric medium as the dipoles are oriented against random collisions one way and then the other way and so on by the field (Kasap 2006:607). The power dissipated in the dielectric medium is related to the imaginary part (ε''_r) and peaks when $\omega = 1/\tau$. The rate of energy storage by the field is determined by ω whereas the rate of energy transfer to molecular collisions is determined by $1/\tau$. When $\omega = 1/\tau$, the two processes, energy storage by the field and energy transfer to random collisions, are then occurring at the same rate, and hence energy is being transferred to heat most efficiently. The relative magnitude of ε''_r is defined with respect to ε'_r through the loss tangent as:

$$\tan\delta = \frac{\varepsilon''_r}{\varepsilon'_r} \tag{4.7}$$

The energy per unit time dissipated as dielectric loss in the medium is defined as (Kasap 2006:607):

$$W_{vol} = \omega \times E^2 \times \varepsilon_o \times \varepsilon'_r \times \tan\delta \tag{4.8}$$

Where

W ≡ losses per unit volume in Watts per square meter (W/m^2)

ω ≡ angular frequency (s^{-1})

E ≡ electric field in Voltage per meter (V/m)

ε_o ≡ permittivity of free space (F/m)

It is frequently convenient to normalize the permittivity of a material by the permittivity of free space as shown by the following equation (Giacoletto 1977):

$$\varepsilon_r(\omega) = \frac{\varepsilon(\omega)}{\varepsilon_o} \tag{4.9}$$

The above equations indicate that the relative dielectric permittivity of a material is closely associated to the frequency of operation, which is one of the electrical properties that can be measured by sophisticated RF measuring instruments.

4.4 RF measurement coupling techniques

Two RF measurement coupling techniques currently exist for determining the RF electrical properties of dielectric materials. They are the:

- Cylindrical capacitor with coaxial electrodes and
- Parallel-plate capacitor (PPC) with disk electrodes.

These coupling techniques may furthermore be used with two different measuring instruments, namely a network analyser or a vector voltmeter. The practical setup for both measuring instruments is presented next. However, the network analyser was used as the primary measuring instrument in this research due to its advanced functionality.

4.4.1 Cylindrical capacitor with coaxial electrodes

Numerous articles list the usefulness of the cylindrical capacitor in measuring electrical impedances (Levitskaya and Sternberg 2000; Bagdassarov and Slutskii 2003; Azimi and Golnabi 2009). Figure 4.3 illustrates a detailed cylindrical capacitor with coaxial electrodes. A cylindrical capacitor consists of a three-part coaxial capacitance sensor in which the middle one acts as the main sensing probe (Azimi and Golnabi 2009). The outer conductor is considered to be a guard ring in order to reduce stray capacitance and error measurements. Aluminium material is often used for manufacturing the capacitor tube electrodes (Rutschlin et al. 2006).

The cylindrical capacitor extends the frequency limit of measurements to 1 GHz for materials with a dielectric permittivity of less than 25 (Levitskaya and Sternberg 2000). However, cutting a sample of marble (dielectric permittivity of 8) into a cylindrical form with exact diameter spacing proves cumbersome and difficult in the absence of a core-drill. For this reason the PPC was reviewed as a possible coupling device.

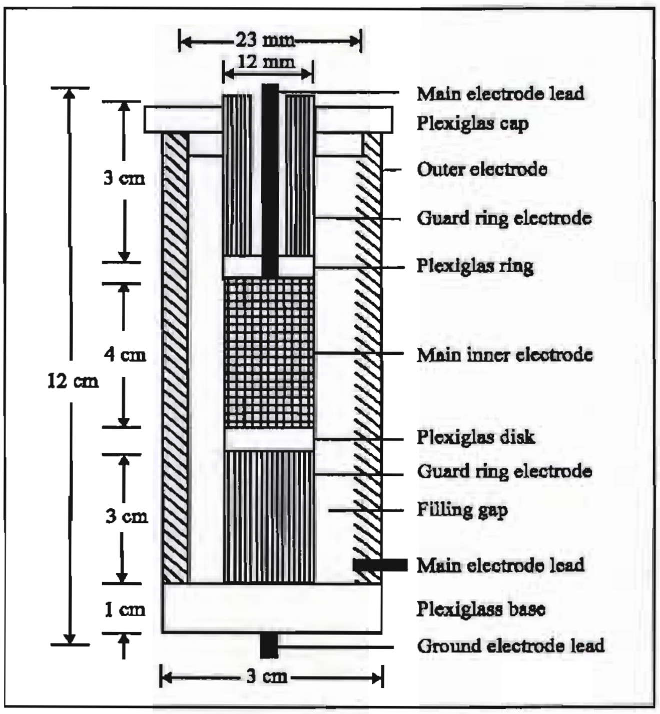

Figure 4.3: Cylindrical capacitor with coaxial electrodes (Azimi and Golnabi 2009)

4.4.2 The parallel-plate capacitor with disk electrodes

A PPC with disk electrodes is formed when a dielectric material or sample is sandwiched between two conducting plates (see Figure 4.4). These conducting plates (made from copper due to its good conductivity (Lu et al. 2004; Zaghloul 2008)) are connected to relevant test equipment via standard RF connectors and coaxial cables. Previous research has shown that the PPC technique is feasible up to frequencies around 100 MHz (Bussey 1979; Levitskaya and Sternberg 2000; Park et al. 2005). This technique has seemingly been found to be incompatible for measurements above 100 MHz due to the following reasons (Levitskaya and Sternberg 2000):

- connections may be a cause of mismatch;
- components become efficient transmitting antennas;
- energy is lost due to radiation;
- difficult to account for stray inductance and capacitance; and
- components become distributed rather than lumped parameters.

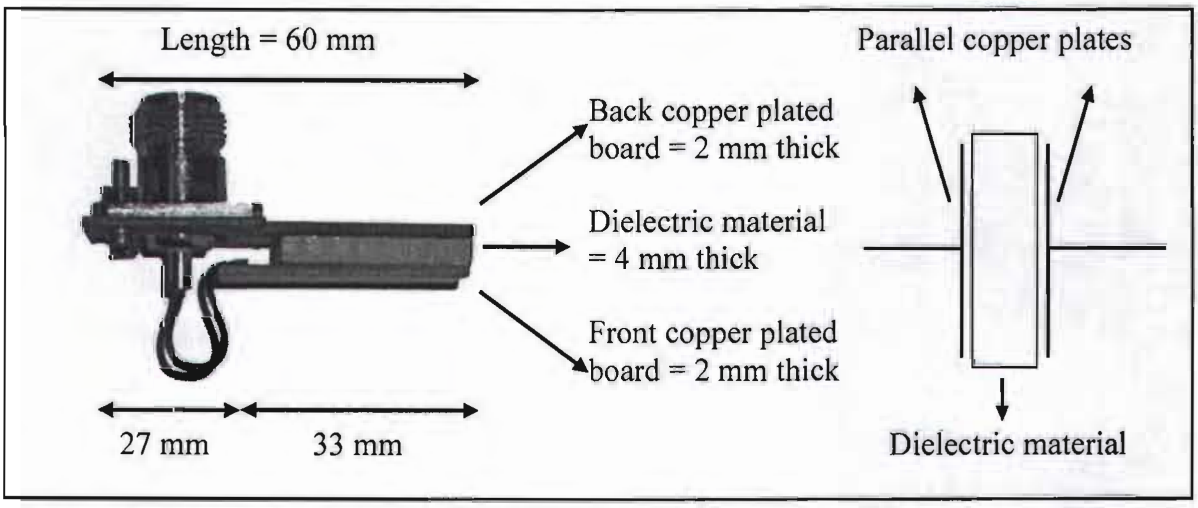

Figure 4.4: PPC showing the rock sample as the dielectric material

Levitskaya and Sternberg (2000) presented the following equation which provides an estimate of the limiting thickness dimensions for the sample to be measured with the PPC technique:

$$thickness < 0.038 \times \frac{\lambda}{\sqrt{\varepsilon'_r}} \quad \text{mm} \tag{4.10}$$

Where

λ ≡ wavelength of the specified frequency in millimetres (mm)

ε'_r ≡ relative dielectric permittivity

This equation suggests that high frequency measurements are easier on material samples with a low dielectric permittivity. Using a relative dielectric permittivity of 8 (Beleznai 2009) for a marble rock sample and a maximum frequency of 950 MHz yields a maximum sample thickness of:

$$thickness < 0.038 \times \frac{315.789}{\sqrt{8}}$$

$$thickness < 4.24 \quad \text{mm}$$

Cutting a sample of rock to a thickness of 4 mm is relatively easy and was done using a rock cutting disk (see Annexure 11). The rock sample acting as the dielectric material may be termed the device under test (DUT).

Hence, the PPC was chosen as the desired coupling device due to the following advantages:

- relatively easy to cut a rock sample into a rectangular shape;
- proliferation of copper plates to act as the disk electrodes;
- custom made jigs to hold the copper plates in place; and
- wide spread use of common connecters to couple the test equipment.

4.5 Constructing the parallel-plate capacitor

The PPC was constructed from single sided printed circuit board (PCB) material (thickness of 2 mm) with copper as the conducting material. The first PPC was built in

2005 and featured a rectangular holder with a BNC connector. This first prototype is shown in Figure 4.5.

The disadvantage of this first prototype was the constant soldering of the PCB when a new rock sample was to be inserted as the dielectric material. For this reason a new clamping jig was designed incorporating a novel wooden frame using a spring and 6 mm dowel. Wood adds no significant stray capacitance to the PPC, as it is a good electrical insulator (Winandy 1994). The spring presses the dielectric material sandwiched between two copper plates against a wooden frame. The conducting copper plates are connected to a BNC connector which facilitates connection to the RF test equipment. This second prototype of the coupling device incorporating a PPC is shown in Figure 4.6.

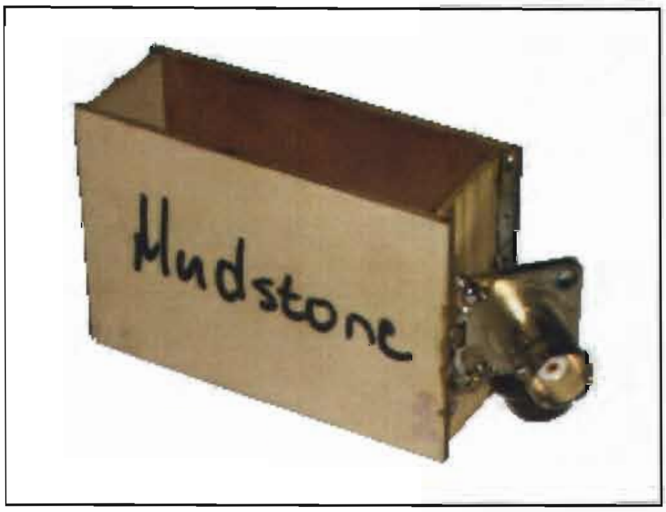

Figure 4.5: First prototype of the PPC with a BNC connector

However, the second prototype also had problems in that the singular spring did not exert sufficient pressure to keep the rock sample in the PPC. An additional BNC to N-Type adapter was further needed as the RF test equipment was fitted with only an N-Type female connector. These problems were resolved in a third prototype which featured an additional spring, wooden dowel and an N-Type female connector. The various parts comprising the novel wooden jig and PPC are depicted in Figure 4.7. In this prototype, the springs attached to the dowels are inserted into two six mm holes which are drilled horizontally between the outer side of the wooden clamp and the cut-out section. The small rectangular PCB with two self tapping screws ensures that the springs are held in position for optimal tension.

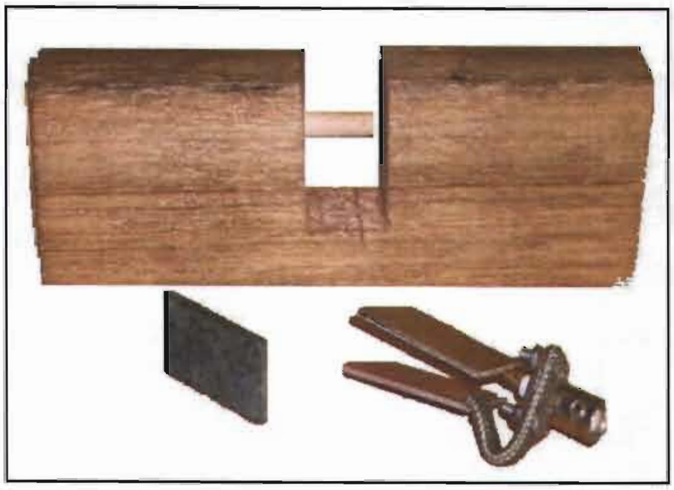

Figure 4.6: Second prototype of the PPC and novel wooden jig

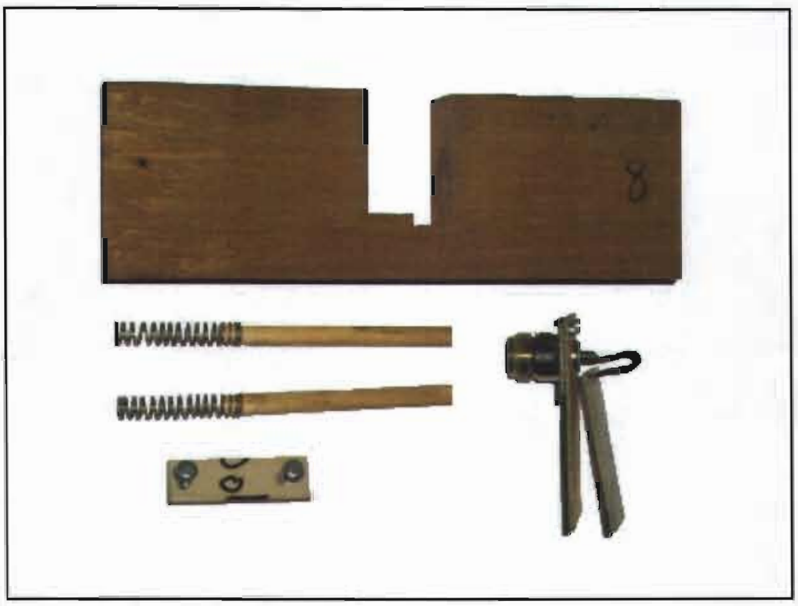

Figure 4.7: Third prototype of the novel wooden jig and PPC

Four different sized PPCs were constructed (see Annexure 12 for photographs) out of 2 mm thick plates coated with copper for the purpose of determining whether the resonating frequency of the sample is influenced by the rock's dimensions. The four sizes (length and width) of the front copper coated plate were:

- 87 x 47 mm referred to as PPC-1;
- 59 x 47 mm termed PPC-2;
- 28 x 47 mm labelled PPC-3; and
- 18 x 33 mm called PPC-4.

The size of the back plate was always 27 mm longer in length (see Figure 4.4) to accommodate the N-Type female connector. These PPCs were then used with corresponding rock sample sizes in two practical setups to determine the electrical properties of the dielectric materials.

4.6 RF measurements of dielectric materials

The electrical properties (impedance and phase angle) of the dielectric material (various rock samples in this research) were determined by using standard RF measuring equipment (vector voltmeter and network analyser) connected to the PPC by means of a coaxial cable. The description of the method used to obtain these measurements follows.

4.6.1 The practical setup of the experiment using the vector voltmeter

The vector voltmeter (HP 8505A used in this research) was used as the primary measuring device in the practical setup. However, the setup also required a power splitter and an external RF signal generator (SMY01) that could generate a range of required frequencies at a constant output level. Figure 4.8 presents the practical setup of the experiment using the vector voltmeter, RF signal generator and power splitter. The second port of the power splitter was connected to the DUT. The vector voltmeter measured the reaction or response of the DUT to the different frequencies generated by the RF signal generator, expressing the reaction as a magnitude ($|Z|$) and a phase angle (θ).

The vector voltmeter, with an input impedance of 50 Ω, was initially calibrated with a pure 50 Ω resistance to obtain a standard reference for all successive measurements. A

100 MHz 0 dBm output signal was generated by the RF signal generator (output impedance of 50 Ω). The output signal applied to the 50 Ω power splitter provided a stable reference signal at the A-input of the vector voltmeter. A pure 50 Ω resistance was then inserted as the DUT, coupled to the B-input of the vector voltmeter. The measuring instrument compared the two signals (A-input and B-input), providing a corresponding impedance and phase angle measurement. The calibration measurement was 50 Ω at 0°. A short circuit was then applied as the DUT with a corresponding calibration measurement of 0 Ω at 0° (Agilent Technologies 2003).

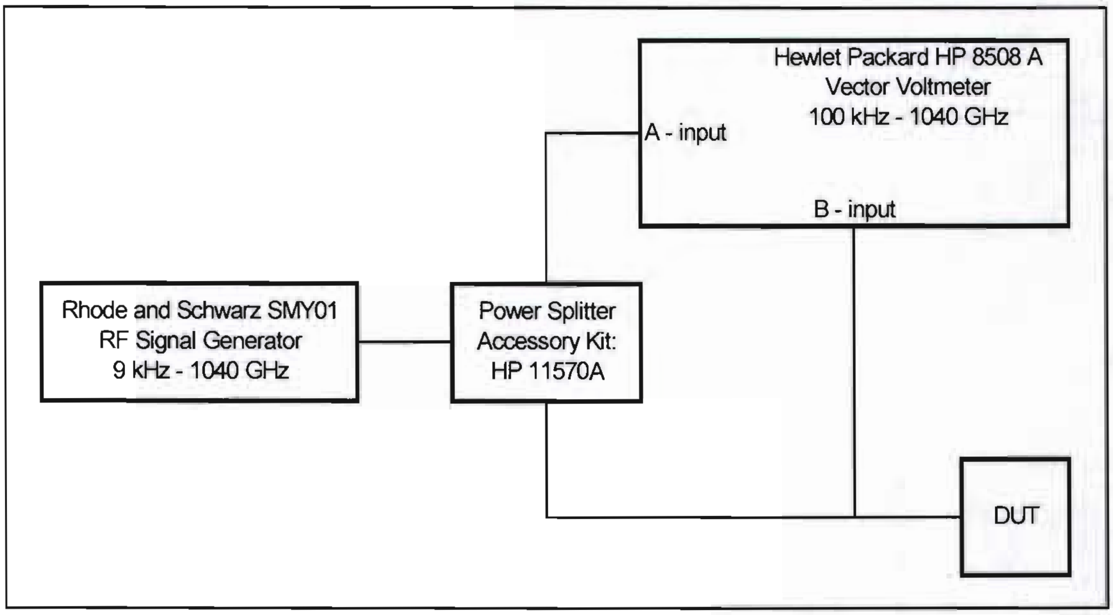

Figure 4.8: Practical setup of the experiment (Swart et al. 2009c)

Successive measurements at different radio-frequencies were taken once the equipment had been calibrated. The output frequency of the RF signal generator was initially set to 50 MHz, with a corresponding impedance and phase measurement being measured by the vector voltmeter. The output frequency of the RF signal generator was changed in 50 MHz steps from 50 MHz up to 950 MHz, with corresponding magnitude and phase measurements being recorded. These measurements where then tabulated and inserted into other equations (equations 4.1 through 4.5) to obtain the resistance, reactance, resistivity and conductivity of the rock samples at each specified frequency change (e.g. see Figure 4.9 for a graphical result of the resistance to frequency curve).

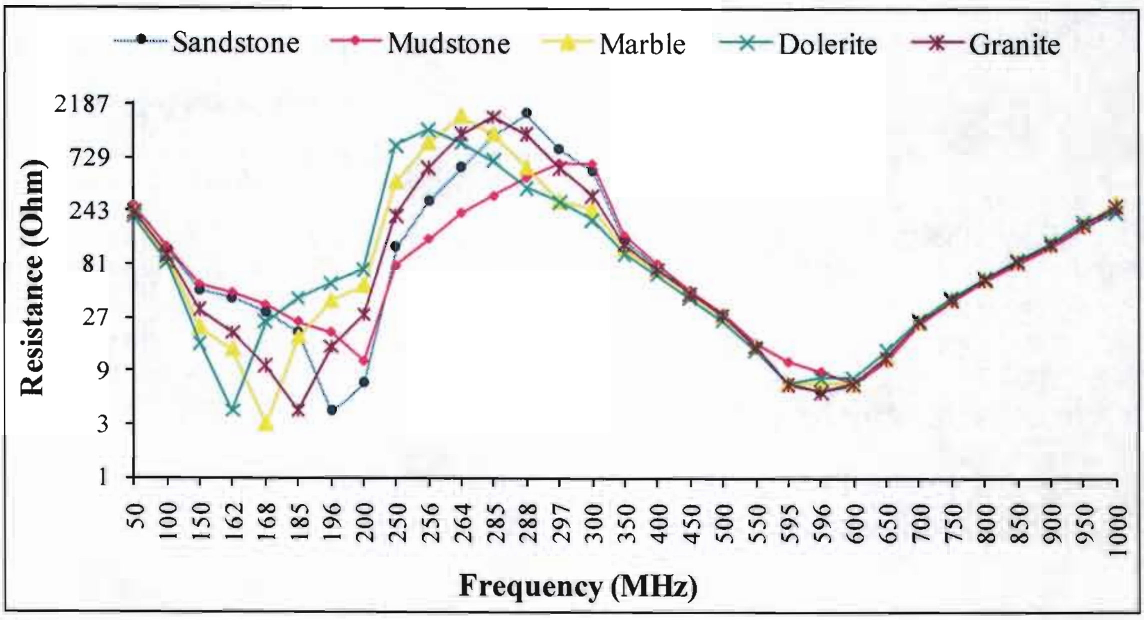

Figure 4.9: Resistance measurements for five different rock samples (57 x 41 x 18 mm) (Swart et al. 2005)

Initial measurements revealed three average resonating points for the different rock samples, at approximately 160, 320 and 600 MHz when using PPC-2 (59 x 47 mm). This method was then applied to measure the resonating frequencies of four different sized marble samples (JSB), two of which were painted with tin (tin powder mixed with an activator which the manufacturer may not disclose), using a small paint brush. This was done in an attempt to enhance the coupling between the rock's surface and the copper conducting plates. Tin exhibits excellent corrosion resistance and metal-like electrical conductivity (Yang and Northwood 2007), while having a low resistivity and interfacial thermal stability (Ding et al. 1988). It is not as expensive as silver or gold which do have better conductivities. Electrical measurements were obtained (shown in Figure 4.10) from four samples, two with a width of 18 mm and two with a width of 4 mm. The reason for using two different thicknesses was to illustrate the importance of the equation given by Levitskaya and Sternberg (2000), which indicates that the thickness of the sample should not exceed 4 mm for a frequency of 950 MHz. The following four marble samples were housed in the corresponding PPC with rectangular electrodes:

- sample (57 x 41 x 18 mm housed in PPC-2) with non-coated tin indicated by a square (□) in Figure 4.10;

- sample (57 x 41 x 18 mm housed in PPC-2) with coated tin denoted by a diamond (◊) in Figure 4.10;
- sample (35 x 19 x 4 mm housed in PPC-4) with non-coated tin denoted by a circle (○) in Figure 4.10; and
- sample (35 x 19 x 4 mm housed in PPC-4) with coated tin shown by a triangle (Δ) in Figure 4.10.

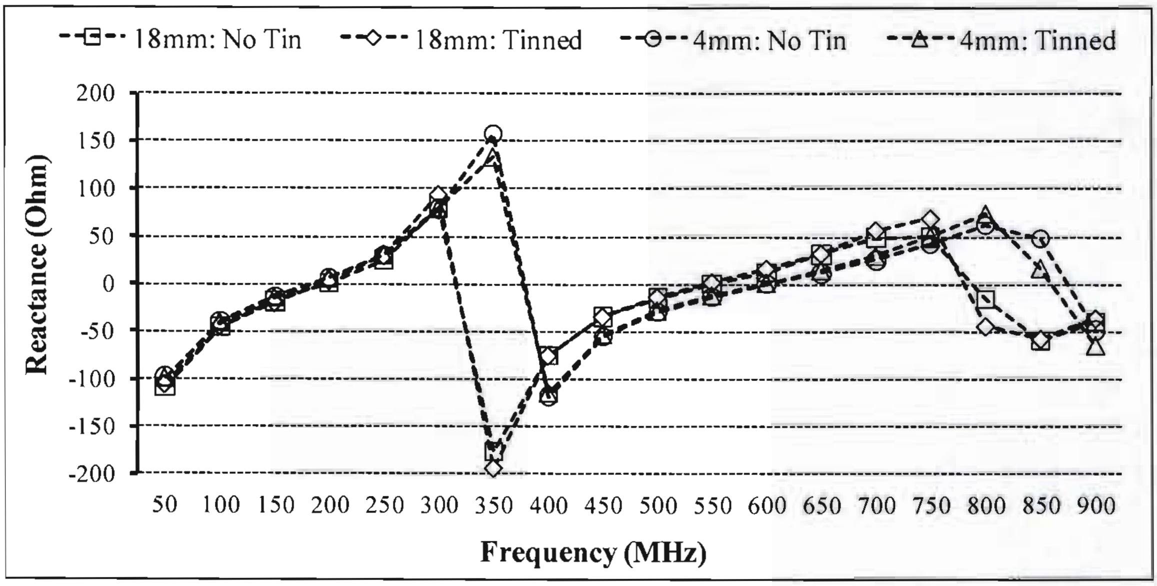

Figure 4.10: Reactance to frequency curve of four different sized marble samples (JSB)

It is noteworthy that the four curves follow the same pattern, with almost the exact same values between 50 and 300 MHz. The significant observable difference between the four samples from 300 MHz onward may well be related to the sample size, which should not exceed 4.24 mm in terms of the equation given by Levitskaya and Sternberg (2000). The results also reveal that the rock sample can be either a little smaller than the PPC (57 x 41 mm in 59 x 47 mm) or a little bigger than the PPC (35 x 19 mm in 33 x 18 mm) for frequencies below 300 MHz. The results of the tin-coated samples further reveal no significant differences below 300 MHz to the non-coated ones which suggest that tin does not really enhance the coupling between the copper conducting plates and the marble rock at frequencies lower than 300 MHz. The dielectric material (of no more than

4 mm in thickness) was subsequently used with no tin coating in subsequent measurements below 300 MHz (being the end of the VHF range).

This measurement procedure proved to be rather cumbersome and time consuming, since at each step the frequency had to be manually set on the RF signal generator, with corresponding measurements recorded. However, this procedure well illustrates the measurement process, where a magnitude ($|Z|$) and phase angle (θ) at different frequencies are obtained for a specific dielectric material. Similar measurements may be easier to obtain from a network analyser.

4.6.2 The practical setup of the experiment using a network analyser

The network analyser (HP 8752C used in this research) has the advantage of having an internal RF signal generator for measuring purposes and no power splitter or calibration resistances are required. The PPC may be connected directly to the reflection port on the network analyser via a 50 Ω coaxial cable with N-type connectors. This setup is shown in Figure 4.11.

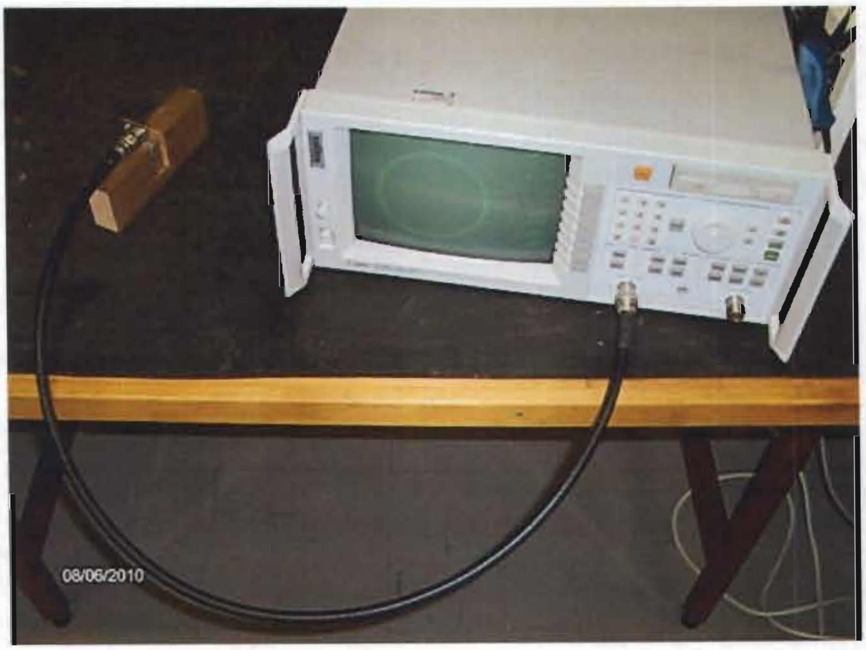

Figure 4.11: Practical setup of the experiment with a HP 8752C network analyser

The integration of the swept synthesized source, test set, and receiver, results in a network analyser that is easy to set up and use and that is ideal for service, incoming inspection, production and final test measurements (Agilent Technologies 2003). The integrated synthesized source provides a maximum port power level of +5 dBm with linear, logarithmic, list, power, and constant wave sweep types. The sensitive, tuned receivers provide 100 dB of dynamic range with two independent display channels available. Simultaneous measurements include reflection and transmission characteristics of the DUT on a crisp colour display. Data can be displayed in either linear or logarithmic magnitudes, standing wave ratios, phase, group delay, polar, real, or Smith chart formats.

The Smith chart format (see Figure 4.12) is especially useful in calculating circuit parameters such as Voltage Standing Wave Ratio (VSWR), reflection coefficient and return losses (Grebennikov 2005:112). This graphical measurement portrays the magnitude and phase in polar coordinates or a real and an imaginary part in XY coordinates (Hutchinson 2001:6.32). The horizontal axis is the pure resistance or zero reactance line (Frenzel 2003:576), where the resonating frequency points ($Xc = Xl$) of the DUT may be discerned. Points below the horizontal line indicates a capacitive reactance while points above the line are indicative of an inductive reactance (Orr 1997:21-14).

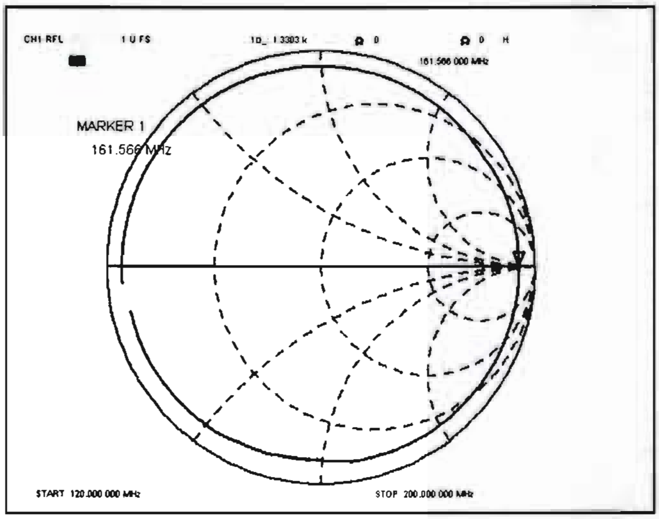

Figure 4.12: Smith chart display indicating the resonating frequency (161.566 MHz) of a rock sample within the PPC (Swart et al. 2009b)

The frequency range (shown on the bottom of the chart being 120 – 200 MHz) is kept purposively small to obtain a more detailed and accurate measurement. It is chosen in accord with the average resonating point of 160 MHz obtained from the vector voltmeter setup. The magnitude (|Z|) and phase angle (θ) of the DUT is shown in the top right hand corner of the display, with the marker frequency just below it. The 0 Ω and 0 H values indicate that no reactance components are present with only a pure resistance value of 1.33 kΩ at 161.566 MHz.

Two identical sized rock samples (30 x 19 x 4 mm) were inserted side by side into PPC-3 (28 x 47 mm front plate and 28 x 64 mm back plate), as shown in Figure 4.13.

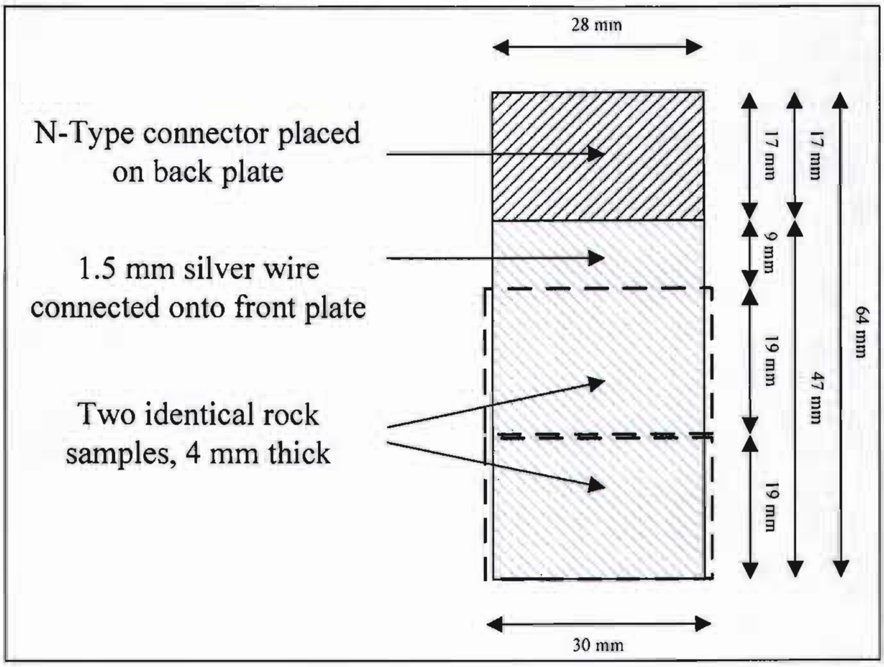

Figure 4.13: Two rock samples (with dimensions 30 x 19 x 4 mm) inserted side by side into PPC-3 (28 x 47 mm front plate)

This resulted in an overall dimension of 30 x 38 x 4 mm, with a 1 mm overlap on either side of the PPC. This was initially done to eliminate the possibility of fringing electric fields, which often results in the abrupt truncation of copper conducting strips at the open circuit (Sainati 1996:26). Moreover, the fringing electric fields store energy and act like a capacitor connected to the end of the copper strip, making the electrical line longer than its physical length. However, no significant resonating frequency variations were observed when this overlap was removed (i.e. the rock sample length was cut to the exact breadth of the PPC). This is portrayed in Table 4.1 where the maximum frequency deviation never exceeded 2%. On the other hand, significant resistance variations were observed for all the rock samples, with some deviating by up to 26% (JS4 sample). However, this resistance variation was not critical because the matching network (from Chapter 4) was designed to operate over a wide range of impedances. It may, therefore, be stated that fringing has no real effects on the frequency of operation in this type of PPC at frequencies within the VHF range. However, all rock samples were cut 2 mm wider than PPC-3 (1 mm overlap on either side) to easily facilitate the contact of K-Type thermocouples without the possibility of short circuiting the two conducting plates. The resonating frequencies obtained from the network analyser for these rock samples were presented at the New Generation University Conference held in Vanderbijlpark during 2009 (Swart et al. 2009a) and are shown in Table 4.1

Table 4.1: Ten untreated rock samples (30 x 38 x 4 mm) housed in PPC-3 (two sizes being 30 x 47 mm and 28 x 47 mm) and analysed with a spectrum analyser with respect to resonating frequencies

Sample code	Rock type	Untreated with 0 mm overlap		Untreated with 1 mm overlap		Frequency variation (Percentage)	Resistance variation (Percentage)
		Frequency (MHz)	Resistance (Ohm)	Frequency (MHz)	Resistance (Ohm)		
JSA	Dolerite	161.01	1101	160.14	1264	-0.5%	12.9%
JSB	Marble	159.78	1135	162.58	1325	1.7%	14.3%
JSC	Granite	165.11	1206	167.85	1545	1.6%	21.9%
JSD	Sandstone	168.99	1259	170.08	1169	0.6%	-7.7%
JSE	Mudstone	151.48	167	154.34	171	1.9%	2.3%
JS1	Marble	160.76	1388	162.61	1630	1.1%	14.8%
JS2	Marble	159.43	939	159.74	940	0.2%	0.1%
JS3	Marble	160.59	1761	162.30	2037	1.1%	13.5%
JS4	Granite	165.11	1340	165.14	1812	0.0%	26.0%
JS5	Marble	158.17	1573	160.43	1339	1.4%	-17.5%

Repeated measurements of a rock sample (Marble called JS5 – See Table 4.1) cut to two different sizes (corresponding to PPC-1 and PPC-3) were made to establish the reliability of the results. These repeated measurements (obtained on the 12th and 30th of June 2009) are shown in Figures 4.14 – 4.17 and indeed indicate repeatability of the resonating frequency measurements for each rock sample. Verification of the resonating frequencies for each rock sample was realized. Significantly, three experimental results reveal that the resonating frequency increases with decreasing sample size (from 145.576 MHz measured with PPC-1 (90 x 38 x 4 mm) to 158.576 MHz measured with PPC-3 (30 x 38 x 4 mm)). This is advantageous as it implies that the sample size may be manipulated to fit within the frequency range of commercially available RF amplifiers. For this reason PPC-3 (28 x 47 mm) and its rock sample size (30 x 38 x 4 mm) was selected for subsequent measurements because its resonating frequency (approximately 159 MHz) falls within the range of a commercially available RF amplifier (MIRAGE PAC30-130 with a frequency range of 154 – 174 MHz and a 130 W maximum output).

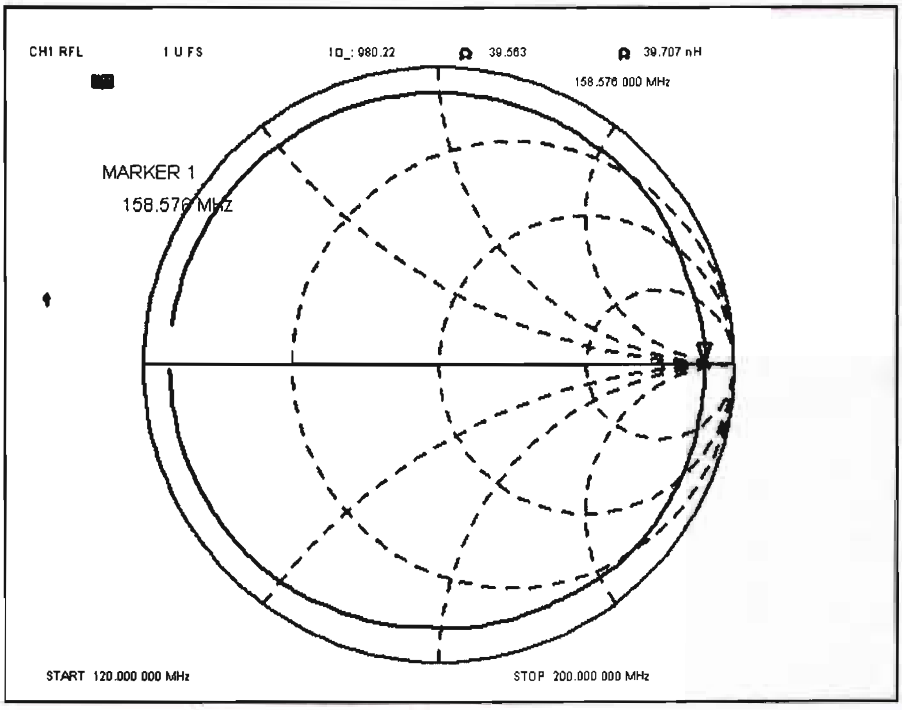

Figure 4.14: Smith chart result of a rock sample (JS5 with dimensions 30 x 38 x 4 mm) taken on the 12th of June 2009 in PPC-3 (28 x 47 mm)

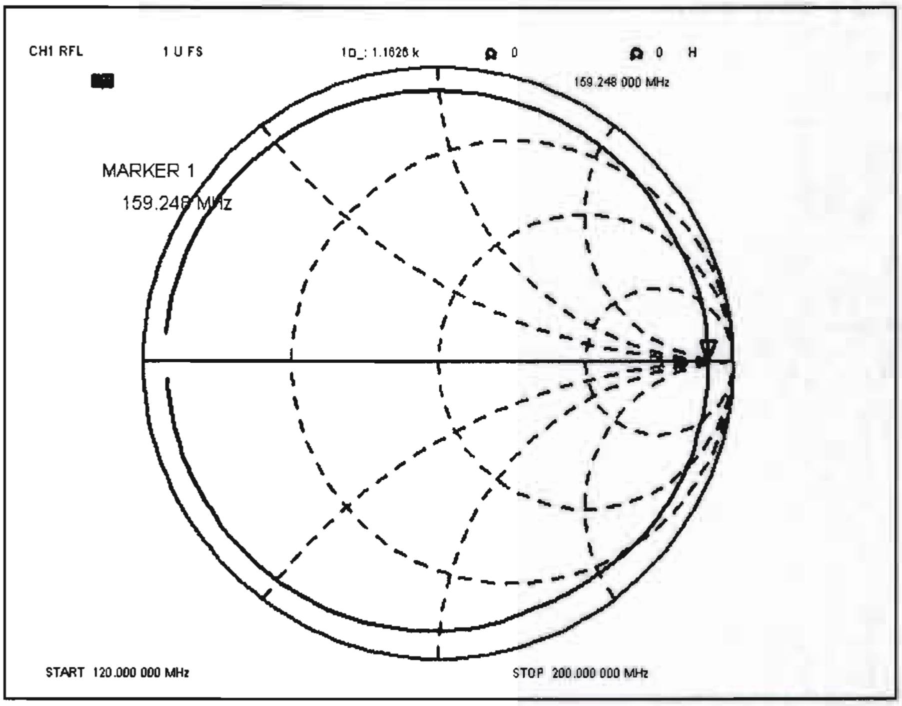

Figure 4.15: Smith chart result of a rock sample (JS5 with dimensions 30 x 38 x 4 mm) taken on the 30th of June 2009 in PPC-3 (28 x 47 mm)

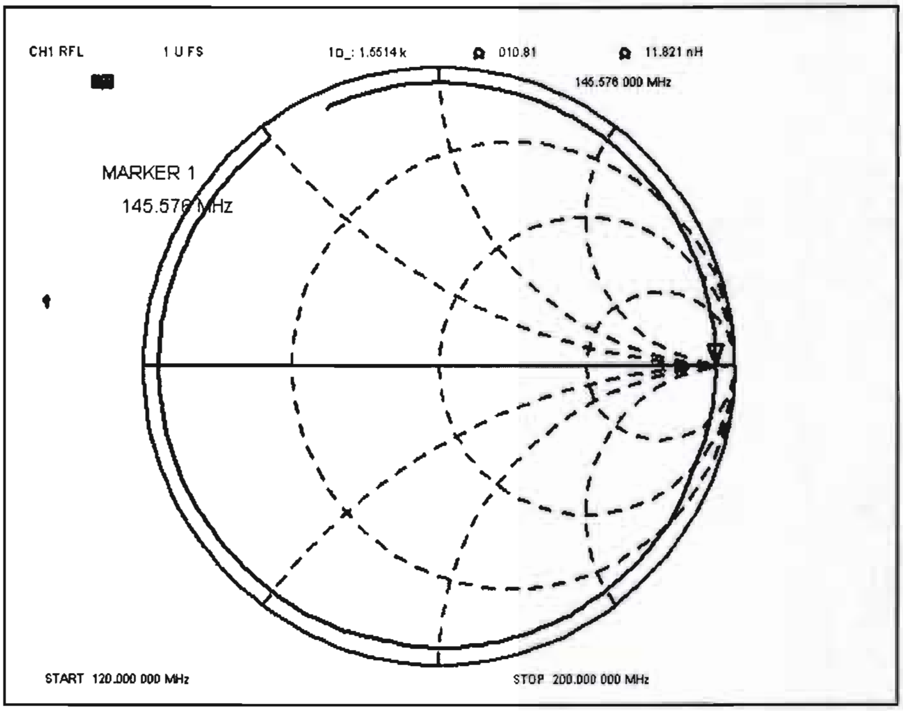

Figure 4.16: Smith chart result of a rock sample (JS5 with dimensions 90 x 38 x 4 mm) taken on the 12th of June 2009 in PPC-1 (87 x 47 mm)

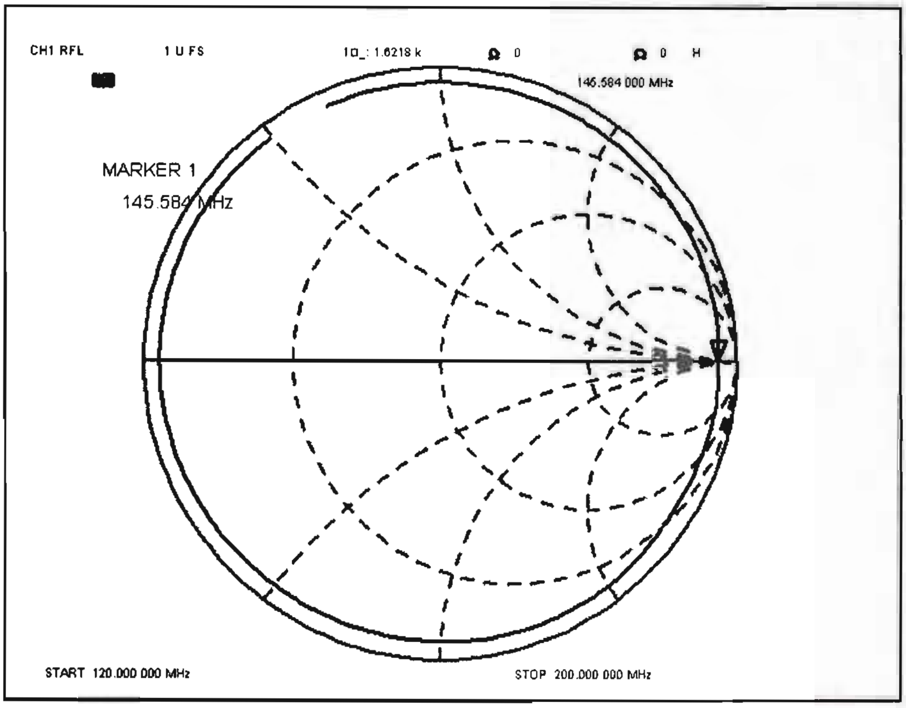

Figure 4.17: Smith chart result of a rock sample (JS5 with dimensions 90 x 38 x 4 mm) taken on the 30th of June 2009 in PPC-1 (87 x 47 mm)

In Figures 4.14 – 4.17, the marker shown on the display is on the resonance line, where *Xc* tends to cancel *Xl*. This point needs to be where the resonance line intersects the 50 Ω circle (second dotted circle from the left hand side in the middle of the display) to ensure that the maximum amount of power is transferred to the rock sample. This was achieved with the design and implementation of a passive matching network (presented in Chapter 5) using the Scattering coefficients obtained from the network analyser.

4.7 Practical results obtained from the network analyser

Scattering coefficient readings (termed the S-parameters and specifically S_{11}) were obtained for each sample (two identical rocks with dimensions 30 x 19 x 4 mm inserted side by side into PPC-3) using the wooden jig. In S-parameter theory an incident component is defined as that component which would exist if the port under consideration were conjugately matched to the normalized impedance at that port, which, in most cases, is 50 Ω (Z_o) (Abrie 1999:9). Two hundred and one samples of these S-parameters were obtained for each rock sample for the VHF range and were then converted into phase angles (Radians and Degrees), resistance (Ohm), resistivity (Ohm-meter) and conductivity (Siemens per meter) (conversion equations are shown in Annexure 23). The results for each untreated rock sample are shown in Annexures 1 – 10. Rock sample JSA was selected for the initial trial in sketching the frequency to phase angle graph as shown in Figure 4.18.

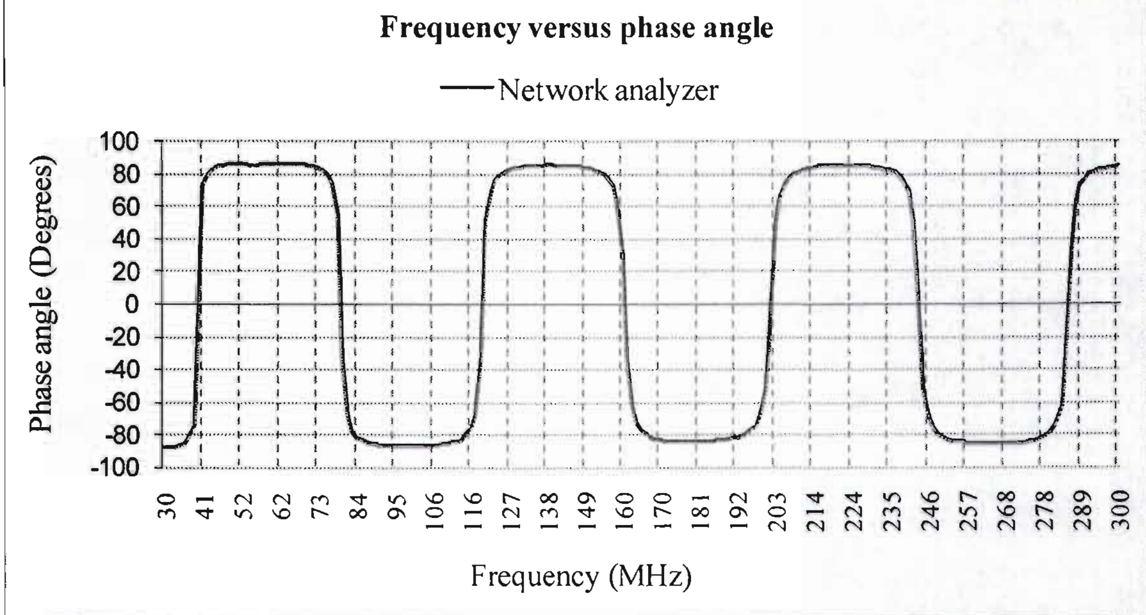

Figure 4.18: Frequency to phase angle of the JSA rock sample for the VHF range

Additional graphs including (a) frequency to resistivity and (b) frequency to conductivity curves are shown in Figure 4.19. These graphs may be reproduced for the other rock samples by using their respective S-parameters (given in Annexures 1 – 10) with the relevant conversion equations shown in Annexure 23. The frequency to phase angle graph (Figure 4.18) of the JSA rock sample depicts a square waveform. This waveform may be derived from a proven scientific equation which was used in the mathematical modelling of the frequency to phase angle graph of the rock samples, and is presented in the next section.

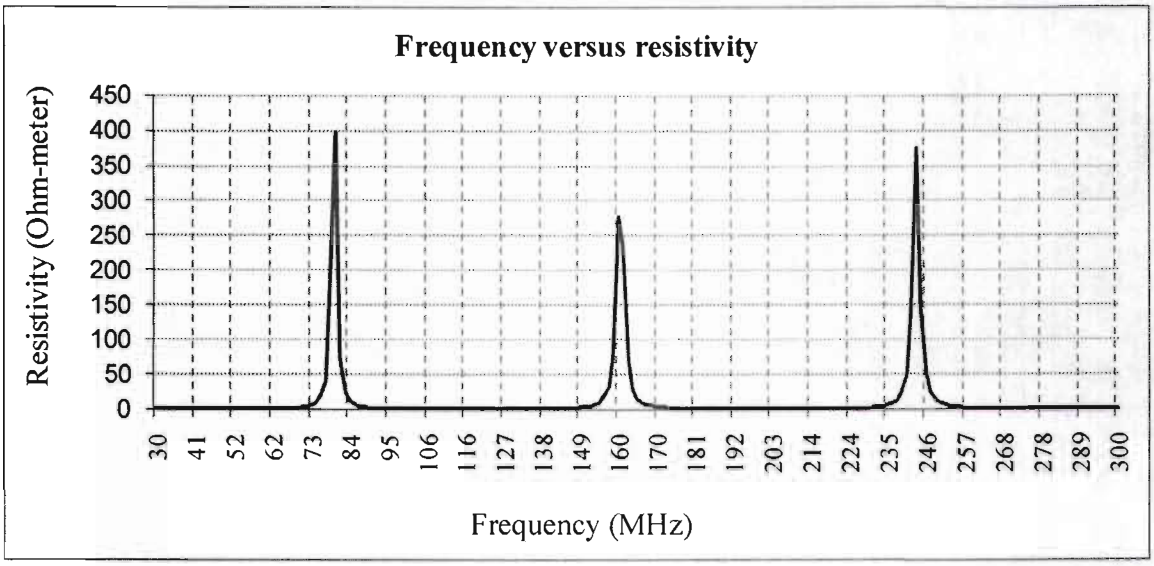

(a)

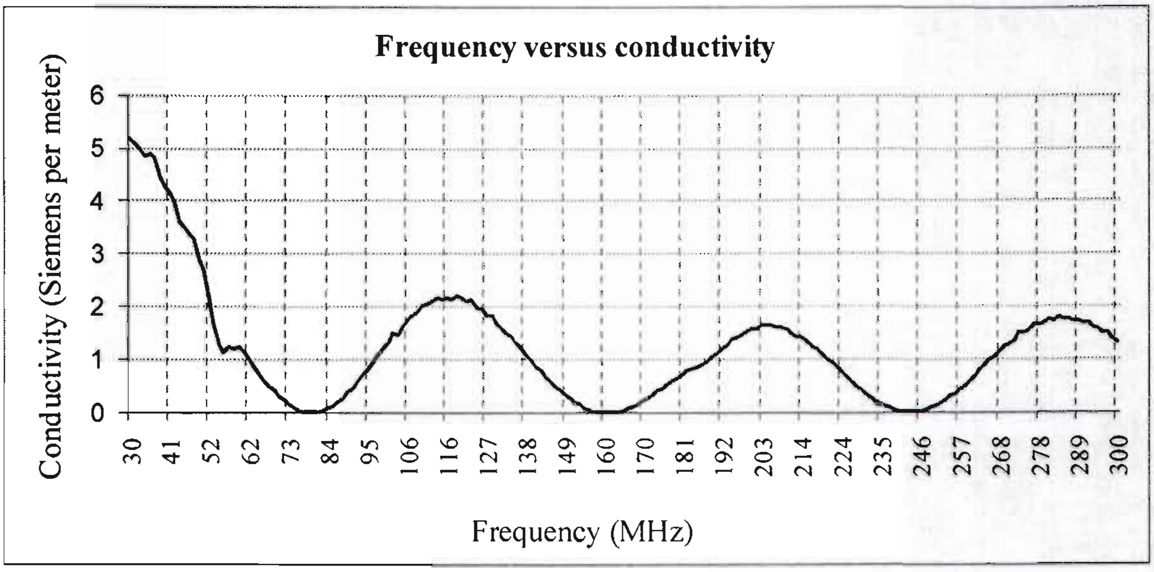

(b)

Figure 4.19: Frequency to resistivity (a) and frequency to conductivity (b) of the JSA rock sample for the VHF range

4.8 Mathematical modelling of the frequency to phase angle equation for the rock samples

A Fourier Frequency Transform (FFT) equation was used as the basis for deriving the mathematical equation for the resonating frequency of rock sample JSA. This modified equation can be used to predict the phase angle of the rock sample at specified frequencies. The original FFT equation is (Young 2004:90; Amidror and Hersch 2009):

$$v(t) = \frac{2 \times A}{\pi} \times \cos(2 \times \pi \times f_o \times t) - \frac{2 \times A}{\pi} \times \cos(2 \times \pi \times 3 \times f_o \times t)... \quad (4.11)$$

Where

A ≡ the amplitude of the signal in Voltage (V)

f_o ≡ the frequency of the waveform in Hertz (Hz)

t ≡ time in seconds (s)

Equation 4.11 may be modified to the following:

$$\phi = \sum_{n=1}^{\infty} [A \times \frac{\sin(n \times \frac{\pi}{2})}{n \times \frac{\pi}{2}}] \times \cos(2 \times \pi \times n \times f_o \times t) \quad (4.12)$$

Where

n ≡ the number of samples

Equation 4.12 was adapted by changing the amplitude (A = 172) of the waveform to represent a +90 to -90 degrees phase shift. The frequency of the waveform was also adjusted (f_o = 0.012278) to coincide with the original waveform obtained from the network analyser. Values for t (30 – 300) were stipulated in terms of the VHF range of frequencies and were advanced by a factor of 22.782 to coincide with the first resonating point at 39.45 MHz. This produces the following equation which was used in MATHCAD to obtain the phase angle calculations for a given frequency:

$$\phi = \sum_{n=1}^{201} [172 \times \frac{\sin(n \times \frac{\pi}{2})}{n \times \frac{\pi}{2}}] \times \cos(2 \times \pi \times n \times 0.012278 \times (f + 22.782)) \quad (4.13)$$

Where

f ≡ must be the frequency of the waveform in MHz

The waveform derived from equation 4.13 is plotted in Figure 4.20, where the original waveform (shown in a solid blue line obtained from the network analyser) is contrasted to the predicted algorithm waveform (black dotted line obtained from the mathematical equation in MATHCAD). Very little difference can be perceived between these two waveforms with the maximum percentage error at the high-frequency side of the waveform being approximately 1%. This technique was used on the other rock samples to obtain their individual mathematical equations for resonance. These results are shown in Annexure 13 and may be used to calculate the exact phase angle of the specified rock sample at a given frequency. The resonating frequency of rock sample JSA was initially used in the design of a passive matching network presented in Chapter 5.

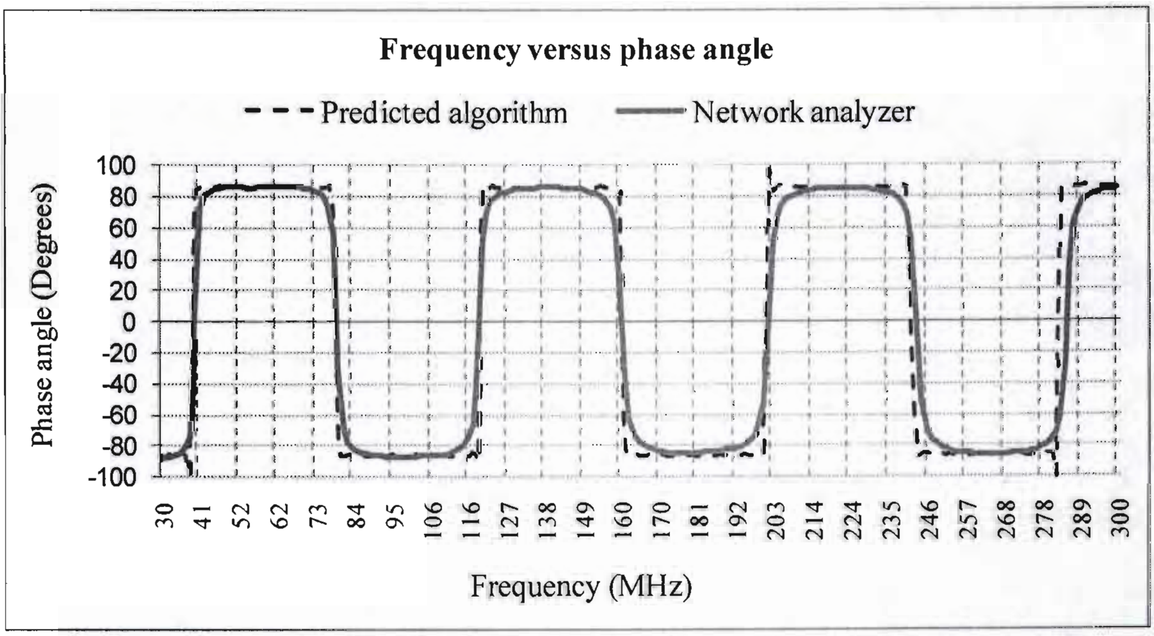

Figure 4.20: Frequency to phase angle waveform of the JSA rock sample obtained from the mathematical equation and network analyser

4.9 Summary

Chapter 4 introduced the various RF electrical properties associated with dielectric materials. The cylindrical and parallel-plate capacitor were introduced as possible coupling techniques which could be used to connect dielectric materials, such as rock samples, to appropriate measuring equipment, such as the network analyser. The PPC technique was chosen due to its simplicity and ease of connection. The vector voltmeter and network analyser were introduced as possible test equipment in determining the electrical properties of dielectric materials. The network analyser was chosen as the preferred test instrument due to its ease of operation. PPC-3 (with dimensions 28 x 47 mm) was used in subsequent measurements with a network analyser to determine various electrical properties associated with the ten specific rock samples. These properties were then used in the mathematical modelling of the phase angle to frequency equation for each rock sample.

The design and analysis of a matching network to ensure maximum power transfer (MPT) between the RF amplifier and the rock sample will be presented in Chapter 5.

Chapter 5 Matching network design and relevant results

5.1 Introduction

Chapter 4 introduced the PPC as the preferred technique in coupling the rock samples to the electrical equipment. However, initial results from the network analyser revealed that the impedance of the rock samples (considered as the load reflection coefficient - Γ_L) varied from 171 + jX Ω to around 2037 + jX Ω at resonance. This impedance cannot be directly connected to the output of a RF amplifier which has an output impedance of 50 Ω (source reflection coefficient - Γ_S). This large mismatch will result in a high percentage of the forward power (power coming from the source) being reflected back (from the load) towards the transmitter and thereby damaging it (Frenzel 2001:230). Preventing this mismatch necessitates the use of a matching network as shown in Figure 5.1, which illustrates the S-parameters of a two-port network as well as various impedances at different points in the system. Normalised impedances to 50 Ω are also shown and are characterized by the term NORM. The aim of this network is to make the load resistance appear to be connected to its same value, when in fact it is connected to a power source of 50 Ω.

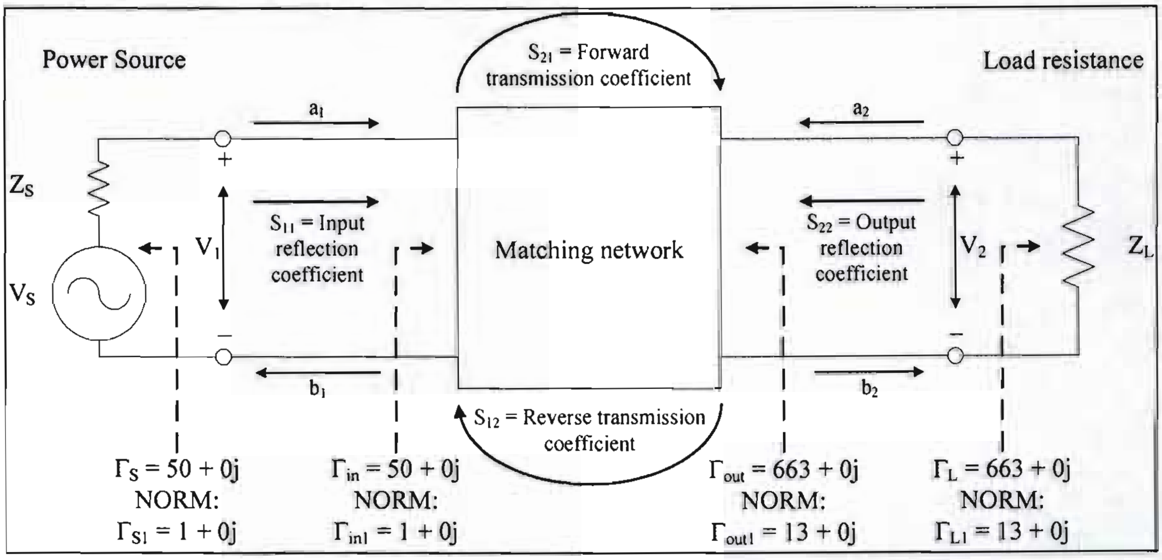

Figure 5.1: Reflection coefficients of a matching configuration

Impedance matching is often necessary in the design of RF circuitry to provide the maximum possible transfer of power between a source and its load (Bowick et al. 2008:63). RF power amplifiers (being the source) consist of an active device, biasing network, input and output reactive filtering and impedance matching networks. These networks are effectively band pass filters offering the required impedance transformation. The input circuit usually provides impedance matching to achieve low return loss and good power transfer. The output network is usually the load network and effectively provides a load to the active device which is chosen to obtain the required operating conditions such as gain, efficiency and stability (Everard 2001:248). Subsequently, maximum power transfer (MPT) is possible between the source and the load (which is the rock sample acting as a dielectric material in PPC-3 for this research).

This chapter will first review three possible inductor capacitor (LC) matching configurations which may be used to provide MPT between a load and its source, followed by the design of the selected matching network by scientific method and computer software (Multimatch). An analysis of this matching network is presented by means of simulation (software model constructed in SIMetrix) and practical models (physical circuit built and tested using a network analyser and practical experiment). A unique value for the coupling coefficient with respect to the transfer of RF power to the dielectric material inside the PPC is substantiated. Experimental results regarding surface temperature rise of the rock samples (housed in PPC-3) treated with RF power are also shown.

5.2 Selecting the appropriate matching network

Three main types of L-C based configurations exist, which may be used to match the output impedance of a transmitter to the input impedance of a transmission line or electronic circuit:

- L network
- T network; and
- Pi network;

The simplest and most widely used matching circuit is the L network (Bowick et al. 2008:64). The component orientation resembles the shape of the letter L as can be seen by the two examples shown below in Figure 5.2.

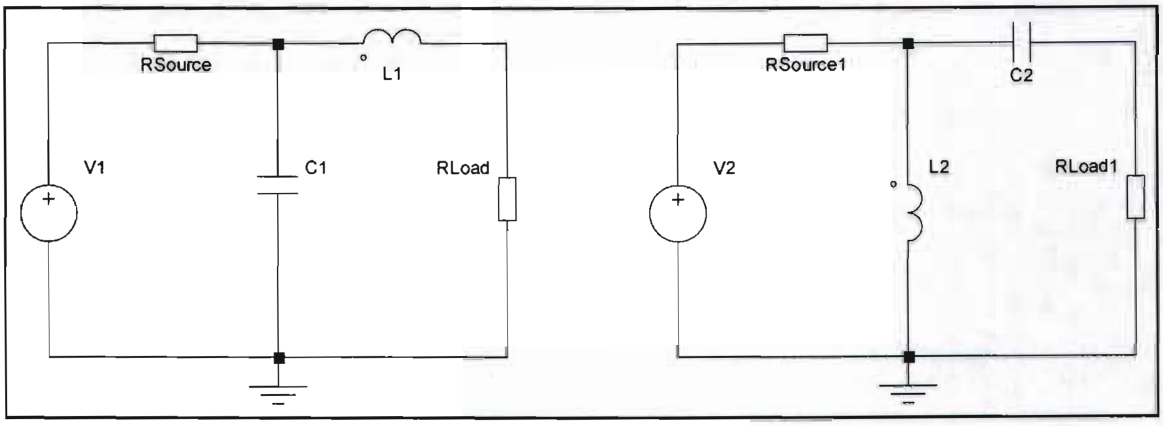

Figure 5.2: High pass and low pass filter based on the L network

L networks provide very little control over the figure of merit (called the Q of a resonating circuit (Carr 2002:278)) and are, therefore, inflexible with regard to selectivity (Frenzel 2003:129). RF transmitters are designed to operate over a narrow range of frequencies which must be confined to the operating frequency of the matching network. L networks tend to cover large frequency ranges and are really not suitable as matching networks where narrow frequency ranges are required. Matching circuits incorporating three elements (such as the Pi and T networks) are generally used to overcome this problem.

The T network (shown in Figure 5.3) matches the load and source to a virtual resistance that is larger than either the load or source resistance (Bowick et al. 2008:69). The T network is the most popular matching circuit (Orr 1997:129) and is often used to match two low-valued impedances when a high-Q arrangement is required (Bowick et al. 2008:69). However, the Pi network is very useful where the source impedance (R1) is greater than the load impedance (R2) or visa versa (Carr 2002:290). It is necessary to set the Q of the network (usually between 5 and 20) to a value greater than:

$$Q > \sqrt{\frac{R1}{R2} - 1} \tag{5.1}$$

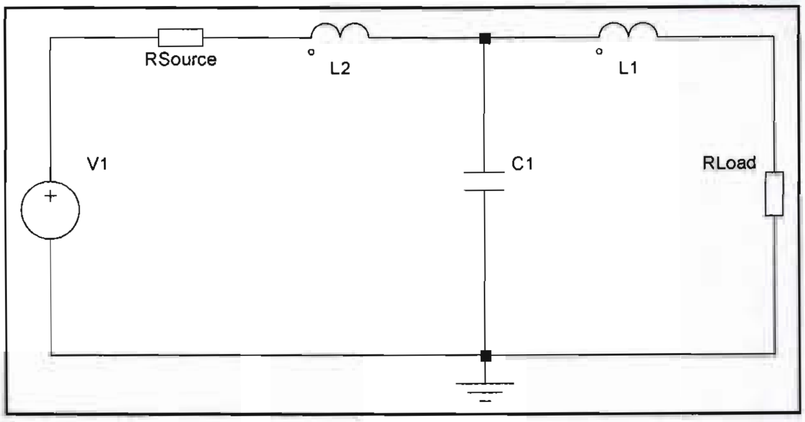

Figure 5.3: T network comprising two L networks

Pi networks offer greater harmonic attenuation than L networks and may be used to match a relatively wide range of impedances (Orr 1997:14-18). The advantage of easily fine-tuning any matching network is very desirable according to Grebennikov (2005:112) and is accomplished through the use of variable capacitors in the shunt branches of the network (Hickman 2007:148). The Pi network may be seen as two L networks placed back to back to match the load and source to an invisible or virtual resistance (R) located at the junction between the two networks (Bowick et al. 2008:68). Figure 5.4 illustrates a Pi network incorporating three reactive elements (two parallel capacitors and one series inductor).

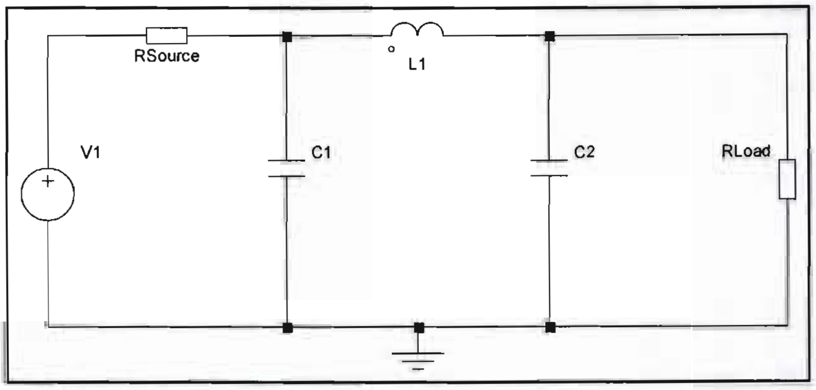

Figure 5.4: Pi network comprising two L networks placed back to back

The Pi network was chosen for this research because it can match a large range of impedances (made possible by the parallel variable capacitors) and because it possesses only one series component (the inductor). It can further match larger impedances to smaller impedances, which is necessary in this research where the RF amplifier has an output impedance of 50 Ω while the rock's input impedance varies between 453 Ω and 2226 Ω.

5.3 The design of a Pi matching network

A Pi network was designed based upon two scientific methods; mathematical equations and a computer software program called Multimatch μlite from AMPSA (2009). The results of these two designs are compared below in this section.

The parameters of the dolerite sample (JSA) were used as the trial in this design as its resonating frequency (160.14 MHz at 1264 Ω derived from the S-parameters shown in Annexure 1 using interpolation) falls in the middle of the frequency range of the RF source (150 – 174 MHz).

Assuming the Q of the circuit to be 10, the load resistance (R_{Load}) 1264 Ω and the source impedance (R_{Source}) 50 Ω, the virtual resistance can be calculated as follows (Bowick et al. 2008:70):

$$R = \frac{R_{Load}}{Q^2 + 1} \qquad (5.2)$$

$$R = \frac{1264}{10^2 + 1}$$

$$R = 12.515\ \Omega$$

The parallel output reactance ($Xp2$) is next calculated:

$$Xp2 = \frac{R_{Load}}{Q} \tag{5.3}$$

$$Xp2 = \frac{1264}{10}$$

$$Xp2 = 126.4\ \Omega$$

The second series reactance ($Xs2$) is calculated to be:

$$Xs2 = Q \times R \tag{5.4}$$

$$Xs2 = 10 \times 12.515$$

$$Xs2 = 125.149\ \Omega$$

The Q for the other L network is now defined by the ratio of R_{Source} to R using equation 5.1:

$$Q1 = \sqrt{\frac{50}{12.515} - 1}$$

$$Q1 = 1.731$$

The parallel input reactance ($Xp1$) can now be calculated using equation 5.3:

$$Xp1 = \frac{R_{Source}}{Q1}$$

$$Xp1 = \frac{50}{1.731}$$

$$Xp1 = 28.89\ \Omega$$

Similarly $Xs1$ (first series reactance) may be calculated using equation 5.4:

$$Xs1 = Q1 \times R$$

$$Xs1 = 1.731 \times 12.515$$

$Xs1 = 21.659\ \Omega$

The two L networks which are connected back to back to form the Pi network are shown in Figure 5.5 with all the calculated parameters.

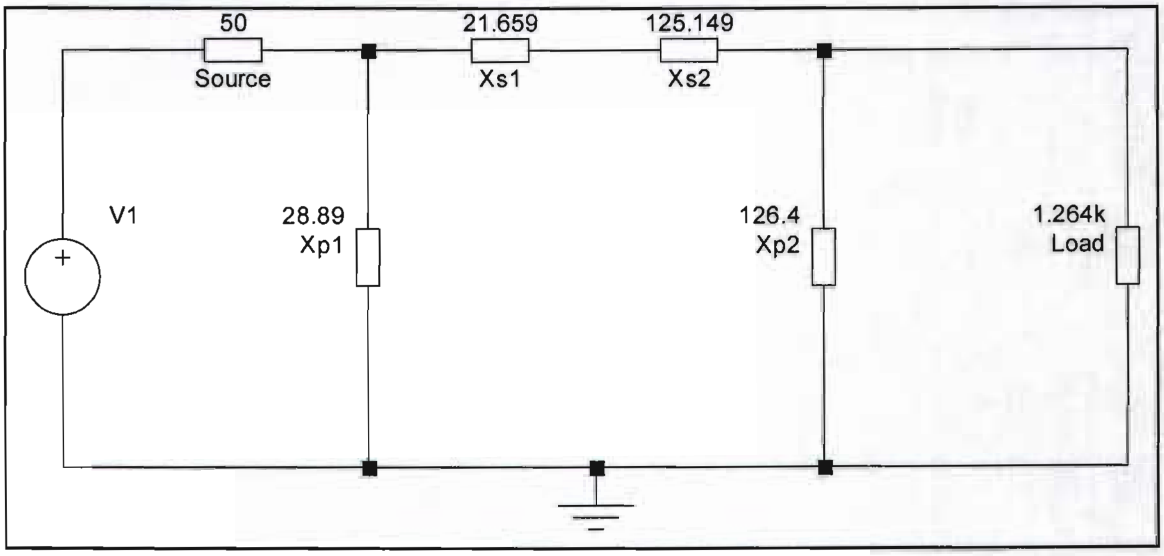

Figure 5.5: Mathematical design of the Pi matching network

The required input ($C1$) and output ($C2$) capacitance can subsequently be calculated using equation 4.1 from Chapter 4 substituting $Xp1$ and $Xp2$ for Xc:

$$Xc = \frac{1}{2 \times \pi \times f \times C}$$

$$C = \frac{1}{2 \times \pi \times f \times Xc}$$

$$C1 = \frac{1}{2 \times \pi \times 160.14 \times 10^6 \times 28.89}$$

$$C1 = 34.4\ \text{pF}$$

$$C2 = \frac{1}{2 \times \pi \times 160.14 \times 10^6 \times 126.4}$$

$$C2 = 7.86\ \text{pF}$$

Next, the required series inductance is calculated using equation 4.2 from Chapter 4 substituting the sum of $Xs1$ and $Xs2$ for Xl:

$$Xl = 2\times\pi\times f\times L$$

$$L = \frac{Xl}{2\times\pi\times fo}$$

$$L1 = \frac{21.659+125.149}{2\times\pi\times160.14\times10^6}$$

$$L1 = 145 \text{ nH}$$

The final matching circuit with all parameters is shown in Figure 5.6. These results can now be compared to the results obtained from the Multimatch computer software program.

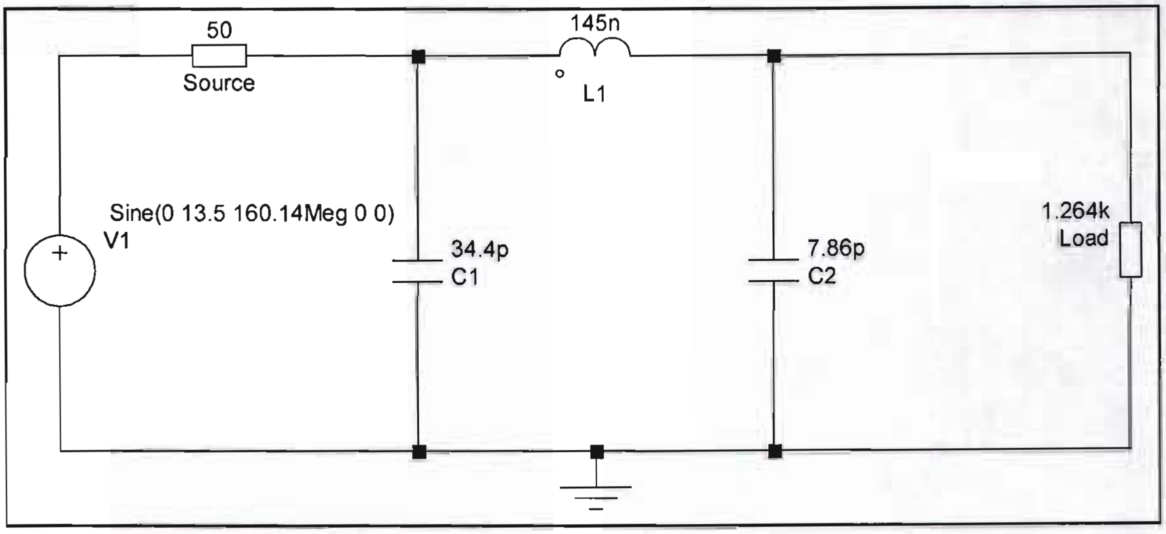

Figure 5.6: Final matching circuit based on the Pi network

The Multimatch µlite impedance matching program facilitates the design of high quality matching networks up to microstrip level (AMPSA 2009). The program requires a number of data inputs as illustrated in Figure 5.7. A number of frequencies from 159.6 – 160.95 MHz were entered along with the source (50 Ω) and load impedances (interpolated from the S-parameters shown in Annexure 1) for the JSA rock sample. The topology of the circuit was set to a low pass filter ("L" selected in the program) with the first element counted from the load side being a shunt element ("P" selected in the program). The final design from the Multimatch software package is shown in Figure 5.8 where the final Q value was calculated to be 10.07. A comparison of the mathematical and software program results (Figures 5.6 and 5.8) yields no significant differences.

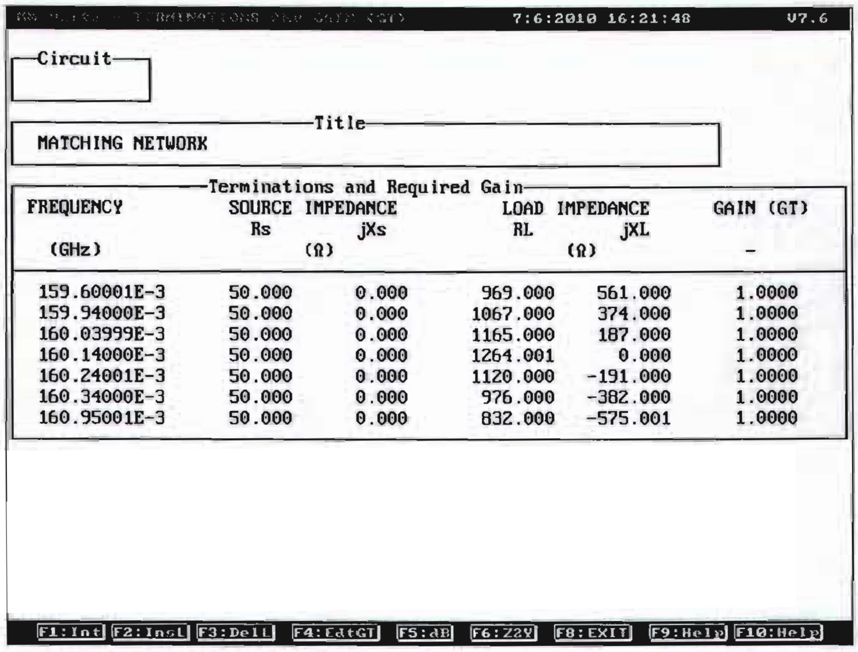

FREQUENCY (GHz)	SOURCE IMPEDANCE Rs (Ω)	jXs	LOAD IMPEDANCE RL (Ω)	jXL	GAIN (GT) -
159.60001E-3	50.000	0.000	969.000	561.000	1.0000
159.94000E-3	50.000	0.000	1067.000	374.000	1.0000
160.03999E-3	50.000	0.000	1165.000	187.000	1.0000
160.14000E-3	50.000	0.000	1264.001	0.000	1.0000
160.24001E-3	50.000	0.000	1120.000	-191.000	1.0000
160.34000E-3	50.000	0.000	976.000	-382.000	1.0000
160.95001E-3	50.000	0.000	832.000	-575.001	1.0000

Figure 5.7: Input data parameters for the matching network programme

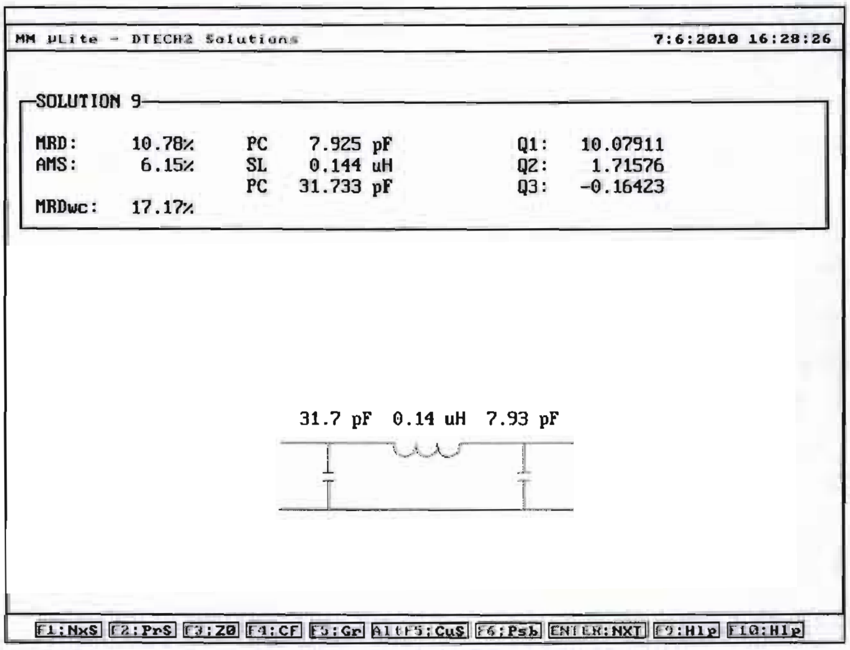

Figure 5.8: Pi network designed in the Multimatch µlite software program

5.4 Pi matching network construction

Mechanical plate trimmer capacitors (5-100 pf) were used and the inductor was constructed from silver wire (silver solder). Silver has a lower resistivity (1.624×10^{-8} Ω-cm) than that of copper (1.728×10^{-8} Ω-cm) at 20 °C and is therefore a better conductor with less attenuation (Rouse 1962:12; Hutchinson 2001:5.2). Hence, it will not heat up as quickly as copper will, which could weaken the soldering joints. Pozar (2005:687) substantiates this claim by noting that the conductivity of silver (6.173×10^7 S/m at 20 °C) is higher than that of copper (5.813×10^7 S/m at 20 °C). Consequently, the inductor will have a lower power dissipation, which increases with frequency due to skin effect. Practically all the current will flow in a very thin layer near the conductors surface, thereby resulting in a higher RF resistance than at direct current (DC) (Hutchinson 2001:10.12). The depth of current (χ) flow is a function of frequency and is determined from the following equation adapted from Whitaker (2002:12-2):

$$\chi = \frac{6.562 \times 10^{-5}}{\sqrt{\mu \times f}} \quad \text{mm} \qquad (5.5)$$

Where

f ≡ frequency in MHz

μ ≡ permeability of the material (copper equal to 1)

Thus if the operating frequency is 160 MHz, then the skin depth in a copper conductor will be:

$$\chi = \frac{6.562 \times 10^{-5}}{\sqrt{1 \times 160}}$$

$$\chi = 5.188 \ \mu\text{m}$$

This means that current will travel in only the top 5.188 μm of the copper conductor, thereby significantly increasing its series impedance at RF. Consider further how the resistance of a 1.5 mm copper wire is affected in this regard. A rough estimate of the cut-off frequency where a non-ferrous wire will begin to show skin effect can be calculated with the following equation adapted from Hutchinson (2001:10.12):

$$f = \frac{124}{(\frac{d}{0.0254})^2} \qquad \text{MHz} \qquad (5.6)$$

Where

d ≡ diameter of the conductor in mm

f ≡ cut-off frequency in MHz

Therefore if the diameter of a copper conductor is 1.5 mm then:

$$f = \frac{124}{(\frac{1.5}{0.0254})^2}$$

$$f = 0.036 \text{ MHz}$$

The resistance of the 1.5 mm copper wire will increase significantly above this frequency (Hutchinson 2001:10-12). The following equation may be used to calculate the new resistance (*Rac*) of a 1 m copper wire (1.5 mm diameter) at 160 MHz (Abrie 1999:102):

$$Rac = [\frac{r}{2 \times \delta}] \times Rdc \qquad \Omega/\text{mm} \qquad (5.7)$$

Where

r ≡ radius of the conductor in mm

Rdc ≡ wire resistance at DC in Ω/mm

Calculation of the wire resistance per unit length (mm) at DC when considering the resistivity of copper can be done using equation 4.4 from Chapter 3:

$$\rho = \frac{R \times A}{l} \ \Omega\text{m}$$

$$R = \frac{l \times \rho}{A} \ \Omega$$

$$R = \frac{100 \times 1.728 \times 10^{-8}}{\pi \times 0.075^2}$$

$$R = 9.778 \times 10^{-6} \ \Omega/\text{mm}$$

Substituting *Rdc* with *R* in equation 5.7 yields the following:

$$Rac = [\frac{0.75}{2 \times 5.188 \times 10^{-6} \times 1000}] \times 9.778 \times 10^{-6}$$

$$Rac = 0.0007068 \ \Omega/\text{mm}$$

This shows that the resistance for both copper and silver is appreciatively higher at 160 MHz than it is at DC (shown in Table 5.1). However, silver still remains the ideal choice due to its lower resistance. For this reason the inductor was constructed from a 1.5 mm silver solder rod using the following design equation adapted from Hutchinson (2001:6.22):

$$L = \frac{(D \times 0.039)^2 \times N^2}{(0.702 \times D) + (1.56 \times l)} \quad \mu\text{H} \qquad (5.8)$$

Where

D ≡ coil outer diameter in mm

l ≡ coil length in mm

N ≡ number of turns

For an outer coil diameter of 7.5 mm, a coil length of 20 mm and 7.75 turns, equation 5.8 returns:

$$L = \frac{(7.75 \times 0.039)^2 \times 7.5^2}{(0.702 \times 7.5) + (1.56 \times 20)}$$

$$L = 141 \text{ nH}$$

Table 5.1: Resistances of 1.5 mm diameter copper and silver at DC and 160 MHz

Conductor	DC resistance per meter	160 MHz resistance per meter
Copper	0.00977 Ω/m	0.70685 Ω/m
Silver	0.00919 Ω/m	0.66431 Ω/m

This result was verified with an online single-layer air-core inductor design program by Meserve (2009). The verified results are shown in Table 5.2 and are almost identical to the calculated result shown above. A 4.5 mm drill bit was used as the form diameter and the coil length was marked off with a mathematical ruler. Figure 5.9 illustrates the completed inductor.

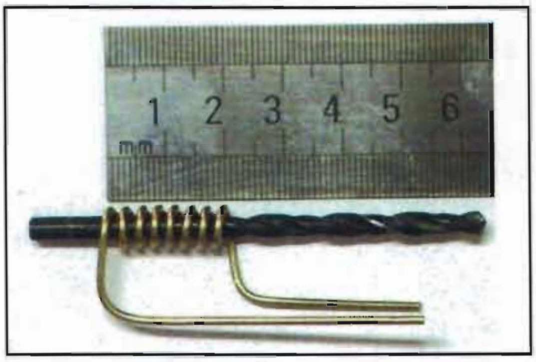

Figure 5.9: 141 nH inductor constructed from 1.5 mm silver wire

Table 5.2: Inductor specifications obtained from an online design (Meserve 2009)

Design Details for a 0.141 uH Coil	Initial Calculations
Number of Turns	7.75
Wire Size	1.5 mm
Wire Type	Insulated Wire
Form Diameter	4.5 mm
Coil Length	20.0 mm

5.5 Simulation model of the matching network

SIMetrix, a simulation package available from SIMetrix Technologies Ltd (2009), was used to simulate the efficiency of the matching network. Figure 5.10 illustrates the schematic diagram of the circuit that was used, with the "Load probe" indicating the point of measurement. The RF amplifier is replaced with a 50 Ω source while the rock sample is represented by the resistance obtained by the network analyser for the JSA rock sample (160.14 MHz at 1264 Ω). The designed values were correlated to the closest E12 international standard for capacitors (see Table 5.3). The last column in Table 5.3 indicates the upper and lower variations of the designed values to test for MPT from the RF amplifier to the rock sample. The simulator was set to provide a transient response with a start time of 53 ns and a stop time of 68 ns.

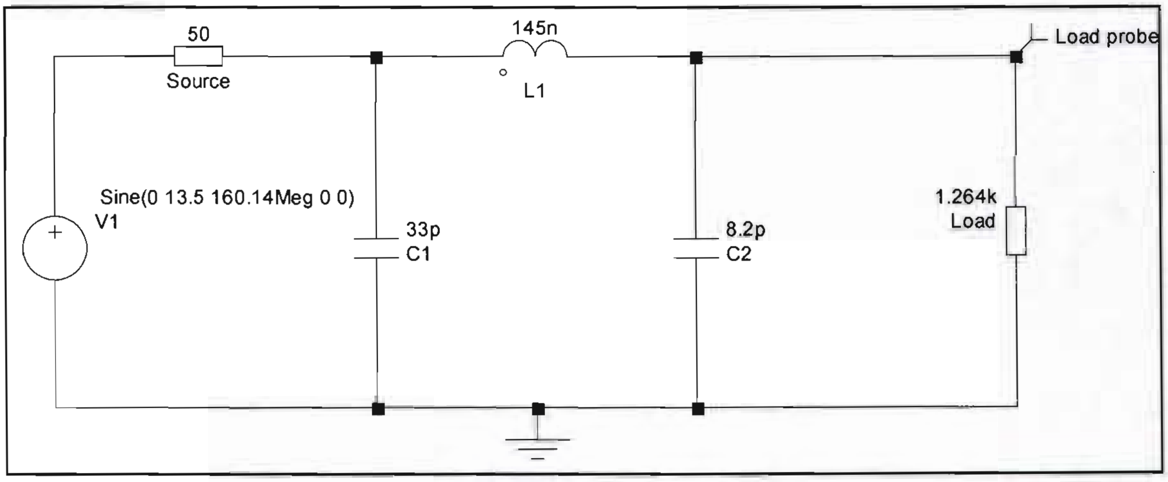

Figure 5.10: Simulation schematic of the matching network

Table 5.3: Component values used in the simulation package

Component	Designed value	Simulation value	Simulation variation
Inductor ($L1$)	145 nH	145 nH	125 – 165 nH
Capacitor ($C1$)	34.4 pF	33 pF	33 pF
Capacitor ($C2$)	7.86 pF	8.2 pF	6.8 – 10 pF

A 13.5 V supply was used to simulate the output voltage of the RF amplifier with a frequency of 160.14 MHz. Three different results are shown for the inductor in Figure 5.11 while keeping the input and output capacitor values constant:

- The designed matching network with a 145 nH inductor (trace shown in red);
- Modified network with the inductor's value decreased to 125 nH (green trace);
- Modified network with the inductor's value increased to 165 nH (blue trace).

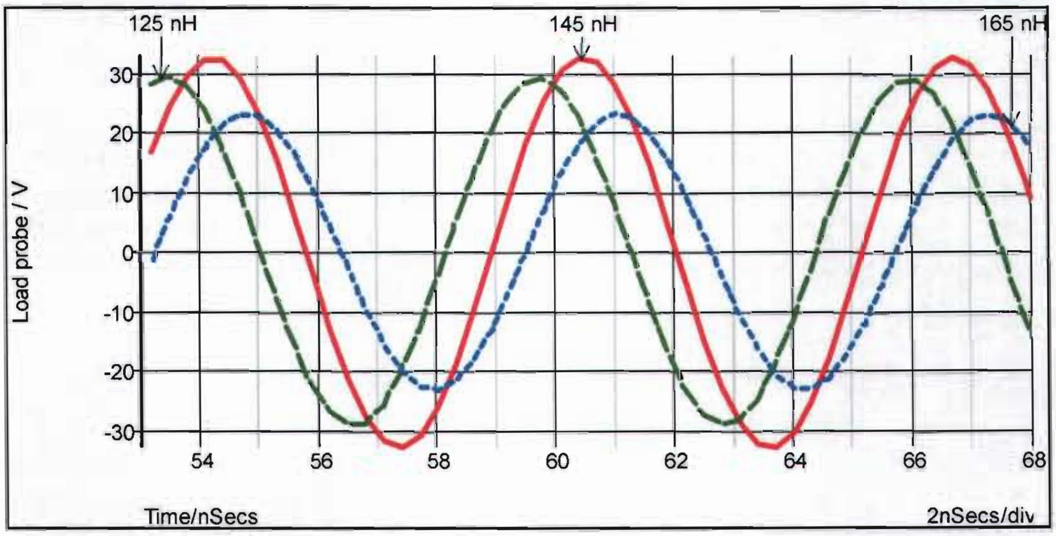

Figure 5.11: Inductor variation results obtained from the simulation package

Another three results are shown in Figure 5.12 representing variation in the output capacitor's value while keeping the input capacitor and inductor constant:

- The designed matching network with a 8.2 pF capacitor (trace shown in red);
- Modified network with output capacitor decreased to 6.8 pF (green trace);
- Modified network with output capacitor increased to 10 pF (blue trace).

The results of the simulation circuit reveal that the highest output voltage of 32.64 V for a source (50 Ω) to load (1264 Ω) connection at 160.14 MHz (time period is 6.245 ns in Figure 5.10) occurs at the values from the scientific design process, thereby indicating MPT. Any variation in component values represents a decline in power transfer, thereby substantiating the design process as reliable and valid. A network analyser was subsequently used to verify the impedance matching ability of the network.

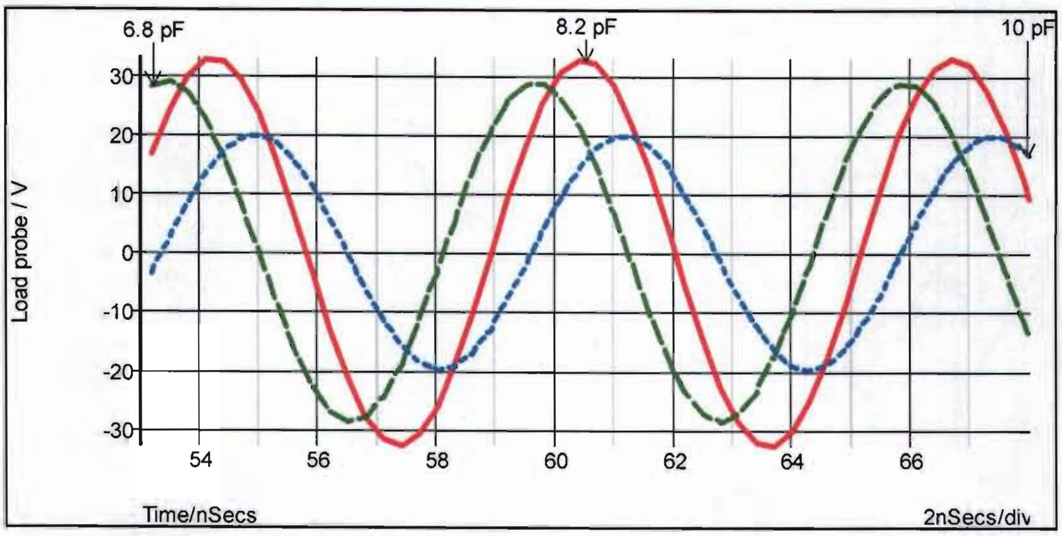

Figure 5.12: Output capacitor variation results from the simulation package

5.6 Verifying the matching network's performance with a network analyser

The matching network's performance was further analysed using the network analyser described in Chapter 4. The JSA rock sample (two identical samples cut to 30 x 19 x 4 mm) was inserted into PPC-3 (clamped in the wooden jig) which was connected to the matching network (see Figure 5.13).

Each trimmer capacitor has two side protruding pins which are inserted into 1.5 mm holes drilled into the side of the wooden jig. This helped to secure the trimmer capacitors to the jig and subsequently to the inductor and PPC. However, the trimmer capacitors were not placed within 10 mm of the PPC so as to minimize any possible stray capacitance. The input and output trimmer capacitors were adjusted until the resonating frequency point of 160.14 MHz was stationary over the 50 Ω centre point. This result is shown in Figure 5.14. At this point, the impedance of the rock (1264 Ω) was matched to an impedance of 50 Ω (which represents the output impedance of the RF amplifier), resulting in MPT with minimum reflected power. The capacitors were then disconnected and measured with a LCR meter to determine whether their values were similar to those obtained from the scientific design process. These results are shown in Table 5.4.

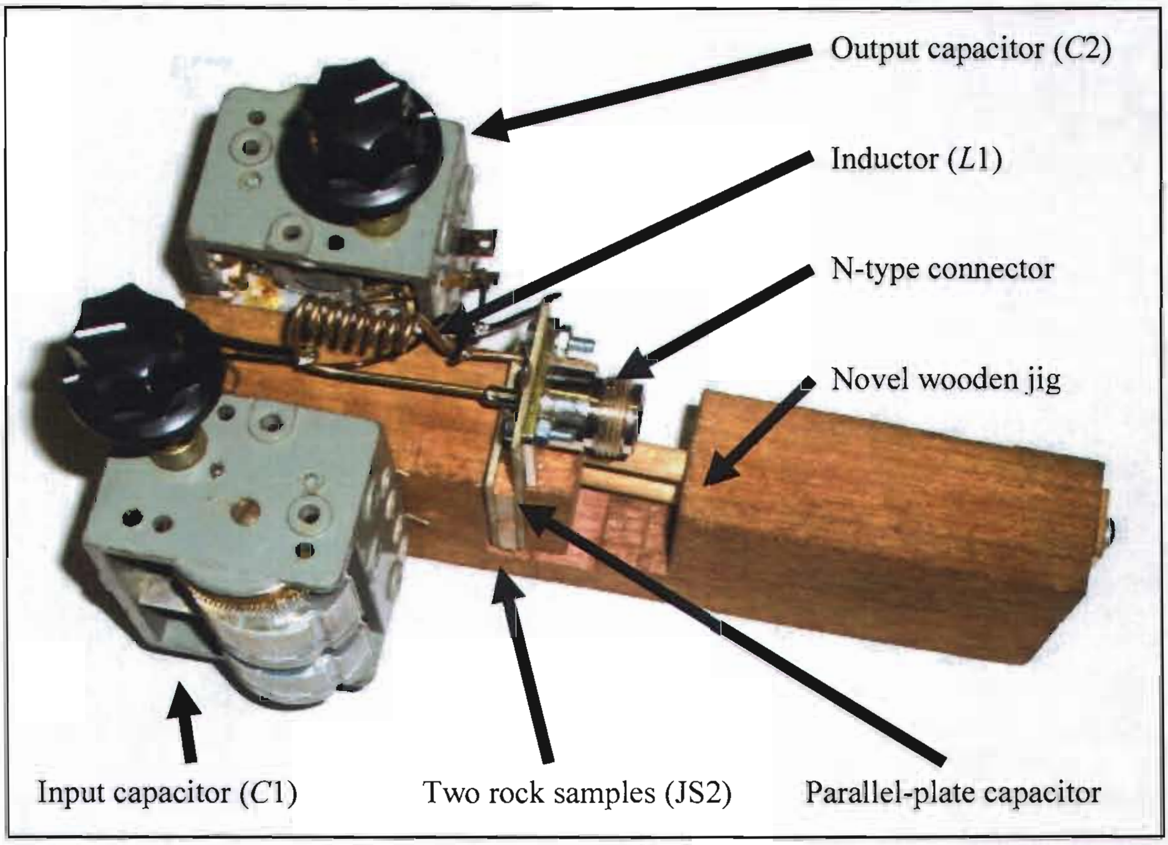

Figure 5.13: Two rock samples (each with dimensions 30 x 19 x 4 mm) inside PPC-3 (28 x 47 mm) with the matching network

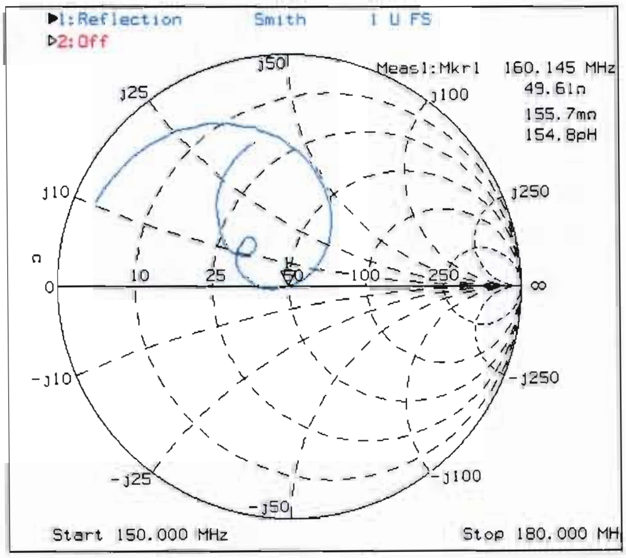

Figure 5.14: Rock sample (JSA) impedance matched to 50 Ω as viewed on a network analyser

A relationship exists between the values for capacitor $C2$. However, no correlation could be established for capacitor $C1$ or inductor $L1$ as stray capacitance and inductance present in the practical model was not accounted for in the theoretical design process. Nevertheless, the design procedure did serve its purpose in providing useful information for the selection process of the components required in the matching network.

Table 5.4: Capacitor values measured after the matching network is tuned to 50 Ω

Component	**Designed values**	**Practical model values (LCR meter)**
Inductor ($L1$)	145 nH	200 nH
Capacitor ($C1$)	34.4 pF	32.3 pF
Capacitor ($C2$)	7.86 pF	15.6 pF

The use of these approximate components, of which the capacitors are adjustable, has resulted in the impedance of the rock sample being matched to 50 Ω. Hence, the objective of impedance matching to ensure MPT has been achieved as shown by the network analyser's results (see Figure 5.14). This result was further validated by a practical experiment, described below, in which RF power is transferred to the rock sample by means of a RF transceiver, amplifier and inline wattmeter (used to measure the forward and reflected power).

5.7 Evaluating the matching network's performance in a practical setup

The matching network's performance was finally evaluated using two RF amplifiers (MIRAGE PAC30-130B) driven by a commercial RF transceiver (ICOM IC-V8000). The RF transceiver generated a 3.2 W RF signal which was amplified by the first RF amplifier to approximately 32 W, an in turn, to approximately 113 W by the second RF amplifier. This was necessary because the RF transceiver was not capable of providing more than 70 W of RF power. The input to the RF amplifiers was limited to 35 W to ensure correct operation of the driver stages. The practical setup is shown in Figure 5.15.

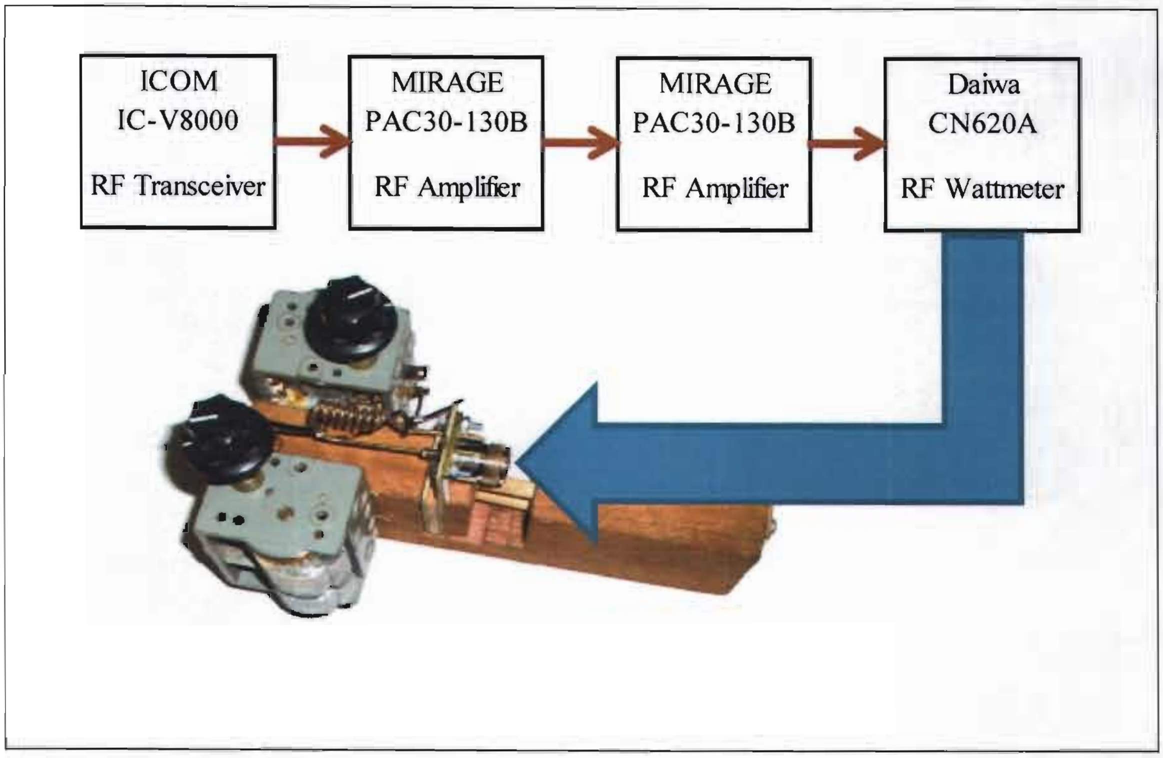

Figure 5.15: Practical setup to determine the efficacy of the matching network

The output of the RF transceiver was first connected straight to the matching network through a RF wattmeter to determine the SWR of the circuit. The reason for this is to ensure that the SWR value remain as close as possible to one, in order to prevent an excess of reflected power damaging the output stage of the RF amplifier. With the two RF amplifiers bypassed, the RF transceiver was activated (keyed) to generate a 3.2 W signal at 160.47 MHz. The trimmer capacitors were then fine tuned to obtain the lowest SWR possible. The RF amplifiers were then switched on (thus connecting the amplifiers directly into the circuit between the RF transceiver and the matching network). The RF transceiver was keyed again and approximately 113 W of forward power was measured with the wattmeter. Two different wattmeters were used to verify the reliability of the measurements. The reflected power measured approximately 1.8 W resulting in a SWR reading of 1.306 (see Table 5.5). The values of the capacitors were once again measured with a LCR meter and the results are shown in Table 5.6. There is very little difference in the capacitor values between the network analyser and practical setup verification.

Therefore, the reliability of the matching network within the practical model was substantiated by two independent measurements (network analyser and practical setup). The successful transfer of RF power to the rock samples was further collaborated by a significant rise in surface temperature, as described in the following subsection.

Table 5.5: Wattmeter readings obtained for the evaluation of the matching network

Parameter	Bird Wattmeter (4304A)	Daiwa Wattmeter (CN620A)
RF transceiver output power	3.2 W	3.3 W
First RF amplifier output power	31 W	31.8 W
Second RF amplifier output power	114 W	114.5 W
Wattmeter forward power	112 W	112.5 W
Wattmeter reflected power	2 W	2 W
SWR value	1.308	1.308

Table 5.6: Capacitor values measured after the matching network is tuned to 50 Ω on the network analyser and then treated with 112 W of RF power

Component	Designed values obtained from the Multimatch software package	Practical model values after network is tuned with a network analyser (LCR meter)	Practical model values after the rock sample is treated with RF power (LCR meter)
Inductor ($L1$)	145 nH	200 nH	200 nH
Capacitor ($C1$)	34.4 pF	32.3 pF	32 pF
Capacitor ($C2$)	7.86 pF	15.6 pF	14 pF

5.8 The relationship between RF power and the surface temperature of the DUT

The JSA and JS2 rock samples were treated with 82 W of RF power at their resonating frequency of approximately 160 MHz. The second result of 112 W (see Table 5.7) was achieved when using an operating frequency of 156 MHz. Figures 5.16 and 5.17 show the temperature curves over a 36 minute period for three different input frequencies (152, 156 and 160 MHz). These measurements were obtained from a LUTRON TM-2000 digital thermometer using K-type thermocouples pressed firmly against the surface of the rock samples (see Annexure 14). Temperature readings were recorded on a personal computer attached via the RS232 port to the digital thermometer. Temperature curves for the other eight samples are shown in Annexures 15 – 18.

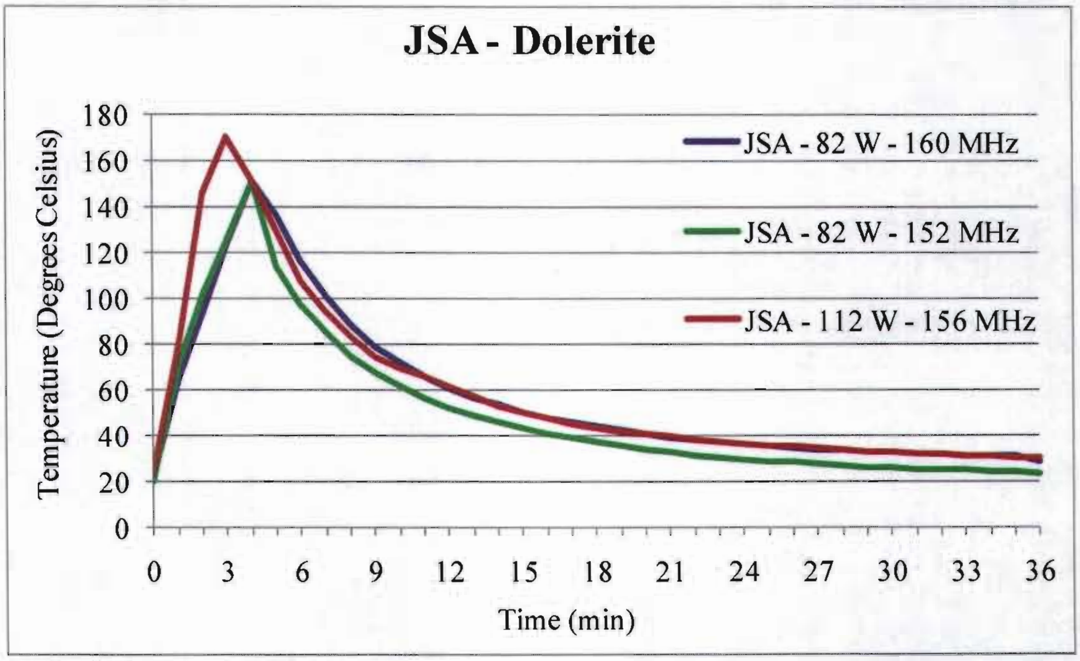

Figure 5.16: Surface temperature rise and fall of the JSA rock sample over a 36 minute period for three different frequencies and input RF powers

Both results indicate that all three frequencies yield a similar variation in temperature over time for an input power of 82 W at 152 and 160 MHz. However, in both cases, a higher input power (112 W at 156 MHz) results in a much quicker rise in temperature. This suggests that the RF input power rather than the frequency of operation is crucial to the surface temperature rise of the rock samples. This validates equation 3.3 which places significant emphasis on the input power as being responsible for the temperature change within the dielectric material. Therefore, it was decided to use an operating frequency of 160 MHz at 82 W for all the rock samples, thereby simplifying the analysis and evaluation of all the results. The data obtained from the LUTRON TM-2000 digital thermometer was further used to determine the coupling coefficient of the PPC, thereby validating the specific heat capacities of the various rock samples.

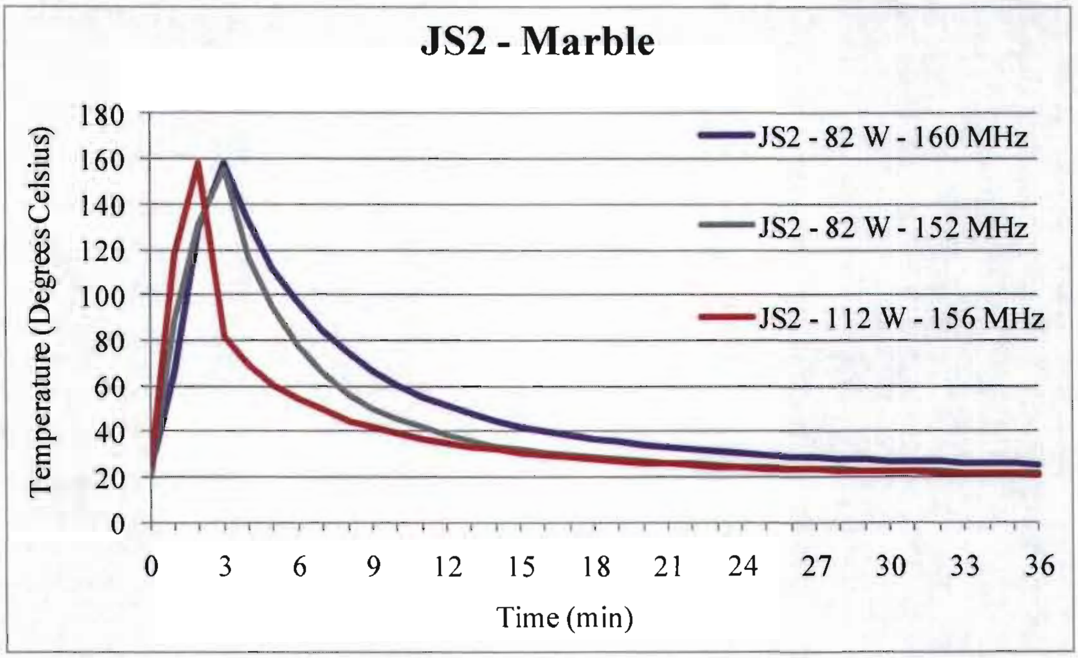

Figure 5.17: Surface temperature rise and fall of the JS2 rock sample over a 36 minute period for three different frequencies and input RF powers

5.9 Determining the coupling coefficient of the PPC using specific heat capacities

The RF heating of a dielectric material is directly related to the amount of RF input power, rather than input frequency. This is deduced from equation 3.3 introduced in Chapter 3 and proposed by Halverson et al. (1996):

$$\Delta T = \frac{\mathrm{k} \times P}{C \times m} \times \Delta t \qquad °\mathrm{C}$$

The amount of input power (P) can be measured by means of a RF wattmeter connected inline between the RF amplifier and PPC (see Figure 5.15). The temperature increase (ΔT) over a specific time period (Δt) was obtained by means of K-Type thermocouples pressed firmly against the surface of the specified rock samples (see Annexure 14). The mass (m) of the rock sample was measured with a digital scale. The value of specific heat capacity for dolerite was taken as 900 J/kg/°C (Waples and Waples 2004). Using the data obtained for rock sample JSA and manipulating equation 3.3 yields the following suggested value for the coupling coefficient (k), which is unique to this PPC.

$$\mathrm{k} = \frac{\Delta T \times C \times m}{P \times \Delta t} \tag{5.9}$$

$$\mathrm{k} = \frac{129 \times 900 \times 13.31 \times 10^{-3}}{82 \times 231}$$

$$\mathrm{k} = 81.58 \times 10^{-3}$$

This value for the coupling coefficient can now be used in the following equation to estimate the specific heat capacity of the other rock samples (listed in Table 5.7):

$$C = \frac{\mathrm{k} \times P}{\Delta T \times m} \times \Delta t \qquad \mathrm{J/kg/°C} \tag{5.10}$$

These calculations were done to establish the reliability of the coupling coefficient which is unique to this sized PPC. The reliability and validity of these results are achieved through repeated measurements (different input powers and mass) which are compared to accepted values (obtained from Waples and Waples (2004)). The specific heat capacities of the rock samples, as calculated with equation 5.10, were all within 5% of the generally accepted values available in the literature. However, the specific heat capacities for rock samples JS3 – JS5 were very different. A possible reason for this could be related to the mineral composition of these rock samples, which is described in detail in Chapter 6.

Table 5.7: Original value for the coupling coefficient (k) substantiated with data obtained from the ten rock samples

Rock sample	Operating frequency (MHz)	Power (W)	Temperature change (°C)	Mass (kg)	Time (s)	Specific heat capacity (J/kg/°C)		Deviation (%)
						Calculated	Accepted	
JSA Dolerite	160.00	82	129	1.33E-02	231	900.00	900.00	0.00%
	156.00	112	146	1.30E-02	189	909.15	900.00	1.01%
	152.00	82	131	1.32E-02	234	908.69	900.00	0.96%
JSB Marble	159.00	90	84	1.20E-02	123	895.18	883.00	1.36%
JSC Granite	160.00	82	33	1.16E-02	66	1156.36	1172.00	-1.35%
JSD Sandstone	159.00	90	49	1.12E-02	60	801.29	775.00	3.28%
JSE Mudstone	160.00	82	50	1.22E-02	75	820.47	860.00	-4.82%
JS1 Marble	160.00	82	119	1.37E-02	225	925.94	883.00	4.64%
JS2 Marble	160.00	82	134	1.12E-02	195	868.40	883.00	-1.68%
	156.00	112	133	1.05E-02	135	884.11	883.00	0.13%
	152.00	82	136	1.10E-02	195	871.18	883.00	-1.36%
JS3 Marble	160.00	82	35	1.39E-02	240	3304.85	883.00	73.28%
JS4 Granite	160.00	82	41	1.37E-02	240	2868.75	1172.00	59.15%
JS5 Marble	160.00	82	39	1.30E-02	240	3161.79	883.00	72.07%

5.10 Summary

Chapter 5 has provided the theoretical design of the matching network based on scientific literature in the field of RF communications. The Pi circuit was chosen as the preferred matching network due to the fact that it can match a large range of impedances (made possible by the parallel variable capacitors) and because it posses only one series component (the inductor). The matching network was analysed and evaluated by means of a simulation model (in SIMetrix) and a practical model (using a network analyser and a practical experiment). The results suggest reliability and validity of the matching network as indicated by low SWR readings. Furthermore, maximum forward power into the rock sample from the RF amplifiers was achieved. A unique value for the coupling coefficient for PPC-3 was partially substantiated. Initial results of transferring RF power to various rock samples confirmed that it is the input power rather than the frequency of operation that is central to the dielectric heating of materials.

Chapter 6 will present the physical results (colour, screening, SEM analysis and power consumption) of the treated and untreated samples using the wooden jig (discussed in Chapter 4) and matching network presented in this chapter.

Chapter 6 Evaluation of the effects of RF treatment on the rock samples

6.1 Introduction

In this chapter the effects of RF treatment on the rock samples are described and interpreted. The possible changes that were considered include textural, phase, grindability, colour and temperature changes. Textural changes (changes in grain size and inter-grain boundary relationships) were considered using polarizing optical microscopy on polished thin sections of the rock samples. Phase changes (changes in mineral assemblage) were determined using polarizing optical microscopy. Grindability, being the changes in the power consumption during grinding and changes in the particle size distribution after grinding, was determined by measuring the power consumption during milling and by performing particle size analyses (sieve tests). Surface colour changes were visually observed while surface temperature changes were measured. Contrasts between the electrical properties (resonating frequency) of the untreated and treated samples are further indicated. The results from the above considerations were interpreted in terms of the mineralogical and chemical composition of the samples.

6.2 Comparative textural description

This section presents the petrographic description and chemical composition of the ten rock samples.

6.2.1 Petrographic description

The petrographic description highlights the main minerals present within the ten rock samples (shown in Table 6.1), determined by examining the polished thin sections under an electronic microscope. Photomicrographs of the untreated and treated rock samples are contrasted in Figures 6.1 – 6.10, where some mineral grain boundaries are indicated.

Table 6.1: Petrographic description of the ten rock samples used in this research

Sample code	Rock type	Petrographic description Minerals Present	Texture
JSA (Figure 6.1)	Dolerite	Plagioclase (50%), clinopyroxene (17%), orthopyroxene (27%), quartz (5%), minor biotite and opaque minerals	The major minerals are typically subhedral, coarse-grained (2-4 mm), interlocked crystals typical of a gabbro
JSB (Figure 6.2)	Marble	Dolomite (50%), calcite (25%), tremolite-actinolite (18%), quartz (5%), and minor clay, serpentine and opaque minerals	The dolomite and calcite grains are variable in grain size but finer than the 1 mm long fibrous laths of tremolite-actinolite
JSC (Figure 6.3)	Granite	Plagioclase (55%), quartz (40%), almandine-pyrope garnet (5%), and minor dolomite, muscovite, biotite and clay minerals	This is a coarse-grained (1-5 mm) leucocratic granite with seriate texture and mainly anhedral grains
JSD (Figure 6.4)	Sandstone	Quartz (90%), calcite (4%), clay (3%), and haematite (3%)	The rock is a clast-supported sandstone with rounded quartz grains (0.3 mm in diameter) and very fine-grained interstitial calcite, clay and haematite
JSE (Figure 6.5)	Mudstone	10% haematite laths (pseudo morphs) in a matrix of sericite and sub microscopic clay	Micron-sized sericite grains and sub microscopic clay material as a matrix with dispersed opaque prismatic laths. Dispersed opaque prismatic laths are composed psuedomorphic haematite after either feldspar or amphibole
JS1 (Figure 6.6)	Marble	Dolomite (20%), calcite (50%), tremolite-actinolite (15%), quartz (6%), clay (5%), and serpentine (4%)	The carbonate minerals occur as 0.5-1 mm sized grains
JS2 (Figure 6.7)	Marble	Calcite (85%) with rare rounded poikilitic garnet grains, sparse magnetite veinlets and limonite coating on grain margins	Calcite grains occur as anhedral to rounded grains up to 2 mm in size that are dispersed within a calcite matrix made up of tiny grains (10 μm)
JS3 (Figure 6.8)	Marble	Calcite (98%)	Calcite grains occurs as 0.25-0.5 mm sized anhedral grains dispersed within a very fine carbonate matrix comprising 1 μm sized calcite
JS4 (Figure 6.9)	Granite	Anhedral quartz (25%), perthitic potassium feldspar (55%), myrmekite (5%) and minor euhedral garnet (15%)	Grain sizes range from 0.1-4 mm
JS5 (Figure 6.10)	Marble	Calcite (90%)	This carbonate rock comprises a matrix of 1 μm sized calcite grains that is crosscut by veins of coarser-grained (0.25 mm) polygonal calcite grains

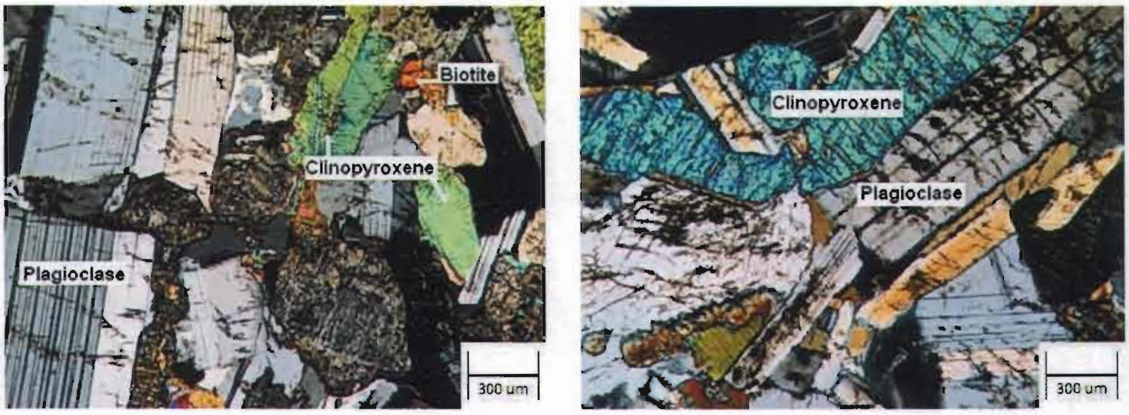

Figure 6.1: Photomicrographs of the untreated (left) and treated (right) JSA rock sample taken under cross-polarized light

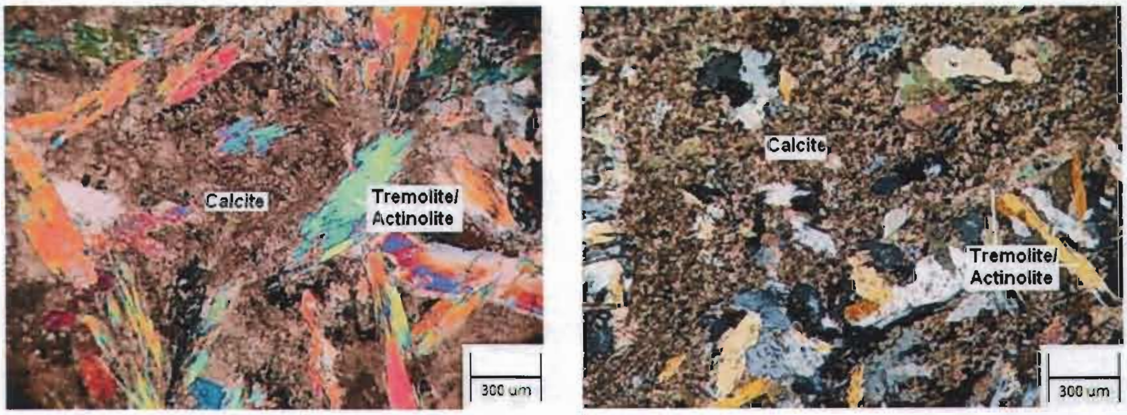

Figure 6.2: Photomicrographs of the untreated (left) and treated (right) JSB rock sample taken under cross-polarized light

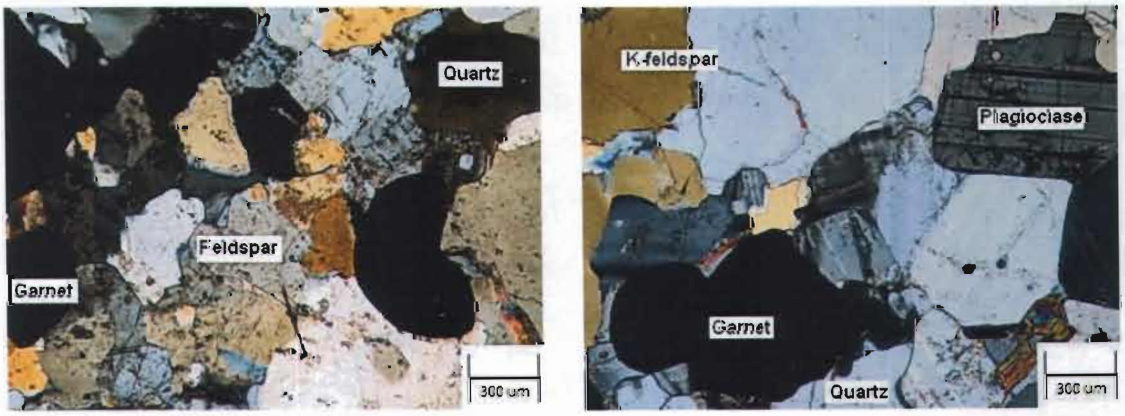

Figure 6.3: Photomicrographs of the untreated (left) and treated (right) JSC rock sample taken under cross-polarized light

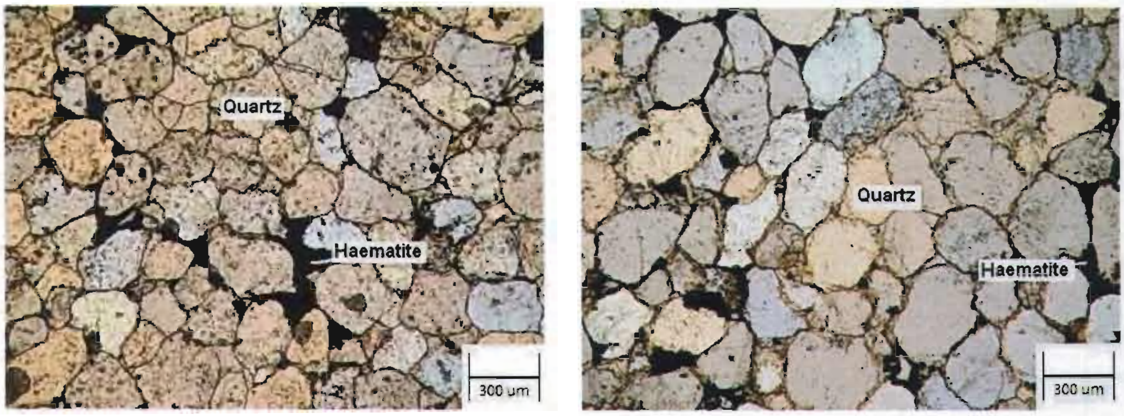

Figure 6.4: Photomicrographs of the untreated (left) and treated (right) JSD rock sample taken under plane-polarized light

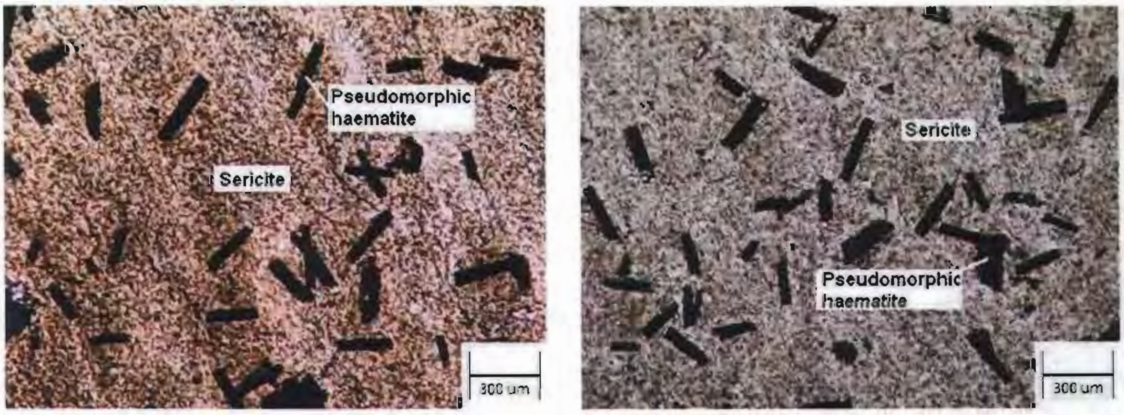

Figure 6.5: Photomicrographs of the untreated (left) and treated (right) JSE rock sample taken under plane-polarized light

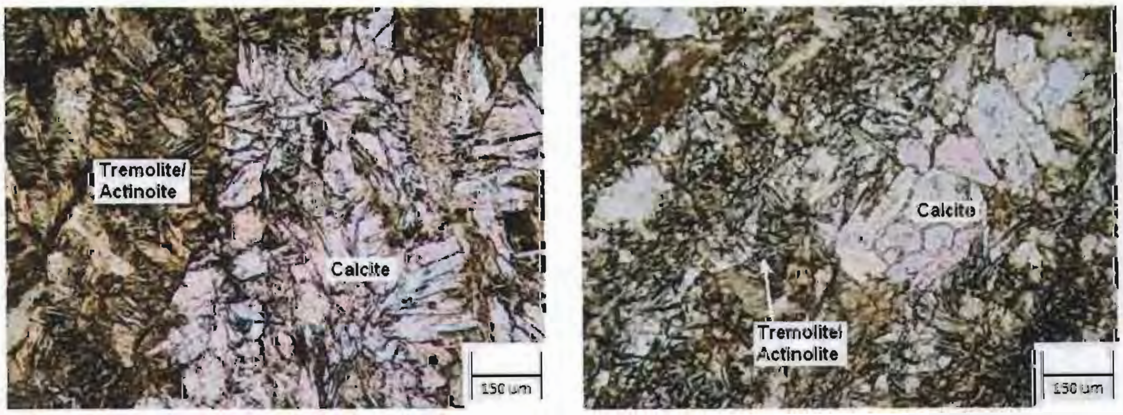

Figure 6.6: Photomicrographs of the untreated (left) and treated (right) JS1 rock sample taken under plane-polarized light

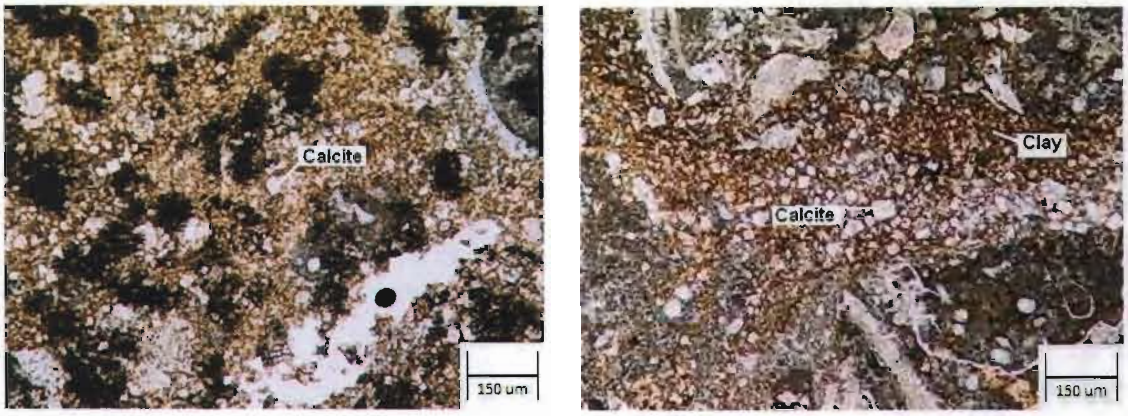

Figure 6.7: Photomicrographs of the untreated (left) and treated (right) JS2 rock sample taken under plane-polarized light

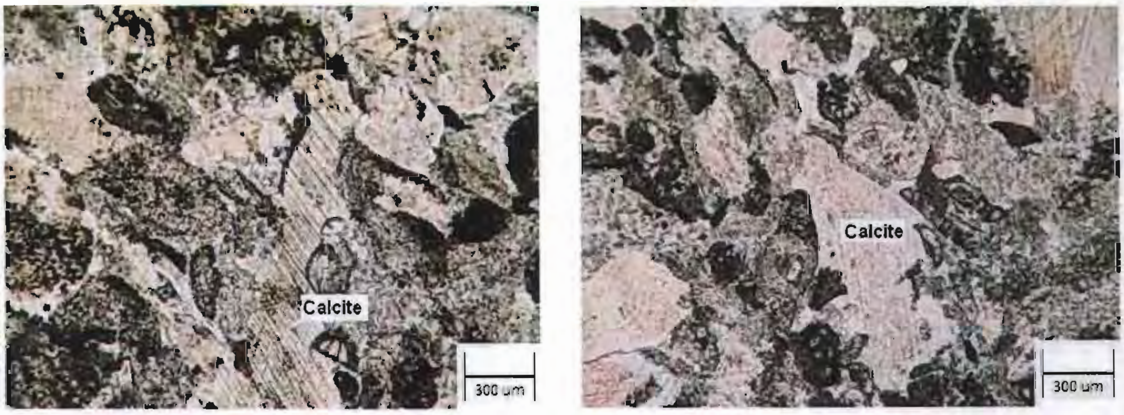

Figure 6.8: Photomicrographs of the untreated (left) and treated (right) JS3 rock sample taken under plane-polarized light

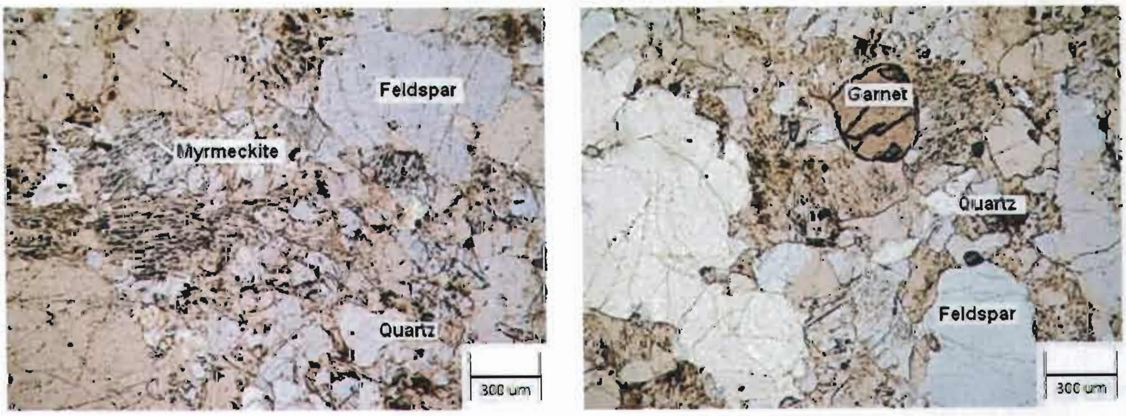

Figure 6.9: Photomicrographs of the untreated (left) and treated (right) JS4 rock sample taken under plane-polarized light

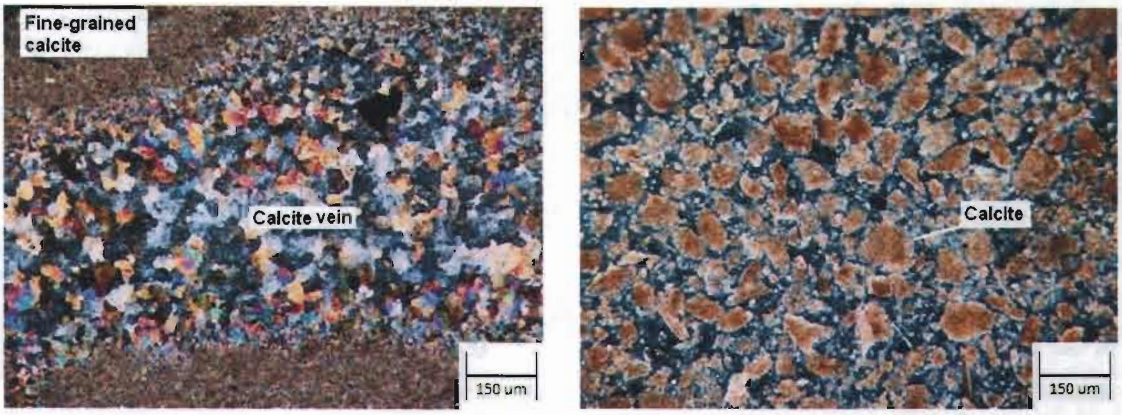

Figure 6.10: Photomicrographs of the untreated (left) and treated (right) JS5 rock sample taken under cross-polarized light

A comparison of the photomicrographs of the untreated and treated rock samples reveals no significant differences in grain size, grain shape, minerals present or inter-granular textures. No visible cracks or fractures exist along the mineral grain boundaries of the treated rock samples. Annexure 24 gives a photograph of the ten thin sections used for the petrographic and chemical analysis.

6.2.2 Chemical composition of the rock samples

The chemical composition of the rock samples was determined using an X-ray fluorescence spectrometer, using a Rigaku Primini instrument. A complete wavelength dispersive scan was done using virtual standards on all the major elements (Table 6.2).

A statistically significant correlation (Pearson) was found to exist between the presence of specific chemical elements and changes in the surface temperature and colour of the treated rocks samples (discussed in section 5.8 of Chapter 5). High temperatures attained during RF treatment were associated with high modal proportions of minerals plagioclase, dolomite and iron oxides in the samples. Visible surface colour changes (shown in Table 6.3 and 6.4) were also associated with high modal proportions of calcite and/or tremolite-actinolite. No correlation was found to exist between the grindability (screen change discussed in the following section) of the rock samples and their chemical composition.

Table 6.2: Pearson correlation between chemical composition and textural changes

Sample code	SiO_2	Al_2O_3	Fe_2O_3	MgO	MnO	CaO	K_2O	Na_2O	P_2O_5	TiO_2	Temperature	Screen change	Color change
JSA	56.2	19.5	9.03	3.2	0.21	9.01	0.81	1.55	0	0.43	151	1	0
JSB	26.1	0.59	19.7	2.5	0.53	49.2	0.17	0	1.26	0	107	0	1
JSC	73	17.6	1.53	0	0.1	3.59	0.87	3.36	0	0	110	0	0
JSD	89.3	1.61	1.6	0	0	2.54	0.82	0	4.12	0	55	1	0
JSE	41.9	18.6	19.5	0	0	1.2	7.81	0	1.45	9.5	104	0	0
JS1	38.9	1.69	11.9	16.6	0.22	30.7	0	0	0	0	155	0	1
JS2	5.7	0.3	1.79	0	0	91.1	0.38	0	0.78	0	158	0	1
JS3	4.46	0	0	0	0	94.9	0	0	0.62	0	65	1	0
JS4	74.7	8.1	1.29	0	0.25	4.67	9.4	0	1.59	0	66	0	0
JS5	4.4	0	0	0	0	95	0	0	0.59	0	69	1	1
	-0.19	0.24	0.38	**0.54**	0.22	-0.02	-0.26	0.23	-0.27	0.02	Pearson		
	0.30	0.25	0.14	0.05	0.27	0.48	0.23	0.26	0.23	0.48	sig.		
	-0.08	-0.15	-0.43	-0.24	-0.39	0.25	-0.40	-0.08	0.20	-0.25		Pearson	
	0.41	0.33	0.10	0.25	0.13	0.24	0.12	0.41	0.28	0.24		sig.	
	-0.62	**-0.63**	0.19	0.42	0.28	**0.59**	-0.46	-0.38	-0.27	-0.29			Pearson
	0.02	0.02	0.30	0.11	0.21	0.03	0.08	0.13	0.22	0.21			sig.

*Correlation is significant at the 0.05 level (1-tailed)

6.3 Grindability differences between untreated and treated rock samples

Determination of the relative grindability of the untreated and treated samples was done by measuring the power consumption during grinding and comparing the particle size distribution after the grinding process. The untreated and treated samples were ground down to powder form in a laboratory swing mill obtained from Effective Laboratory

Supplies in South Africa (Effective Laboratory Supplies 2010). A photo of this mill, which is powered by a 3-phase AC power supply, is shown in Annexure 19. The swing mill pot consists of a shallow cylinder; two internal rings and a heavy disc (see Annexure 19 for a photo of these rings). The sample is placed in the space between the disc and rings and the mill is securely clamped into a vibrating barrel. These mills are designed for reduction of materials to extremely fine powders for preparation of samples for spectra analysis. All samples were milled for 2 minutes with corresponding power measurements taken of the power consumed using a HIOKI 3286-20 clamp on power meter (see Annexure 20). A small brush was used to clean out the grounded samples (in the form of powder or dust) from the pot, which were then weighed with a digital scale.

The powder samples were next transferred to particle screening sieves (250 μm, 150 μm, 90 μm and 38 μm screens placed on top of each other – see Annexure 21). This screen combination was placed in an ENDECOTTS EFL2000 shaker for 5 minutes. Rock sample particles left behind in each screen was weighed individually. These weightings were converted into percentages by dividing each weighting by the total mass and cumulative mass percentages by adding successive mass percentages. The results of this evaluation are shown in Figures 6.11 – 6.20, where the untreated samples are shown by means of a triangle or cross. The treated samples are indicated by means of a diamond or square. The left sketch indicates the particle size distribution to cumulative mass, while the right hand sketch shows the frequency of occurrence for each grain size.

JSB, JSC, JSE, JS2 and JS4 show little or no variation in post-grinding particle size distribution between the untreated and treated rock samples. However, JSA, JSD, JS1, JS3 and JS4 reveal minor to major variations.

The treated JSA sample (dolerite) shows a significant coarser grain size distribution with a mode value of 38 μm, whereas it is 90 μm for the untreated sample (discerned from the right hand graph in Figure 6.11). Similarly, the d_{80} (nominal sieve size allowing 80% of the powered sample to pass through – left hand graph in Figure 6.11) is less than 38 μm for the treated samples, but approximately 85 μm for the untreated ones. This means that for the same amount of grinding (2 minutes) the treated samples were reduced in size to a lesser extent than the untreated samples, suggesting reduced grindability. This may also indicate that fewer fines (smaller particles) are generated and therefore over grinding is reduced. A similar situation is evident for the JSD sample, which is a sandstone with granular textures in which sand grains are cemented with matrix material such as haematite, whereas the JSA sample has a typical igneous texture of interlocking crystals. Yet they behaved similarly during grinding of the treated samples. The JS1 (marble) sample shows a similar but smaller difference in the grindability between the untreated and treated rock samples.

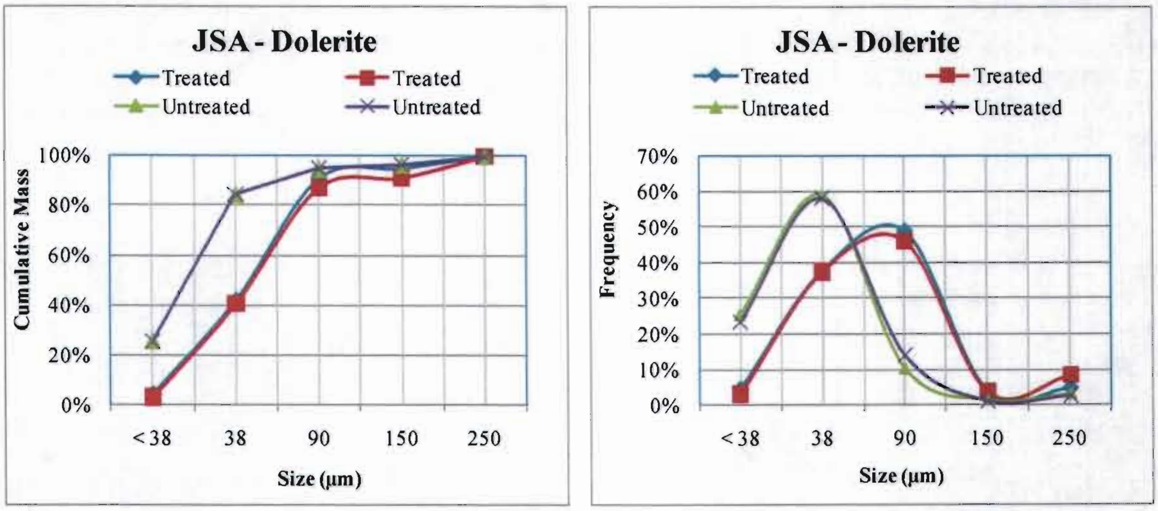

Figure 6.11: Particle screen results for the untreated and treated JSA sample

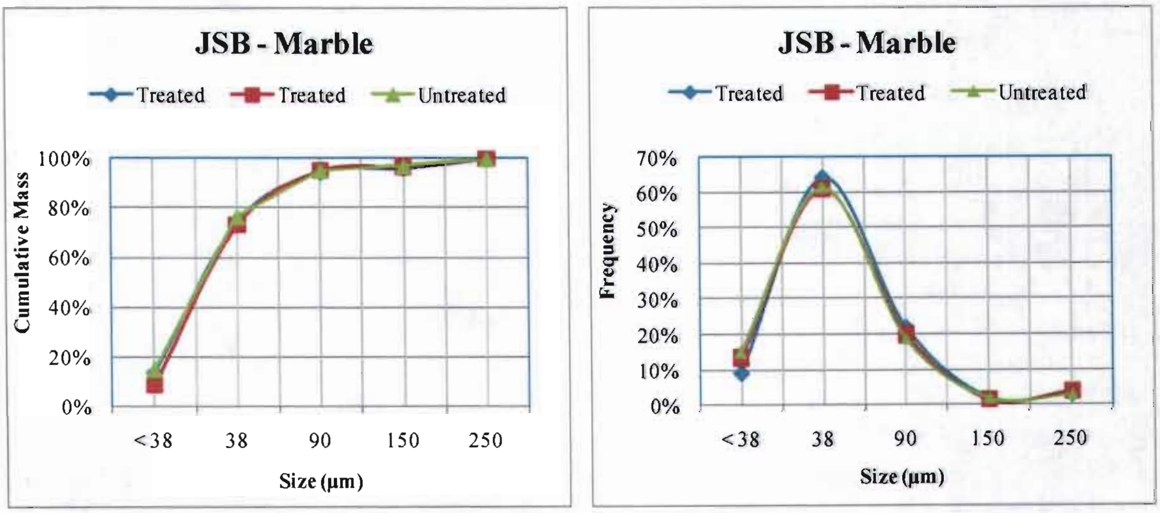

Figure 6.12: Particle screen results for the untreated and treated JSB sample

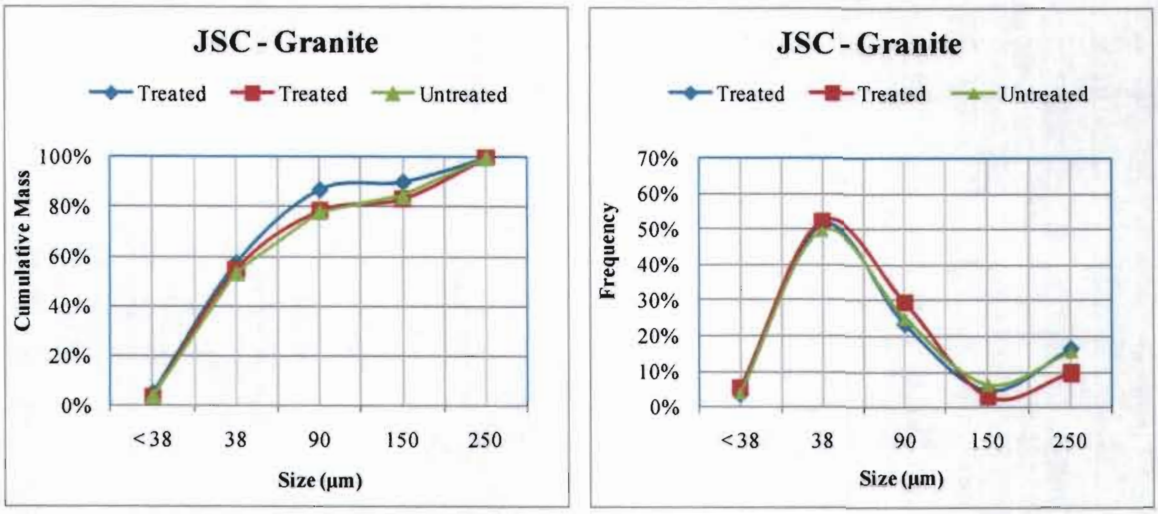

Figure 6.13: Particle screen results for the untreated and treated JSC sample

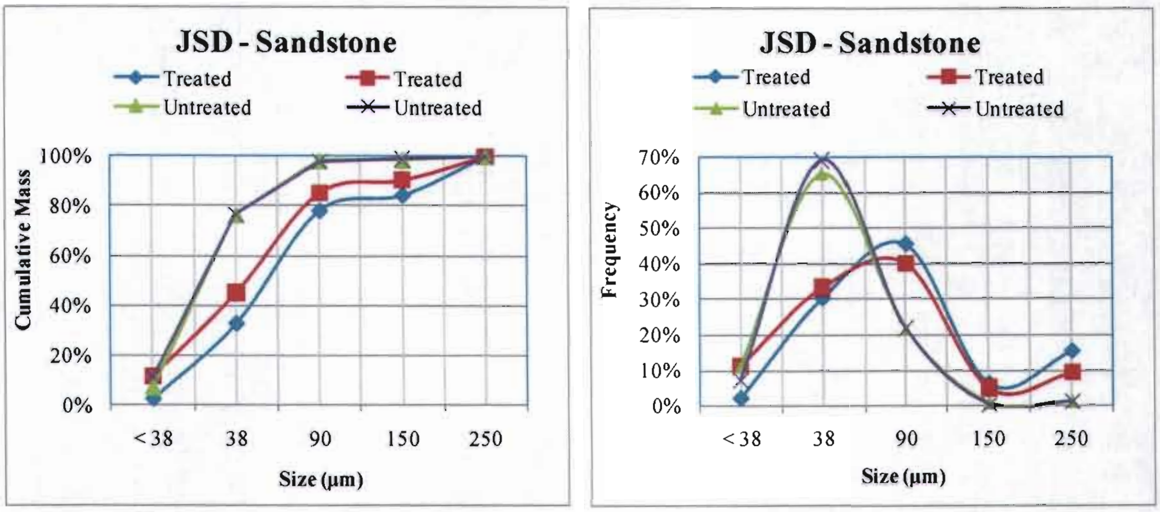

Figure 6.14: Particle screen results for the untreated and treated JSD sample

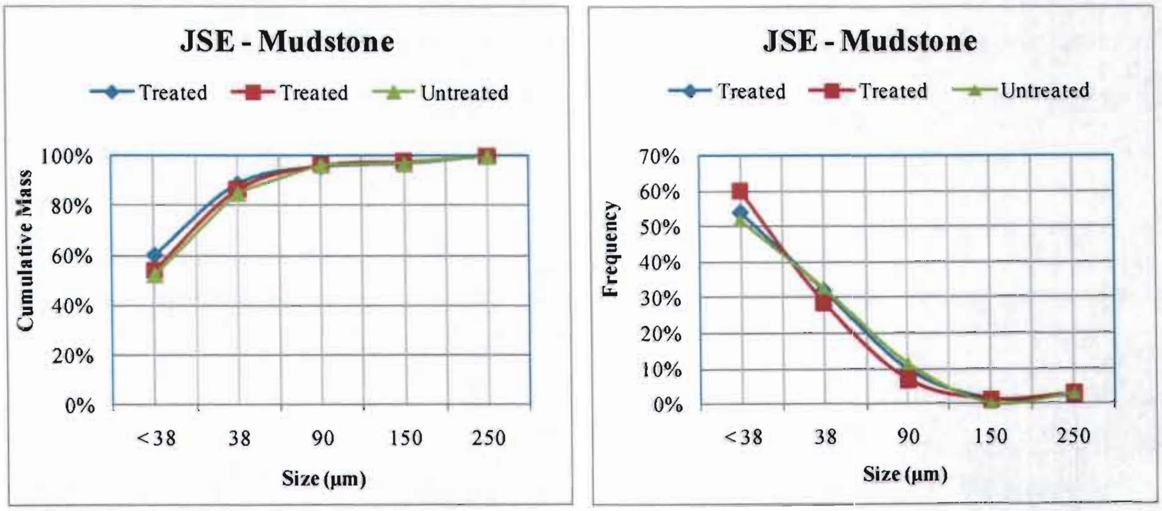

Figure 6.15: Particle screen results for the untreated and treated JSE sample

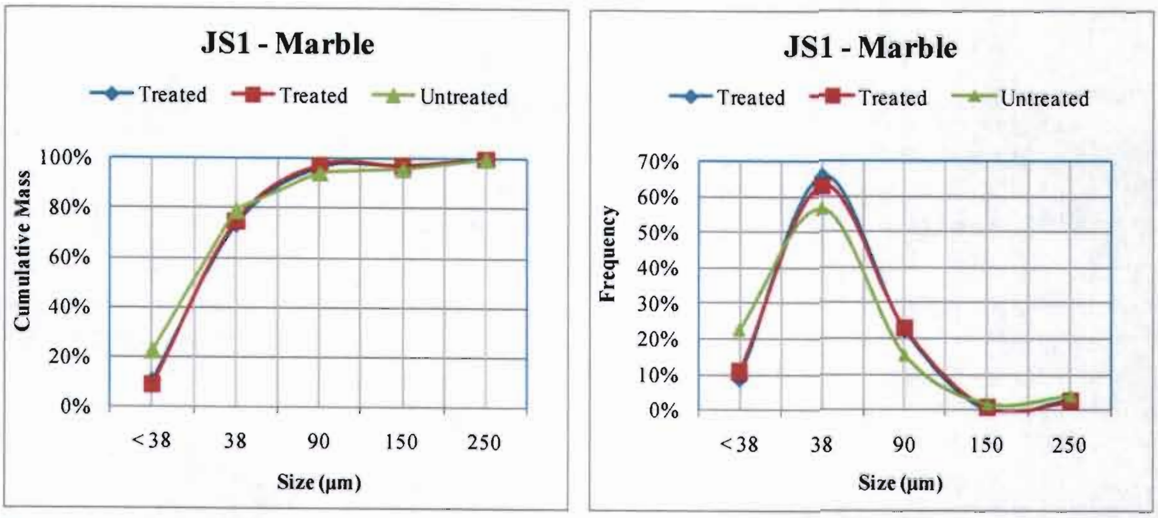

Figure 6.16: Particle screen results for the untreated and treated JS1 sample

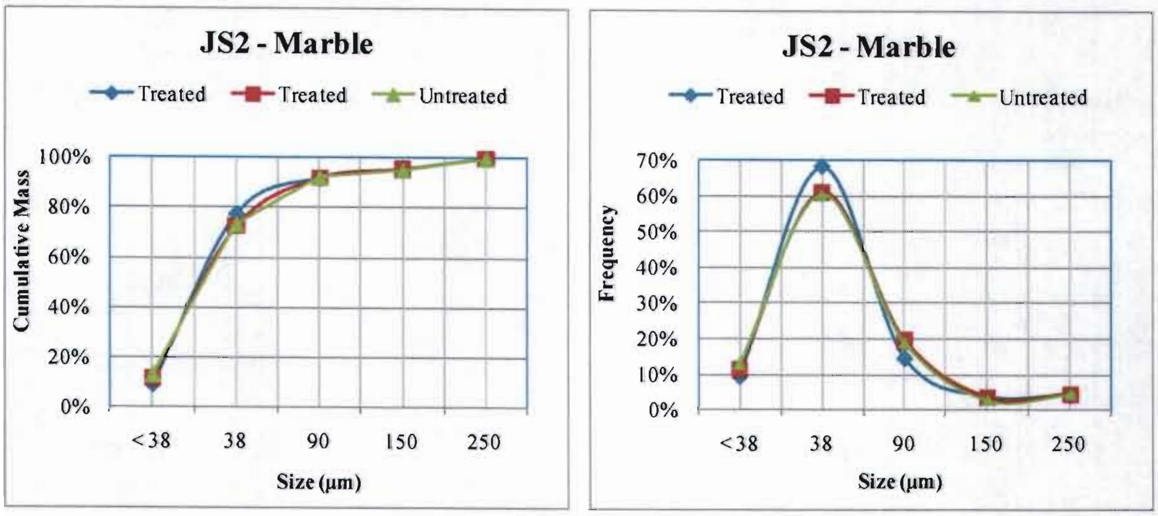

Figure 6.17: Particle screen results for the untreated and treated JS2 sample

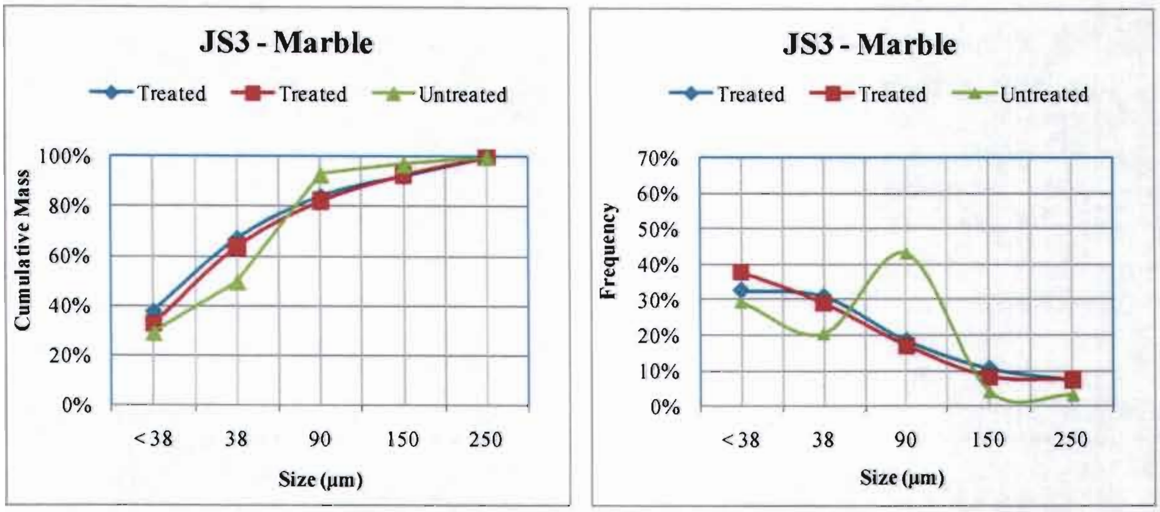

Figure 6.18: Particle screen results for the untreated and treated JS3 sample

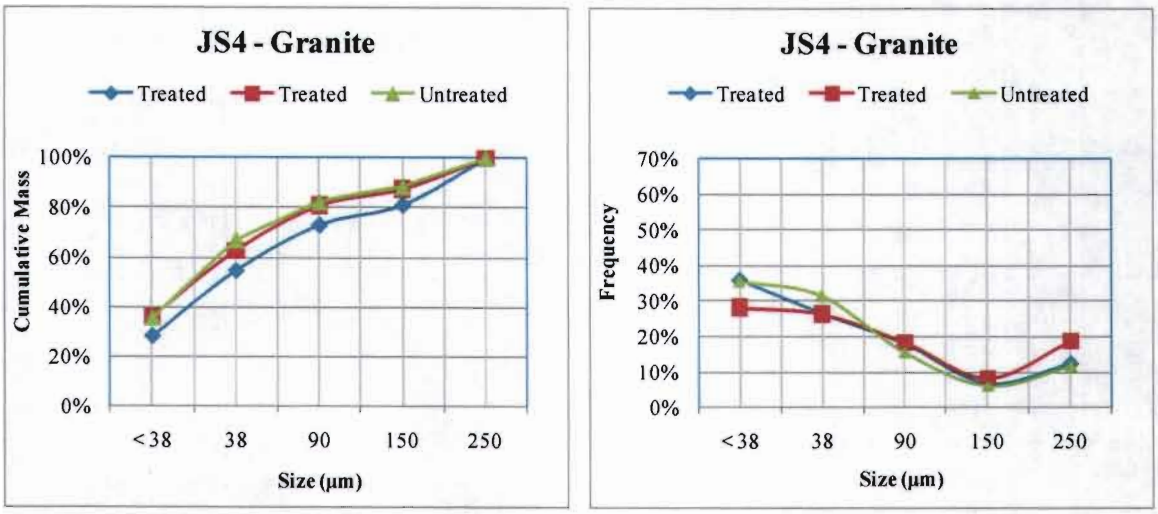

Figure 6.19: Particle screen results for the untreated and treated JS4 sample

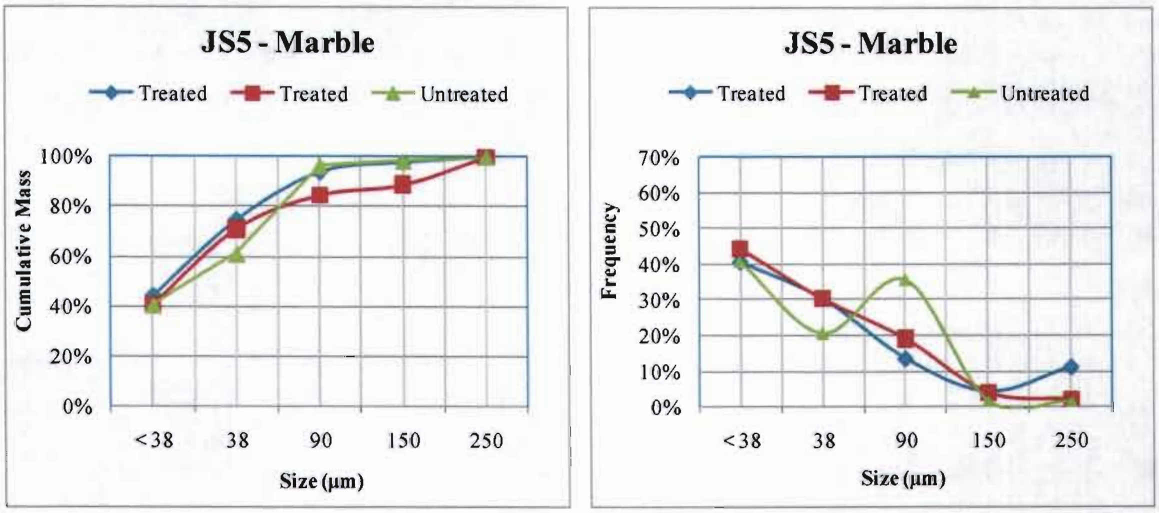

Figure 6.20: Particle screen results for the untreated and treated JS5 sample

The untreated JS3 and JS5 samples (marble) indicate a grain size distribution with high percentages of fines (< 38 μm), but with an otherwise almost normal distribution (see the right hand graphs in Figures 6.18 and 6.20). The treated samples did not produce a normal particle size distribution indicating a larger amount of fines being produced.

Polished sections of the powdered samples (see Annexure 25 for photograph) were obtained to check for textural changes with regard to particle sizes of the untreated and treated samples (see Figures 6.21 – 6.30). The size of the mineral grains is indicated, revealing no significant reduction in size between the untreated and treated samples.

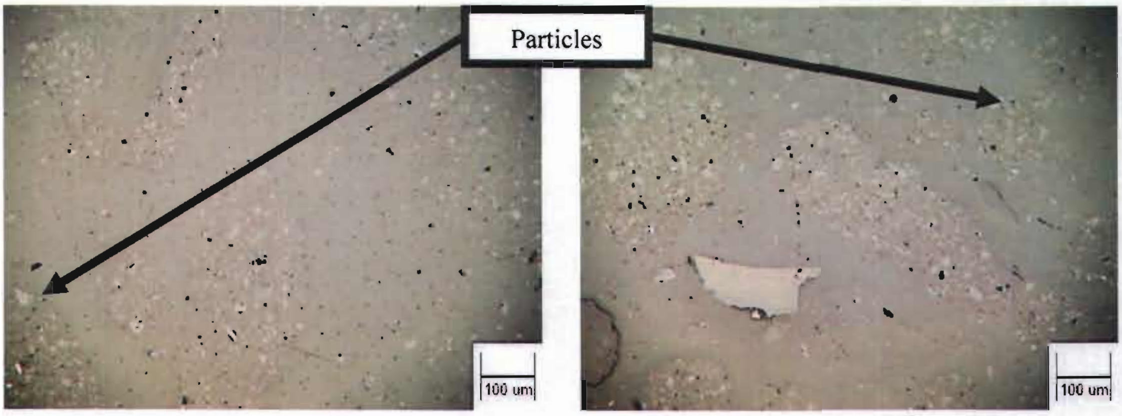

Figure 6.21: Photomicrographs of the untreated (left) and treated (right) JSA sample (polished section of the powered rock)

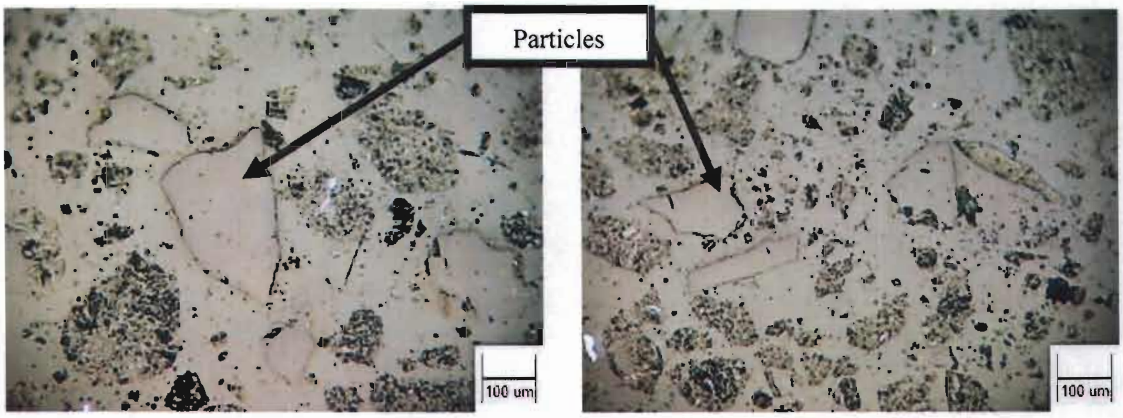

Figure 6.22: Photomicrographs of the untreated (left) and treated (right) JSB sample (polished section of the powered rock)

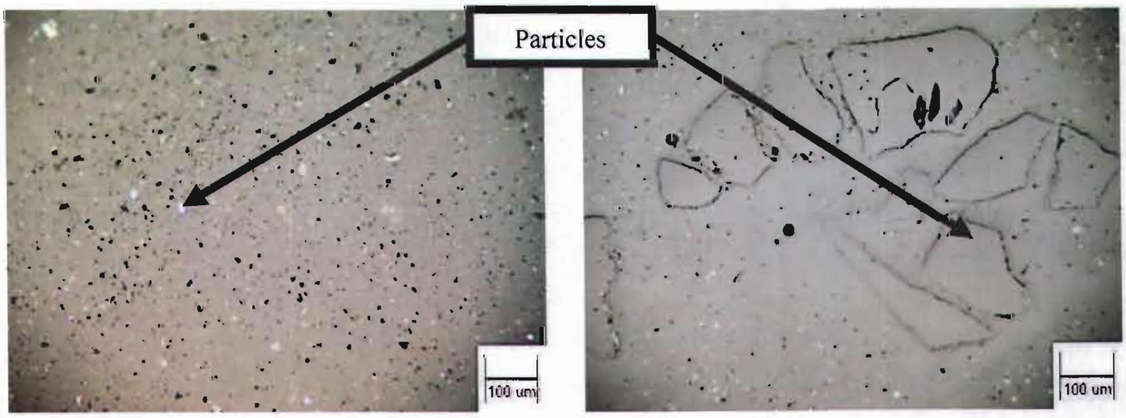

Figure 6.23: Photomicrographs of the untreated (left) and treated (right) JSC sample (polished section of the powered rock)

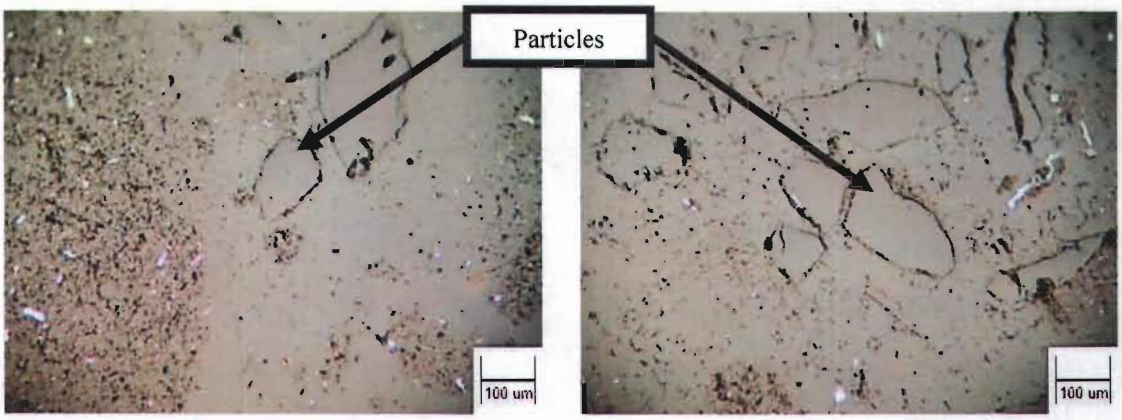

Figure 6.24: Photomicrographs of the untreated (left) and treated (right) JSD sample (polished section of the powered rock)

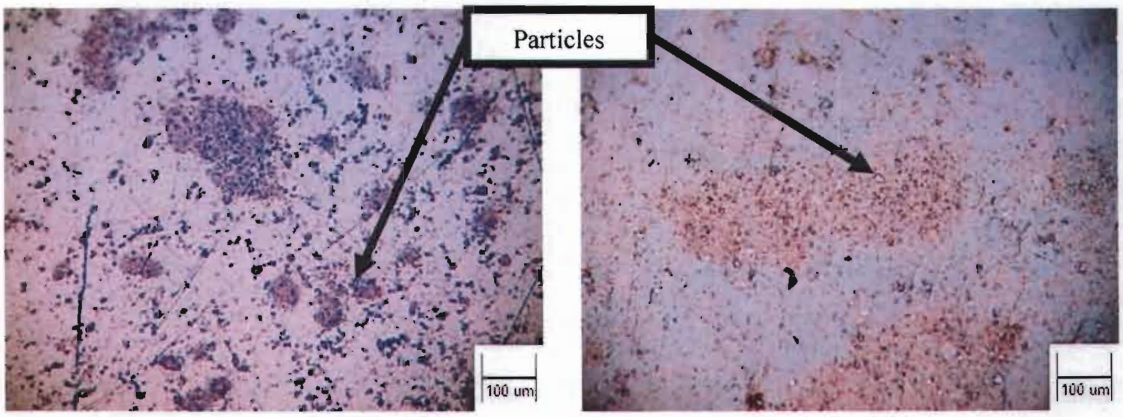

Figure 6.25: Photomicrographs of the untreated (left) and treated (right) JSE sample (polished section of the powered rock)

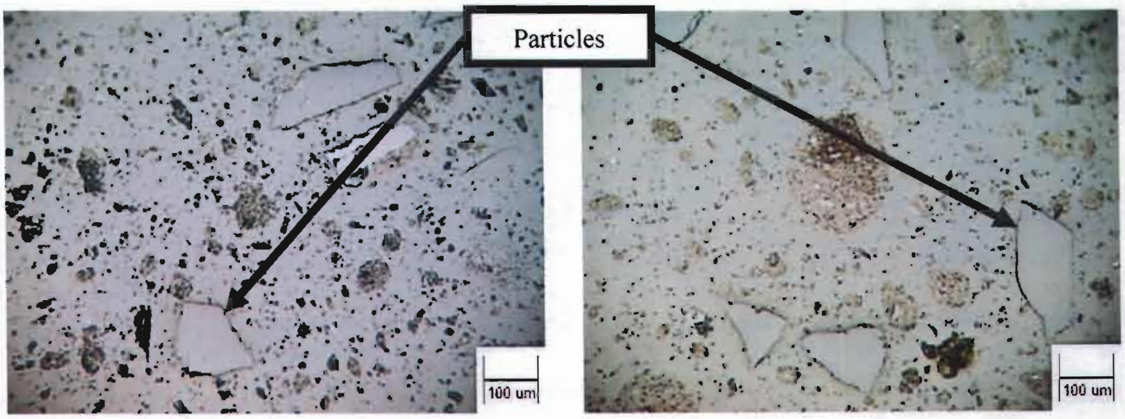

Figure 6.26: Photomicrographs of the untreated (left) and treated (right) JS1 sample (polished section of the powered rock)

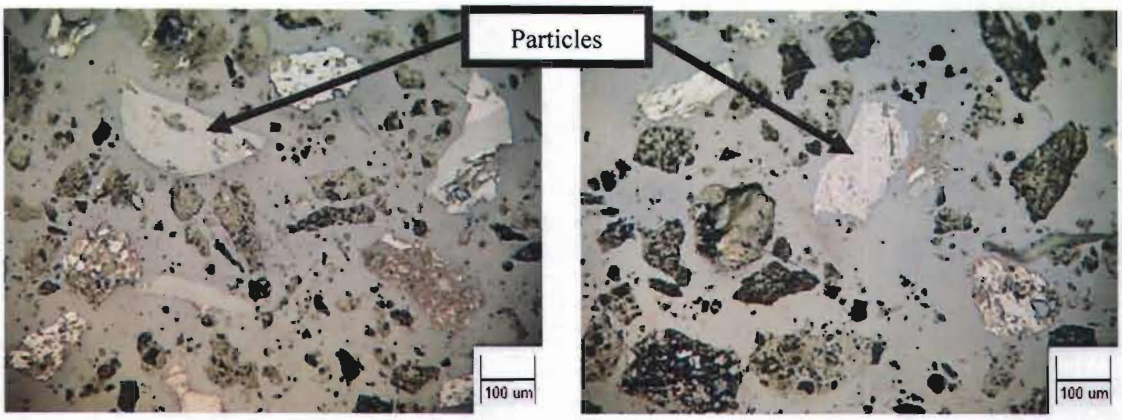

Figure 6.27: Photomicrographs of the untreated (left) and treated (right) JS2 sample (polished section of the powered rock)

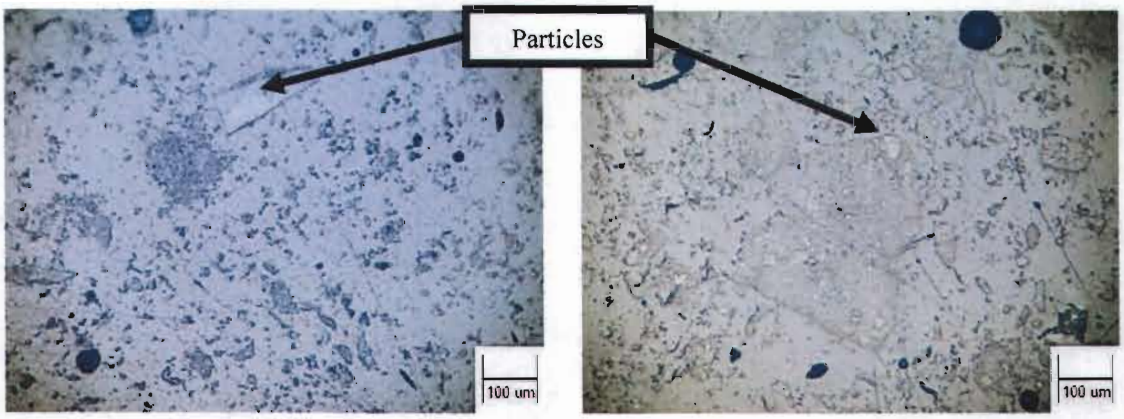

Figure 6.28: Photomicrographs of the untreated (left) and treated (right) JS3 sample (polished section of the powered rock)

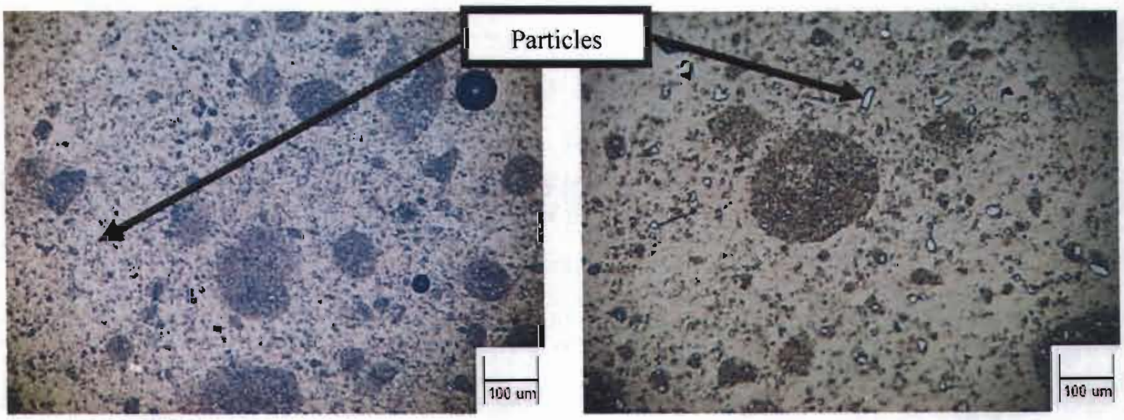

Figure 6.29: Photomicrographs of the untreated (left) and treated (right) JS4 sample (polished section of the powered rock)

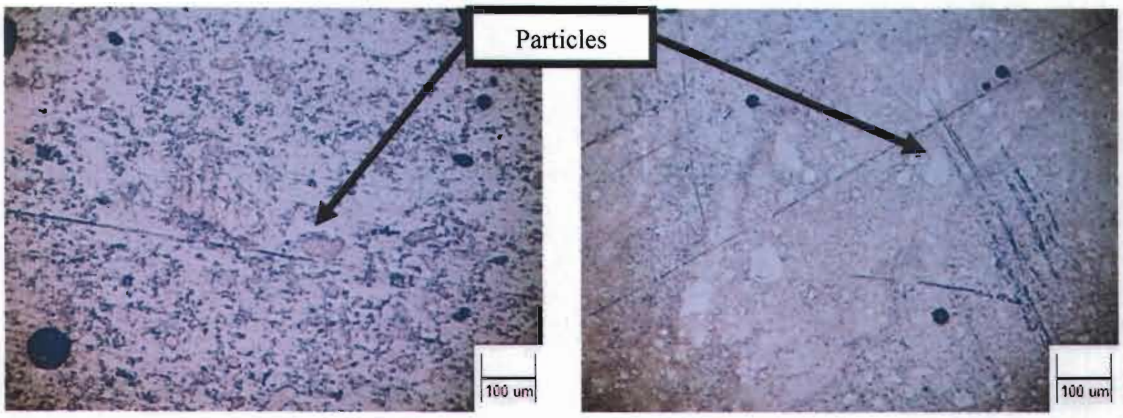

Figure 6.30: Photomicrographs of the untreated (left) and treated (right) JS5 sample (polished section of the powered rock)

6.4 Visual effects of RF heating on the rock samples and PPC

The transfer of RF power to the rock samples resulted in a surface temperature rise due to RF heating of the dielectric material. This transfer of RF power resulted in another significant effect being observed in the surface colour of the novel jig and PPC. Figure 6.31 indicates these visual colour changes of the PPC (a) and wooden clamp (b).

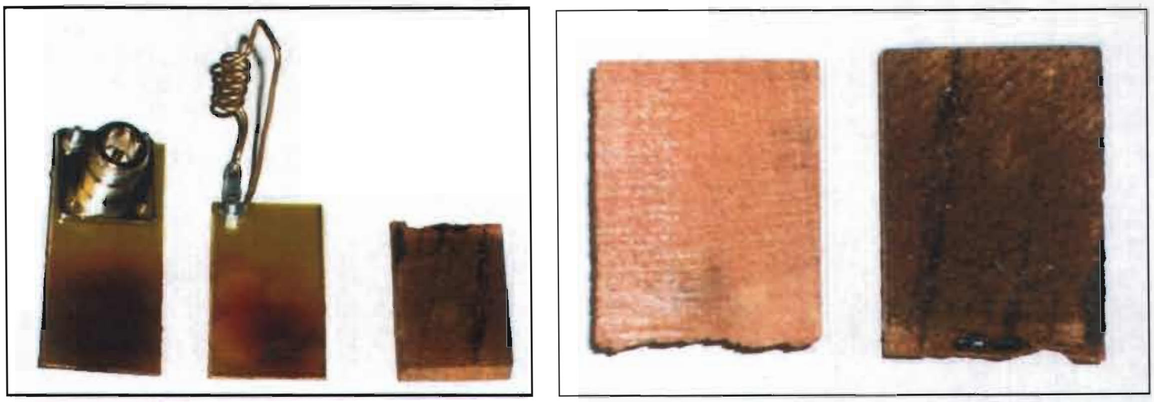

Figure 6.31: Effects of RF heating on the (a) PPC and (b) wooden clamp

Table 6.3 presents visual effects of RF heating on the first five rock samples (JSA – JSE), while Table 6.4 illustrates the next five samples (JS1 – JS5). Colour changes and maximum temperature reached with 82 W of RF power at 160 MHz is indicated.

Table 6.3: Surface colour changes and maximum temperatures reached for samples JSA – JSE (untreated on the left and treated on the right)

Sample code and type	Maximum temperature (Degrees Celsius)	Time (min)	Screen change	Colour change	Untreated sample	Treated sample
JSA 30 x 19 x 4 mm Dolerite Igneous	151	4	Yes	No		
JSB 31 x 19 x 4 mm Marble Metamorphic	107	2	No	Yes		
JSC 30 x 19 x 4 mm Granite Igneous	110	8	No	No		
JSD 30 x 19 x 4 mm Sandstone Sedimentary	55	5	Yes	No		
JSE 32 x 19 x 4 mm Mudstone Sedimentary	104	6	No	No		

Table 6.4: Surface colour changes and maximum temperatures reached for samples JS1 – JS5 (untreated on the left and treated on the right)

Sample code and type	Maximum temperature (Degrees Celsius)	Time (seconds)	Screen change	Colour change	Untreated sample	Treated sample
JS1 29 x 20 x 4 mm Marble Metamorphic	155	6	No	Yes		
JS2 30 x 19 x 4 mm Marble Metamorphic	158	3	No	Yes		
JS3 30 x 21 x 4 mm Marble Metamorphic	65	9	Yes	No		
JS4 30 x 20 x 4 mm Granite Igneous	66	6	No	No		
JS5 30 x 20 x 4 mm Marble Metamorphic	69	7	Yes	Yes		

6.5 Power usage of the practical setup and grinding mill

One of the aims of this research was to evaluate if the use of RF power would weaken mineral grain boundaries, leading subsequently to a reduction in energy consumption of current comminution equipment, such as the swing-pot mill. The electrical power consumed in treating the individual rock samples with 82 W, 90 W and 112 W of RF power is shown in Table 6.5. A photograph of the RF amplifiers is shown in Annexure 22.

Table 6.5: Power consumed by the RF equipment and grinding mill

Sample code	Rock sample	RF power (in W)	RF equipment (> 3 minutes) (power in W)	Grinding mill (2 minutes) (power in W)	Total power consumed (in W)
JSA	Dolerite	112	484	935	1419
JSB	Marble	90	437	920	1357
JSC	Granite	82	415	950	1365
JSD	Sandstone	90	437	920	1357
JSE	Mudstone	82	408	950	1358
JS1	Marble	82	415	950	1365
JS2	Marble	112	484	935	1419
JS3	Marble	82	412	950	1362
JS4	Granite	82	412	950	1362
JS5	Marble	82	412	950	1362

A consistent observation is that a higher RF power (112 W compared to 82 W) requires more energy from local energy utilities, such as ESKOM. The power consumed by the swing-pot mill for the untreated rock samples ranged from 920 – 950 W. The total power consumed by both the RF amplifiers and swing-pot mill varies between 1358 and 1419 W for the different rock samples. Subsequently it must be stated that no power reduction was realized, and therefore no improved efficiency was achieved with the RF treated samples.

6.6 Contrasting the resonating frequencies of the untreated and treated samples

S-parameters (in the form of Cartesian Coordinates) for the treated rock samples were also obtained from the network analyser. Equations listed in Annexure 23 were used to calculate the resonating frequency and resistance (Table 6.6) of the untreated and treated rock samples, which overlapped PPC-3 by 1 mm on either side (see Figure 4.13).

Table 6.6: Resonating frequencies for the untreated and treated rock samples

Sample code	Rock type	Untreated with 1 mm overlap		Treated with 1 mm overlap		Frequency variation (Percentage)	Resistance variation (Percentage)
		Frequency (MHz)	Resistance (Ohm)	Frequency (MHz)	Resistance (Ohm)		
JSA	Dolerite	160.14	1264	164.37	1319	2.6%	4.2%
JSB	Marble	162.58	1325	161.57	1467	-0.6%	9.7%
JSC	Granite	167.85	1545	166.57	1592	-0.8%	3.0%
JSD	Sandstone	170.08	1169	169.86	1292	-0.1%	9.5%
JSE	Mudstone	154.34	171	164.31	453	6.1%	62.3%
JS1	Marble	162.61	1630	162.48	1799	-0.1%	9.4%
JS2	Marble	159.74	940	159.82	1043	0.1%	9.9%
JS3	Marble	162.30	2037	160.78	2226	-0.9%	8.5%
JS4	Granite	165.14	1812	164.93	1988	-0.1%	8.9%
JS5	Marble	160.43	1339	159.22	1475	-0.8%	9.2%

No significant changes in resonating frequency (variation less than 1%) were observed between most of the rock samples as shown in Table 6.6. However, the treated JSA and JSE samples revealed a higher resonating frequency than the untreated samples, giving rise to a 2.6% and 6.1% variation. JSA and JSE were the only two samples with measureable amounts of T_1O_2. Moreover, the resistance of the JSE sample increased dramatically by 62.3%, while the resistance values of the other samples varied with less than 10%.

6.7 Summary

Chapter 6 presented the results of the textural, phase, grindability, colour and temperature changes for the treated rock samples. This analysis proved useful in identifying the chemical composition of the rocks as well as the rock type. The photomicrographs of the thin sections obtained from the untreated and treated samples revealed no fractures or breakages along the mineral grain boundaries. The grindability analysis of the untreated and treated samples indicated the particle size distribution for five different screens (250 µm, 150 µm, 90 µm, 38 µm and less than 38 µm). Significant variations between the particle size distribution of the JSA, JSD, JS3 and JS5 samples were observed. The photomicrographs from the polished sections indicated no differences in particle size reduction and shape between the untreated and treated samples. The amount of power used to mill the untreated and treated rock samples was consistently the same, being approximately 935 W.

Chapter 7 will present the conclusions and succinct recommendations.

Chapter 7 Conclusions and recommendations

7.1 Introduction

The final chapter of this research presents the conclusions reached with regard to the effects that RF power treatment exerts on specific rock samples. A brief review of what has been presented will first be given. The original purpose will be reviewed together with the various results. Recommendations for future research conclude this chapter.

7.2 Brief review

Chapter 1 presented the background to the possible use of RF power in assisting with rock comminution. The methodology and overview of the research were reviewed as well as the delimitations of the project, which does not include the design and development of a VHF amplifier. The importance of the research was highlighted with particular emphasis on significant contributions to the scientific community.

Chapter 2 reviewed the description and classification of minerals and rocks and their physical properties, followed by a more detailed description and characterization of ten rock samples chosen for this research. All three rock groups are represented with the majority of the samples being selected from the metamorphic group (five marble samples). The principles of rock comminution and mineral liberation were introduced as a possible objective of the research was to develop an alternative, non-conventional method to aid the comminution process.

Chapter 3 reviewed four current treatment techniques (microwave pre-treatment, ultrasound pre-treatment, high voltage electrical pulses and RF power) used to achieve specific goals with regard to various materials, specimens or liquids. Disadvantages of these treatment techniques included the use of sophisticated precision-type technology (such as the design and construction of the magnetron and cavity) requiring specialist knowledge and expensive equipment if meaningful results are to be obtained. Further disadvantages of using high voltage pulsed power included the relatively short lifetime of the spark-gap switches. Rationale for using RF power in the dielectric heating of materials was grounded in this review. A new electrical treatment technique for rocks was introduced based on RF heating of materials. The practical setup of the equipment used in the transfer of RF power to a dielectric material was covered.

Chapter 4 presented various RF electrical properties associated with dielectric materials, reviewing two current RF methods of connecting dielectric materials to electrical test equipment, being the cylindrical and parallel-plate capacitor (PPC). Significant advantages associated with the PPC included its simplicity and ease of connection, and was therefore chosen as the preferred coupling device. A PPC with dimensions 28 x 47 mm was used in subsequent measurements with a network analyser to determine the resonating frequency of ten specific rock samples. The primary reason for using this type of PPC (being PPC-3) was because the rock samples resonating frequency coincided with the frequency range of commercially available VHF amplifiers. Readings between 30 and 300 MHz were recorded in the form of comprehensive S-parameters, which were subsequently used in the mathematical modelling of the phase angle to frequency equation for each rock sample. Resonance, resistivity and conductivity graphs were included for the JSA sample. However initial results from the network analyser revealed that the impedance of the rock samples at resonance varied from 171 + jX Ω to around 2037 + jX Ω. This impedance could not be directly connected to the output of a RF amplifier which has an output impedance of 50 Ω. This large mismatch would result in a high percentage of forward power (power coming from the source) being reflected back (from the load) towards the transmitter and thereby damaging it.

Chapter 5 subsequently discussed impedance matching as an important requirement in assuring MPT between the source (RF amplifier) and the load (dielectric material in the PPC). These matching networks are effectively band pass filters offering the required impedance transformation. A Pi type network was chosen as the preferred matching network due to the fact that it can match a large range of impedances (made possible by the parallel variable capacitors) and because it posses only one series component (the inductor). The matching network was analysed and evaluated by means of a simulation model (in SIMetrix) and a practical model (using a network analyser and a practical experiment). The results indicated reliability and validity of the matching network as a low SWR reading was achieved. Subsequent maximum forward power into the rock sample from the RF amplifiers was realized. A unique value for the coupling coefficient of the PPC was presented based on power and temperature measurements used in conjunction with the specific heat capacity of the individual rocks. Initial observations relating to the temperature rise of the sample verified that input power rather than resonating frequency is critical in the successful transfer of RF power to a dielectric material.

Chapter 6 introduced the effects of RF treatment on the rock samples. The possible changes that were considered included textural, phase, grindability, colour and temperature changes. Significant variations between the particle distribution of the JSA, JSD, JS3 and JS5 samples were observed, which indicated rock strengthening. The amount of power used to mill the untreated and treated samples was revealed to be the same, around 935 W.

7.3 Conclusions

One of the primary aims of this research was to design and develop a suitable coupling device to connect relevant electronic equipment (test instruments and amplifiers) to various rock samples. MPT to the rock sample at a specific frequency of operation was noted to be of greatest importance. This was achieved with the use of a PPC and matching network housed in a novel wooden jig. Inserting specific sized rock samples into this coupling device proved simple and effective, being neither time consuming or difficult. Similarly, tuning the capacitors to obtain a SWR close to one for each rock sample was easily done with the use of the network analyser.

This research further highlighted that the input power rather than the resonating frequency is critical to the successful transfer of power to rock samples within a PPC.

The rise in temperature as well as change in particle size distribution for different input frequencies substantiates this claim. However, there may still be other frequencies within the UHF range which could result in more textural changes within specified rock samples.

This research made **four valuable scientific contributions** to the fields of metallurgical and electrical engineering. Firstly, it introduced a **new technique for the treatment of rock samples**, being the use of RF power. The effect of RF power on the textural changes of the rocks was presented in Chapter 6.

Using RF power in heating specific rock samples could subsequently be used in the colouring of rock surfaces. However, only four samples (JSA, JSD, JS3 and JS4) revealed a notable change in their particle size distribution. The fact that the percentage of larger sized particles increased (from 38 μm to 90 μm as seen in Chapter 6) suggests that the rock was **strengthened** rather than weakened. A possible application could be the prevention of over grinding during comminution, which may have benefits during mineral processing.

Secondly, **an innovative coupling technique** to connect rock samples to high powered RF electronic equipment, using a PPC with dimensions of 28 x 47 mm, was described. The feasibility of this technique was confirmed by repeated correlated measurements taken on a vector voltmeter and network analyser. Low SWR readings obtained from a RF Wattmeter in a practical setup also proved the viability of the matching network used in the coupling technique.

Thirdly, **an original coupling coefficient** (81.58×10^{-3}) for the PPC was presented. This value may be used in similar sized capacitors to determine the specific heat capacity of dielectric materials. However, the value of the coupling coefficient was only verified for seven out of the ten rock samples. The value of the coupling coefficient should hold true for all rock samples, as it represents the coupling of energy between the PPC and rock sample. This suggests that the specific heat capacity for white marble or white granite should be higher (around 3200 J/kg/°C for marble and 2800 J/kg/°C for granite) than those values for dark coloured samples. No current literature was found to substantiate this claim.

Finally, this research **defined the mathematical models** for 10 rock samples for the VHF range of frequencies (30 – 300 MHz), providing unique phase angle to resonance equations for each sample. These equations can be used with each specific rock to determine the resonating frequency where the maximum current flows and the minimum resistance is present.

Current physical methods used for crushing of rocks in the mineral processing industry result in erratic breakages that do not efficiently liberate the economically valuable minerals. The purpose of this research was to evaluate the effect that RF power exerts on rock samples with particular focus on textural changes. This evaluation brought to light that mineral grain boundaries within ten specified rock samples treated with RF power are not significantly weakened. This was firstly determined by the similar electrical properties of the untreated and treated samples, where consistent values for resonating frequency were obtained from the network analyser. This was clarified by the SEM analysis of the untreated and treated samples. Photomicrographs obtained for both samples revealed no significant changes in the form of fractures or breakages along the mineral grain boundaries. The particle size distribution after milling of both samples further revealed no weakening or softening of the rock, as the percentage of smaller sized particles did not increase in the treated samples. Therefore, it may be stated that treating rock samples with RF power within the VHF range may not significantly improve rock comminution and mineral liberation.

7.4 Recommendations

This research incorporated the use of commercially available RF amplifiers in the RF heating of a dielectric material housed within a PPC. The transfer of 82 W of RF power at 160 MHz to a specific sample size proved significant in changing the particle size distribution of dolerite (JSA), sandstone (JSD) and marble (JS3 and JS5) samples. The particle size distribution of other treated rock samples may through be influenced through use of a higher input power, around 500 W. This may be the focus of future research in evaluating the effects of RF power on textural changes of rocks.

The effect of RF heating on the PPC was also shown to be significant, with burn marks evident on the copper conducting plates. In two instances, 112 W of RF power was transferred to the dielectric material housed in the PPC. However, this resulted in arcing within the variable capacitors, and a subsequent dramatic increase in the SWR. Larger power handling capacitors will therefore be required if the input power is to be increased to 500 W. Thicker copper plates will further be required to handle the larger amount of RF power.

The methods that have been developed here could be applied in determining the electrical properties of rocks, which in turn, may find use in other geophysical applications.

Future research surrounding the effects of RF power on the textural changes of rocks is limitless and begs the attention of dedicated researches in the field of metallurgical and electrical engineering to “find remedies in the thorniest of trees”.

REFERENCES

ABRIE, P. L. D. 1999. *Design of RF and Microwave Amplifiers and Oscillators.* Boston: Artech House.

AGILENT TECHNOLOGIES. 2003. The Impedance Measurement handbook. A guide to Measurement Technology and Techniques. [Online] Available at: http://literature.agilent.com/LitWeb/Admin/SNSelectForTM.cfm, Accessed on 1 August, 2003

AMANKWAH, R. K., KHAN, A. U., PICKLES, C. A. & YEN, W. T. 2005. Improved grindability and gold liberation by microwave pretreatment of a free-milling gold ore. *International Journal of Mineral Processing and Extractive Metallurgy Review,* 114(C): 30-36.

AMETHYST GALLERIES. 2000. The physical characteristics of Minerals. [Online] Available at: http://mineral.galleries.com/minerals/physical.htm#phy, Accessed on 22 July, 2005

AMIDROR, I. & HERSCH, R. D. 2009. The role of Fourier theory and of modulation in the prediction of visible moirÃ© effects. *Journal of Modern Optics,* 56(9): 1103 - 1118.

AMPSA. 2009. The Ultimate in Microwave and RF Amplifier Design Software. [Online] Available at: http://www.ampsa.com/, Accessed on 26 November, 2009

ANDRES, U., TIMOSHKIN, I. & SOLOVIEV, M. 2001. Energy consumption and liberation of minerals in explosive electrical breakdown of ores. *Mineral Processing and Extractive Metallurgy: Transactions of the Institute of Mining and Metallurgy, Section C,* 110149-157.

AZIMI, P. & GOLNABI, H. 2009. Precise formulation of electrical capacitance for a cylindrical capacitive sensor. *Journal of Applied Science,* (9): 1556-1561.

BAGDASSAROV, N. S. & SLUTSKII, A. B. 2003. Phase transformations in calcite from electrical impedance measurements. *Phase Transitions: A Multinational Journal,* 76(12): 1015 - 1028.

BAKER, R. J. & JOHNSON, B. P. 1993. Applying the Marx bank circuit configuration to power MOSFETs. *Electronics Letters,* 29(1): 56-57.

BEASLEY, J. S. & MILLER, G. M. 2008. *Modern Electronic Communication.* New Jersey: Pearson Prentice-Hall.

BELEZNAI, S. 2009. *Development of mercury-free dielectric barrier discharge light sources.* Budapest: Budapest University of Technology and Economics.

BERRY, T. F. & BRUCE, R. W. 1966. A Simple Method of Determining the Grindability of Ores. *Canadian Mining Journal,* 196663-65.

BEST, M. G. & CHRISTIANSEN, E. H. 2001. *Igneous Petrology.* Massachusetts: Blackwell Science.

BOWICK, C., BLYLER, J. & AJLUNI, C. 2008. *RF circuit design.* 2nd Ed. Amsterdam: Elsevier.

BRADSHAW, S. M., VAN WYK, E. J. & DE SWARDT, J. B. 1998. Microwave heating principles and the application to the regeneration of granular activated carbon. *The Journal of The South African Institute of Mining and Metallurgy,* July/August201-210.

BUDENSTEIN, P. P. 1980. One mechanism of breakdown in solids. *IEEE Transactions on Electrical Insulation,* 225-240.

BUSSEY, H. E. 1979. Microwave dielectric measurements of lunar soil with a coaxial line resonator method. *10th Lunar and Planetary Science Conference.* Houston, Texax, 19-23 March.

BUTKEWITSCH, S. & SCHEINBEIM, J. 2006. Dielectric properties of a hydrated sulfonated poly(styrene-ethylene/butylenes-styrene) triblock copolymer. *Applied Surface Science,* 252(23): 8277-8286.

CARLSON, D. H., PLUMMER, C. C. & MCGEARY, D. 2008. *Physical Geology: Earth Revealed.* 7th Ed. New York: McGraw-Hill.

CARR, J. 2002. *RF components and circuits.* Oxford: Newnes.

CHEE, S. N., JOHANSEN, A. L., GU, L., KARLSEN, J. & HENG, P. W. S. 2005. Microwave Drying of Granules Containing a Moisture-Sensitive Drug: A Promising Alternative to Fluid Bed and Hot Air Oven Drying. *Chemical & Pharmaceutical Bulletin,* 53(7): 770-775.

CHEN, T. T., DUTRIZAC, J. E., HAQUE, K. E., WYSLOUZIL, W. & KASHYAP, S. 1984. The relative transparency of minerals to microwave radiation. *Canadian*

Metallurgical Quarterly, 23(3): 349-351.

CHEN, X., ZHOU, D., HUANG, G., XU, J., ZHANG, D. & LU, W. 2003. A new method for microwave dielectric measurement of low loss ceramics. *Materials Science and Engineering B,* 99(1-3): 390-393.

CHERNICOFF, S. & FOX, H. A. 1997. *Essential of Geology.* New York: Worth Publishers.

CHO, S. H., MOHANTY, B., ITO, M., NAKAMIYA, Y., OWADA, S., KUBOTA, S., OGATA, Y., TSUBAYAMA, A., YOKOTA, M. & KANEKO, K. 2006. Dynamic fragmentation of rock by high-voltage pulses. *The 41st U.S. Symposium on Rock Mechanics (USRMS).* Golden, Colorado, June 17-21.

COLLET, L. S. & KATSUBE, T. J. 1973. Electrical parameters of rocks in developing geophysical techniques. *Geophysics,* 38(1): 76-91.

DANA, J. D. 1963. *Dana's manual of mineralogy.* 17th Ed. New York: John Wiley and Sons.

DANIELS, J. J. & DYCK, A. V. 1984. Borehole resistivity and electromagnetic methods applied to mineral exploration. *IEEE Geoscience and Remote Sensing Society,* 1(22): 80-87.

DEISTER, R. J. 1987. How to determine the Bond work index using lab ball mill grindability tests. *Engineering and Mining Journal,* 188(2): 42-45.

DEV, S. R. S., PADMINI, T., ADEDEJI, A., GARIEPY, Y. & RAGHAVAN, G. S. V. 2008. A comparative study on the effect of chemical, microwave, and pulsed electric pretreatments on convective drying and quality of raisins. *Drying Technology,* 26(10): 1238-1243.

DIETRICH, R. V. & SKINNER, B. J. 1979. *Rocks and rock minerals.* New York: John Wiley and Sons.

DING, J., LILIENTAL-WEBER, Z., WEBER, E. R., WASHBURN, J., FOURKAS, R. M. & CHEUNG, N. W. 1988. Structure and electrical properties of TIN/GaAs Schottky contacts. *American Institute of Physics,* 52(25): 2160.

DYAL, P. & PARKIN, C. W. 1973. Global electromagnetic induction in the moon and planets. *Physics of the Earth and Planetary Interiors,* 7251-265.

EFFECTIVE LABORATORY SUPPLIES. 2010. [Online] Available at:

http://www.effectivelab.co.za/, Accessed on 15 May 2010,

EVANS, I. O. 1972. *Rocks, Minerals & Gemstones.* London: The Hamlyn Publishing Group.

EVERARD, J. 2001. *Fundamentals of RF Circuit Design with Low Noise Oscillators.* Chichester: John Wiley & Sons.

FONTANA, R. J. 2004. Recent System Applications of Short-Pulse Ultra-Wideband (UWB) Technology. *IEEE Transactions on Microwave Theory and Techniques,* 52(9): 2087-2104.

FRENZEL, L. E. 2001. *Communication Electronics Principles and Applications.* 3rd Ed. New York: Glencoe/McGraw-Hill.

FRENZEL, L. E. 2003. *Principles of Electronic Communication Systems.* 2nd Ed. New York: McGraw-Hill.

GAETE-GARRETÓN, L., VARGAS-HERNANDEZ, Y., CHAMAYOU, A., DODDS, J. A., VALDERAMA-REYES, W. & MONTOYA-VITINI, F. 2003. Development of an ultrasonic high-pressure roller press. *Chemical Engineering Science,* 58(19): 4317-4322.

GAETE-GARRETÓN, L. F., VARGAS-HERMÁNDEZ, Y. P. & VELASQUEZ-LAMBERT, C. 2000. Application of ultrasound in comminution. *Ultrasonics,* 38(1-8): 345-352.

GÄRTNER, W. 1953. Über die Möglichkeit der zerkleinerung suspendierter stoffe durch ultrashall. *Acustica,* 3124-128.

GIACOLETTO, L. J. 1977. *Electronics Designers' Handbook.* 2nd. New York: McGraw-Hill.

GIANCOLI, D. C. 2005. *Physics - principles with applications.* 6th Ed. New Jersey: Pearson Prentice Hall.

GREBENNIKOV, A. 2005. *RF and microwave power amplifier design.* New York: McGraw-Hill.

GRIFFITH, A. A. 1921. The phenomena of rupture and flow in solids. *Philosophical Transactions of the Royal Society of London,* 221163-198.

HALVERSON, S. L., BURKHOLDER, W. E., BIGELOW, T. S., NORSHEIM, E. V. & MISENHEIMER, M. E. 1996. High-power microwave radiation as an alternative insect control method for stored products. *J. Econ. Entomol,* 891638-1648.

HAMMON, J., HOPWOOD, D., INGRAM, M., KLATT, M. & TATMAN, T. 2000. Electric pulse rock sample disaggregator. *24th International Power Modulator Symopsium.* Norfolk, Virginia, 26-29 June.

HAQUE, K. E. 1999. Microwave energy for mineral treatment processes—a brief review. *Int. J. Miner. Process,* 571-24.

HENAN CHUANGXIN CO. 2009. Building-material Equipment. [Online] Available at: http://www.enchuangxin.com/Mineral%20Processing%20Equipment/, Accessed on 6 November, 2009

HICKMAN, I. 2007. *Practical RF handbook.* 4th Ed. Amsterdam: Elsevier - Newnes.

HU, Z., WANG, Y. & WEN, Z. 2008. Alkali (NaOH) pretreatment of switchgrass by radio frequency-based dielectric heating. *Applied Biochemistry and Biotechnology,* 148(1-3): 71-81.

HU, Z. & WEN, Z. 2008. Enhancing enzymatic digestibility of switchgrass by microwave-assisted alkali pretreatment. *Biochemical Engineering Journal,* 38(3): 369-378.

HUTCHINSON, C. (Ed.) 2001. *The ARRL Handbook for Radio Amateurs,* Newington: ARRL.

HUTTON, V. R. S. 1976. The electrical conductivity of the Earth and planets. *Reports on Progress in Physics,* 39487-572.

IKEDIALA, J. N., HANSEN, J. D., TANG, J., DRAKE, S. R. & WANG, S. 2002. Development of a saline water immersion technique with RF energy as a postharvest treatment against codling moth in cherries. *Postharvest Biology and Technology,* 24209-221.

INGLIS, C. E. 1913. Stresses in a plate due to the presence of cracks and sharp corners. *Transactions of the Institution of Naval Architects 55,* 55219-230.

IXER, R. A. & DULLER, A. R. 1998. Virtual Atlas of Opaque and Ore Minerals in their Associations. [Online] Available at: http://www.smenet.org/opaque-ore/, Accessed on 5 February, 2010

JONES, D. A., KINGMAN, S. W., WHITTLES, D. N. & LOWNDES, I. S. 2007. The influence of microwave energy delivery method on strength reduction in ore samples. *Chemical Engineering and Processing,* 46(4): 291-299.

JONES, D. A., LELYVELD, T. P., MAVROFIDIS, S. D., KINGMAN, S. W. & MILES, N. J. 2002. Microwave heating applications in environmental engineering--a review. *Resources, Conservation and Recycling,* 34(2): 75-90.

KANDALA, C. V. K. & NELSON, S. O. 2007. RF impedance method for nondestructive moisture content determination for in-shell peanuts. *Measurement Science and Technology,* 18991-996.

KASAP, S. O. 2006. *Principles of Electronic Materials and Devices.* 3rd. Boston: McGraw-Hill.

KAWALA, Z. & ATAMANCZUK, T. 1998. Microwave-enhanced thermal decontamination of soil. *Environmental Science and Technology,* 32(17): 2602-7.

KEHEW, A. E. 1995. *Geology for Engineers and Environmental Scientists.* 2nd Ed. New Jersey: Prentice-Hall.

KELLY, R. M. & ROWSON, N. A. 1995. Microwave reduction of oxidised ilmenite concentrates. *Minerals Engineering,* 8(11): 1427-1438.

KING, R. P. 2001. *Modelling and simulation of mineral processing systems.* Oxford: Butterworth-Heinemann.

KINGMAN, S. W., JACKSON, K., CUMBANE, A., BRADSHAW, S. M., ROWSON, N. A. & GREENWOOD, R. 2004. Recent developments in microwave-assisted comminution. *Int. J. Min. Proc,* 74(1-4): 71-83.

KLEIN, C. 2002. *The 22nd edition of the manual of Mineral Science.* New York: John Wiley & Sons.

KOSTAROPOULOS, A. E. & SARAVACOS, G. D. 1995. Microwave Pre-treatment for Sun-Dried Raisins. *Journal of Food Science,* 60(2): 344-347.

KU, H. S., BALL, J. A. R., SIORES, E. & HORSFIELD, B. 1999. Microwave processing and permittivity measurement of thermoplastic composites at elevated temperature. *Journal of Materials Processing Technology,* 89-90419-424.

LEACH, M. F. & RUBIN, G. A. 1988. Fragmentation of Rocks Under Ultrasonic Loading. *Ultrasonic Symp of the IEEE.* Chicago, USA,

LEVIN, J. 1989. Observations on the bond standard grindability test and a proposal for a standard grindability test for fine materials. *Journal of the South African Institute*

Mining and Metallurgy, 89(1): 13-21.

LEVITSKAYA, T. M. & STERNBERG, B. K. 2000. Laboratory measurement of material electrical properties: extending the application of lumped-circuit equivalent models to 1 GHz. *Radio Science,* 35(2): 371-383.

LI, X., ZHANG, B., LI, W. & LI, Y. 2005. Research on the effect of microwave pretreatment on moisture diffusion coefficient of wood. *Wood Science and Technology,* 39(7): 521-528.

LU, L., SHEN, Y., CHEN, X., QIAN, L. & LU, K. 2004. Ultrahigh Strength and High Electrical Conductivity in Copper. *Science,* 304(5669): 422-426.

MCGEARY, D., PLUMMER, C. C. & CARLSON, D. 2001. *Physical Geology EARTH REVEALED.* 4th Ed. New York: WCB/McGraw-Hill.

MESERVE, M. E. 2009. Javascripe Electronic Notebook Single-Layer Air-Core Inductor Design. [Online] Available at: http://www.k7mem.150m.com/Electronic_Notebook/inductors/coildsgn.html#Initial_Design, Accessed on 21 December, 2009

MONTALBO-LOMBOY, M., SRINIVASAN, G., RAMAN, D. R., ANEX JR, R. P. & GREWELL, D. 2007. Influence of ultrasonics in ammonia steeped switchgrass for enzymatic hydrolysis. *2007 ASABE Annual International Meeting, Technical Papers.* Minneapolis, MN, United states,

MORAN, C. 2009. Submission to the Australian Government Energy White Paper. University of Queensland, Sustainable Minerals Institute.

MUSSET & KHAN, A. U. 2000. *Looking into the earth An introduction to geological geophysics.* New York: Cambridge University Press.

NELSON, S. O. 1996. Review and assessment of radio-frequency and microwave energy for stored-grain insect control. *Trans. ASAE,* 391475-1484.

NITAYAVARDHANA, S., RAKSHIT, S. K., GREWELL, D., VAN LEEUWEN, J. & KHANAL, S. K. 2008. Ultrasound pretreatment of cassava chip slurry to enhance sugar release for subsequent ethanol production. *Biotechnology and Bioengineering,* 101(3): 487-496.

NOVER, G. 2005. Electrical properties of crustal and mantle rocks – a review of laboratory measurements and their explanation. *Surveys in Geophysics,* 26593-

651.

OESPCHUCK, J. M. 1984. A history of microwave heating applications. *IEEE Transactions on Microwave Theory and Techniques,* 32(9): 1200-1224.

ORR, W. I. 1997. *Radio Handbook.* 23rd Ed. Boston: Butterworth-Heinemann.

OWADA, S., ITO, M., OTA, T., NISHIMURA, T., ANDO, T., YAMASHITA, T. & SHINOZAKI, S. 2003. Application of electrical disintegration to coal. *22th International Mineral Processing Congress.* Cape Town, South Africa, 28 September - 3 October.

PAN, S., LO, K. V., PING, H. L. & SCHREIER, H. 2006. Microwave pretreatment for enhancement of phosphorus release from dairy manure. *Journal of Environmental Science and Health - Part B Pesticides, Food Contaminants, and Agricultural Wastes,* 41(4): 451-458.

PENG, B., SHI, B., SUN, D., CHEN, Y. & SHELLY, D. C. 2007. Ultrasonic effects on titanium tanning of leather. *Ultrasonics Sonochemistry,* 14(3): 305-313.

PERKINS, D. 1998. *Mineralogy.* New Jersey: Prentice Hall.

PHILIPS, W. J. 1984. Resonance effects in complex resistivity data and their significance in mineral exploration. *Institution of mining and metallurgy transactions,* 93(February): 1-11.

PIENAAR, H. C. 2002. *Design and development of a class E dielectric blood heater.* DTech. Vanderbijlpark: Vaal Triangle Technikon.

POZAR, D. M. 2005. *Microwave Engineering.* 3rd Ed. Massachusetts: John Wiley & Sons.

READ, H. H. 1984. *Rutley's elements of mineralogy.* 26th Ed. London: George Allen & Unwin.

ROLAND, U., BUCHENHORST, D., HOLZER, F. & KOPINKE, F. D. 2008. Engineering Aspects of Radio-Wave Heating for Soil Remediation and Compatibility with Biodegradation. *Environmental Science & Technology,* 42(4): 1232-1237.

ROUSE, J. A. (Ed.) 1962. *The Amateur Radio Handbook,* London: Radio Society of Great Britain.

ROY, I., MONDAL, K. & GUPTA, M. N. 2003. Accelerating Enzymatic Hydrolysis of

Chitin by Microwave Pretreatment. *Biotechnology Progress,* 19(6): 1648-1653.

RUTSCHLIN, M., CLOETE, J. H. & PALMER, K. D. 2006. A guarded cylindrical capacitor for the non-destructive measurement of hard rock core samples. *Measurement Science and Technology,* 17(6): 1390-1398.

SAINATI, R. A. 1996. *CAD of microstrip antennas for wireless applications.* Boston: Artech House.

SCOTT, G., BRADSHAW, S. M. & EKSTEEN, J. J. 2008. The effect of microwave pretreatment on the liberation of a copper carbonatite ore after milling. *International Journal of Mineral Processing,* 85121-128.

SHAFIEE, S. & TOPAL, E. 2009. When will fossil fuel reserves be diminished? *Energy Policy,* 37(1): 181-189.

SIMETRIX TECHNOLOGIES LTD. 2009. Homepage. [Online] Available at: http://www.simetrix.co.uk/, Accessed on 10 January, 2009

SKINNER, B. J. & PORTER, S. C. 1992. *The Dynamic Earth an introduction to physical geology.* 2nd Ed. New York: John Wiley & Sons.

SMITH, R. D. 1993. Large industrial microwave power supplies. *Proc. Microwave-Induced reactions workshops.* Pacific Grove, California,

SMITH, R. W. & LEE, K. H. 1968. A comparison of data from Bond type simulated closed-circuit and batch type grindability tests. *Transactions of the Society of Mineral Engineering,* 24191-99.

SOLENHOFEN, A. 2003. Rock properties and their importance to stoneworking, carving, and lapidary working of rocks and minerals by the ancient Egyptians. [Online] Available at: http://www.geocities.com/unforbidden_geology/rock_properties.htm#a%29%20Rock%20hardness, Accessed on 2 August, 2005

SOMASUNDARAN, P. & SHROTI, S. (Eds.) 1995. *Grinding aids: A review of their use, effects and mechanisms,* New Delhi: Wiley Eastern Limited.

SPIERINGS, E. L. H., BREVARD, J. A. & KATZ, N. P. 2008. Two-Minute Skin Anesthesia Through Ultrasound Pretreatment and Iontophoretic Delivery of a Topical Anesthetic: A Feasibility Study. *Pain Medicine,* 9(1): 55-59.

STASZEWSKI, L. 2010. Lightning Phenomenon – Introduction and Basic Information to

Understand the Power of Nature. *International Conference Environment and Electrical Engineering 2010.* Prague, Czech Republic, 16-19 May.

SWART, A. J., PIENAAR, H. C. V. & MENDONIDIS, P. 2009a. Investigating the use of RF power in rock comminution. *New Generation University Conference.* Emerald Casino Resort, Vanderbijlpark, RSA, 17-19 November 2009.

SWART, A. J., PIENAAR, H. C. V. & MENDONIDIS, P. 2005. Radio frequencies effect on rock comminution. *Annual Faculty Research Seminar, Vaal University of Technology.* Emfuleni Conference Centre, Vanderbijlpark, July.

SWART, A. J., PIENAAR, H. C. V. & MENDONIDIS, P. 2009b. RF radiation of calcite/dolomite samples *Die Suid-Afrikaanse Akademie vir Wetenskap en Kuns - Studentesimposium 2009.* University of the Free State, Bloemfontein, 29-30 October 2009.

SWART, J., MENDONIDIS, P. & PIENAAR, C. 2009c. The Electrical Properties of Chlorite Tremolite Marble measured for a range of Radio-Frequencies. *Mineral Processing and Extractive Metallurgy Review: An International Journal,* 30(4): 307 - 326.

TARBUCK, E. J. & LUTGENS, F. K. 1999. *Earth An introduction to physical geology.* 6th Ed. New Jersey: Prentice Hall.

THOMPSON, G. R. & TURK, J. 1997. *Modern Physical Geology.* 2nd Ed. New York: Saunders College Publishing.

THOMPSON, G. R. & TURK, J. 2007. *Earth Science and the Environment.* 4th Ed. Belmont: Thompson Brooks/Cole.

TIEHM, A., NICKEL, K. & NEIS, U. 1997. The use of ultrasound to accelerate the anaerobic digestion of sewage sludge. *Water Science and Technology,* 36121-128.

TOURYAN, K. J. & BENZE, J. W. 1991. Enhanced Coal Comminution And Beneficiation using Pulsed Power Generated Shocks. *Pulsed Power Conference, 8th IEEE International.* San Diego, California, 16-19 June.

TREFIL, J. & HAZEN, R. M. 2007. *The Sciences An integrated approach.* 5th Ed. New York: John Wiley and Sons.

TROMANS, D. 2008. Mineral comminution: Energy efficiency considerations. *Minerals Engineering,* 21(8): 613-620.

UQUICHE, E., JEREZ, M. & ORTIZ, J. 2008. Effect of pretreatment with microwaves on mechanical extraction yield and quality of vegetable oil from Chilean hazelnuts (Gevuina avellana Mol). *Innovative Food Science and Emerging Technologies,* 9(4): 495-500.

WALKIEWICZ, J. W., KAZONICH, G. & MCGILL, S. L. 1988. Microwave heating characteristics of selected minerals and compounds. *Minerals and Metallurgical Processing,* 39-42.

WALTHER, J. V. 2005. *Essentials of geochemistry.* Massachusetts: Jones & Bartlett Publishers.

WANG, S., BIRLA, S. L., TANG, J. & HANSEN, J. D. 2006. Postharvest treatment to control codling moth in fresh apples using water assisted radio frequency heating. *Postharvest Biology and Technology,* 40(1): 89-96.

WANG, S., IKEDIALA, J. N., TANG, J., HANSEN, J. D., MITCHAM, E., MAO, R. & SWANSON, B. 2001. Radio frequency treatments to control codling moth in in-shell walnuts. *Postharvest Biology and Technology,* 2229-38.

WANG, Y. & FORSSBERG, E. 2007. Enhancement of energy efficiency for mechanical production of fine and ultra-fine particles in comminution. *China Particuology,* 5(3): 193-201.

WAPLES, D. W. & WAPLES, J. S. 2004. A Review and Evaluation of Specific Heat Capacities of Rocks, Minerals, and Subsurface Fluids. Part 1: Minerals and Nonporous Rocks. *Natural Resources Research,* 13(2): 97-122.

WENK, H. R. & BULAKH, A. 2004. *Minerals their Constitution and Origin.* Cambridge: Cambridge University Press.

WHITAKER, J. C. (Ed.) 2002. *The RF Transmission Systems Handbook,* Boca Raton: CRC Press.

WILLS, B. A. 1992. *Mineral processing technology.* 5th Ed. Oxford: Pergamon Press.

WILSON, M. P., BALMER, L., GIVEN, M. J., MACGREGOR, S. J., MACKERSIE, J. W. & TIMOSHKIN, I. V. 2006. Application of electric spark generated high power ultrasound to recover ferrous and non-ferrous metals from slag waste. *Minerals Engineering,* 19(5): 491-499.

WINANDS, G. J. J., LIU, Z., PEMEN, A. J. M., VAN HEESCH, E. J. M. & YAN, K.

2005. Long lifetime, triggered, spark-gap switch for repetitive pulsed power applications. *Review of Scientific Instruments,* 76(8): 085107-6.

WINANDY, J. E. 1994. Wood Properties. ARNTZEN, C. J. (Ed.) *Encyclopedia of Agricultural Science.* Orlando, Academic Press.

WOLDE-RUFAEL, Y. 2010. Coal consumption and economic growth revisited. *Applied Energy,* 87(1): 160-167.

WOOLLACOTT, L. C. & ERIC, R. H. 1994. *The South African Institute of Mining and Metallurgy.* Johannesburg.

YANG, W. & NORTHWOOD, D. O. 2007. An investigation into TIN-coated 316L stainless steel as a bipolar plate material for PEM fuel cells. *Journal of Power Sources,* 165293-298.

YARAR, B. & DOGAN, Z. M. (Eds.) 1987. *Mineral processing design,* Dordrecht: Martinus Nijhoff Publishers.

YERKOVIC, C., MENACHO, J. & GAETE, L. 1993. Exploring the ultrasonic comminution of copper ores. *Minerals Engineering,* 6(6): 607-617.

YOUNG, P. H. 2004. *Electronic Communication Techniques.* 5th Ed. New Jersey: Pearson Prentice-Hall.

ZHANG, W. & YAO, Y. L. 2002. Micro scale laser shock processing of metallic components. *Journal of Manufacturing Science and Engineering Transactions of ASME,* 124369-378.

ANNEXURE 1 Electrical parameters of the untreated JSA rock sample for the VHF range

Frequency (Hertz)	VNA Real (r)	VNA Imaginary (x)	Resistance (Ohm)	Reactance (Ohm)	Magnitude (Ohm)	Angle (Radians)	Angle (Degrees)	Frequency (MegaHertz)	Resistivity (Ohm-meter)	Conductivity (Siemens per meter)	Rock Area (Square Meters)	
30000000	-0.713	-0.668	0.676	-19.746	19.758	-1.537	-88	30.000	0.193	5.192	1.140E-03	
31350000	-0.778	-0.588	0.690	-16.754	16.769	-1.530	-88	31.350	0.197	5.083	1.140E-03	
32700000	-0.834	-0.503	0.701	-13.903	13.921	-1.520	-87	32.700	0.200	5.002	1.140E-03	
34050000	-0.883	-0.407	0.725	-10.963	10.987	-1.505	-86	34.050	0.207	4.842	1.140E-03	
35400000	-0.921	-0.313	0.717	-8.267	8.298	-1.484	-85	35.400	0.204	4.890	1.140E-03	
36750000	-0.951	-0.200	0.727	-5.189	5.240	-1.432	-82	36.750	0.207	4.824	1.140E-03	
38100000	-0.963	-0.106	0.789	-2.725	2.837	-1.289	-74	38.100	0.225	4.447	1.140E-03	
39450000	-0.968	-0.002	0.814	-0.050	0.816	-0.061	-3	39.450	0.232	4.308	1.140E-03	
40800000	-0.961	0.107	0.848	2.772	2.899	1.274	73	40.800	0.242	4.137	1.140E-03	
42150000	-0.943	0.207	0.882	5.415	5.487	1.409	81	42.150	0.251	3.980	1.140E-03	
43500000	-0.915	0.298	0.977	7.937	7.997	1.448	83	43.500	0.279	3.590	1.140E-03	
44850000	-0.874	0.404	0.999	10.983	11.028	1.480	85	44.850	0.285	3.514	1.140E-03	
46200000	-0.823	0.498	1.043	13.933	13.972	1.496	86	46.200	0.297	3.365	1.140E-03	
47550000	-0.768	0.581	1.061	16.780	16.814	1.508	86	47.550	0.302	3.306	1.140E-03	
48900000	-0.694	0.662	1.211	20.007	20.044	1.510	87	48.900	0.345	2.898	1.140E-03	
50250000	-0.614	0.736	1.308	23.385	23.422	1.515	87	50.250	0.373	2.682	1.140E-03	
51600000	-0.526	0.792	1.636	26.804	26.854	1.510	87	51.600	0.466	2.145	1.140E-03	
52950000	-0.428	0.838	2.082	30.553	30.624	1.503	86	52.950	0.593	1.685	1.140E-03	
54300000	-0.351	0.858	2.742	33.498	33.610	1.489	85	54.300	0.782	1.279	1.140E-03	
55650000	-0.266	0.883	3.139	37.053	37.186	1.486	85	55.650	0.895	1.118	1.140E-03	
57000000	-0.174	0.919	2.834	41.328	41.425	1.502	86	57.000	0.808	1.238	1.140E-03	
58350000	-0.090	0.934	2.888	45.322	45.414	1.507	86	58.350	0.823	1.215	1.140E-03	
59700000	0.011	0.945	2.837	50.483	50.562	1.515	87	59.700	0.809	1.237	1.140E-03	
61050000	0.118	0.941	3.040	56.475	56.556	1.517	87	61.050	0.866	1.154	1.140E-03	
62400000	0.222	0.923	3.418	63.346	63.439	1.517	87	62.400	0.974	1.027	1.140E-03	
63750000	0.319	0.891	4.122	70.849	70.969	1.513	87	63.750	1.175	0.851	1.140E-03	
65100000	0.402	0.857	4.755	78.508	78.652	1.510	87	65.100	1.355	0.738	1.140E-03	
66450000	0.497	0.803	6.039	89.490	89.693	1.503	86	66.450	1.721	0.581	1.140E-03	
67800000	0.574	0.752	7.016	100.695	100.940	1.501	86	67.800	2.000	0.500	1.140E-03	
69150000	0.660	0.686	8.053	116.966	117.243	1.502	86	69.150	2.295	0.436	1.140E-03	
70500000	0.724	0.614	10.783	135.500	135.928	1.491	85	70.500	3.073	0.325	1.140E-03	
71850000	0.780	0.539	14.992	159.133	159.837	1.477	85	71.850	4.273	0.234	1.140E-03	
73200000	0.839	0.447	21.398	198.003	199.216	1.463	84	73.200	6.098	0.164	1.140E-03	
74550000	0.878	0.362	33.602	247.854	250.121	1.436	82	74.550	9.577	0.104	1.140E-03	
75900000	0.911	0.268	61.536	336.373	341.956	1.390	80	75.900	17.538	0.057	1.140E-03	
77250000	0.934	0.173	143.901	504.311	524.439	1.293	74	77.250	41.012	0.024	1.140E-03	
78600000	0.947	0.071	622.252	907.059	1099.979	0.970	56	78.600	177.342	0.006	1.140E-03	
79950000	0.949	-0.030	1398.869	-850.130	1636.935	-0.546	-31	79.950	398.676	0.003	1.140E-03	
81300000	0.941	-0.125	258.051	-652.488	701.664	-1.194	-68	81.300	73.544	0.014	1.140E-03	
82650000	0.923	-0.227	83.797	-394.421	403.224	-1.361	-78	82.650	23.882	0.042	1.140E-03	
84000000	0.894	-0.329	40.186	-277.301	280.198	-1.427	-82	84.000	11.453	0.087	1.140E-03	
85350000	0.855	-0.411	26.138	-216.290	217.864	-1.451	-83	85.350	7.449	0.134	1.140E-03	
86700000	0.802	-0.505	17.229	-171.766	172.628	-1.471	-84	86.700	4.910	0.204	1.140E-03	
88050000	0.746	-0.586	12.281	-143.720	144.244	-1.486	-85	88.050	3.500	0.286	1.140E-03	
89400000	0.680	-0.662	9.140	-122.500	122.840	-1.496	-86	89.400	2.605	0.384	1.140E-03	
90750000	0.607	-0.727	7.566	-106.453	106.722	-1.500	-86	90.750	2.156	0.464	1.140E-03	
92100000	0.529	-0.785	6.225	-93.724	93.931	-1.504	-86	92.100	1.774	0.564	1.140E-03	
93450000	0.440	-0.840	4.935	-82.370	82.518	-1.511	-87	93.450	1.406	0.711	1.140E-03	
94800000	0.347	-0.883	4.150	-73.231	73.348	-1.514	-87	94.800	1.183	0.846	1.140E-03	
96150000	0.259	-0.912	3.684	-66.041	66.143	-1.515	-87	96.150	1.050	0.952	1.140E-03	
97500000	0.159	-0.935	3.174	-59.120	59.205	-1.517	-87	97.500	0.905	1.105	1.140E-03	
98850000	0.053	-0.945	2.896	-52.791	52.870	-1.516	-87	98.850	0.825	1.211	1.140E-03	
100200000	-0.042	-0.946	2.626	-47.784	47.856	-1.516	-87	100.200	0.748	1.336	1.140E-03	
101550000	-0.146	-0.936	2.337	-42.762	42.826	-1.516	-87	101.550	0.666	1.502	1.140E-03	
102900000	-0.232	-0.913	2.392	-38.807	38.881	-1.509	-86	102.900	0.682	1.467	1.140E-03	
104250000	-0.330	-0.883	2.163	-34.637	34.705	-1.508	-86	104.250	0.616	1.622	1.140E-03	
105600000	-0.436	-0.837	1.969	-30.312	30.376	-1.506	-86	105.600	0.561	1.782	1.140E-03	
106950000	-0.515	-0.789	1.919	-27.060	27.128	-1.500	-86	106.950	0.547	1.828	1.140E-03	
108300000	-0.597	-0.729	1.819	-23.664	23.734	-1.494	-86	108.300	0.518	1.929	1.140E-03	
109650000	-0.667	-0.667	1.717	-20.678	20.749	-1.488	-85	109.650	0.489	2.044	1.140E-03	
111000000	-0.730	-0.594	1.703	-17.739	17.821	-1.475	-85	111.000	0.485	2.060	1.140E-03	
112350000	-0.792	-0.507	1.659	-14.614	14.708	-1.458	-84	112.350	0.473	2.114	1.140E-03	
113700000	-0.842	-0.420	1.612	-11.780	11.890	-1.435	-82	113.700	0.459	2.177	1.140E-03	
115050000	-0.883	-0.318	1.635	-8.707	8.859	-1.385	-79	115.050	0.466	2.146	1.140E-03	
116400000	-0.911	-0.227	1.608	-6.142	6.349	-1.315	-75	116.400	0.458	2.181	1.140E-03	
117750000	-0.927	-0.140	1.628	-3.742	4.081	-1.160	-66	117.750	0.464	2.155	1.140E-03	
119100000	-0.937	-0.036	1.598	-0.952	1.861	-0.537	-31	119.100	0.456	2.195	1.140E-03	
120450000	-0.935	0.074	1.602	1.970	2.539	0.888	51	120.450	0.457	2.190	1.140E-03	
121800000	-0.921	0.165	1.668	4.447	4.750	1.212	69	121.800	0.475	2.104	1.140E-03	
123150000	-0.899	0.265	1.656	7.203	7.391	1.345	77	123.150	0.472	2.119	1.140E-03	
124500000	-0.865	0.352	1.773	9.763	9.922	1.391	80	124.500	0.505	1.979	1.140E-03	
125850000	-0.822	0.446	1.785	12.662	12.787	1.431	82	125.850	0.509	1.966	1.140E-03	
127200000	-0.767	0.530	1.918	15.566	15.684	1.448	83	127.200	0.547	1.829	1.140E-03	
128550000	-0.711	0.608	1.905	18.443	18.541	1.468	84	128.550	0.543	1.842	1.140E-03	
129900000	-0.644	0.674	2.057	21.345	21.444	1.475	84	129.900	0.586	1.706	1.140E-03	
131250000	-0.565	0.740	2.212	24.689	24.788	1.481	85	131.250	0.630	1.586	1.140E-03	
132600000	-0.484	0.796	2.345	28.079	28.176	1.487	85	132.600	0.668	1.496	1.140E-03	
133950000	-0.398	0.845	2.424	31.721	31.814	1.495	86	133.950	0.691	1.448	1.140E-03	
135300000	-0.310	0.878	2.672	35.311	35.412	1.495	86	135.300	0.762	1.313	1.140E-03	
136650000	-0.216	0.905	2.912	39.370	39.477	1.497	86	136.650	0.830	1.205	1.140E-03	
138000000	-0.121	0.923	3.157	43.777	43.891	1.499	86	138.000	0.900	1.111	1.140E-03	
139350000	-0.025	0.929	3.546	48.569	48.699	1.498	86	139.350	1.011	0.990	1.140E-03	
140700000	0.072	0.926	3.990	53.897	54.045	1.497	86	140.700	1.137	0.879	1.140E-03	
142050000	0.172	0.914	4.424	60.107	60.269	1.497	86	142.050	1.261	0.793	1.140E-03	
143400000	0.267	0.891	5.025	66.850	67.138	1.496	86	143.400	1.432	0.698	1.140E-03	
144750000	0.356	0.857	6.022	74.556	74.799	1.490	85	144.750	1.716	0.583	1.140E-03	
146100000	0.438	0.819	6.941	83.048	83.338	1.487	85	146.100	1.978	0.506	1.140E-03	
147450000	0.519	0.769	8.490	93.489	93.873	1.480	85	147.450	2.420	0.413	1.140E-03	
148800000	0.598	0.711	10.219	106.548	107.036	1.475	85	148.800	2.912	0.343	1.140E-03	
150150000	0.673	0.642	12.971	123.618	124.296	1.466	84	150.150	3.697	0.270	1.140E-03	
151500000	0.737	0.567	17.399	145.156	146.195	1.452	83	151.500	4.959	0.202	1.140E-03	
152850000	0.790	0.490	23.866	172.545	174.187	1.433	82	152.850	6.802	0.147	1.140E-03	
154200000	0.831	0.410	35.977	208.465	211.547	1.400	80	154.200	10.254	0.098	1.140E-03	**Resonating**
155550000	0.872	0.316	60.046	272.141	278.686	1.354	78	155.550	17.115	0.058	1.140E-03	**frequency**
156900000	0.898	0.232	110.493	358.265	374.917	1.272	73	156.900	31.490	0.032	1.140E-03	**interpolated**
158250000	0.915	0.140	268.535	521.714	586.768	1.095	63	158.250	76.533	0.013	1.140E-03	**1.6014E+08**
159600000	0.925	0.041	969.609	561.855	1120.640	0.525	30	159.600	276.339	0.004	1.140E-03	
160950000	0.921	-0.052	832.875	-575.875	1012.343	-0.605	-35	160.950	237.309	0.004	1.140E-03	
162300000	0.911	-0.148	248.255	-495.438	554.157	-1.106	-63	162.300	70.753	0.014	1.140E-03	**Resistance**
163650000	0.890	-0.241	106.843	-343.831	359.762	-1.269	-73	163.650	30.450	0.033	1.140E-03	**interpolated**
165000000	0.861	-0.332	57.480	-256.217	262.586	-1.350	-77	165.000	18.382	0.054	1.140E-03	**1264.001**
166350000	0.819	-0.428	36.567	-200.620	203.923	-1.391	-80	166.350	10.417	0.096	1.140E-03	

Frequency (Hertz)	VNA Real (r)	VNA Imaginary (x)	Resistance (Ohm)	Reactance (Ohm)	Magnitude (Ohm)	Angle (Radians)	Angle (Degrees)	Frequency (MegaHertz)	Resistivity (Ohm-meter)	Conductivity (Siemens per meter)	Rock Area (Square Meters)
167700000	0.773	-0.497	25.997	-166.574	168.591	-1.416	-81	167.700	7.409	0.135	1.140E-03
169050000	0.721	-0.570	19.401	-141.561	142.884	-1.435	-82	169.050	5.529	0.181	1.140E-03
170400000	0.652	-0.646	14.581	-120.006	120.888	-1.450	-83	170.400	4.156	0.241	1.140E-03
171750000	0.587	-0.704	11.955	-105.604	106.278	-1.458	-84	171.750	3.407	0.294	1.140E-03
173100000	0.504	-0.765	9.667	-92.067	92.573	-1.466	-84	173.100	2.755	0.363	1.140E-03
174450000	0.424	-0.811	8.201	-81.971	82.380	-1.471	-84	174.450	2.337	0.428	1.140E-03
175800000	0.335	-0.846	7.433	-73.057	73.434	-1.469	-84	175.800	2.118	0.472	1.140E-03
177150000	0.250	-0.873	6.653	-65.877	66.213	-1.470	-84	177.150	1.896	0.527	1.140E-03
178500000	0.157	-0.894	5.850	-59.227	59.515	-1.472	-84	178.500	1.667	0.600	1.140E-03
179850000	0.071	-0.904	5.317	-53.785	54.047	-1.472	-84	179.850	1.515	0.660	1.140E-03
181200000	-0.020	-0.905	4.870	-48.669	48.912	-1.471	-84	181.200	1.388	0.720	1.140E-03
182550000	-0.121	-0.896	4.486	-43.516	43.747	-1.468	-84	182.550	1.279	0.782	1.140E-03
183900000	-0.210	-0.877	4.176	-39.280	39.501	-1.465	-84	183.900	1.190	0.840	1.140E-03
185250000	-0.201	-0.850	4.054	-35.569	35.799	-1.457	-83	185.250	1.155	0.866	1.140E-03
186600000	-0.372	-0.814	3.893	-31.972	32.208	-1.450	-83	186.600	1.109	0.901	1.140E-03
187950000	-0.455	-0.776	3.521	-28.526	28.742	-1.448	-83	187.950	1.004	0.996	1.140E-03
189300000	-0.529	-0.729	3.293	-25.415	25.627	-1.442	-83	189.300	0.938	1.066	1.140E-03
190650000	-0.599	-0.673	3.116	-22.369	22.585	-1.432	-82	190.650	0.888	1.126	1.140E-03
192000000	-0.668	-0.609	2.913	-19.308	19.527	-1.421	-81	192.000	0.830	1.205	1.140E-03
193350000	-0.727	-0.540	2.744	-16.493	16.720	-1.406	-81	193.350	0.782	1.279	1.140E-03
194700000	-0.784	-0.462	2.533	-13.609	13.843	-1.387	-79	194.700	0.722	1.385	1.140E-03
196050000	-0.825	-0.383	2.481	-11.011	11.287	-1.349	-77	196.050	0.707	1.414	1.140E-03
197400000	-0.865	-0.290	2.363	-8.146	8.482	-1.289	-74	197.400	0.673	1.485	1.140E-03
198750000	-0.892	-0.198	2.277	-5.460	5.916	-1.176	-67	198.750	0.649	1.541	1.140E-03
200100000	-0.909	-0.106	2.231	-2.913	3.669	-0.917	-53	200.100	0.636	1.573	1.140E-03
201450000	-0.914	-0.016	2.236	-0.440	2.279	-0.194	-11	201.450	0.637	1.569	1.140E-03
202800000	-0.915	0.091	2.109	2.483	3.258	0.867	50	202.800	0.601	1.663	1.140E-03
204150000	-0.902	0.173	2.138	4.742	5.202	1.147	66	204.150	0.609	1.641	1.140E-03
205500000	-0.880	0.272	2.110	7.535	7.824	1.298	74	205.500	0.601	1.663	1.140E-03
206850000	-0.846	0.364	2.146	10.289	10.510	1.365	78	206.850	0.612	1.635	1.140E-03
208200000	-0.806	0.449	2.156	12.956	13.134	1.406	81	208.200	0.615	1.627	1.140E-03
209550000	-0.757	0.526	2.240	15.633	15.792	1.429	82	209.550	0.638	1.567	1.140E-03
210900000	-0.695	0.600	2.327	18.496	18.642	1.446	83	210.900	0.663	1.508	1.140E-03
212250000	-0.632	0.671	2.430	21.554	21.691	1.459	84	212.250	0.693	1.444	1.140E-03
213600000	-0.554	0.739	2.472	24.958	25.080	1.472	84	213.600	0.704	1.420	1.140E-03
214950000	-0.479	0.792	2.565	28.143	28.260	1.480	85	214.950	0.731	1.368	1.140E-03
216300000	-0.399	0.832	2.787	31.396	31.519	1.482	85	216.300	0.794	1.259	1.140E-03
217650000	-0.314	0.870	2.920	35.016	35.138	1.488	85	217.650	0.832	1.202	1.140E-03
219000000	-0.221	0.897	3.207	39.060	39.192	1.489	85	219.000	0.914	1.094	1.140E-03
220350000	-0.123	0.917	3.412	43.617	43.750	1.493	86	220.350	0.973	1.028	1.140E-03
221700000	-0.028	0.926	3.702	48.368	48.510	1.494	86	221.700	1.055	0.948	1.140E-03
223050000	0.058	0.924	4.101	53.052	53.210	1.494	86	223.050	1.169	0.855	1.140E-03
224400000	0.151	0.911	4.729	58.723	58.913	1.490	85	224.400	1.348	0.742	1.140E-03
225750000	0.245	0.893	5.177	65.297	65.502	1.492	85	225.750	1.475	0.678	1.140E-03
227100000	0.338	0.861	6.095	72.981	73.235	1.487	85	227.100	1.737	0.576	1.140E-03
228450000	0.420	0.825	7.075	81.091	81.399	1.484	85	228.450	2.016	0.496	1.140E-03
229800000	0.502	0.778	8.341	91.201	91.582	1.480	85	229.800	2.377	0.421	1.140E-03
231150000	0.576	0.724	10.217	102.800	103.306	1.472	84	231.150	2.912	0.343	1.140E-03
232500000	0.646	0.662	12.740	117.476	118.165	1.463	84	232.500	3.631	0.275	1.140E-03
233850000	0.706	0.596	16.629	135.045	136.065	1.448	83	233.850	4.739	0.211	1.140E-03
235200000	0.767	0.520	21.671	160.116	161.575	1.436	82	235.200	6.176	0.162	1.140E-03
236550000	0.817	0.440	30.398	193.699	196.070	1.415	81	236.550	8.663	0.115	1.140E-03
237900000	0.856	0.356	47.422	241.242	245.859	1.377	79	237.900	13.515	0.074	1.140E-03
239250000	0.886	0.267	85.289	316.843	328.122	1.308	75	239.250	24.307	0.041	1.140E-03
240600000	0.907	0.185	165.979	431.300	462.135	1.203	69	240.600	47.304	0.021	1.140E-03
241950000	0.922	0.091	492.647	633.340	802.385	0.910	52	241.950	140.404	0.007	1.140E-03
243300000	0.927	-0.004	1314.210	-72.152	1316.189	-0.055	-3	243.300	374.550	0.003	1.140E-03
244650000	0.923	-0.090	500.983	-642.881	815.034	-0.909	-52	244.650	142.780	0.007	1.140E-03
246000000	0.908	-0.185	166.127	-434.299	464.987	-1.205	-69	246.000	47.346	0.021	1.140E-03
247350000	0.885	-0.274	80.199	-310.381	320.575	-1.318	-76	247.350	22.857	0.044	1.140E-03
248700000	0.858	-0.353	48.345	-243.925	248.669	-1.375	-79	248.700	13.778	0.073	1.140E-03
250050000	0.816	-0.443	30.096	-192.504	194.842	-1.416	-81	250.050	8.577	0.117	1.140E-03
251400000	0.769	-0.521	21.181	-160.452	161.844	-1.440	-82	251.400	6.037	0.166	1.140E-03
252750000	0.716	-0.593	15.738	-137.251	138.150	-1.457	-83	252.750	4.485	0.223	1.140E-03
254100000	0.648	-0.667	11.877	-117.289	117.889	-1.470	-84	254.100	3.385	0.295	1.140E-03
255450000	0.577	-0.727	9.800	-102.813	103.279	-1.476	-85	255.450	2.793	0.358	1.140E-03
256800000	0.506	-0.777	8.235	-91.630	92.000	-1.481	-85	256.800	2.347	0.426	1.140E-03
258150000	0.424	-0.825	6.883	-81.450	81.740	-1.486	-85	258.150	1.962	0.510	1.140E-03
259500000	0.346	-0.859	6.086	-73.663	73.914	-1.488	-85	259.500	1.734	0.577	1.140E-03
260850000	0.248	-0.893	5.146	-65.549	65.751	-1.492	-86	260.850	1.467	0.682	1.140E-03
262200000	0.162	-0.915	4.457	-59.442	59.609	-1.496	-86	262.200	1.270	0.787	1.140E-03
263550000	0.064	-0.927	3.924	-53.410	53.554	-1.497	-86	263.550	1.118	0.894	1.140E-03
264900000	-0.025	-0.928	3.615	-48.532	48.687	-1.496	-86	264.900	1.030	0.971	1.140E-03
266250000	-0.111	-0.923	3.265	-44.225	44.346	-1.497	-86	266.250	0.931	1.075	1.140E-03
267600000	-0.199	-0.905	3.133	-40.127	40.249	-1.493	-86	267.600	0.893	1.120	1.140E-03
268950000	-0.302	-0.877	2.816	-35.596	35.707	-1.492	-85	268.950	0.803	1.246	1.140E-03
270300000	-0.376	-0.846	2.752	-32.427	32.544	-1.486	-85	270.300	0.784	1.275	1.140E-03
271650000	-0.459	-0.803	2.603	-28.958	29.075	-1.481	-85	271.650	0.742	1.348	1.140E-03
273000000	-0.545	-0.752	2.330	-25.487	25.593	-1.480	-85	273.000	0.664	1.506	1.140E-03
274350000	-0.617	-0.689	2.321	-22.299	22.420	-1.467	-84	274.350	0.662	1.512	1.140E-03
275700000	-0.673	-0.634	2.251	-19.808	19.936	-1.458	-84	275.700	0.642	1.558	1.140E-03
277050000	-0.740	-0.558	2.109	-16.705	16.837	-1.445	-83	277.050	0.601	1.664	1.140E-03
278400000	-0.793	-0.474	2.119	-13.780	13.942	-1.418	-81	278.400	0.604	1.656	1.140E-03
279750000	-0.832	-0.403	2.064	-11.464	11.649	-1.393	-80	279.750	0.588	1.700	1.140E-03
281100000	-0.872	-0.309	1.993	-8.582	8.811	-1.343	-77	281.100	0.568	1.760	1.140E-03
282450000	-0.896	-0.225	2.018	-6.164	6.486	-1.254	-72	282.450	0.575	1.739	1.140E-03
283800000	-0.915	-0.134	1.955	-3.635	4.127	-1.077	-62	283.800	0.557	1.795	1.140E-03
285150000	-0.923	-0.039	1.993	-1.039	2.248	-0.481	-28	285.150	0.568	1.760	1.140E-03
286500000	-0.922	0.052	1.996	1.413	2.446	0.616	35	286.500	0.569	1.758	1.140E-03
287850000	-0.910	0.144	2.051	3.937	4.439	1.090	62	287.850	0.585	1.711	1.140E-03
289200000	-0.892	0.240	2.018	6.604	6.906	1.274	73	289.200	0.575	1.738	1.140E-03
290550000	-0.865	0.321	2.081	8.952	9.191	1.342	77	290.550	0.593	1.686	1.140E-03
291900000	-0.827	0.413	2.072	11.761	11.942	1.396	80	291.900	0.590	1.694	1.140E-03
293250000	-0.784	0.487	2.182	14.235	14.399	1.420	81	293.250	0.616	1.623	1.140E-03
294600000	-0.730	0.567	2.204	17.100	17.241	1.443	83	294.600	0.628	1.592	1.140E-03
295950000	-0.670	0.635	2.312	19.899	20.033	1.455	83	295.950	0.659	1.518	1.140E-03
297300000	-0.601	0.704	2.356	23.024	23.144	1.469	84	297.300	0.671	1.490	1.140E-03
298650000	-0.530	0.755	2.542	25.934	26.058	1.473	84	298.650	0.724	1.380	1.140E-03
300000000	-0.457	0.803	2.652	29.022	29.143	1.480	85	300.000	0.756	1.323	1.140E-03

ANNEXURE 2 Electrical parameters of the untreated JSB rock sample for the VHF range

Frequency (Hertz)	VNA Real (r)	VNA Imaginary (x)	Resistance (Ohm)	Reactance (Ohm)	Magnitude (Ohm)	Angle (Radians)	Angle (Degrees)	Frequency (MegaHertz)	Resistivity (Ohm-meter)	Conductivity (Siemens per meter)	Rock Area (Square Meters)	
30000000	-0.674	-0.695	0.961	-21.157	21.179	-1.525	-87	30	0.283	3.535	1.178E-03	
31350000	-0.738	-0.625	0.944	-18.314	18.338	-1.519	-87	31	0.278	3.597	1.178E-03	
32700000	-0.797	-0.544	0.971	-15.417	15.447	-1.508	-86	33	0.286	3.495	1.178E-03	
34050000	-0.858	-0.444	0.913	-12.180	12.214	-1.496	-86	34	0.269	3.718	1.178E-03	
35400000	-0.896	-0.358	0.927	-9.630	9.675	-1.475	-85	35	0.273	3.663	1.178E-03	
36750000	-0.928	-0.265	0.895	-6.990	7.047	-1.443	-83	37	0.264	3.794	1.178E-03	
38100000	-0.948	-0.157	1.013	-4.114	4.237	-1.329	-76	38	0.298	3.354	1.178E-03	
39450000	-0.962	-0.058	0.926	-1.455	1.724	-1.004	-58	39	0.273	3.668	1.178E-03	
40800000	-0.956	0.034	1.106	0.891	1.420	0.678	39	41	0.326	3.070	1.178E-03	
42150000	-0.948	0.140	1.067	3.659	3.811	1.287	74	42	0.314	3.183	1.178E-03	
43500000	-0.927	0.248	1.061	6.568	6.653	1.411	81	44	0.313	3.199	1.178E-03	
44850000	-0.895	0.334	1.173	9.026	9.102	1.442	83	45	0.345	2.896	1.178E-03	
46200000	-0.851	0.432	1.230	11.960	12.023	1.468	84	46	0.362	2.760	1.178E-03	
47550000	-0.802	0.517	1.269	14.720	14.775	1.465	85	48	0.374	2.676	1.178E-03	
48900000	-0.741	0.601	1.336	17.710	17.760	1.496	86	49	0.393	2.543	1.178E-03	
50250000	-0.673	0.670	1.527	20.624	20.681	1.497	86	50	0.450	2.224	1.178E-03	
51600000	-0.585	0.745	1.668	24.299	24.356	1.502	86	52	0.491	2.035	1.178E-03	
52950000	-0.502	0.790	2.137	27.435	27.518	1.493	86	53	0.629	1.589	1.178E-03	
54300000	-0.411	0.828	2.726	30.929	31.049	1.483	85	54	0.803	1.245	1.178E-03	
55650000	-0.327	0.849	3.488	34.217	34.394	1.469	84	56	1.027	0.974	1.178E-03	
57000000	-0.288	0.877	3.341	36.911	37.061	1.481	85	57	0.984	1.016	1.178E-03	
58350000	-0.175	0.909	3.244	41.212	41.339	1.492	85	58	0.955	1.047	1.178E-03	
59700000	-0.072	0.930	3.214	46.163	46.275	1.501	86	60	0.946	1.057	1.178E-03	
61050000	0.014	0.937	3.284	50.669	50.775	1.506	86	61	0.967	1.034	1.178E-03	
62400000	0.120	0.930	3.705	56.725	56.846	1.506	86	62	1.091	0.917	1.178E-03	
63750000	0.220	0.914	4.014	63.270	63.398	1.507	86	64	1.182	0.846	1.178E-03	
65100000	0.310	0.888	4.573	70.250	70.399	1.506	86	65	1.347	0.743	1.178E-03	
66450000	0.402	0.849	5.490	78.712	78.903	1.501	86	66	1.617	0.619	1.178E-03	
67800000	0.491	0.797	6.936	89.166	89.435	1.493	86	68	2.043	0.490	1.178E-03	
69150000	0.559	0.753	7.880	98.658	99.172	1.491	85	69	2.321	0.431	1.178E-03	
70500000	0.647	0.689	8.962	114.923	115.272	1.493	86	71	2.639	0.379	1.178E-03	
71850000	0.713	0.620	11.499	132.951	133.447	1.485	85	72	3.386	0.295	1.178E-03	
73200000	0.767	0.547	15.871	154.785	155.596	1.469	84	73	4.674	0.214	1.178E-03	
74550000	0.827	0.453	23.468	192.603	194.028	1.450	83	75	6.911	0.145	1.178E-03	
75900000	0.870	0.367	35.662	242.415	245.024	1.425	82	76	10.502	0.095	1.178E-03	
77250000	0.901	0.278	63.143	319.070	325.258	1.375	79	77	18.596	0.054	1.178E-03	
78600000	0.924	0.189	131.715	455.545	474.205	1.289	74	79	38.790	0.026	1.178E-03	
79950000	0.942	0.082	524.767	811.286	966.214	0.997	57	80	154.544	0.006	1.178E-03	
81300000	0.946	-0.009	1738.522	-301.006	1764.490	-0.172	-10	81	511.996	0.002	1.178E-03	
82650000	0.937	-0.117	309.856	-661.895	730.832	-1.133	-65	83	91.253	0.011	1.178E-03	
84000000	0.922	-0.205	112.434	-426.020	440.607	-1.313	-75	84	33.112	0.030	1.178E-03	
85350000	0.894	-0.307	50.364	-291.409	295.730	-1.400	-80	85	14.832	0.067	1.178E-03	
86700000	0.859	-0.392	31.469	-225.845	228.027	-1.432	-82	87	9.268	0.108	1.178E-03	
88050000	0.810	-0.482	20.672	-179.703	180.888	-1.456	-83	88	6.088	0.164	1.178E-03	
89400000	0.756	-0.565	14.420	-149.051	149.746	-1.474	-84	89	4.247	0.235	1.178E-03	
90750000	0.694	-0.639	10.975	-127.190	127.662	-1.485	-85	91	3.232	0.309	1.178E-03	
92100000	0.622	-0.707	8.834	-109.980	110.335	-1.491	-85	92	2.602	0.384	1.178E-03	
93450000	0.549	-0.765	7.207	-96.969	97.236	-1.497	-86	93	2.122	0.471	1.178E-03	
94800000	0.469	-0.817	5.964	-86.089	86.296	-1.502	-86	95	1.756	0.569	1.178E-03	
96150000	0.381	-0.860	5.146	-76.632	76.804	-1.504	-86	96	1.515	0.660	1.178E-03	
97500000	0.292	-0.894	4.417	-68.714	68.856	-1.507	-86	98	1.301	0.769	1.178E-03	
98850000	0.188	-0.929	3.633	-61.047	61.155	-1.511	-87	99	1.070	0.935	1.178E-03	
100200000	0.095	-0.937	3.323	-55.217	55.317	-1.511	-87	100	0.979	1.022	1.178E-03	
101550000	-0.004	-0.940	3.101	-49.718	49.814	-1.509	-86	102	0.913	1.095	1.178E-03	
102900000	-0.102	-0.937	2.666	-44.767	44.847	-1.511	-87	103	0.785	1.274	1.178E-03	
104250000	-0.205	-0.919	2.479	-40.015	40.092	-1.509	-86	104	0.730	1.370	1.178E-03	
105600000	-0.291	-0.894	2.350	-36.271	36.347	-1.506	-86	106	0.692	1.445	1.178E-03	
106950000	-0.392	-0.857	2.086	-32.060	32.148	-1.506	-86	107	0.614	1.628	1.178E-03	
108300000	-0.479	-0.808	2.065	-28.457	28.532	-1.498	-86	108	0.608	1.645	1.178E-03	
109650000	-0.563	-0.753	1.921	-25.016	25.090	-1.494	-86	110	0.566	1.768	1.178E-03	
111000000	-0.631	-0.696	1.860	-22.148	22.226	-1.487	-85	111	0.548	1.826	1.178E-03	
112350000	-0.701	-0.624	1.818	-19.018	19.105	-1.476	-85	112	0.535	1.868	1.178E-03	
113700000	-0.765	-0.544	1.749	-15.949	16.044	-1.462	-84	114	0.515	1.942	1.178E-03	
115050000	-0.813	-0.465	1.741	-13.271	13.385	-1.440	-83	115	0.513	1.950	1.178E-03	
116400000	-0.860	-0.373	1.693	-10.368	10.505	-1.409	-81	116	0.499	2.005	1.178E-03	
117750000	-0.895	-0.277	1.686	-7.544	7.726	-1.354	-78	118	0.491	2.039	1.178E-03	
119100000	-0.914	-0.193	1.728	-5.226	5.504	-1.252	-72	119	0.509	1.965	1.178E-03	
120450000	-0.928	-0.088	1.759	-2.370	2.952	-0.932	-53	120	0.518	1.931	1.178E-03	
121800000	-0.934	0.013	1.711	0.350	1.747	0.202	12	122	0.504	1.984	1.178E-03	
123150000	-0.929	0.103	1.691	2.757	3.234	1.021	58	123	0.498	2.008	1.178E-03	
124500000	-0.911	0.194	1.805	5.271	5.572	1.241	71	125	0.532	1.881	1.178E-03	
125850000	-0.884	0.295	1.813	8.104	8.304	1.351	77	126	0.534	1.873	1.178E-03	
127200000	-0.845	0.392	1.858	11.032	11.187	1.404	80	127	0.547	1.828	1.178E-03	
128550000	-0.803	0.471	1.912	13.583	13.687	1.431	82	129	0.563	1.776	1.178E-03	
129900000	-0.749	0.561	2.006	16.399	16.522	1.448	83	130	0.591	1.692	1.178E-03	
131250000	-0.685	0.630	2.064	19.480	19.589	1.465	84	131	0.608	1.645	1.178E-03	
132600000	-0.616	0.699	2.118	22.539	22.638	1.477	85	133	0.624	1.604	1.178E-03	
133950000	-0.543	0.754	2.327	25.556	25.661	1.480	85	134	0.685	1.459	1.178E-03	
135300000	-0.456	0.810	2.453	29.194	29.297	1.487	85	135	0.723	1.384	1.178E-03	
136650000	-0.373	0.851	2.625	32.613	32.718	1.490	85	137	0.773	1.293	1.178E-03	
138000000	-0.284	0.885	2.800	36.397	36.505	1.494	86	138	0.825	1.213	1.178E-03	
139350000	-0.196	0.908	3.030	40.249	40.362	1.496	86	139	0.892	1.121	1.178E-03	
140700000	-0.097	0.923	3.352	44.906	45.031	1.496	86	141	0.987	1.013	1.178E-03	
142050000	0.001	0.931	3.587	49.922	50.050	1.499	86	142	1.056	0.947	1.178E-03	
143400000	0.095	0.924	4.114	55.245	55.398	1.496	86	143	1.212	0.825	1.178E-03	
144750000	0.189	0.911	4.520	61.241	61.408	1.497	86	145	1.331	0.751	1.178E-03	
146100000	0.277	0.888	5.296	67.740	67.947	1.493	86	146	1.560	0.641	1.178E-03	
147450000	0.375	0.851	6.076	76.351	76.593	1.491	85	147	1.789	0.559	1.178E-03	
148800000	0.462	0.806	7.304	85.793	86.104	1.486	85	149	2.151	0.465	1.178E-03	
150150000	0.537	0.757	8.792	96.203	96.604	1.480	85	150	2.589	0.386	1.178E-03	
151500000	0.617	0.694	10.899	110.481	111.017	1.472	84	152	3.210	0.312	1.178E-03	Resonating
152850000	0.681	0.629	14.149	126.450	127.240	1.459	84	153	4.167	0.240	1.178E-03	frequency
154200000	0.744	0.565	18.502	148.496	149.644	1.447	83	154	5.449	0.184	1.178E-03	interpolated
155550000	0.797	0.476	26.028	177.711	179.607	1.425	82	156	7.665	0.130	1.178E-03	1.6258E+08
156900000	0.842	0.391	38.863	219.513	222.926	1.396	80	157	11.445	0.087	1.178E-03	
158250000	0.877	0.299	68.054	285.828	293.818	1.337	77	158	20.042	0.050	1.178E-03	
159600000	0.900	0.210	135.064	388.674	411.473	1.236	71	160	39.776	0.025	1.178E-03	Resistance
160950000	0.914	0.119	349.020	550.338	651.680	1.006	58	161	102.786	0.010	1.178E-03	interpolated
162300000	0.923	0.027	1104.524	403.770	1176.012	0.350	20	162	325.282	0.003	1.178E-03	1325.915
163650000	0.918	-0.065	699.786	-596.538	919.543	-0.706	-40	164	206.087	0.005	1.178E-03	
165000000	0.907	-0.167	203.973	-455.435	499.026	-1.150	-66	165	60.070	0.017	1.178E-03	
166350000	0.884	-0.250	102.920	-329.240	344.951	-1.268	-73	166	30.310	0.033	1.178E-03	

Frequency (Hertz)	VNA Real (r)	VNA Imaginary (x)	Resistance (Ohm)	Reactance (Ohm)	Magnitude (Ohm)	Angle (Radians)	Angle (Degrees)	Frequency (MegaHertz)	Resistivity (Ohm-meter)	Conductivity (Siemens per meter)	Rock Area (Square Meters)
167700000	0.853	-0.341	56.887	-247.237	253.697	-1.345	-77	168	16.753	0.060	1.178E-03
169050000	0.811	-0.431	35.244	-194.640	197.805	-1.392	-80	169	10.379	0.096	1.178E-03
170400000	0.766	-0.501	26.470	-163.731	165.857	-1.411	-81	170	7.796	0.128	1.178E-03
171750000	0.706	-0.586	18.540	-136.318	137.573	-1.436	-82	172	5.460	0.183	1.178E-03
173100000	0.643	-0.653	14.446	-117.874	118.756	-1.449	-83	173	4.254	0.235	1.178E-03
174450000	0.571	-0.714	11.801	-102.854	103.529	-1.457	-83	174	3.475	0.288	1.178E-03
175800000	0.499	-0.765	9.932	-91.470	92.007	-1.463	-84	176	2.925	0.342	1.178E-03
177150000	0.413	-0.809	8.729	-81.017	81.486	-1.463	-84	177	2.571	0.389	1.178E-03
178500000	0.326	-0.849	7.327	-72.491	72.860	-1.470	-84	179	2.158	0.463	1.178E-03
179850000	0.244	-0.873	6.720	-65.438	65.782	-1.468	-84	180	1.979	0.505	1.178E-03
181200000	0.149	-0.894	5.884	-58.705	58.999	-1.471	-84	181	1.733	0.577	1.178E-03
182550000	0.058	-0.901	5.418	-53.024	53.300	-1.469	-84	183	1.596	0.627	1.178E-03
183900000	-0.035	-0.902	4.934	-47.847	48.100	-1.468	-84	184	1.453	0.688	1.178E-03
185250000	-0.124	-0.890	4.706	-43.312	43.567	-1.463	-84	185	1.386	0.721	1.178E-03
186600000	-0.208	-0.869	4.544	-39.228	39.491	-1.455	-83	187	1.338	0.747	1.178E-03
187950000	-0.307	-0.838	4.203	-34.791	35.044	-1.451	-83	188	1.238	0.808	1.178E-03
189300000	-0.379	-0.808	3.985	-31.628	31.878	-1.445	-83	189	1.174	0.852	1.178E-03
190650000	-0.453	-0.768	3.811	-28.441	28.695	-1.438	-82	191	1.122	0.891	1.178E-03
192000000	-0.524	-0.724	3.528	-25.418	25.662	-1.433	-82	192	1.039	0.963	1.178E-03
193350000	-0.608	-0.659	3.246	-21.807	22.048	-1.423	-82	193	0.956	1.046	1.178E-03
194700000	-0.668	-0.605	2.987	-19.208	19.436	-1.417	-81	195	0.880	1.137	1.178E-03
196050000	-0.730	-0.529	2.845	-16.167	16.416	-1.397	-80	196	0.838	1.194	1.178E-03
197400000	-0.784	-0.456	2.605	-13.440	13.690	-1.379	-79	197	0.767	1.303	1.178E-03
198750000	-0.824	-0.380	2.535	-10.937	11.227	-1.343	-77	199	0.747	1.339	1.178E-03
200100000	-0.861	-0.292	2.457	-8.228	8.587	-1.281	-73	200	0.724	1.382	1.178E-03
201450000	-0.886	-0.202	2.413	-5.626	6.121	-1.166	-67	201	0.711	1.407	1.178E-03
202800000	-0.904	-0.111	2.332	-3.039	3.831	-0.916	-52	203	0.687	1.456	1.178E-03
204150000	-0.915	-0.001	2.231	-0.033	2.231	-0.015	-1	204	0.657	1.522	1.178E-03
205500000	-0.911	0.082	2.220	2.238	3.152	0.789	45	206	0.654	1.530	1.178E-03
206850000	-0.901	0.178	2.158	4.876	5.332	1.154	66	207	0.635	1.574	1.178E-03
208200000	-0.874	0.275	2.246	7.668	7.991	1.286	74	208	0.661	1.512	1.178E-03
209550000	-0.846	0.358	2.192	10.130	10.365	1.358	78	210	0.646	1.549	1.178E-03
210900000	-0.805	0.449	2.161	12.979	13.158	1.406	81	211	0.636	1.571	1.178E-03
212250000	-0.755	0.529	2.240	15.745	15.904	1.429	82	212	0.660	1.516	1.178E-03
213600000	-0.695	0.608	2.276	18.737	18.874	1.450	83	214	0.670	1.492	1.178E-03
214950000	-0.634	0.673	2.324	21.565	21.690	1.463	84	215	0.684	1.461	1.178E-03
216300000	-0.557	0.737	2.470	24.843	24.966	1.472	84	216	0.727	1.375	1.178E-03
217650000	-0.482	0.789	2.592	27.996	28.115	1.478	85	218	0.763	1.310	1.178E-03
219000000	-0.405	0.832	2.715	31.203	31.320	1.484	85	219	0.800	1.251	1.178E-03
220350000	-0.311	0.873	2.863	35.203	35.319	1.490	85	220	0.843	1.186	1.178E-03
221700000	-0.223	0.895	3.256	38.983	39.119	1.487	85	222	0.960	1.042	1.178E-03
223050000	-0.126	0.917	3.402	43.494	43.627	1.493	86	223	1.002	0.998	1.178E-03
224400000	-0.031	0.926	3.701	48.218	48.360	1.494	86	224	1.090	0.917	1.178E-03
225750000	0.058	0.922	4.218	53.044	53.212	1.491	85	226	1.242	0.805	1.178E-03
227100000	0.162	0.911	4.664	59.454	59.636	1.493	86	227	1.374	0.728	1.178E-03
228450000	0.240	0.892	5.269	64.976	65.189	1.490	85	228	1.552	0.644	1.178E-03
229800000	0.339	0.864	5.857	73.015	73.249	1.491	85	230	1.725	0.580	1.178E-03
231150000	0.419	0.825	7.037	81.031	81.336	1.484	85	231	2.072	0.483	1.178E-03
232500000	0.499	0.779	8.368	90.846	91.230	1.479	85	233	2.464	0.406	1.178E-03
233850000	0.572	0.727	10.067	102.183	102.678	1.473	84	234	2.965	0.337	1.178E-03
235200000	0.655	0.657	12.559	119.315	119.974	1.466	84	235	3.699	0.270	1.178E-03
236550000	0.713	0.591	16.443	136.797	137.782	1.451	83	237	4.842	0.207	1.178E-03
237900000	0.769	0.517	22.191	161.192	162.712	1.434	82	238	6.535	0.153	1.178E-03
239250000	0.813	0.443	30.755	191.507	193.961	1.412	81	239	9.057	0.110	1.178E-03
240600000	0.855	0.358	47.389	240.131	244.762	1.376	79	241	13.956	0.072	1.178E-03
241950000	0.887	0.270	81.389	315.287	325.623	1.318	76	242	23.969	0.042	1.178E-03
243300000	0.908	0.184	167.097	434.822	465.823	1.204	69	243	49.210	0.020	1.178E-03
244650000	0.924	0.091	487.035	646.450	810.981	0.927	53	245	143.432	0.007	1.178E-03
246000000	0.931	-0.003	1390.726	-62.644	1392.136	-0.045	-3	246	409.569	0.002	1.178E-03
247350000	0.924	-0.098	445.951	-639.341	779.506	-0.962	-55	247	131.333	0.008	1.178E-03
248700000	0.910	-0.192	149.771	-427.204	452.697	-1.234	-71	249	44.108	0.023	1.178E-03
250050000	0.887	-0.282	72.879	-305.544	314.115	-1.337	-77	250	21.463	0.047	1.178E-03
251400000	0.856	-0.366	42.953	-236.469	240.338	-1.391	-80	251	12.650	0.079	1.178E-03
252750000	0.815	-0.447	28.984	-191.194	193.378	-1.420	-81	253	8.536	0.117	1.178E-03
254100000	0.766	-0.529	19.888	-158.250	159.495	-1.446	-83	254	5.857	0.171	1.178E-03
255450000	0.714	-0.597	15.259	-136.162	137.014	-1.459	-84	255	4.494	0.223	1.178E-03
256800000	0.646	-0.671	11.505	-116.630	117.196	-1.472	-84	257	3.388	0.295	1.178E-03
258150000	0.574	-0.731	9.551	-102.177	102.622	-1.478	-85	258	2.813	0.356	1.178E-03
259500000	0.501	-0.784	7.794	-90.756	91.090	-1.485	-85	260	2.295	0.436	1.178E-03
260850000	0.427	-0.824	6.907	-81.766	82.057	-1.487	-85	261	2.034	0.492	1.178E-03
262200000	0.328	-0.874	5.319	-71.897	72.093	-1.497	-86	262	1.566	0.638	1.178E-03
263550000	0.246	-0.898	4.861	-65.318	65.499	-1.497	-86	264	1.431	0.699	1.178E-03
264900000	0.158	-0.916	4.415	-59.166	59.330	-1.496	-86	265	1.300	0.769	1.178E-03
266250000	0.063	-0.928	3.861	-53.334	53.474	-1.499	-86	266	1.137	0.879	1.178E-03
267600000	-0.042	-0.931	3.361	-47.708	47.826	-1.500	-86	268	0.990	1.010	1.178E-03
268950000	-0.118	-0.923	3.185	-43.899	44.014	-1.498	-86	269	0.938	1.066	1.178E-03
270300000	-0.219	-0.906	2.859	-39.279	39.383	-1.498	-86	270	0.842	1.188	1.178E-03
271650000	-0.314	-0.876	2.689	-35.141	35.243	-1.494	-86	272	0.792	1.263	1.178E-03
273000000	-0.394	-0.843	2.519	-31.764	31.863	-1.492	-86	273	0.742	1.348	1.178E-03
274350000	-0.474	-0.798	2.464	-28.411	28.517	-1.484	-85	274	0.726	1.378	1.178E-03
275700000	-0.559	-0.744	2.249	-24.928	25.030	-1.481	-85	276	0.662	1.510	1.178E-03
277050000	-0.625	-0.688	2.187	-22.097	22.205	-1.472	-84	277	0.644	1.553	1.178E-03
278400000	-0.695	-0.617	2.090	-18.976	19.091	-1.461	-84	278	0.615	1.625	1.178E-03
279750000	-0.751	-0.545	2.060	-16.191	16.322	-1.444	-83	280	0.607	1.648	1.178E-03
281100000	-0.803	-0.467	1.974	-13.447	13.591	-1.425	-82	281	0.581	1.720	1.178E-03
282450000	-0.843	-0.388	1.962	-10.932	11.106	-1.393	-80	282	0.578	1.731	1.178E-03
283800000	-0.879	-0.292	1.955	-8.073	8.306	-1.333	-76	284	0.576	1.737	1.178E-03
285150000	-0.905	-0.203	1.912	-5.532	5.853	-1.238	-71	285	0.563	1.776	1.178E-03
286500000	-0.916	-0.114	2.002	-3.092	3.683	-0.996	-57	287	0.590	1.696	1.178E-03
287850000	-0.924	-0.029	1.968	-0.784	2.119	-0.379	-22	288	0.580	1.725	1.178E-03
289200000	-0.923	0.074	1.925	1.988	2.767	0.802	46	289	0.567	1.764	1.178E-03
290550000	-0.907	0.173	2.022	4.714	5.129	1.166	67	291	0.596	1.679	1.178E-03
291900000	-0.886	0.260	2.028	7.173	7.454	1.295	74	292	0.597	1.674	1.178E-03
293250000	-0.860	0.333	2.102	9.333	9.567	1.349	77	293	0.619	1.615	1.178E-03
294600000	-0.817	0.433	2.063	12.414	12.584	1.406	81	295	0.607	1.646	1.178E-03
295950000	-0.773	0.504	2.193	14.834	14.995	1.424	82	296	0.646	1.548	1.178E-03
297300000	-0.722	0.578	2.205	17.524	17.662	1.446	83	297	0.649	1.540	1.178E-03
298650000	-0.658	0.649	2.308	20.459	20.588	1.458	84	299	0.680	1.471	1.178E-03
300000000	-0.585	0.718	2.384	23.709	23.826	1.471	84	300	0.698	1.436	1.178E-03

ANNEXURE 3 Electrical parameters of the untreated JSC rock sample for the VHF range

Frequency (Hertz)	VNA Real (r)	VNA Imaginary (x)	Resistance (Ohm)	Reactance (Ohm)	Magnitude (Ohm)	Angle (Radians)	Angle (Degrees)	Frequency (MegaHertz)	Resistivity (Ohm-meter)	Conductivity (Siemens per meter)	Rock Area (Square Meters)
30000000	-0.604	-0.781	0.390	-24.550	24.553	-1.555	-89	30	0.111	9.007	1.140E-03
31350000	-0.691	-0.706	0.387	-21.019	21.022	-1.553	-89	31	0.105	9.563	1.140E-03
32700000	-0.752	-0.639	0.384	-18.364	18.368	-1.550	-89	33	0.109	9.145	1.140E-03
34050000	-0.813	-0.555	0.430	-15.427	15.433	-1.543	-88	34	0.122	8.164	1.140E-03
35400000	-0.866	-0.471	0.390	-12.717	12.723	-1.540	-88	35	0.111	8.988	1.140E-03
36750000	-0.910	-0.374	0.429	-9.882	9.892	-1.527	-88	37	0.122	8.181	1.140E-03
38100000	-0.942	-0.285	0.409	-7.392	7.403	-1.516	-87	38	0.116	8.588	1.140E-03
39450000	-0.962	-0.186	0.523	-4.792	4.821	-1.462	-84	39	0.149	6.711	1.140E-03
40800000	-0.977	-0.094	0.464	-2.408	2.453	-1.381	-79	41	0.132	7.564	1.140E-03
42150000	-0.979	0.010	0.530	0.244	0.584	0.432	25	42	0.151	6.617	1.140E-03
43500000	-0.971	0.117	0.553	2.996	3.047	1.388	80	44	0.158	6.339	1.140E-03
44850000	-0.954	0.210	0.600	5.448	5.481	1.461	84	45	0.171	5.849	1.140E-03
46200000	-0.927	0.306	0.620	8.001	8.025	1.493	86	46	0.177	5.656	1.140E-03
47550000	-0.889	0.397	0.686	10.660	10.682	1.507	86	48	0.195	5.116	1.140E-03
48900000	-0.842	0.494	0.652	13.597	13.613	1.523	87	49	0.186	5.379	1.140E-03
50250000	-0.786	0.570	0.815	16.216	16.237	1.521	87	50	0.232	4.304	1.140E-03
51600000	-0.719	0.647	0.948	19.180	19.204	1.521	87	52	0.270	3.703	1.140E-03
52950000	-0.639	0.716	1.243	22.393	22.428	1.515	87	53	0.354	2.822	1.140E-03
54300000	-0.556	0.764	1.787	25.439	25.502	1.501	86	54	0.509	1.964	1.140E-03
55650000	-0.480	0.795	2.426	28.164	28.268	1.485	85	56	0.691	1.446	1.140E-03
57000000	-0.417	0.844	2.107	31.037	31.108	1.503	86	57	0.601	1.665	1.140E-03
58350000	-0.339	0.883	2.036	34.321	34.381	1.512	87	58	0.580	1.723	1.140E-03
59700000	-0.251	0.918	1.905	38.158	38.205	1.521	87	60	0.543	1.842	1.140E-03
61050000	-0.158	0.945	1.851	42.319	42.360	1.527	87	61	0.527	1.896	1.140E-03
62400000	-0.065	0.955	2.053	46.680	46.725	1.527	87	62	0.585	1.709	1.140E-03
63750000	0.027	0.968	2.193	51.406	51.453	1.528	88	64	0.625	1.600	1.140E-03
65100000	0.136	0.953	2.236	57.625	57.668	1.532	88	65	0.637	1.569	1.140E-03
66450000	0.227	0.931	2.795	63.554	63.615	1.527	87	66	0.796	1.256	1.140E-03
67800000	0.314	0.902	3.465	70.214	70.299	1.521	87	68	0.987	1.013	1.140E-03
69150000	0.393	0.875	3.515	77.137	77.217	1.525	87	69	1.002	0.998	1.140E-03
70500000	0.492	0.831	3.604	87.577	87.651	1.530	88	71	1.027	0.974	1.140E-03
71850000	0.572	0.778	4.291	98.720	98.813	1.527	88	72	1.223	0.818	1.140E-03
73200000	0.651	0.715	5.162	112.989	113.107	1.525	87	73	1.471	0.680	1.140E-03
74550000	0.719	0.643	7.087	130.654	130.846	1.517	87	75	2.020	0.495	1.140E-03
75900000	0.781	0.571	8.554	152.600	152.839	1.515	87	76	2.438	0.410	1.140E-03
77250000	0.835	0.486	12.440	184.412	184.831	1.503	86	77	3.546	0.282	1.140E-03
78600000	0.881	0.401	18.244	229.082	229.808	1.491	85	79	5.200	0.192	1.140E-03
79950000	0.913	0.312	32.703	297.777	299.568	1.461	84	80	9.320	0.107	1.140E-03
81300000	0.942	0.219	63.353	426.693	431.371	1.423	82	81	18.055	0.055	1.140E-03
82650000	0.959	0.125	183.565	721.331	744.321	1.322	76	83	52.316	0.019	1.140E-03
84000000	0.967	0.022	2034.465	1403.333	2471.516	0.604	35	84	579.823	0.002	1.140E-03
85350000	0.965	-0.070	515.679	-1140.643	1251.795	-1.146	-66	85	146.969	0.007	1.140E-03
86700000	0.953	-0.166	109.303	-560.708	571.262	-1.378	-79	87	31.151	0.032	1.140E-03
88050000	0.928	-0.265	45.277	-350.969	353.877	-1.442	-83	88	12.904	0.077	1.140E-03
89400000	0.899	-0.352	25.539	-262.326	263.566	-1.474	-84	89	7.279	0.137	1.140E-03
90750000	0.856	-0.448	15.115	-202.104	202.668	-1.496	-86	91	4.308	0.232	1.140E-03
92100000	0.809	-0.526	10.897	-167.999	168.352	-1.506	-86	92	3.106	0.322	1.140E-03
93450000	0.757	-0.595	8.827	-143.931	144.202	-1.510	-86	93	2.516	0.398	1.140E-03
94800000	0.690	-0.672	6.593	-122.587	122.764	-1.517	-87	95	1.879	0.532	1.140E-03
96150000	0.615	-0.743	5.060	-106.099	106.219	-1.523	-87	96	1.442	0.693	1.140E-03
97500000	0.540	-0.798	4.231	-94.081	94.176	-1.526	-87	98	1.206	0.829	1.140E-03
98850000	0.462	-0.845	3.590	-84.203	84.280	-1.528	-88	99	1.023	0.977	1.140E-03
100200000	0.364	-0.894	2.874	-74.251	74.307	-1.532	-88	100	0.819	1.221	1.140E-03
101550000	0.273	-0.925	2.543	-66.854	66.902	-1.533	-88	102	0.725	1.380	1.140E-03
102900000	0.184	-0.946	2.293	-60.642	60.686	-1.533	-88	103	0.653	1.531	1.140E-03
104250000	0.081	-0.959	2.077	-54.380	54.420	-1.533	-88	104	0.592	1.689	1.140E-03
105600000	-0.024	-0.966	1.677	-48.759	48.788	-1.536	-88	106	0.478	2.093	1.140E-03
106950000	-0.111	-0.958	1.619	-44.522	44.551	-1.534	-88	107	0.461	2.167	1.140E-03
108300000	-0.215	-0.940	1.465	-39.828	39.855	-1.534	-88	108	0.418	2.395	1.140E-03
109650000	-0.301	-0.912	1.545	-36.145	36.178	-1.528	-88	110	0.440	2.272	1.140E-03
111000000	-0.392	-0.879	1.445	-32.395	32.428	-1.526	-87	111	0.412	2.428	1.140E-03
112350000	-0.484	-0.830	1.326	-28.727	28.758	-1.525	-87	112	0.378	2.646	1.140E-03
113700000	-0.566	-0.780	1.166	-25.481	25.507	-1.525	-87	114	0.332	3.009	1.140E-03
115050000	-0.636	-0.720	1.213	-22.541	22.574	-1.517	-87	115	0.346	2.893	1.140E-03
116400000	-0.709	-0.648	1.167	-19.395	19.430	-1.511	-87	116	0.333	3.007	1.140E-03
117750000	-0.769	-0.572	1.170	-16.546	16.587	-1.500	-86	118	0.334	2.998	1.140E-03
119100000	-0.827	-0.486	1.118	-13.604	13.650	-1.489	-85	119	0.319	3.139	1.140E-03
120450000	-0.873	-0.395	1.125	-10.776	10.834	-1.467	-84	120	0.321	3.119	1.140E-03
121600000	-0.903	-0.315	1.144	-8.462	8.539	-1.436	-82	122	0.326	3.066	1.140E-03
123150000	-0.929	-0.219	1.169	-5.809	5.925	-1.372	-79	123	0.333	3.001	1.140E-03
124500000	-0.950	-0.117	1.086	-3.074	3.260	-1.231	-71	125	0.310	3.231	1.140E-03
125850000	-0.955	-0.024	1.137	-0.640	1.305	-0.512	-29	126	0.324	3.085	1.140E-03
127200000	-0.950	0.084	1.175	2.214	2.506	1.083	62	127	0.335	2.985	1.140E-03
128550000	-0.937	0.175	1.203	4.638	4.792	1.317	75	129	0.343	2.918	1.140E-03
129900000	-0.915	0.273	1.188	7.297	7.393	1.409	81	130	0.339	2.954	1.140E-03
131250000	-0.886	0.351	1.246	9.549	9.630	1.441	83	131	0.355	2.816	1.140E-03
132600000	-0.840	0.448	1.301	12.498	12.565	1.467	84	133	0.371	2.697	1.140E-03
133950000	-0.792	0.526	1.374	15.089	15.151	1.480	85	134	0.391	2.555	1.140E-03
135300000	-0.734	0.604	1.423	17.922	17.979	1.492	85	135	0.406	2.466	1.140E-03
136650000	-0.666	0.676	1.507	20.955	21.009	1.499	86	137	0.429	2.329	1.140E-03
138000000	-0.595	0.740	1.586	23.945	23.998	1.505	86	138	0.452	2.213	1.140E-03
139350000	-0.519	0.795	1.677	27.050	27.102	1.509	86	139	0.478	2.092	1.140E-03
140700000	-0.430	0.841	1.810	30.265	30.320	1.511	87	141	0.516	1.939	1.140E-03
142050000	-0.344	0.886	1.884	34.195	34.246	1.516	87	142	0.537	1.862	1.140E-03
143400000	-0.255	0.915	2.007	37.935	37.988	1.518	87	143	0.572	1.748	1.140E-03
144750000	-0.156	0.936	2.243	42.301	42.360	1.518	87	145	0.639	1.564	1.140E-03
146100000	-0.058	0.944	2.560	46.463	46.533	1.516	87	146	0.730	1.371	1.140E-03
147450000	0.030	0.947	2.785	51.542	51.617	1.517	87	147	0.794	1.260	1.140E-03
148800000	0.127	0.939	3.080	57.123	57.206	1.517	87	149	0.878	1.139	1.140E-03
150150000	0.225	0.921	3.478	63.536	63.632	1.516	87	150	0.991	1.009	1.140E-03
151500000	0.320	0.890	4.209	70.935	71.059	1.512	87	152	1.200	0.834	1.140E-03
152850000	0.408	0.854	4.930	78.892	79.046	1.508	86	153	1.405	0.712	1.140E-03
154200000	0.489	0.810	5.756	88.302	88.489	1.506	86	154	1.641	0.610	1.140E-03
155550000	0.567	0.755	7.199	99.652	99.912	1.499	86	156	2.052	0.487	1.140E-03
156900000	0.638	0.697	8.759	113.013	113.352	1.493	86	157	2.496	0.401	1.140E-03
158250000	0.702	0.625	12.145	130.259	130.824	1.478	85	158	3.461	0.289	1.140E-03
159600000	0.762	0.550	16.318	153.148	154.015	1.465	84	160	4.651	0.215	1.140E-03
160950000	0.816	0.469	23.577	185.777	187.267	1.445	83	161	6.719	0.149	1.140E-03
162300000	0.858	0.381	35.966	230.723	233.509	1.416	81	162	10.250	0.098	1.140E-03
163650000	0.885	0.298	62.493	292.316	298.921	1.360	78	164	17.811	0.056	1.140E-03
165000000	0.913	0.204	126.111	414.798	433.545	1.276	73	165	35.942	0.028	1.140E-03
166350000	0.925	0.117	337.155	606.103	693.566	1.063	61	166	96.089	0.010	1.140E-03

Frequency (Hertz)	VNA Real (r)	VNA Imaginary (x)	Resistance (Ohm)	Reactance (Ohm)	Magnitude (Ohm)	Angle (Radians)	Angle (Degrees)	Frequency (MegaHertz)	Resistivity (Ohm-meter)	Conductivity (Siemens per meter)	Rock Area (Square Meters)
167700000	0.934	0.018	1360.153	384.074	1413.340	0.275	16	168	387.644	0.003	1.140E-03
169050000	0.928	-0.081	503.489	-692.052	892.444	-0.887	-51	169	160.594	0.006	1.140E-03
170400000	0.916	-0.174	176.658	-464.688	497.135	-1.208	-69	170	50.347	0.020	1.140E-03
171750000	0.894	-0.260	93.729	-338.818	351.544	-1.301	-75	172	26.713	0.037	1.140E-03
173100000	0.860	-0.347	49.727	-247.606	252.550	-1.373	-79	173	14.172	0.071	1.140E-03
174450000	0.819	-0.430	33.137	-197.248	200.012	-1.404	-80	174	9.444	0.106	1.140E-03
175800000	0.771	-0.507	23.850	-163.902	165.629	-1.426	-82	176	6.797	0.147	1.140E-03
177150000	0.713	-0.584	17.781	-137.850	138.992	-1.443	-83	177	5.068	0.197	1.140E-03
178500000	0.652	-0.648	14.334	-119.768	120.612	-1.452	-83	179	4.085	0.245	1.140E-03
179850000	0.581	-0.710	11.677	-104.514	105.164	-1.460	-84	180	3.328	0.300	1.140E-03
181200000	0.507	-0.761	9.949	-92.490	93.023	-1.464	-84	181	2.835	0.353	1.140E-03
182550000	0.421	-0.809	8.454	-81.774	82.209	-1.468	-84	183	2.409	0.415	1.140E-03
183900000	0.331	-0.846	7.528	-72.745	73.134	-1.468	-84	184	2.145	0.466	1.140E-03
185250000	0.249	-0.868	6.994	-65.903	66.273	-1.465	-84	185	1.993	0.502	1.140E-03
186600000	0.159	-0.884	6.466	-59.390	59.741	-1.462	-84	187	1.843	0.543	1.140E-03
187950000	0.081	-0.889	6.205	-54.387	54.740	-1.457	-83	188	1.769	0.565	1.140E-03
189300000	-0.012	-0.893	5.580	-49.033	49.350	-1.457	-84	189	1.590	0.629	1.140E-03
190650000	-0.100	-0.884	5.254	-44.366	44.676	-1.453	-83	191	1.497	0.668	1.140E-03
192000000	-0.186	-0.871	4.750	-40.212	40.492	-1.453	-83	192	1.354	0.739	1.140E-03
193350000	-0.265	-0.850	4.456	-36.602	36.872	-1.450	-83	193	1.270	0.787	1.140E-03
194700000	-0.344	-0.826	3.997	-33.195	33.435	-1.451	-83	195	1.139	0.878	1.140E-03
196050000	-0.433	-0.788	3.572	-29.463	29.678	-1.450	-83	196	1.018	0.982	1.140E-03
197400000	-0.510	-0.742	3.352	-26.223	26.436	-1.444	-83	197	0.956	1.047	1.140E-03
198750000	-0.581	-0.695	3.020	-23.312	23.507	-1.442	-83	199	0.861	1.162	1.140E-03
200100000	-0.646	-0.637	2.831	-20.437	20.632	-1.433	-82	200	0.807	1.239	1.140E-03
201450000	-0.715	-0.562	2.650	-17.252	17.455	-1.418	-81	201	0.755	1.324	1.140E-03
202800000	-0.766	-0.496	2.475	-14.750	14.956	-1.405	-80	203	0.705	1.418	1.140E-03
204150000	-0.820	-0.409	2.311	-11.759	11.984	-1.377	-79	204	0.659	1.519	1.140E-03
205500000	-0.862	-0.317	2.201	-8.892	9.160	-1.328	-76	206	0.627	1.594	1.140E-03
206850000	-0.892	-0.233	2.060	-6.404	6.727	-1.260	-72	207	0.587	1.703	1.140E-03
208200000	-0.916	-0.134	1.932	-3.641	4.121	-1.083	-62	208	0.550	1.817	1.140E-03
209550000	-0.923	-0.052	1.976	-1.393	2.418	-0.614	-35	210	0.563	1.776	1.140E-03
210900000	-0.926	0.053	1.890	1.431	2.370	0.648	37	211	0.539	1.857	1.140E-03
212250000	-0.917	0.149	1.853	4.018	4.424	1.139	65	212	0.528	1.893	1.140E-03
213600000	-0.899	0.233	1.878	6.375	6.646	1.284	74	214	0.535	1.869	1.140E-03
214950000	-0.870	0.331	1.846	9.182	9.366	1.372	79	215	0.526	1.900	1.140E-03
216300000	-0.828	0.425	1.901	12.071	12.220	1.415	81	216	0.542	1.845	1.140E-03
217650000	-0.780	0.510	1.915	14.865	14.988	1.443	83	218	0.546	1.832	1.140E-03
219000000	-0.728	0.582	1.976	17.489	17.600	1.458	84	219	0.563	1.775	1.140E-03
220350000	-0.665	0.654	2.031	20.454	20.555	1.472	84	220	0.579	1.727	1.140E-03
221700000	-0.590	0.724	2.091	23.703	23.795	1.483	85	222	0.596	1.679	1.140E-03
223050000	-0.516	0.782	2.101	26.882	26.964	1.493	86	223	0.599	1.670	1.140E-03
224400000	-0.429	0.830	2.319	30.399	30.487	1.495	86	224	0.661	1.513	1.140E-03
225750000	-0.344	0.867	2.537	33.883	33.977	1.496	86	226	0.723	1.383	1.140E-03
227100000	-0.252	0.900	2.680	37.864	37.959	1.500	86	227	0.764	1.309	1.140E-03
228450000	-0.160	0.919	2.974	41.977	42.082	1.500	86	228	0.848	1.180	1.140E-03
229800000	-0.064	0.929	3.325	46.539	46.657	1.499	86	230	0.945	1.055	1.140E-03
231150000	0.033	0.931	3.651	51.680	51.809	1.500	86	231	1.041	0.961	1.140E-03
232500000	0.124	0.923	4.122	56.997	57.146	1.499	86	233	1.175	0.851	1.140E-03
233850000	0.225	0.905	4.564	63.713	63.876	1.499	86	234	1.301	0.769	1.140E-03
235200000	0.316	0.876	5.384	70.886	71.090	1.495	86	235	1.534	0.652	1.140E-03
236550000	0.403	0.840	6.190	79.072	79.314	1.493	86	237	1.764	0.567	1.140E-03
237900000	0.481	0.798	7.280	88.108	88.409	1.488	85	238	2.075	0.482	1.140E-03
239250000	0.552	0.750	8.728	98.239	98.626	1.482	85	239	2.487	0.402	1.140E-03
240600000	0.633	0.683	10.957	113.601	114.128	1.475	84	241	3.123	0.320	1.140E-03
241950000	0.699	0.618	13.778	130.854	131.577	1.466	84	242	3.927	0.255	1.140E-03
243300000	0.757	0.543	18.769	153.339	154.484	1.449	83	243	5.349	0.187	1.140E-03
244650000	0.810	0.465	25.160	184.416	186.125	1.435	82	245	7.171	0.139	1.140E-03
246000000	0.848	0.388	37.598	223.393	226.535	1.404	80	246	10.715	0.093	1.140E-03
247350000	0.885	0.298	63.209	291.952	298.717	1.358	78	247	18.015	0.056	1.140E-03
248700000	0.912	0.207	123.621	409.772	428.013	1.278	73	249	35.232	0.028	1.140E-03
250050000	0.926	0.118	332.015	611.300	695.645	1.073	61	250	94.624	0.011	1.140E-03
251400000	0.935	0.022	1332.430	460.420	1409.736	0.333	19	251	379.742	0.003	1.140E-03
252750000	0.933	-0.086	512.548	-719.395	883.309	-0.952	-55	253	146.076	0.007	1.140E-03
254100000	0.918	-0.174	171.809	-470.910	501.204	-1.221	-70	254	48.909	0.020	1.140E-03
255450000	0.898	-0.255	84.663	-338.090	348.530	-1.325	-76	255	24.129	0.041	1.140E-03
256800000	0.867	-0.348	45.434	-250.823	254.905	-1.392	-80	257	12.949	0.077	1.140E-03
258150000	0.827	-0.436	28.632	-198.073	200.132	-1.427	-82	258	8.160	0.123	1.140E-03
259500000	0.779	-0.513	20.800	-164.349	165.660	-1.445	-83	260	5.928	0.169	1.140E-03
260850000	0.722	-0.568	15.691	-138.876	139.760	-1.458	-84	261	4.472	0.224	1.140E-03
262200000	0.660	-0.658	12.000	-119.961	120.560	-1.471	-84	262	3.420	0.292	1.140E-03
263550000	0.584	-0.729	9.066	-103.438	103.835	-1.483	-85	264	2.584	0.387	1.140E-03
264900000	0.516	-0.779	7.582	-92.606	92.915	-1.489	-85	265	2.161	0.463	1.140E-03
266250000	0.430	-0.829	6.293	-81.945	82.186	-1.494	-86	266	1.794	0.558	1.140E-03
267600000	0.347	-0.865	5.598	-73.634	73.846	-1.495	-86	268	1.596	0.627	1.140E-03
268950000	0.257	-0.897	4.734	-66.118	66.287	-1.499	-86	269	1.349	0.741	1.140E-03
270300000	0.174	-0.916	4.320	-60.221	60.375	-1.499	-86	270	1.231	0.812	1.140E-03
271650000	0.067	-0.931	3.734	-53.569	53.699	-1.501	-86	272	1.064	0.940	1.140E-03
273000000	-0.023	-0.929	3.547	-48.651	48.780	-1.498	-86	273	1.011	0.989	1.140E-03
274350000	-0.112	-0.925	3.137	-44.215	44.326	-1.500	-86	274	0.894	1.119	1.140E-03
275700000	-0.212	-0.905	2.966	-39.553	39.664	-1.496	-86	276	0.845	1.183	1.140E-03
277050000	-0.303	-0.880	2.703	-35.596	35.698	-1.495	-86	277	0.770	1.298	1.140E-03
278400000	-0.395	-0.841	2.572	-31.707	31.811	-1.490	-85	278	0.733	1.364	1.140E-03
279750000	-0.468	-0.799	2.545	-28.606	28.719	-1.482	-85	280	0.725	1.379	1.140E-03
281100000	-0.547	-0.748	2.389	-25.330	25.443	-1.477	-85	281	0.681	1.469	1.140E-03
282450000	-0.627	-0.681	2.292	-21.879	21.998	-1.466	-84	282	0.653	1.531	1.140E-03
283800000	-0.691	-0.615	2.229	-18.978	19.109	-1.454	-83	284	0.635	1.574	1.140E-03
285150000	-0.747	-0.543	2.200	-16.230	16.378	-1.436	-82	285	0.627	1.595	1.140E-03
286500000	-0.804	-0.456	2.108	-13.173	13.340	-1.412	-81	287	0.601	1.665	1.140E-03
287850000	-0.840	-0.380	2.118	-10.754	10.960	-1.376	-79	288	0.604	1.657	1.140E-03
289200000	-0.874	-0.286	2.150	-7.970	8.255	-1.307	-75	289	0.613	1.632	1.140E-03
290550000	-0.897	-0.199	2.143	-5.481	5.885	-1.198	-69	291	0.611	1.638	1.140E-03
291900000	-0.913	-0.109	2.097	-2.971	3.636	-0.956	-55	292	0.598	1.673	1.140E-03
293250000	-0.920	-0.015	2.076	-0.408	2.116	-0.194	-11	293	0.592	1.690	1.140E-03
294600000	-0.914	0.072	2.172	1.974	2.935	0.738	42	295	0.619	1.615	1.140E-03
295950000	-0.903	0.178	2.089	4.825	5.258	1.162	67	296	0.595	1.680	1.140E-03
297300000	-0.881	0.262	2.153	7.250	7.563	1.282	73	297	0.614	1.630	1.140E-03
298650000	-0.848	0.354	2.200	9.985	10.225	1.354	78	299	0.627	1.595	1.140E-03
300000000	-0.813	0.433	2.172	12.452	12.640	1.398	80	300	0.619	1.615	1.140E-03

Resonating frequency interpolated 1.6785E+08

Resistance interpolated 1545.583

ANNEXURE 4 Electrical parameters of the untreated JSD rock sample for the VHF range

Frequency (Hertz)	VNA Real (r)	VNA Imaginary (x)	Resistance (Ohm)	Reactance (Ohm)	Magnitude (Ohm)	Angle (Radians)	Angle (Degrees)	Frequency (MegaHertz)	Resistivity (Ohm-meter)	Conductivity (Siemens per meter)	Rock Area (Square Meters)
30000000	-0.590	-0.789	0.467	-25.039	25.043	-1.552	-89	30	0.133	7.517	1.140E-03
31350000	-0.658	-0.730	0.517	-22.232	22.238	-1.548	-89	31	0.147	6.787	1.140E-03
32700000	-0.730	-0.655	0.558	-19.141	19.149	-1.542	-88	33	0.159	6.290	1.140E-03
34050000	-0.785	-0.585	0.579	-16.575	16.585	-1.536	-88	34	0.165	6.056	1.140E-03
35400000	-0.844	-0.499	0.535	-13.679	13.690	-1.532	-88	35	0.152	6.564	1.140E-03
36750000	-0.889	-0.411	0.545	-10.999	11.012	-1.521	-87	37	0.155	6.444	1.140E-03
38100000	-0.924	-0.322	0.557	-8.458	8.476	-1.505	-86	38	0.159	6.298	1.140E-03
39450000	-0.952	-0.225	0.561	-5.831	5.858	-1.475	-85	39	0.160	6.260	1.140E-03
40800000	-0.967	-0.128	0.614	-3.303	3.359	-1.387	-79	41	0.175	5.716	1.140E-03
42150000	-0.976	-0.033	0.590	-0.848	1.033	-0.963	-55	42	0.168	5.944	1.140E-03
43500000	-0.974	0.066	0.610	1.695	1.802	1.225	70	44	0.174	5.749	1.140E-03
44850000	-0.961	0.167	0.630	4.324	4.370	1.426	82	45	0.180	5.569	1.140E-03
46200000	-0.938	0.256	0.722	6.689	6.727	1.463	84	46	0.206	4.862	1.140E-03
47550000	-0.904	0.352	0.788	9.387	9.420	1.487	85	48	0.225	4.451	1.140E-03
48900000	-0.865	0.438	0.824	11.944	11.973	1.502	86	49	0.235	4.261	1.140E-03
50250000	-0.812	0.520	0.999	14.634	14.668	1.503	86	50	0.285	3.511	1.140E-03
51600000	-0.752	0.602	1.065	17.535	17.567	1.510	87	52	0.304	3.294	1.140E-03
52950000	-0.686	0.668	1.249	20.306	20.345	1.509	86	53	0.356	2.809	1.140E-03
54300000	-0.614	0.730	1.431	23.252	23.296	1.509	86	54	0.408	2.451	1.140E-03
55650000	-0.531	0.778	1.916	26.378	26.448	1.498	86	56	0.546	1.831	1.140E-03
57000000	-0.458	0.815	2.239	29.204	29.290	1.494	86	57	0.638	1.567	1.140E-03
58350000	-0.379	0.858	2.275	32.526	32.605	1.501	86	58	0.648	1.543	1.140E-03
59700000	-0.309	0.894	2.089	35.562	35.624	1.512	87	60	0.595	1.679	1.140E-03
61050000	-0.218	0.925	2.061	39.543	39.597	1.519	87	61	0.587	1.703	1.140E-03
62400000	-0.131	0.944	2.120	43.499	43.550	1.522	87	62	0.604	1.655	1.140E-03
63750000	-0.025	0.950	2.464	48.640	48.703	1.520	87	64	0.702	1.424	1.140E-03
65100000	0.061	0.943	2.996	53.256	53.340	1.515	87	65	0.854	1.171	1.140E-03
66450000	0.151	0.937	3.105	58.625	58.707	1.518	87	66	0.885	1.130	1.140E-03
67800000	0.249	0.921	3.139	65.242	65.317	1.523	87	68	0.895	1.118	1.140E-03
69150000	0.335	0.896	3.444	71.993	72.076	1.523	87	69	0.982	1.019	1.140E-03
70500000	0.425	0.859	3.862	80.393	80.486	1.523	87	71	1.101	0.908	1.140E-03
71850000	0.504	0.818	4.204	89.409	89.506	1.524	87	72	1.198	0.835	1.140E-03
73200000	0.595	0.758	4.800	102.571	102.683	1.524	87	73	1.368	0.731	1.140E-03
74550000	0.653	0.707	5.990	113.995	114.152	1.518	87	75	1.707	0.586	1.140E-03
75900000	0.735	0.624	7.733	135.778	135.998	1.514	87	76	2.204	0.454	1.140E-03
77250000	0.790	0.551	10.467	158.450	158.795	1.505	86	77	2.983	0.335	1.140E-03
78600000	0.840	0.470	14.838	190.642	191.220	1.493	86	79	4.229	0.236	1.140E-03
79950000	0.879	0.389	22.704	234.517	235.613	1.474	84	80	6.471	0.155	1.140E-03
81300000	0.914	0.305	35.807	304.094	306.195	1.454	83	81	10.205	0.098	1.140E-03
82650000	0.938	0.214	75.480	431.179	437.736	1.397	80	83	21.512	0.046	1.140E-03
84000000	0.957	0.109	259.332	794.183	835.452	1.255	72	84	73.910	0.014	1.140E-03
85350000	0.963	0.014	2295.945	881.560	2459.372	0.367	21	85	654.344	0.002	1.140E-03
86700000	0.960	-0.077	483.848	-1016.625	1125.892	-1.127	-65	87	137.896	0.007	1.140E-03
88050000	0.945	-0.178	107.289	-513.285	524.378	-1.365	-78	88	30.577	0.033	1.140E-03
89400000	0.924	-0.273	44.664	-339.818	342.741	-1.440	-83	89	12.729	0.079	1.140E-03
90750000	0.894	-0.361	25.094	-254.755	255.988	-1.473	-84	91	7.152	0.140	1.140E-03
92100000	0.852	-0.453	15.134	-199.658	200.230	-1.495	-86	92	4.313	0.232	1.140E-03
93450000	0.805	-0.523	12.707	-167.867	168.347	-1.495	-86	93	3.621	0.276	1.140E-03
94800000	0.749	-0.606	8.832	-140.361	140.639	-1.508	-86	95	2.517	0.397	1.140E-03
96150000	0.685	-0.676	6.603	-121.597	121.776	-1.517	-87	96	1.882	0.531	1.140E-03
97500000	0.611	-0.739	5.788	-106.024	106.182	-1.516	-87	98	1.650	0.606	1.140E-03
98850000	0.534	-0.798	4.575	-93.473	93.585	-1.522	-87	99	1.304	0.767	1.140E-03
100200000	0.457	-0.841	4.167	-83.880	83.984	-1.521	-87	100	1.188	0.842	1.140E-03
101550000	0.373	-0.881	3.593	-75.318	75.403	-1.523	-87	102	1.024	0.977	1.140E-03
102900000	0.281	-0.918	2.871	-67.494	67.555	-1.528	-88	103	0.818	1.222	1.140E-03
104250000	0.179	-0.944	2.470	-60.336	60.388	-1.530	-88	104	0.704	1.420	1.140E-03
105600000	0.096	-0.955	2.254	-55.198	55.244	-1.530	-88	106	0.642	1.557	1.140E-03
106950000	-0.009	-0.959	2.052	-49.496	49.538	-1.529	-88	107	0.585	1.710	1.140E-03
108300000	-0.110	-0.955	1.753	-44.566	44.601	-1.531	-88	108	0.500	2.002	1.140E-03
109650000	-0.201	-0.939	1.673	-40.385	40.420	-1.529	-88	110	0.477	2.097	1.140E-03
111000000	-0.292	-0.911	1.694	-36.441	36.481	-1.524	-87	111	0.483	2.072	1.140E-03
112350000	-0.383	-0.881	1.437	-32.752	32.784	-1.527	-87	112	0.410	2.442	1.140E-03
113700000	-0.474	-0.835	1.346	-29.098	29.129	-1.525	-87	114	0.384	2.606	1.140E-03
115050000	-0.553	-0.784	1.305	-25.914	25.947	-1.520	-87	115	0.372	2.688	1.140E-03
116400000	-0.623	-0.724	1.388	-22.936	22.978	-1.510	-87	116	0.396	2.527	1.140E-03
117750000	-0.697	-0.655	1.291	-19.809	19.851	-1.506	-86	118	0.368	2.717	1.140E-03
119100000	-0.760	-0.577	1.307	-16.813	16.864	-1.493	-86	119	0.372	2.685	1.140E-03
120450000	-0.814	-0.499	1.249	-14.098	14.153	-1.482	-85	120	0.356	2.809	1.140E-03
121800000	-0.859	-0.418	1.200	-11.510	11.573	-1.467	-84	122	0.342	2.923	1.140E-03
123150000	-0.898	-0.327	1.178	-8.805	8.883	-1.438	-82	123	0.336	2.980	1.140E-03
124500000	-0.921	-0.240	1.261	-6.392	6.515	-1.376	-79	125	0.359	2.782	1.140E-03
125850000	-0.942	-0.136	1.239	-3.583	3.791	-1.238	-71	126	0.353	2.831	1.140E-03
127200000	-0.949	-0.046	1.282	-1.222	1.772	-0.762	-44	127	0.365	2.736	1.140E-03
128550000	-0.950	0.061	1.256	1.339	1.836	0.817	47	129	0.358	2.793	1.140E-03
129900000	-0.942	0.148	1.205	3.899	4.081	1.271	73	130	0.343	2.913	1.140E-03
131250000	-0.921	0.235	1.289	6.277	6.408	1.368	78	131	0.367	2.722	1.140E-03
132600000	-0.890	0.338	1.283	9.167	9.257	1.432	82	133	0.366	2.735	1.140E-03
133950000	-0.850	0.423	1.364	11.743	11.822	1.455	83	134	0.389	2.572	1.140E-03
135300000	-0.806	0.502	1.405	14.305	14.374	1.473	84	135	0.400	2.497	1.140E-03
136650000	-0.752	0.581	1.435	17.046	17.106	1.487	85	137	0.409	2.446	1.140E-03
138000000	-0.680	0.661	1.562	20.282	20.342	1.494	86	138	0.445	2.247	1.140E-03
139350000	-0.606	0.726	1.689	23.378	23.439	1.499	86	139	0.481	2.078	1.140E-03
140700000	-0.535	0.779	1.756	26.217	26.276	1.504	86	141	0.501	1.998	1.140E-03
142050000	-0.459	0.824	1.958	29.344	29.409	1.504	86	142	0.558	1.792	1.140E-03
143400000	-0.380	0.866	1.984	32.634	32.694	1.510	87	143	0.566	1.768	1.140E-03
144750000	-0.278	0.903	2.193	36.858	36.924	1.511	87	145	0.625	1.600	1.140E-03
146100000	-0.185	0.927	2.347	40.964	41.031	1.514	87	146	0.669	1.495	1.140E-03
147450000	-0.093	0.939	2.621	45.244	45.320	1.513	87	147	0.747	1.339	1.140E-03
148800000	-0.002	0.944	2.880	49.826	49.909	1.513	87	149	0.821	1.218	1.140E-03
150150000	0.100	0.938	3.275	55.520	55.616	1.512	87	150	0.933	1.071	1.140E-03
151500000	0.187	0.926	3.543	60.970	61.073	1.513	87	152	1.010	0.990	1.140E-03
152850000	0.278	0.898	4.407	67.662	67.805	1.506	86	153	1.256	0.796	1.140E-03
154200000	0.367	0.868	4.830	75.222	75.377	1.507	86	154	1.377	0.726	1.140E-03
155550000	0.455	0.824	5.814	84.436	84.636	1.502	86	156	1.657	0.604	1.140E-03
156900000	0.541	0.771	6.997	95.802	96.057	1.498	86	157	1.994	0.501	1.140E-03
158250000	0.611	0.715	8.799	107.922	108.280	1.489	85	158	2.508	0.399	1.140E-03
159600000	0.678	0.648	11.462	123.835	124.364	1.478	85	160	3.267	0.306	1.140E-03
160950000	0.742	0.575	15.016	144.804	145.580	1.467	84	161	4.280	0.234	1.140E-03
162300000	0.791	0.500	21.241	170.104	171.426	1.447	83	162	6.054	0.165	1.140E-03
163650000	0.836	0.418	31.536	207.435	209.819	1.420	81	164	8.988	0.111	1.140E-03
165000000	0.873	0.326	53.469	266.563	271.877	1.373	79	165	15.244	0.066	1.140E-03
166350000	0.898	0.245	94.238	347.726	360.270	1.306	75	166	26.858	0.037	1.140E-03

Frequency (Hertz)	VNA Real (r)	VNA Imaginary (x)	Resistance (Ohm)	Reactance (Ohm)	Magnitude (Ohm)	Angle (Radians)	Angle (Degrees)	Frequency (MegaHertz)	Resistivity (Ohm-meter)	Conductivity (Siemens per meter)	Rock Area (Square Meters)	
167700000	0.921	0.139	261.384	543.470	603.060	1.123	64	168	74.495	0.013	1.140E-03	
169050000	0.924	0.056	803.005	627.243	1018.946	0.663	38	169	228.857	0.004	1.140E-03	
170400000	0.925	-0.037	1024.323	-527.889	1152.256	-0.476	-27	170	291.932	0.003	1.140E-03	**Resonating**
171750000	0.915	-0.130	300.166	-538.661	616.648	-1.062	-61	172	85.547	0.012	1.140E-03	**frequency**
173100000	0.897	-0.223	120.440	-369.664	388.790	-1.256	-72	173	34.325	0.029	1.140E-03	**interpolated**
174450000	0.871	-0.310	64.556	-274.597	282.083	-1.340	-77	174	18.399	0.054	1.140E-03	**1.7008E+08**
175800000	0.835	-0.392	41.506	-216.705	220.644	-1.382	-79	176	11.829	0.085	1.140E-03	
177150000	0.786	-0.479	27.984	-174.005	176.241	-1.411	-81	177	7.976	0.125	1.140E-03	
178500000	0.729	-0.556	20.772	-145.247	146.725	-1.429	-82	179	5.920	0.169	1.140E-03	**Resistance**
179850000	0.669	-0.621	16.837	-125.457	126.582	-1.437	-82	180	4.798	0.208	1.140E-03	**interpolated**
181200000	0.596	-0.679	14.754	-108.855	109.850	-1.436	-82	181	4.205	0.238	1.140E-03	**1169.994**
182550000	0.520	-0.733	12.531	-95.461	96.280	-1.440	-83	183	3.571	0.280	1.140E-03	
183900000	0.445	-0.774	11.227	-85.333	86.069	-1.440	-83	184	3.200	0.313	1.140E-03	
185250000	0.360	-0.810	10.069	-75.987	76.651	-1.439	-82	185	2.870	0.348	1.140E-03	
186600000	0.271	-0.838	9.107	-67.953	68.560	-1.438	-82	187	2.595	0.385	1.140E-03	
187950000	0.190	-0.852	8.618	-61.661	62.260	-1.432	-82	188	2.456	0.407	1.140E-03	
189300000	0.117	-0.858	8.227	-56.621	57.216	-1.427	-82	189	2.345	0.426	1.140E-03	
190650000	0.034	-0.858	7.868	-51.402	52.001	-1.419	-81	191	2.242	0.446	1.140E-03	
192000000	-0.048	-0.855	7.303	-46.723	47.290	-1.416	-81	192	2.081	0.480	1.140E-03	
193350000	-0.125	-0.847	6.739	-42.716	43.244	-1.414	-81	193	1.920	0.521	1.140E-03	
194700000	-0.196	-0.836	6.164	-39.281	39.762	-1.415	-81	195	1.757	0.569	1.140E-03	
196050000	-0.271	-0.819	5.591	-35.808	36.241	-1.416	-81	196	1.594	0.628	1.140E-03	
197400000	-0.357	-0.796	4.840	-32.171	32.533	-1.421	-81	197	1.379	0.725	1.140E-03	
198750000	-0.427	-0.763	4.486	-29.147	29.490	-1.418	-81	199	1.278	0.782	1.140E-03	
200100000	-0.509	-0.720	3.980	-25.739	26.045	-1.417	-81	200	1.134	0.882	1.140E-03	
201450000	-0.580	-0.666	3.697	-22.688	22.987	-1.409	-81	201	1.054	0.949	1.140E-03	
202800000	-0.649	-0.609	3.362	-19.719	20.003	-1.402	-80	203	0.958	1.044	1.140E-03	
204150000	-0.713	-0.545	3.014	-16.853	17.120	-1.394	-80	204	0.859	1.164	1.140E-03	
205500000	-0.766	-0.470	2.883	-14.090	14.382	-1.369	-78	206	0.822	1.217	1.140E-03	
206850000	-0.821	-0.380	2.630	-10.993	11.304	-1.336	-77	207	0.749	1.334	1.140E-03	
208200000	-0.858	-0.297	2.493	-8.394	8.757	-1.282	-73	208	0.711	1.407	1.140E-03	
209550000	-0.887	-0.206	2.368	-5.727	6.197	-1.179	-68	210	0.675	1.482	1.140E-03	
210900000	-0.903	-0.117	2.351	-3.208	3.977	-0.938	-54	211	0.670	1.493	1.140E-03	
212250000	-0.913	-0.019	2.264	-0.529	2.325	-0.230	-13	212	0.645	1.550	1.140E-03	
213600000	-0.914	0.074	2.172	2.009	2.959	0.746	43	214	0.619	1.615	1.140E-03	
214950000	-0.904	0.173	2.093	4.731	5.174	1.154	66	215	0.596	1.676	1.140E-03	
216300000	-0.881	0.262	2.144	7.251	7.562	1.283	74	216	0.611	1.636	1.140E-03	
217650000	-0.851	0.351	2.150	9.890	10.121	1.357	78	218	0.613	1.632	1.140E-03	
219000000	-0.809	0.436	2.241	12.590	12.788	1.395	80	219	0.639	1.566	1.140E-03	
220350000	-0.761	0.520	2.232	15.429	15.589	1.427	82	220	0.636	1.572	1.140E-03	
221700000	-0.700	0.604	2.227	18.546	18.679	1.451	83	222	0.635	1.575	1.140E-03	
223050000	-0.641	0.663	2.378	21.176	21.309	1.459	84	223	0.678	1.475	1.140E-03	
224400000	-0.562	0.730	2.533	24.567	24.687	1.468	84	224	0.722	1.385	1.140E-03	
225750000	-0.488	0.781	2.680	27.642	27.771	1.474	84	226	0.764	1.309	1.140E-03	
227100000	-0.410	0.825	2.832	30.910	31.040	1.479	85	227	0.807	1.239	1.140E-03	
228450000	-0.312	0.863	3.193	34.993	35.138	1.480	85	228	0.910	1.099	1.140E-03	
229800000	-0.224	0.893	3.339	38.914	39.057	1.485	85	230	0.952	1.051	1.140E-03	
231150000	-0.134	0.910	3.635	43.038	43.191	1.487	85	231	1.036	0.965	1.140E-03	
232500000	-0.037	0.916	4.144	47.844	48.023	1.484	85	233	1.181	0.847	1.140E-03	
233850000	0.054	0.918	4.461	52.836	53.024	1.487	85	234	1.271	0.787	1.140E-03	
235200000	0.141	0.909	4.946	58.127	58.337	1.486	85	235	1.410	0.709	1.140E-03	
236550000	0.241	0.889	5.545	65.072	65.307	1.486	85	237	1.580	0.633	1.140E-03	
237900000	0.322	0.862	6.349	71.625	71.906	1.482	85	238	1.809	0.553	1.140E-03	
239250000	0.418	0.823	7.302	80.979	81.308	1.481	85	239	2.081	0.481	1.140E-03	
240600000	0.493	0.780	8.603	90.174	90.583	1.476	85	241	2.452	0.408	1.140E-03	
241950000	0.572	0.725	10.306	102.314	102.832	1.470	84	242	2.937	0.340	1.140E-03	
243300000	0.643	0.663	12.915	117.000	117.710	1.461	84	243	3.681	0.272	1.140E-03	
244650000	0.711	0.595	15.964	136.043	136.976	1.454	83	245	4.550	0.220	1.140E-03	
246000000	0.765	0.521	21.889	159.847	161.042	1.434	82	246	6.238	0.160	1.140E-03	
247350000	0.817	0.439	30.808	193.847	196.280	1.413	81	247	8.780	0.114	1.140E-03	
248700000	0.857	0.356	47.302	242.118	246.696	1.378	79	249	13.481	0.074	1.140E-03	
250050000	0.890	0.262	85.962	324.831	336.013	1.312	75	250	24.499	0.041	1.140E-03	
251400000	0.912	0.173	184.393	458.898	494.558	1.189	68	251	52.552	0.019	1.140E-03	
252750000	0.924	0.083	551.648	659.180	859.554	0.874	50	253	157.220	0.006	1.140E-03	
254100000	0.929	-0.016	1291.623	-293.164	1324.476	-0.223	-13	254	368.113	0.003	1.140E-03	
255450000	0.921	-0.112	370.418	-595.691	701.468	-1.014	-58	255	105.569	0.009	1.140E-03	
256800000	0.906	-0.204	136.600	-403.586	426.077	-1.244	-71	257	38.931	0.026	1.140E-03	
258150000	0.881	-0.284	75.241	-299.669	308.970	-1.325	-76	258	21.444	0.047	1.140E-03	
259500000	0.844	-0.382	41.809	-224.445	228.306	-1.387	-79	260	11.916	0.084	1.140E-03	
260850000	0.804	-0.456	29.468	-184.826	187.259	-1.413	-81	261	8.398	0.119	1.140E-03	
262200000	0.754	-0.538	20.341	-153.607	154.948	-1.439	-82	262	5.797	0.173	1.140E-03	
263550000	0.690	-0.615	15.401	-129.721	130.632	-1.453	-83	264	4.389	0.228	1.140E-03	
264900000	0.627	-0.680	12.039	-113.019	113.659	-1.465	-84	265	3.431	0.291	1.140E-03	
266250000	0.557	-0.736	10.076	-99.742	100.249	-1.470	-84	266	2.872	0.348	1.140E-03	
267600000	0.475	-0.789	8.423	-87.816	88.220	-1.475	-85	268	2.401	0.417	1.140E-03	
268950000	0.392	-0.832	7.239	-78.329	78.663	-1.479	-85	269	2.063	0.485	1.140E-03	
270300000	0.304	-0.868	6.251	-70.105	70.384	-1.482	-85	270	1.782	0.561	1.140E-03	
271650000	0.211	-0.892	5.613	-62.889	63.139	-1.482	-85	272	1.600	0.625	1.140E-03	
273000000	0.121	-0.907	5.084	-56.858	57.085	-1.482	-85	273	1.449	0.690	1.140E-03	
274350000	0.030	-0.910	4.846	-51.457	51.685	-1.477	-85	274	1.381	0.724	1.140E-03	
275700000	-0.065	-0.907	4.403	-46.368	46.577	-1.476	-85	276	1.255	0.797	1.140E-03	
277050000	-0.153	-0.896	4.071	-42.002	42.199	-1.474	-84	277	1.160	0.862	1.140E-03	
278400000	-0.246	-0.875	3.763	-37.743	37.931	-1.471	-84	278	1.073	0.932	1.140E-03	
279750000	-0.334	-0.845	3.513	-33.894	34.076	-1.468	-84	280	1.001	0.999	1.140E-03	
281100000	-0.413	-0.808	3.311	-30.489	30.668	-1.463	-84	281	0.944	1.060	1.140E-03	
282450000	-0.490	-0.763	3.171	-27.246	27.430	-1.455	-83	282	0.904	1.107	1.140E-03	
283800000	-0.571	-0.706	2.969	-23.798	23.983	-1.447	-83	284	0.846	1.182	1.140E-03	
285150000	-0.638	-0.645	2.865	-20.810	21.007	-1.434	-82	285	0.817	1.224	1.140E-03	
286500000	-0.701	-0.573	2.807	-17.798	18.018	-1.414	-81	287	0.800	1.250	1.140E-03	
287850000	-0.749	-0.506	2.743	-15.263	15.508	-1.393	-80	288	0.782	1.279	1.140E-03	
289200000	-0.803	-0.416	2.665	-12.166	12.455	-1.355	-78	289	0.759	1.317	1.140E-03	
290550000	-0.838	-0.335	2.666	-9.595	9.959	-1.300	-74	291	0.760	1.316	1.140E-03	
291900000	-0.869	-0.246	2.585	-6.907	7.375	-1.213	-69	292	0.737	1.357	1.140E-03	
293250000	-0.886	-0.159	2.641	-4.446	5.173	-1.035	-59	293	0.753	1.329	1.140E-03	
294600000	-0.900	-0.073	2.560	-2.023	3.263	-0.669	-38	295	0.730	1.371	1.140E-03	
295950000	-0.903	0.019	2.538	0.515	2.590	0.200	11	296	0.723	1.383	1.140E-03	
297300000	-0.896	0.111	2.554	3.076	3.998	0.878	50	297	0.728	1.374	1.140E-03	
298650000	-0.879	0.212	2.560	5.938	6.466	1.164	67	299	0.730	1.370	1.140E-03	
300000000	-0.853	0.299	2.588	8.464	8.870	1.275	73	300	0.738	1.356	1.140E-03	

ANNEXURE 5 Electrical parameters of the untreated JSE rock sample for the VHF range

Frequency (Hertz)	VNA Real (r)	VNA Imaginary (x)	Resistance (Ohm)	Reactance (Ohm)	Magnitude (Ohm)	Angle (Radians)	Angle (Degrees)	Frequency (MegaHertz)	Resistivity (Ohm-meter)	Conductivity (Siemens per meter)	Rock Area (Square Meters)	
30000000	-0.649	-0.246	9.328	-8.833	12.847	-0.758	-43	30	2.836	0.353	1.216E-03	
31350000	-0.668	-0.163	9.369	-5.795	11.017	-0.554	-32	31	2.848	0.351	1.216E-03	
32700000	-0.673	-0.084	9.614	-3.002	10.072	-0.303	-17	33	2.923	0.342	1.216E-03	
34050000	-0.672	0.007	9.812	0.256	9.815	0.026	1	34	2.983	0.335	1.216E-03	
35400000	-0.662	0.066	10.069	2.369	10.344	0.231	13	35	3.081	0.327	1.216E-03	
36750000	-0.645	0.137	10.377	5.019	11.527	0.450	26	37	3.155	0.317	1.216E-03	
38100000	-0.619	0.209	10.753	7.834	13.304	0.630	36	38	3.269	0.306	1.216E-03	
39450000	-0.587	0.273	11.195	10.528	15.368	0.755	43	39	3.403	0.294	1.216E-03	
40800000	-0.545	0.337	11.762	13.485	17.894	0.854	49	41	3.576	0.280	1.216E-03	
42150000	-0.499	0.395	12.379	16.450	20.587	0.926	53	42	3.763	0.266	1.216E-03	
43500000	-0.449	0.443	13.102	19.293	23.321	0.974	56	44	3.983	0.251	1.216E-03	
44850000	-0.394	0.486	13.978	22.257	26.283	1.010	58	45	4.249	0.235	1.216E-03	
46200000	-0.332	0.524	15.016	25.554	29.639	1.040	60	46	4.565	0.219	1.216E-03	
47550000	-0.274	0.551	16.100	28.600	32.820	1.058	61	48	4.894	0.204	1.216E-03	
48900000	-0.209	0.574	17.522	32.047	36.525	1.070	61	49	5.327	0.188	1.216E-03	
50250000	-0.141	0.590	19.152	35.730	40.540	1.079	62	50	5.822	0.172	1.216E-03	
51600000	-0.072	0.598	21.127	39.663	44.938	1.081	62	52	6.422	0.156	1.216E-03	
52950000	-0.007	0.595	23.580	43.502	49.482	1.074	62	53	7.168	0.140	1.216E-03	
54300000	0.058	0.588	26.385	47.714	54.524	1.066	61	54	8.021	0.125	1.216E-03	
55650000	0.124	0.570	30.233	52.170	60.298	1.046	60	56	9.191	0.109	1.216E-03	
57000000	0.178	0.546	34.411	56.024	65.748	1.020	58	57	10.461	0.096	1.216E-03	
58350000	0.229	0.524	38.745	60.317	71.689	1.000	57	58	11.778	0.085	1.216E-03	
59700000	0.283	0.497	44.136	65.290	78.809	0.976	56	60	13.417	0.075	1.216E-03	
61050000	0.339	0.460	51.857	70.898	87.839	0.926	54	61	15.765	0.063	1.216E-03	
62400000	0.383	0.424	60.105	75.554	96.545	0.899	51	62	18.272	0.055	1.216E-03	
63750000	0.423	0.379	71.170	79.583	106.765	0.841	48	64	21.636	0.046	1.216E-03	
65100000	0.458	0.327	85.261	81.572	117.997	0.763	44	65	25.919	0.039	1.216E-03	
66450000	0.488	0.277	101.107	81.590	129.925	0.679	39	66	30.737	0.033	1.216E-03	
67800000	0.515	0.223	120.140	78.276	143.390	0.577	33	68	36.523	0.027	1.216E-03	
69150000	0.532	0.167	139.546	67.899	155.184	0.453	26	69	42.422	0.024	1.216E-03	
70500000	0.548	0.109	159.178	49.758	166.774	0.303	17	71	48.390	0.021	1.216E-03	
71850000	0.555	0.050	172.018	24.968	173.820	0.144	8	72	52.293	0.019	1.216E-03	
73200000	0.555	-0.011	174.525	-5.481	174.610	-0.031	-2	73	53.056	0.019	1.216E-03	
74550000	0.550	-0.071	166.706	-34.116	170.161	-0.202	-12	75	50.679	0.020	1.216E-03	
75900000	0.538	-0.127	151.391	-55.243	161.155	-0.350	-20	76	46.023	0.022	1.216E-03	
77250000	0.518	-0.188	130.928	-70.326	147.828	-0.496	-28	77	39.520	0.025	1.216E-03	
78600000	0.495	-0.239	111.777	-76.479	135.436	-0.600	-34	79	33.980	0.029	1.216E-03	
79950000	0.464	-0.291	94.051	-78.123	122.265	-0.693	-40	80	28.591	0.035	1.216E-03	
81300000	0.429	-0.337	79.911	-76.607	110.699	-0.764	-44	81	24.293	0.041	1.216E-03	
82650000	0.390	-0.379	68.318	-73.460	100.315	-0.822	-47	83	20.767	0.048	1.216E-03	
84000000	0.346	-0.420	58.210	-69.468	90.632	-0.873	-50	84	17.696	0.057	1.216E-03	
85350000	0.297	-0.452	50.594	-64.750	82.173	-0.908	-52	85	15.381	0.065	1.216E-03	
86700000	0.248	-0.480	44.483	-60.261	74.901	-0.935	-54	87	13.523	0.074	1.216E-03	
88050000	0.195	-0.504	39.211	-55.836	68.229	-0.959	-55	88	11.920	0.084	1.216E-03	
89400000	0.142	-0.519	35.383	-51.565	62.537	-0.969	-56	89	10.756	0.093	1.216E-03	
90750000	0.085	-0.529	31.898	-47.399	57.133	-0.978	-56	91	9.697	0.103	1.216E-03	
92100000	0.022	-0.535	28.672	-43.040	51.716	-0.983	-56	92	8.716	0.115	1.216E-03	
93450000	-0.035	-0.533	26.395	-39.329	47.365	-0.980	-56	93	8.024	0.125	1.216E-03	
94800000	-0.091	-0.526	24.364	-35.839	43.336	-0.974	-56	95	7.407	0.135	1.216E-03	
96150000	-0.142	-0.513	22.862	-32.710	39.908	-0.961	-55	96	6.950	0.144	1.216E-03	
97500000	-0.198	-0.493	21.387	-29.365	36.333	-0.941	-54	98	6.505	0.154	1.216E-03	
98850000	-0.247	-0.469	20.265	-26.408	33.287	-0.916	-52	99	6.161	0.162	1.216E-03	
100200000	-0.295	-0.438	19.317	-23.448	30.381	-0.882	-51	100	5.872	0.170	1.216E-03	
101550000	-0.338	-0.404	18.515	-20.669	27.749	-0.840	-48	102	5.629	0.178	1.216E-03	
102900000	-0.381	-0.363	17.732	-17.818	25.138	-0.788	-45	103	5.391	0.186	1.216E-03	
104250000	-0.418	-0.321	17.101	-15.181	22.867	-0.726	-42	104	5.199	0.192	1.216E-03	
105600000	-0.446	-0.279	16.693	-12.879	21.084	-0.657	-38	106	5.075	0.197	1.216E-03	
106950000	-0.472	-0.228	16.347	-10.289	19.316	-0.562	-32	107	4.970	0.201	1.216E-03	
108300000	-0.495	-0.177	15.978	-7.825	17.791	-0.455	-26	108	4.857	0.206	1.216E-03	
109650000	-0.511	-0.118	15.764	-5.153	16.585	-0.316	-18	110	4.792	0.209	1.216E-03	
111000000	-0.518	-0.070	15.715	-3.045	16.007	-0.191	-11	111	4.777	0.209	1.216E-03	
112350000	-0.523	-0.020	15.635	-0.857	15.659	-0.055	-3	112	4.753	0.210	1.216E-03	
113700000	-0.521	0.040	15.717	1.726	15.812	0.109	6	114	4.778	0.209	1.216E-03	
115050000	-0.513	0.099	15.807	4.295	16.380	0.265	15	115	4.805	0.208	1.216E-03	
116400000	-0.502	0.148	15.957	6.494	17.228	0.387	22	116	4.851	0.206	1.216E-03	
117750000	-0.484	0.200	16.181	8.910	18.472	0.503	29	118	4.919	0.203	1.216E-03	
119100000	-0.458	0.253	16.579	11.570	20.217	0.609	35	119	5.040	0.198	1.216E-03	
120450000	-0.431	0.296	17.007	13.875	21.948	0.684	39	120	5.170	0.193	1.216E-03	
121800000	-0.396	0.342	17.575	16.544	24.137	0.755	43	122	5.343	0.187	1.216E-03	
123150000	-0.359	0.381	18.210	19.135	26.415	0.810	46	123	5.536	0.181	1.216E-03	
124500000	-0.319	0.415	18.993	21.725	28.857	0.852	49	125	5.774	0.173	1.216E-03	
125850000	-0.272	0.449	19.909	24.647	31.684	0.891	51	126	6.052	0.165	1.216E-03	
127200000	-0.224	0.476	20.996	27.598	34.677	0.920	53	127	6.383	0.157	1.216E-03	
128550000	-0.176	0.494	22.259	30.347	37.636	0.938	54	129	6.767	0.148	1.216E-03	
129900000	-0.122	0.512	23.755	33.657	41.196	0.956	55	130	7.222	0.138	1.216E-03	
131250000	-0.071	0.521	25.468	36.716	44.684	0.964	55	131	7.742	0.129	1.216E-03	
132600000	-0.015	0.528	27.517	40.329	48.822	0.972	56	133	8.365	0.120	1.216E-03	
133950000	0.041	0.527	30.079	44.046	53.337	0.972	56	134	9.144	0.109	1.216E-03	
135300000	0.092	0.521	32.823	47.511	57.746	0.966	55	135	9.978	0.100	1.216E-03	
136650000	0.148	0.509	36.495	51.643	63.237	0.956	55	137	11.095	0.090	1.216E-03	
138000000	0.198	0.493	40.470	55.588	68.759	0.941	54	138	12.303	0.081	1.216E-03	
139350000	0.249	0.470	45.718	59.899	75.353	0.919	53	139	13.898	0.072	1.216E-03	
140700000	0.296	0.441	51.967	63.930	82.387	0.888	51	141	15.798	0.063	1.216E-03	
142050000	0.340	0.410	59.407	67.896	90.217	0.852	49	142	18.060	0.055	1.216E-03	
143400000	0.380	0.374	68.267	71.357	98.753	0.808	46	143	20.753	0.048	1.216E-03	
144750000	0.414	0.338	78.118	73.802	107.467	0.757	43	145	23.748	0.042	1.216E-03	
146100000	0.449	0.290	92.070	74.940	118.714	0.683	39	146	27.989	0.036	1.216E-03	
147450000	0.477	0.244	107.195	73.251	129.833	0.599	34	147	32.587	0.031	1.216E-03	Resonating
148800000	0.499	0.196	123.155	67.838	140.603	0.503	29	149	37.439	0.027	1.216E-03	frequency
150150000	0.517	0.146	139.846	57.371	151.156	0.389	22	150	42.513	0.024	1.216E-03	interpolated
151500000	0.530	0.091	154.944	39.757	159.963	0.251	14	152	47.103	0.021	1.216E-03	1.5434E+08
152850000	0.537	0.039	164.469	18.214	165.474	0.110	6	153	49.999	0.020	1.216E-03	
154200000	0.539	-0.018	166.603	-8.380	166.812	-0.050	-3	154	50.647	0.020	1.216E-03	
155550000	0.536	-0.072	160.266	-32.813	163.590	-0.202	-12	156	48.721	0.021	1.216E-03	Resistance
156900000	0.526	-0.125	147.275	-52.072	156.209	-0.340	-19	157	44.771	0.022	1.216E-03	interpolated
158250000	0.511	-0.183	129.505	-67.108	145.859	-0.478	-27	158	39.369	0.025	1.216E-03	171.683
159600000	0.491	-0.231	113.006	-73.988	135.072	-0.580	-33	160	34.354	0.029	1.216E-03	
160950000	0.466	-0.277	97.679	-76.530	124.089	-0.665	-38	161	29.694	0.034	1.216E-03	
162300000	0.437	-0.327	82.802	-77.168	113.186	-0.750	-43	162	25.172	0.040	1.216E-03	
163650000	0.401	-0.369	71.013	-74.612	103.004	-0.810	-46	164	21.588	0.046	1.216E-03	
165000000	0.362	-0.407	61.379	-71.032	93.877	-0.858	-49	165	18.659	0.054	1.216E-03	
166350000	0.320	-0.441	53.502	-67.166	85.870	-0.898	-51	166	18.265	0.061	1.216E-03	

Frequency (Hertz)	VNA Real (r)	VNA Imaginary (x)	Resistance (Ohm)	Reactance (Ohm)	Magnitude (Ohm)	Angle (Radians)	Angle (Degrees)	Frequency (MegaHertz)	Resistivity (Ohm-meter)	Conductivity (Siemens per meter)	Rock Area (Square Meters)
167700000	0.272	-0.473	46.659	-62.767	78.210	-0.932	-53	168	14.184	0.071	1.216E-03
169050000	0.226	-0.498	41.349	-58.745	71.838	-0.957	-55	169	12.570	0.080	1.216E-03
170400000	0.170	-0.520	36.501	-54.246	65.383	-0.979	-56	170	11.096	0.090	1.216E-03
171750000	0.119	-0.535	32.912	-50.340	60.146	-0.992	-57	172	10.005	0.100	1.216E-03
173100000	0.062	-0.545	29.683	-46.319	55.014	-1.001	-57	173	9.024	0.111	1.216E-03
174450000	0.009	-0.549	27.171	-42.767	50.668	-1.005	-58	174	8.260	0.121	1.216E-03
175800000	-0.051	-0.547	24.835	-38.978	46.217	-1.004	-57	176	7.550	0.132	1.216E-03
177150000	-0.104	-0.540	23.086	-35.740	42.553	-0.997	-57	177	7.021	0.142	1.216E-03
178500000	-0.159	-0.528	21.457	-32.534	38.973	-0.988	-57	179	6.523	0.153	1.216E-03
179850000	-0.211	-0.510	20.123	-29.567	35.757	-0.973	-56	180	6.117	0.163	1.216E-03
181200000	-0.262	-0.488	18.950	-26.646	32.697	-0.953	-55	181	5.761	0.174	1.216E-03
182550000	-0.315	-0.454	17.935	-23.471	29.539	-0.918	-53	183	5.452	0.183	1.216E-03
183900000	-0.357	-0.420	17.223	-20.818	27.019	-0.880	-50	184	5.236	0.191	1.216E-03
185250000	-0.402	-0.379	16.456	-17.976	24.371	-0.830	-48	185	5.003	0.200	1.216E-03
186600000	-0.435	-0.340	15.992	-15.818	22.353	-0.774	-44	187	4.862	0.206	1.216E-03
187950000	-0.469	-0.290	15.513	-12.927	20.193	-0.695	-40	188	4.716	0.212	1.216E-03
189300000	-0.498	-0.237	15.137	-10.307	18.313	-0.598	-34	189	4.602	0.217	1.216E-03
190650000	-0.516	-0.192	14.939	-8.219	17.050	-0.503	-29	191	4.541	0.220	1.216E-03
192000000	-0.531	-0.138	14.805	-5.832	15.913	-0.375	-22	192	4.501	0.222	1.216E-03
193350000	-0.541	-0.081	14.700	-3.393	15.087	-0.227	-13	193	4.469	0.224	1.216E-03
194700000	-0.546	-0.031	14.643	-1.285	14.700	-0.088	-5	195	4.452	0.225	1.216E-03
196050000	-0.546	0.028	14.665	1.161	14.711	0.079	5	196	4.458	0.224	1.216E-03
197400000	-0.542	0.078	14.690	3.284	15.053	0.220	13	197	4.466	0.224	1.216E-03
198750000	-0.533	0.130	14.749	5.480	15.734	0.356	20	199	4.484	0.223	1.216E-03
200100000	-0.517	0.188	14.927	8.050	16.960	0.495	28	200	4.538	0.220	1.216E-03
201450000	-0.499	0.238	15.090	10.318	18.280	0.600	34	201	4.587	0.218	1.216E-03
202800000	-0.474	0.287	15.374	12.749	19.972	0.692	40	203	4.674	0.214	1.216E-03
204150000	-0.445	0.332	15.735	15.083	21.797	0.764	44	204	4.784	0.209	1.216E-03
205500000	-0.412	0.375	16.182	17.562	23.880	0.826	47	206	4.919	0.203	1.216E-03
206850000	-0.371	0.420	16.702	20.435	26.392	0.886	51	207	5.078	0.197	1.216E-03
208200000	-0.330	0.456	17.301	23.062	28.831	0.927	53	208	5.259	0.190	1.216E-03
209550000	-0.282	0.490	18.058	26.040	31.689	0.964	55	210	5.490	0.182	1.216E-03
210900000	-0.237	0.514	18.915	28.645	34.327	0.987	57	211	5.750	0.174	1.216E-03
212250000	-0.187	0.536	19.950	31.608	37.377	1.008	58	212	6.065	0.165	1.216E-03
213600000	-0.131	0.555	21.263	34.880	40.936	1.025	59	214	6.464	0.155	1.216E-03
214950000	-0.075	0.568	22.748	38.405	44.637	1.036	59	215	6.915	0.145	1.216E-03
216300000	-0.020	0.575	24.424	41.915	48.512	1.043	60	216	7.425	0.135	1.216E-03
217650000	0.036	0.574	26.557	45.619	52.786	1.044	60	218	8.073	0.124	1.216E-03
219000000	0.093	0.571	28.929	49.740	57.541	1.044	60	219	8.794	0.114	1.216E-03
220350000	0.146	0.561	31.782	53.705	62.405	1.036	59	220	9.662	0.104	1.216E-03
221700000	0.209	0.545	35.706	59.037	68.995	1.027	59	222	10.855	0.092	1.216E-03
223050000	0.265	0.522	40.424	64.183	75.852	1.009	58	223	12.289	0.081	1.216E-03
224400000	0.308	0.499	45.067	68.587	82.069	0.989	57	224	13.700	0.073	1.216E-03
225750000	0.359	0.467	51.916	74.300	90.641	0.961	55	226	15.783	0.063	1.216E-03
227100000	0.403	0.431	60.185	79.501	99.713	0.923	53	227	18.296	0.055	1.216E-03
228450000	0.445	0.390	70.488	84.692	110.188	0.877	50	228	21.428	0.047	1.216E-03
229800000	0.485	0.343	84.622	89.549	123.208	0.814	47	230	25.725	0.039	1.216E-03
231150000	0.515	0.297	99.937	91.889	135.761	0.743	43	231	30.381	0.033	1.216E-03
232500000	0.542	0.249	118.338	91.554	149.620	0.658	38	233	35.975	0.028	1.216E-03
233850000	0.566	0.193	142.478	85.648	166.239	0.541	31	234	43.313	0.023	1.216E-03
235200000	0.584	0.135	167.603	70.822	181.952	0.400	23	235	50.951	0.020	1.216E-03
236550000	0.597	0.079	188.727	46.764	194.435	0.243	14	237	57.373	0.017	1.216E-03
237900000	0.603	0.021	201.074	13.197	201.507	0.066	4	238	61.127	0.016	1.216E-03
239250000	0.604	-0.041	199.935	-26.105	201.632	-0.130	-7	239	60.780	0.016	1.216E-03
240600000	0.597	-0.100	184.003	-58.026	192.936	-0.305	-18	241	55.937	0.018	1.216E-03
241950000	0.587	-0.156	161.908	-79.983	180.586	-0.459	-26	242	49.220	0.020	1.216E-03
243300000	0.572	-0.210	138.151	-92.256	166.123	-0.589	-34	243	41.998	0.024	1.216E-03
244650000	0.549	-0.265	114.920	-96.918	150.332	-0.701	-40	245	34.936	0.029	1.216E-03
246000000	0.523	-0.315	95.912	-96.449	136.020	-0.788	-45	246	29.157	0.034	1.216E-03
247350000	0.490	-0.367	79.131	-93.011	122.118	-0.866	-50	247	24.056	0.042	1.216E-03
248700000	0.453	-0.414	66.199	-88.081	110.185	-0.926	-53	249	20.125	0.050	1.216E-03
250050000	0.410	-0.460	55.459	-82.116	99.090	-0.977	-56	250	16.860	0.059	1.216E-03
251400000	0.365	-0.500	47.273	-76.590	90.004	-1.018	-58	251	14.371	0.070	1.216E-03
252750000	0.309	-0.538	40.124	-70.182	80.842	-1.051	-60	253	12.198	0.082	1.216E-03
254100000	0.263	-0.562	35.798	-65.399	74.555	-1.070	-61	254	10.882	0.092	1.216E-03
255450000	0.211	-0.583	32.000	-60.591	68.522	-1.085	-62	255	9.728	0.103	1.216E-03
256800000	0.149	-0.603	28.200	-55.455	62.214	-1.100	-63	257	8.573	0.117	1.216E-03
258150000	0.086	-0.618	25.091	-50.779	56.639	-1.112	-64	258	7.628	0.131	1.216E-03
259500000	0.028	-0.624	22.845	-46.755	52.038	-1.116	-64	260	6.945	0.144	1.216E-03
260850000	-0.032	-0.623	21.001	-42.901	47.765	-1.116	-64	261	6.384	0.157	1.216E-03
262200000	-0.097	-0.620	19.106	-39.029	43.455	-1.116	-64	262	5.808	0.172	1.216E-03
263550000	-0.155	-0.609	17.747	-35.729	39.894	-1.110	-64	264	5.395	0.185	1.216E-03
264900000	-0.216	-0.589	16.585	-32.272	36.284	-1.096	-63	265	5.042	0.198	1.216E-03
266250000	-0.269	-0.570	15.583	-29.475	33.340	-1.084	-62	266	4.737	0.211	1.216E-03
267600000	-0.326	-0.540	14.685	-26.324	30.143	-1.062	-61	268	4.464	0.224	1.216E-03
268950000	-0.377	-0.506	13.984	-23.541	27.382	-1.035	-59	269	4.251	0.235	1.216E-03
270300000	-0.428	-0.465	13.315	-20.605	24.533	-0.997	-57	270	4.048	0.247	1.216E-03
271650000	-0.471	-0.424	12.759	-18.071	22.122	-0.956	-55	272	3.879	0.258	1.216E-03
273000000	-0.509	-0.377	12.382	-15.594	19.912	-0.900	-52	273	3.764	0.266	1.216E-03
274350000	-0.548	-0.320	11.937	-12.802	17.504	-0.820	-47	274	3.629	0.276	1.216E-03
275700000	-0.577	-0.269	11.631	-10.504	15.672	-0.735	-42	276	3.536	0.283	1.216E-03
277050000	-0.603	-0.205	11.370	-7.863	13.824	-0.605	-35	277	3.456	0.289	1.216E-03
278400000	-0.625	-0.140	11.093	-5.280	12.286	-0.444	-25	278	3.372	0.297	1.216E-03
279750000	-0.632	-0.088	11.093	-3.292	11.571	-0.288	-17	280	3.372	0.297	1.216E-03
281100000	-0.641	-0.025	10.938	-0.931	10.978	-0.085	-5	281	3.325	0.301	1.216E-03
282450000	-0.637	0.038	11.037	1.455	11.132	0.131	8	282	3.355	0.298	1.216E-03
283800000	-0.633	0.103	11.000	3.861	11.658	0.338	19	284	3.344	0.299	1.216E-03
285150000	-0.622	0.168	11.004	6.317	12.688	0.521	30	285	3.345	0.299	1.216E-03
286500000	-0.605	0.221	11.157	8.413	13.973	0.646	37	287	3.392	0.295	1.216E-03
287850000	-0.578	0.290	11.285	11.268	15.947	0.785	45	288	3.431	0.291	1.216E-03
289200000	-0.550	0.341	11.539	13.532	17.784	0.865	50	289	3.508	0.285	1.216E-03
290550000	-0.516	0.390	11.844	15.921	19.844	0.931	53	291	3.601	0.278	1.216E-03
291900000	-0.475	0.444	12.164	18.711	22.317	0.994	57	292	3.698	0.270	1.216E-03
293250000	-0.430	0.489	12.617	21.418	24.858	1.038	59	293	3.836	0.261	1.216E-03
294600000	-0.382	0.529	13.102	24.168	27.491	1.074	62	295	3.983	0.251	1.216E-03
295950000	-0.332	0.563	13.676	26.909	30.185	1.101	63	296	4.158	0.241	1.216E-03
297300000	-0.269	0.598	14.480	30.381	33.655	1.126	65	297	4.402	0.227	1.216E-03
298650000	-0.215	0.621	15.248	33.384	36.683	1.142	65	299	4.636	0.216	1.216E-03
300000000	-0.154	0.641	16.252	36.781	40.212	1.155	66	300	4.941	0.202	1.216E-03

ANNEXURE 6 Electrical parameters of the untreated JS1 rock sample for the VHF range

Frequency (Hertz)	VNA Real (r)	VNA Imaginary (x)	Resistance (Ohm)	Reactance (Ohm)	Magnitude (Ohm)	Angle (Radians)	Angle (Degrees)	Frequency (MegaHertz)	Resistivity (Ohm-meter)	Conductivity (Siemens per meter)	Rock Area (Square Meters)	
30000000	-0.672	-0.720	0.459	-21.716	21.721	-1.550	-89	30	0.133	7.507	1.160E-03	
31350000	-0.748	-0.642	0.424	-18.510	18.515	-1.548	-89	31	0.123	8.127	1.160E-03	
32700000	-0.811	-0.559	0.429	-15.554	15.560	-1.543	-88	33	0.124	8.045	1.160E-03	
34050000	-0.865	-0.467	0.454	-12.635	12.643	-1.535	-88	34	0.132	7.593	1.160E-03	
35400000	-0.902	-0.384	0.523	-10.195	10.208	-1.520	-87	35	0.152	6.598	1.160E-03	
36750000	-0.938	-0.283	0.522	-7.378	7.396	-1.500	-86	37	0.151	6.612	1.160E-03	
38100000	-0.963	-0.182	0.517	-4.696	4.724	-1.461	-84	38	0.150	6.665	1.160E-03	
39450000	-0.975	-0.072	0.562	-1.851	1.935	-1.276	-73	39	0.163	6.138	1.160E-03	
40800000	-0.975	0.020	0.630	0.510	0.810	0.681	39	41	0.183	5.479	1.160E-03	
42150000	-0.965	0.135	0.651	3.471	3.532	1.385	79	42	0.189	5.295	1.160E-03	
43500000	-0.945	0.234	0.674	6.097	6.134	1.461	84	44	0.195	5.119	1.160E-03	
44850000	-0.916	0.331	0.687	8.748	8.775	1.492	86	45	0.199	5.019	1.160E-03	
46200000	-0.876	0.419	0.772	11.350	11.376	1.503	86	46	0.224	4.464	1.160E-03	
47550000	-0.820	0.518	0.819	14.454	14.477	1.514	87	48	0.238	4.208	1.160E-03	
48900000	-0.762	0.601	0.833	17.339	17.359	1.523	87	49	0.241	4.141	1.160E-03	
50250000	-0.695	0.675	0.915	20.283	20.304	1.526	87	50	0.265	3.769	1.160E-03	
51600000	-0.617	0.739	1.157	23.370	23.399	1.521	87	52	0.336	2.982	1.160E-03	
52950000	-0.528	0.798	1.425	26.850	26.888	1.518	87	53	0.413	2.419	1.160E-03	
54300000	-0.441	0.833	2.028	30.066	30.134	1.503	86	54	0.588	1.701	1.160E-03	
55650000	-0.353	0.857	2.729	33.418	33.529	1.489	85	56	0.791	1.264	1.160E-03	
57000000	-0.276	0.892	2.633	36.799	36.893	1.499	86	57	0.764	1.310	1.160E-03	
58350000	-0.190	0.923	2.485	40.678	40.754	1.510	87	58	0.721	1.388	1.160E-03	
59700000	-0.088	0.944	2.416	45.496	45.560	1.518	87	60	0.701	1.427	1.160E-03	
61050000	0.015	0.956	2.255	50.728	50.778	1.526	87	61	0.654	1.529	1.160E-03	
62400000	0.104	0.947	2.720	55.718	55.784	1.522	87	62	0.789	1.268	1.160E-03	
63750000	0.202	0.935	2.842	61.862	61.927	1.525	87	64	0.824	1.213	1.160E-03	
65100000	0.294	0.912	3.064	68.563	68.622	1.526	87	65	0.889	1.125	1.160E-03	
66450000	0.408	0.867	3.695	78.609	78.696	1.524	87	66	1.072	0.933	1.160E-03	
67800000	0.481	0.820	5.069	87.104	87.251	1.513	87	68	1.470	0.680	1.160E-03	
69150000	0.567	0.778	5.221	97.067	97.207	1.517	87	69	1.514	0.661	1.160E-03	
70500000	0.635	0.723	5.603	110.160	110.302	1.520	87	71	1.625	0.615	1.160E-03	
71850000	0.711	0.651	6.977	128.376	128.565	1.516	87	72	2.023	0.494	1.160E-03	
73200000	0.775	0.569	10.001	161.994	162.322	1.505	86	73	2.900	0.345	1.160E-03	
74550000	0.832	0.483	14.326	184.518	185.073	1.493	86	75	4.155	0.241	1.160E-03	
75900000	0.878	0.397	20.790	230.384	231.320	1.481	85	76	6.029	0.166	1.160E-03	
77250000	0.916	0.305	34.356	304.801	306.731	1.459	84	77	9.963	0.100	1.160E-03	
78600000	0.941	0.207	77.338	446.476	453.125	1.399	80	79	22.428	0.045	1.160E-03	
79950000	0.959	0.104	276.091	830.452	875.144	1.250	72	80	80.066	0.012	1.160E-03	
81300000	0.964	0.008	2615.593	556.233	2674.500	0.210	12	81	758.522	0.001	1.160E-03	
82650000	0.960	-0.094	330.235	-900.627	959.169	-1.219	-70	83	95.768	0.010	1.160E-03	
84000000	0.945	-0.188	92.192	-489.611	498.215	-1.385	-79	84	26.736	0.037	1.160E-03	
85350000	0.921	-0.296	34.901	-315.942	317.864	-1.461	-84	85	10.121	0.099	1.160E-03	
86700000	0.884	-0.383	22.254	-239.025	240.059	-1.478	-85	87	6.454	0.155	1.160E-03	
88050000	0.838	-0.471	15.210	-189.962	190.570	-1.491	-85	88	4.411	0.227	1.160E-03	
89400000	0.786	-0.558	9.859	-156.245	156.556	-1.508	-86	89	2.859	0.350	1.160E-03	
90750000	0.723	-0.638	7.364	-131.876	132.081	-1.515	-87	91	2.136	0.468	1.160E-03	
92100000	0.652	-0.705	6.225	-114.097	114.267	-1.516	-87	92	1.805	0.554	1.160E-03	
93450000	0.565	-0.762	5.117	-101.280	101.410	-1.520	-87	93	1.484	0.674	1.160E-03	
94800000	0.492	-0.828	3.829	-87.734	87.818	-1.527	-88	95	1.110	0.901	1.160E-03	
96150000	0.404	-0.871	3.475	-78.225	78.302	-1.526	-87	96	1.008	0.992	1.160E-03	
97500000	0.311	-0.910	2.893	-69.819	69.879	-1.529	-88	98	0.839	1.192	1.160E-03	
98850000	0.220	-0.934	2.650	-63.105	63.161	-1.529	-88	99	0.769	1.301	1.160E-03	
100200000	0.112	-0.956	2.176	-56.173	56.215	-1.532	-88	100	0.631	1.584	1.160E-03	
101550000	0.016	-0.961	1.926	-50.778	50.817	-1.531	-88	102	0.579	1.726	1.160E-03	
102900000	-0.082	-0.957	1.846	-45.871	45.908	-1.531	-88	103	0.535	1.868	1.160E-03	
104250000	-0.189	-0.943	1.626	-40.946	40.979	-1.531	-88	104	0.471	2.121	1.160E-03	
105600000	-0.281	-0.921	1.481	-37.008	37.037	-1.531	-88	106	0.430	2.328	1.160E-03	
106950000	-0.365	-0.887	1.522	-33.477	33.512	-1.525	-87	107	0.441	2.266	1.160E-03	
108300000	-0.470	-0.837	1.349	-29.244	29.276	-1.525	-87	108	0.391	2.557	1.160E-03	
109650000	-0.556	-0.783	1.274	-25.810	25.841	-1.521	-87	110	0.369	2.707	1.160E-03	
111000000	-0.631	-0.722	1.252	-22.688	22.722	-1.516	-87	111	0.363	2.755	1.160E-03	
112350000	-0.704	-0.649	1.263	-19.526	19.567	-1.506	-86	112	0.366	2.731	1.160E-03	
113700000	-0.760	-0.581	1.250	-16.908	16.955	-1.497	-86	114	0.362	2.759	1.160E-03	
115050000	-0.819	-0.494	1.186	-13.907	13.957	-1.486	-85	115	0.344	2.907	1.160E-03	
116400000	-0.871	-0.397	1.145	-10.866	10.927	-1.466	-84	116	0.332	3.012	1.160E-03	
117750000	-0.908	-0.304	1.106	-8.149	8.224	-1.436	-82	118	0.321	3.117	1.160E-03	
119100000	-0.933	-0.210	1.142	-5.551	5.667	-1.368	-78	119	0.331	3.019	1.160E-03	
120450000	-0.947	-0.116	1.177	-3.043	3.263	-1.202	-69	120	0.341	2.930	1.160E-03	
121800000	-0.953	-0.012	1.209	-0.313	1.249	-0.253	-15	122	0.351	2.852	1.160E-03	
123150000	-0.951	0.088	1.158	2.311	2.585	1.106	63	123	0.336	2.979	1.160E-03	
124500000	-0.935	0.197	1.147	5.203	5.328	1.354	78	125	0.333	3.006	1.160E-03	
125850000	-0.909	0.279	1.288	7.504	7.614	1.401	80	126	0.374	2.676	1.160E-03	
127200000	-0.871	0.382	1.310	10.467	10.549	1.446	83	127	0.380	2.632	1.160E-03	
128550000	-0.831	0.460	1.359	12.904	12.976	1.466	84	129	0.394	2.538	1.160E-03	
129900000	-0.778	0.552	1.291	15.926	15.980	1.490	85	130	0.374	2.671	1.160E-03	
131250000	-0.721	0.621	1.414	18.571	18.625	1.495	86	131	0.410	2.438	1.160E-03	
132600000	-0.648	0.694	1.549	21.717	21.772	1.500	86	133	0.449	2.227	1.160E-03	
133950000	-0.557	0.770	1.592	25.529	25.579	1.509	86	134	0.462	2.165	1.160E-03	
135300000	-0.478	0.820	1.741	28.713	28.765	1.510	87	135	0.505	1.980	1.160E-03	
136650000	-0.407	0.856	1.881	31.568	31.624	1.511	87	137	0.546	1.833	1.160E-03	
138000000	-0.310	0.896	1.998	35.569	35.625	1.515	87	138	0.580	1.726	1.160E-03	
139350000	-0.210	0.927	2.056	39.886	39.939	1.519	87	139	0.596	1.677	1.160E-03	
140700000	-0.113	0.942	2.329	44.288	44.349	1.518	87	141	0.675	1.481	1.160E-03	
142050000	-0.015	0.940	2.579	49.128	49.198	1.518	87	142	0.748	1.337	1.160E-03	
143400000	0.087	0.948	2.726	54.741	54.809	1.521	87	143	0.791	1.265	1.160E-03	
144750000	0.181	0.933	3.173	60.513	60.596	1.518	87	145	0.920	1.087	1.160E-03	
146100000	0.279	0.908	3.606	67.529	67.625	1.517	87	146	1.046	0.956	1.160E-03	
147450000	0.363	0.876	4.299	74.685	74.808	1.513	87	147	1.247	0.802	1.160E-03	
148800000	0.451	0.833	5.120	83.729	83.886	1.510	87	149	1.485	0.673	1.160E-03	
150150000	0.532	0.764	6.135	93.956	94.156	1.506	86	150	1.779	0.562	1.160E-03	**Resonating**
151500000	0.610	0.723	7.834	107.207	107.493	1.498	86	152	2.272	0.440	1.160E-03	**frequency**
152850000	0.684	0.656	8.797	123.877	124.264	1.492	85	153	2.541	0.392	1.160E-03	**interpolated**
154200000	0.750	0.592	12.347	145.185	145.709	1.486	85	154	3.581	0.279	1.160E-03	**1.6261E+08**
155550000	0.804	0.498	18.039	173.546	174.481	1.467	84	156	5.231	0.191	1.160E-03	
156900000	0.856	0.403	27.875	219.368	221.144	1.444	83	157	8.113	0.123	1.160E-03	
158250000	0.885	0.327	45.685	272.634	276.435	1.405	80	158	13.249	0.075	1.160E-03	**Resistance**
159600000	0.915	0.230	92.032	382.254	393.177	1.335	76	160	26.689	0.037	1.160E-03	**interpolated**
160950000	0.932	0.140	230.723	577.321	621.718	1.191	68	161	66.910	0.015	1.160E-03	**1630.204**
162300000	0.944	0.031	1324.600	750.297	1522.283	0.515	30	162	384.134	0.003	1.160E-03	
163650000	0.947	-0.067	692.760	-836.951	1086.491	-0.879	-50	164	200.900	0.005	1.160E-03	
165000000	0.927	-0.148	216.235	-543.354	584.781	-1.192	-68	165	62.708	0.016	1.160E-03	
166350000	0.908	-0.243	86.358	-365.822	370.798	-1.336	-77	166	25.044	0.040	1.160E-03	

Frequency (Hertz)	VNA Real (r)	VNA Imaginary (x)	Resistance (Ohm)	Reactance (Ohm)	Magnitude (Ohm)	Angle (Radians)	Angle (Degrees)	Frequency (MegaHertz)	Resistivity (Ohm-meter)	Conductivity (Siemens per meter)	Rock Area (Square Meters)
167700000	0.877	-0.332	48.323	-264.660	269.035	-1.390	-80	168	14.014	0.071	1.160E-03
169050000	0.839	-0.423	28.619	-206.516	208.489	-1.433	-82	169	8.299	0.120	1.160E-03
170400000	0.786	-0.512	19.575	-166.393	167.540	-1.454	-83	170	5.677	0.176	1.160E-03
171750000	0.732	-0.584	15.025	-141.421	142.217	-1.469	-84	172	4.357	0.230	1.160E-03
173100000	0.672	-0.649	12.108	-122.757	123.363	-1.472	-84	173	3.511	0.285	1.160E-03
174450000	0.597	-0.719	9.381	-105.828	106.242	-1.483	-85	174	2.715	0.368	1.160E-03
175800000	0.512	-0.781	7.597	-92.077	92.390	-1.488	-85	176	2.203	0.454	1.160E-03
177150000	0.434	-0.823	6.764	-82.462	82.739	-1.489	-85	177	1.962	0.510	1.160E-03
178500000	0.345	-0.865	5.619	-73.499	73.714	-1.494	-86	179	1.630	0.614	1.160E-03
179850000	0.257	-0.894	4.945	-66.183	66.367	-1.496	-86	180	1.434	0.697	1.160E-03
181200000	0.160	-0.917	4.336	-59.325	59.483	-1.498	-86	181	1.257	0.795	1.160E-03
182550000	0.069	-0.924	4.126	-53.725	53.883	-1.494	-86	183	1.196	0.836	1.160E-03
183900000	-0.037	-0.925	3.686	-47.926	48.068	-1.494	-86	184	1.069	0.936	1.160E-03
185250000	-0.126	-0.915	3.478	-43.461	43.599	-1.491	-85	185	1.008	0.992	1.160E-03
186600000	-0.215	-0.890	3.553	-39.257	39.418	-1.481	-85	187	1.030	0.971	1.160E-03
187950000	-0.307	-0.863	3.297	-35.169	35.323	-1.477	-85	188	0.956	1.046	1.160E-03
189300000	-0.391	-0.823	3.240	-31.492	31.658	-1.468	-84	189	0.940	1.064	1.160E-03
190650000	-0.470	-0.781	3.071	-28.184	28.351	-1.462	-84	191	0.891	1.123	1.160E-03
192000000	-0.541	-0.729	3.016	-25.074	25.255	-1.451	-83	192	0.875	1.143	1.160E-03
193350000	-0.616	-0.669	2.837	-21.871	22.054	-1.442	-83	193	0.823	1.216	1.160E-03
194700000	-0.675	-0.606	2.789	-19.092	19.295	-1.426	-82	195	0.809	1.236	1.160E-03
196050000	-0.743	-0.527	2.557	-15.905	16.109	-1.411	-81	196	0.742	1.348	1.160E-03
197400000	-0.785	-0.463	2.498	-13.606	13.834	-1.389	-80	197	0.725	1.380	1.160E-03
198750000	-0.830	-0.382	2.368	-10.932	11.185	-1.357	-78	199	0.687	1.450	1.160E-03
200100000	-0.870	-0.286	2.267	-7.995	8.310	-1.294	-74	200	0.657	1.521	1.160E-03
201450000	-0.891	-0.204	2.269	-5.629	6.069	-1.188	-68	201	0.658	1.519	1.160E-03
202800000	-0.915	-0.107	2.065	-2.906	3.564	-0.953	-55	203	0.599	1.670	1.160E-03
204150000	-0.920	-0.022	2.081	-0.603	2.166	-0.282	-16	204	0.603	1.657	1.160E-03
205500000	-0.922	0.087	1.819	2.352	3.036	0.886	51	206	0.557	1.797	1.160E-03
206850000	-0.911	0.178	1.875	4.786	5.140	1.197	69	207	0.544	1.839	1.160E-03
208200000	-0.889	0.272	1.849	7.474	7.699	1.328	76	208	0.536	1.865	1.160E-03
209550000	-0.857	0.367	1.815	10.250	10.410	1.396	80	210	0.526	1.900	1.160E-03
210900000	-0.818	0.450	1.843	12.831	12.962	1.428	82	211	0.534	1.871	1.160E-03
212250000	-0.766	0.535	1.869	15.704	15.815	1.452	83	212	0.542	1.845	1.160E-03
213600000	-0.710	0.610	1.879	18.511	18.606	1.470	84	214	0.545	1.835	1.160E-03
214950000	-0.644	0.681	1.930	21.497	21.584	1.481	85	215	0.560	1.787	1.160E-03
216300000	-0.571	0.745	1.983	24.648	24.727	1.491	85	216	0.575	1.739	1.160E-03
217650000	-0.488	0.800	2.113	28.025	28.105	1.496	86	218	0.613	1.632	1.160E-03
219000000	-0.404	0.847	2.233	31.517	31.596	1.500	86	219	0.647	1.544	1.160E-03
220350000	-0.313	0.887	2.317	35.337	35.413	1.505	86	220	0.672	1.488	1.160E-03
221700000	-0.221	0.914	2.469	39.278	39.356	1.508	86	222	0.716	1.396	1.160E-03
223050000	-0.126	0.931	2.745	43.629	43.715	1.508	86	223	0.796	1.256	1.160E-03
224400000	-0.037	0.940	2.929	47.986	48.075	1.510	87	224	0.849	1.177	1.160E-03
225750000	0.062	0.938	3.287	53.325	53.426	1.509	86	226	0.953	1.049	1.160E-03
227100000	0.165	0.927	3.649	59.586	59.698	1.510	86	227	1.058	0.945	1.160E-03
228450000	0.261	0.904	4.212	66.272	66.406	1.507	86	228	1.222	0.819	1.160E-03
229800000	0.341	0.874	4.975	72.977	73.146	1.503	86	230	1.443	0.693	1.160E-03
231150000	0.434	0.834	5.709	82.119	82.317	1.501	86	231	1.656	0.604	1.160E-03
232500000	0.516	0.784	6.994	92.400	92.665	1.495	86	233	2.028	0.493	1.160E-03
233850000	0.593	0.732	8.084	104.345	104.658	1.493	86	234	2.344	0.427	1.160E-03
235200000	0.662	0.668	10.280	119.090	119.533	1.485	85	236	2.981	0.335	1.160E-03
236550000	0.724	0.599	13.462	137.829	138.485	1.473	84	237	3.904	0.256	1.160E-03
237900000	0.783	0.522	18.004	163.330	164.319	1.461	84	238	5.221	0.192	1.160E-03
239250000	0.834	0.437	26.131	199.967	201.667	1.441	83	239	7.578	0.132	1.160E-03
240600000	0.866	0.363	39.402	242.609	245.788	1.410	81	241	11.427	0.088	1.160E-03
241950000	0.904	0.265	71.471	333.044	341.213	1.360	78	242	20.727	0.048	1.160E-03
243300000	0.928	0.170	162.332	499.161	524.893	1.256	72	243	47.076	0.021	1.160E-03
244650000	0.939	0.082	537.437	783.406	950.033	0.970	56	245	155.857	0.006	1.160E-03
246000000	0.943	-0.013	1618.451	-388.460	1664.417	-0.236	-13	246	469.351	0.002	1.160E-03
247350000	0.936	-0.107	364.405	-686.934	777.605	-1.083	-62	247	105.678	0.009	1.160E-03
248700000	0.921	-0.201	118.687	-431.084	447.105	-1.302	-75	249	34.419	0.029	1.160E-03
250050000	0.898	-0.292	56.102	-305.299	310.411	-1.389	-80	250	16.269	0.061	1.160E-03
251400000	0.865	-0.377	34.362	-235.214	237.710	-1.426	-82	251	9.965	0.100	1.160E-03
252750000	0.822	-0.464	22.085	-187.661	188.956	-1.454	-83	253	6.405	0.156	1.160E-03
254100000	0.770	-0.544	15.860	-155.991	156.795	-1.469	-84	254	4.599	0.217	1.160E-03
255450000	0.713	-0.619	11.713	-132.991	133.506	-1.483	-85	255	3.397	0.294	1.160E-03
256800000	0.650	-0.683	9.431	-116.038	116.420	-1.490	-85	257	2.735	0.366	1.160E-03
258150000	0.575	-0.750	7.213	-100.994	101.251	-1.499	-86	258	2.092	0.478	1.160E-03
259500000	0.490	-0.807	5.964	-88.578	88.778	-1.504	-86	260	1.729	0.578	1.160E-03
260850000	0.414	-0.848	5.146	-79.849	80.014	-1.506	-86	261	1.492	0.670	1.160E-03
262200000	0.325	-0.886	4.395	-71.452	71.587	-1.509	-86	262	1.275	0.785	1.160E-03
263550000	0.235	-0.914	3.830	-64.339	64.453	-1.511	-87	264	1.111	0.900	1.160E-03
264900000	0.144	-0.931	3.540	-58.197	58.304	-1.510	-87	265	1.026	0.974	1.160E-03
266250000	0.052	-0.941	3.114	-52.721	52.813	-1.512	-87	266	0.903	1.107	1.160E-03
267600000	-0.049	-0.939	2.911	-47.388	47.477	-1.509	-86	268	0.844	1.184	1.160E-03
268950000	-0.153	-0.930	2.525	-42.383	42.458	-1.511	-87	269	0.732	1.365	1.160E-03
270300000	-0.237	-0.912	2.372	-38.613	38.685	-1.509	-86	270	0.688	1.454	1.160E-03
271650000	-0.330	-0.883	2.182	-34.648	34.717	-1.508	-86	272	0.633	1.580	1.160E-03
273000000	-0.414	-0.843	2.156	-31.101	31.176	-1.502	-86	273	0.625	1.599	1.160E-03
274350000	-0.500	-0.797	2.001	-27.635	27.707	-1.499	-86	274	0.580	1.723	1.160E-03
275700000	-0.580	-0.742	1.867	-24.358	24.430	-1.494	-86	276	0.542	1.847	1.160E-03
277050000	-0.647	-0.682	1.843	-21.464	21.543	-1.485	-85	277	0.535	1.871	1.160E-03
278400000	-0.712	-0.615	1.738	-18.583	18.664	-1.478	-85	278	0.504	1.985	1.160E-03
279750000	-0.772	-0.532	1.765	-15.558	15.658	-1.458	-84	280	0.512	1.953	1.160E-03
281100000	-0.821	-0.456	1.682	-12.951	13.060	-1.442	-83	281	0.488	2.050	1.160E-03
282450000	-0.860	-0.370	1.711	-10.293	10.434	-1.406	-81	282	0.496	2.016	1.160E-03
283800000	-0.892	-0.268	1.684	-7.878	8.052	-1.363	-78	284	0.482	2.073	1.160E-03
285150000	-0.917	-0.187	1.682	-5.050	5.322	-1.249	-72	285	0.488	2.050	1.160E-03
286500000	-0.930	-0.097	1684	-2.586	3.092	-0.991	-57	287	0.491	2.035	1.160E-03
287850000	-0.935	0.003	1677	0.082	1.680	0.049	3	288	0.486	2.058	1.160E-03
289200000	-0.930	0.093	1727	2.481	3.012	0.968	55	289	0.495	2.020	1.160E-03
290550000	-0.915	0.194	1698	5.238	5.506	1.257	72	291	0.492	2.031	1.160E-03
291900000	-0.891	0.279	1746	7.636	7.833	1.346	77	292	0.506	1.978	1.160E-03
293250000	-0.855	0.372	1813	10.399	10.556	1.398	80	293	0.526	1.902	1.160E-03
294600000	-0.817	0.452	1828	12.882	13.011	1.430	82	295	0.530	1.888	1.160E-03
295950000	-0.772	0.522	1937	15.309	15.431	1.445	83	296	0.562	1.781	1.160E-03
297300000	-0.709	0.605	2011	18.414	18.524	1.462	84	297	0.583	1.715	1.160E-03
298650000	-0.645	0.677	1990	21.398	21.490	1.478	85	299	0.577	1.732	1.160E-03
300000000	-0.586	0.726	2.129	23.880	23.975	1.482	85	300	0.617	1.620	1.160E-03

ANNEXURE 7 Electrical parameters of the untreated JS2 rock sample for the VHF range

Frequency (Hertz)	VNA Real (r)	VNA Imaginary (x)	Resistance (Ohm)	Reactance (Ohm)	Magnitude (Ohm)	Angle (Radians)	Angle (Degrees)	Frequency (MegaHertz)	Resistivity (Ohm-meter)	Conductivity (Siemens per meter)	Rock Area (Square Meters)	
30000000	-0.702	-0.673	0.819	-20.101	20.117	-1.530	-88	30	0.233	4.283	1.140E-03	
31350000	-0.765	-0.598	0.816	-17.224	17.243	-1.523	-87	31	0.232	4.302	1.140E-03	
32700000	-0.828	-0.507	0.805	-14.094	14.117	-1.514	-87	33	0.229	4.358	1.140E-03	
34050000	-0.884	-0.408	0.699	-10.976	10.998	-1.507	-86	34	0.199	5.018	1.140E-03	
35400000	-0.916	-0.318	0.821	-8.445	8.484	-1.474	-84	35	0.234	4.274	1.140E-03	
36750000	-0.941	-0.223	0.855	-5.830	5.893	-1.425	-82	37	0.244	4.105	1.140E-03	
38100000	-0.960	-0.118	0.848	-3.058	3.173	-1.300	-75	38	0.242	4.140	1.140E-03	
39450000	-0.964	-0.015	0.926	-0.386	1.003	-0.395	-23	39	0.264	3.790	1.140E-03	
40800000	-0.960	0.096	0.896	2.504	2.659	1.227	70	41	0.255	3.917	1.140E-03	
42150000	-0.943	0.196	0.941	5.144	5.229	1.390	80	42	0.268	3.729	1.140E-03	
43500000	-0.915	0.291	1.047	7.767	7.837	1.437	82	44	0.298	3.352	1.140E-03	
44850000	-0.878	0.384	1.121	10.447	10.507	1.464	84	45	0.319	3.131	1.140E-03	
46200000	-0.827	0.488	1.078	13.648	13.691	1.492	85	46	0.307	3.255	1.140E-03	
47550000	-0.772	0.566	1.201	16.360	16.404	1.498	86	48	0.342	2.922	1.140E-03	
48900000	-0.707	0.642	1.322	19.317	19.363	1.502	86	49	0.377	2.655	1.140E-03	
50250000	-0.628	0.721	1.368	22.743	22.785	1.511	87	50	0.390	2.565	1.140E-03	
51600000	-0.544	0.777	1.660	26.004	26.057	1.507	86	52	0.473	2.113	1.140E-03	
52950000	-0.449	0.830	1.960	29.765	29.829	1.505	86	53	0.559	1.790	1.140E-03	
54300000	-0.362	0.854	2.684	33.032	33.141	1.490	85	54	0.765	1.307	1.140E-03	
55650000	-0.267	0.876	3.404	36.932	37.088	1.479	85	56	0.970	1.031	1.140E-03	
57000000	-0.190	0.902	3.345	40.443	40.581	1.488	85	57	0.953	1.049	1.140E-03	
58350000	-0.108	0.924	3.260	44.482	44.601	1.498	86	58	0.929	1.076	1.140E-03	
59700000	-0.007	0.934	3.359	49.533	49.647	1.503	86	60	0.957	1.045	1.140E-03	
61050000	0.095	0.934	3.511	55.206	55.317	1.507	86	61	1.000	1.000	1.140E-03	
62400000	0.194	0.920	3.895	61.485	61.608	1.508	86	62	1.110	0.901	1.140E-03	
63750000	0.288	0.895	4.426	68.452	68.595	1.506	86	64	1.262	0.793	1.140E-03	
65100000	0.384	0.861	4.961	76.855	77.015	1.506	86	65	1.414	0.707	1.140E-03	
66450000	0.470	0.816	5.987	86.235	86.442	1.501	86	66	1.706	0.586	1.140E-03	
67800000	0.547	0.758	8.066	97.210	97.544	1.488	85	68	2.299	0.435	1.140E-03	
69150000	0.632	0.697	9.232	112.096	112.476	1.489	85	69	2.631	0.380	1.140E-03	
70500000	0.701	0.635	10.668	128.812	129.253	1.488	85	71	3.040	0.329	1.140E-03	
71850000	0.764	0.558	14.279	152.055	152.724	1.477	85	72	4.069	0.246	1.140E-03	
73200000	0.819	0.472	20.759	184.580	185.744	1.459	84	73	5.916	0.169	1.140E-03	
74550000	0.864	0.384	32.055	231.167	233.379	1.423	82	75	9.136	0.109	1.140E-03	
75900000	0.900	0.291	56.226	307.276	312.378	1.390	80	76	16.024	0.062	1.140E-03	
77250000	0.925	0.197	117.991	443.865	459.280	1.311	75	77	33.628	0.030	1.140E-03	
78600000	0.942	0.089	464.962	787.266	914.319	1.037	59	79	132.514	0.008	1.140E-03	
79950000	0.946	-0.002	1791.715	-60.287	1792.729	-0.034	-2	80	510.639	0.002	1.140E-03	
81300000	0.941	-0.103	370.883	-731.605	820.244	-1.102	-63	81	105.702	0.009	1.140E-03	
82650000	0.925	-0.205	107.762	-430.216	443.507	-1.325	-76	83	30.712	0.033	1.140E-03	
84000000	0.897	-0.296	54.256	-301.337	306.182	-1.393	-80	84	15.463	0.065	1.140E-03	
85350000	0.861	-0.397	28.515	-224.710	226.512	-1.445	-83	85	8.127	0.123	1.140E-03	
86700000	0.817	-0.472	21.473	-184.036	185.284	-1.455	-83	87	6.120	0.163	1.140E-03	
88050000	0.761	-0.557	14.975	-151.529	152.267	-1.472	-84	88	4.268	0.234	1.140E-03	
89400000	0.689	-0.650	9.887	-125.268	125.657	-1.492	-85	89	2.818	0.355	1.140E-03	
90750000	0.626	-0.708	8.311	-110.415	110.727	-1.496	-86	91	2.369	0.422	1.140E-03	
92100000	0.550	-0.764	7.274	-97.132	97.404	-1.496	-86	92	2.073	0.482	1.140E-03	
93450000	0.462	-0.821	5.799	-85.237	85.434	-1.503	-86	93	1.653	0.605	1.140E-03	
94800000	0.372	-0.866	4.873	-75.686	75.843	-1.507	-86	95	1.389	0.720	1.140E-03	
96150000	0.286	-0.897	4.315	-68.232	68.369	-1.508	-86	96	1.230	0.813	1.140E-03	
97500000	0.177	-0.926	3.591	-60.340	60.447	-1.511	-87	98	1.023	0.977	1.140E-03	
98850000	0.086	-0.938	3.278	-54.676	54.774	-1.511	-87	99	0.934	1.071	1.140E-03	
100200000	-0.014	-0.943	2.900	-48.180	48.265	-1.512	-87	100	0.827	1.210	1.140E-03	
101550000	-0.111	-0.936	2.655	-44.340	44.419	-1.511	-87	102	0.757	1.322	1.140E-03	
102900000	-0.203	-0.918	2.532	-40.082	40.162	-1.508	-86	103	0.722	1.386	1.140E-03	
104250000	-0.308	-0.890	2.254	-35.540	35.611	-1.507	-86	104	0.642	1.557	1.140E-03	
105600000	-0.393	-0.854	2.190	-31.993	32.068	-1.502	-86	106	0.624	1.602	1.140E-03	
106950000	-0.489	-0.803	2.033	-28.051	28.125	-1.498	-86	107	0.580	1.726	1.140E-03	
108300000	-0.563	-0.751	1.973	-24.984	25.062	-1.492	-85	108	0.562	1.779	1.140E-03	
109650000	-0.641	-0.685	1.893	-21.647	21.729	-1.484	-85	110	0.539	1.854	1.140E-03	
111000000	-0.716	-0.609	1.750	-18.367	18.450	-1.476	-85	111	0.499	2.005	1.140E-03	
112350000	-0.772	-0.532	1.770	-15.564	15.654	-1.457	-84	112	0.505	1.982	1.140E-03	
113700000	-0.824	-0.449	1.682	-12.727	12.837	-1.439	-82	114	0.479	2.086	1.140E-03	
115050000	-0.865	-0.361	1.690	-10.012	10.154	-1.404	-80	115	0.482	2.076	1.140E-03	
116400000	-0.900	-0.260	1.677	-7.073	7.269	-1.338	-77	116	0.478	2.092	1.140E-03	
117750000	-0.918	-0.169	1.730	-4.555	4.873	-1.208	-69	118	0.493	2.029	1.140E-03	
119100000	-0.932	-0.067	1.691	-1.804	2.473	-0.818	-47	119	0.482	2.075	1.140E-03	
120450000	-0.932	0.030	1.759	0.813	1.938	0.433	25	120	0.501	1.995	1.140E-03	
121800000	-0.924	0.129	1.741	3.471	3.883	1.106	63	122	0.496	2.016	1.140E-03	
123150000	-0.905	0.225	1.763	6.122	6.371	1.290	74	123	0.503	1.990	1.140E-03	
124500000	-0.877	0.318	1.782	8.779	8.958	1.371	79	125	0.508	1.969	1.140E-03	
125850000	-0.838	0.410	1.827	11.564	11.707	1.414	81	126	0.521	1.921	1.140E-03	
127200000	-0.788	0.492	1.987	14.299	14.436	1.433	82	127	0.566	1.768	1.140E-03	
128550000	-0.733	0.573	2.002	17.200	17.316	1.455	83	129	0.571	1.752	1.140E-03	
129900000	-0.669	0.649	2.046	20.229	20.332	1.470	84	130	0.583	1.715	1.140E-03	
131250000	-0.600	0.713	2.141	23.231	23.330	1.470	85	131	0.610	1.639	1.140E-03	
132600000	-0.516	0.776	2.286	26.758	26.855	1.486	85	133	0.651	1.535	1.140E-03	
133950000	-0.437	0.821	2.482	29.975	30.078	1.488	85	134	0.708	1.413	1.140E-03	
135300000	-0.343	0.864	2.644	33.868	33.971	1.493	86	135	0.753	1.327	1.140E-03	
136650000	-0.249	0.896	2.861	37.943	38.051	1.496	86	137	0.815	1.226	1.140E-03	
138000000	-0.160	0.914	3.181	41.924	42.044	1.495	86	138	0.907	1.103	1.140E-03	
139350000	-0.066	0.926	3.450	46.470	46.598	1.497	86	139	0.983	1.017	1.140E-03	
140700000	0.032	0.929	3.789	51.584	51.723	1.497	86	141	1.080	0.926	1.140E-03	
142050000	0.129	0.922	4.149	57.335	57.485	1.499	86	142	1.182	0.846	1.140E-03	
143400000	0.224	0.903	4.708	63.709	63.883	1.497	86	143	1.342	0.745	1.140E-03	
144750000	0.320	0.873	5.570	71.282	71.500	1.493	86	145	1.587	0.630	1.140E-03	
146100000	0.405	0.835	6.587	79.471	79.744	1.488	85	146	1.877	0.533	1.140E-03	
147450000	0.498	0.785	7.828	90.396	90.735	1.484	85	147	2.231	0.448	1.140E-03	
148800000	0.570	0.734	9.362	101.431	101.862	1.479	85	149	2.668	0.375	1.140E-03	
150150000	0.638	0.672	12.092	115.358	115.990	1.466	84	150	3.446	0.290	1.140E-03	
151500000	0.707	0.602	15.303	134.165	135.055	1.457	83	152	4.361	0.229	1.140E-03	
152850000	0.768	0.524	20.581	159.523	160.845	1.442	83	153	5.866	0.170	1.140E-03	
154200000	0.811	0.451	29.119	188.742	190.975	1.418	81	154	8.299	0.120	1.140E-03	Resonating frequency interpolated 1.5974E+08
155550000	0.856	0.359	46.487	239.752	244.217	1.379	79	156	13.249	0.075	1.140E-03	
156900000	0.890	0.267	82.328	320.265	330.677	1.319	76	157	23.463	0.043	1.140E-03	
158250000	0.911	0.174	182.793	453.975	489.394	1.188	68	158	52.096	0.019	1.140E-03	
159600000	0.923	0.075	612.885	648.616	892.519	0.814	47	160	174.672	0.006	1.140E-03	
160950000	0.924	-0.015	1210.938	-250.843	1236.648	-0.204	-12	161	345.117	0.003	1.140E-03	
162300000	0.917	-0.118	359.911	-570.450	674.500	-1.008	-58	162	102.575	0.010	1.140E-03	Resistance interpolated 940.484
163650000	0.901	-0.190	165.818	-414.538	446.472	-1.190	-68	164	47.258	0.021	1.140E-03	
165000000	0.877	-0.292	72.863	-290.498	299.497	-1.325	-76	165	20.766	0.048	1.140E-03	
166350000	0.840	-0.379	44.571	-223.596	227.995	-1.374	-79	166	12.703	0.079	1.140E-03	

Frequency (Hertz)	VNA Real (r)	VNA Imaginary (x)	Resistance (Ohm)	Reactance (Ohm)	Magnitude (Ohm)	Angle (Radians)	Angle (Degrees)	Frequency (MegaHertz)	Resistivity (Ohm-meter)	Conductivity (Siemens per meter)	Rock Area (Square Meters)
167700000	0.796	-0.460	28.601	-180.087	182.344	-1.413	-81	168	8.151	0.123	1.140E-03
169050000	0.742	-0.548	20.679	-149.792	151.212	-1.434	-82	169	5.893	0.170	1.140E-03
170400000	0.679	-0.622	15.646	-126.936	127.897	-1.448	-83	170	4.459	0.224	1.140E-03
171750000	0.620	-0.675	13.304	-112.497	113.281	-1.453	-83	172	3.792	0.264	1.140E-03
173100000	0.536	-0.747	9.972	-96.596	97.110	-1.468	-84	173	2.842	0.352	1.140E-03
174450000	0.465	-0.789	8.908	-86.800	87.256	-1.469	-84	174	2.539	0.394	1.140E-03
175800000	0.373	-0.836	7.460	-76.520	76.883	-1.474	-84	176	2.126	0.470	1.140E-03
177150000	0.288	-0.868	6.498	-68.871	69.177	-1.477	-85	177	1.851	0.540	1.140E-03
178500000	0.196	-0.894	5.637	-61.848	62.104	-1.480	-85	179	1.606	0.622	1.140E-03
179850000	0.106	-0.906	5.205	-55.931	56.172	-1.478	-85	180	1.483	0.674	1.140E-03
181200000	0.008	-0.913	4.575	-50.208	50.416	-1.480	-85	181	1.304	0.767	1.140E-03
182550000	-0.086	-0.907	4.249	-45.279	45.478	-1.477	-85	183	1.211	0.826	1.140E-03
183900000	-0.176	-0.892	3.996	-40.919	41.114	-1.473	-84	184	1.139	0.878	1.140E-03
185250000	-0.264	-0.865	3.876	-36.890	37.094	-1.466	-84	185	1.105	0.905	1.140E-03
186600000	-0.351	-0.830	3.752	-33.006	33.219	-1.458	-84	187	1.069	0.935	1.140E-03
187950000	-0.437	-0.788	3.495	-29.353	29.560	-1.452	-83	188	0.996	1.004	1.140E-03
189300000	-0.510	-0.741	3.380	-26.194	26.411	-1.442	-83	189	0.963	1.038	1.140E-03
190650000	-0.577	-0.689	3.249	-23.260	23.486	-1.432	-82	191	0.926	1.080	1.140E-03
192000000	-0.648	-0.623	3.086	-20.066	20.302	-1.418	-81	192	0.880	1.137	1.140E-03
193350000	-0.705	-0.560	2.943	-17.391	17.638	-1.403	-80	193	0.839	1.192	1.140E-03
194700000	-0.759	-0.489	2.786	-14.673	14.935	-1.383	-79	195	0.794	1.259	1.140E-03
196050000	-0.809	-0.406	2.633	-11.785	12.075	-1.351	-77	196	0.750	1.333	1.140E-03
197400000	-0.852	-0.317	2.447	-8.989	9.316	-1.305	-75	197	0.697	1.434	1.140E-03
198750000	-0.879	-0.230	2.433	-6.418	6.864	-1.208	-69	199	0.693	1.442	1.140E-03
200100000	-0.899	-0.141	2.358	-3.886	4.546	-1.025	-59	200	0.672	1.488	1.140E-03
201450000	-0.910	-0.049	2.333	-1.339	2.690	-0.521	-30	201	0.665	1.504	1.140E-03
202800000	-0.912	0.041	2.276	1.117	2.535	0.456	26	203	0.649	1.542	1.140E-03
204150000	-0.904	0.147	2.208	4.024	4.590	1.069	61	204	0.629	1.589	1.140E-03
205500000	-0.886	0.237	2.193	6.570	6.926	1.249	72	206	0.625	1.600	1.140E-03
206850000	-0.860	0.323	2.193	9.066	9.330	1.333	76	207	0.625	1.600	1.140E-03
208200000	-0.822	0.410	2.250	11.764	11.978	1.382	79	208	0.641	1.559	1.140E-03
209550000	-0.775	0.496	2.249	14.609	14.781	1.418	81	210	0.641	1.560	1.140E-03
210900000	-0.724	0.567	2.343	17.202	17.361	1.435	82	211	0.668	1.498	1.140E-03
212250000	-0.660	0.650	2.233	20.445	20.566	1.462	84	212	0.636	1.571	1.140E-03
213600000	-0.592	0.708	2.463	23.324	23.454	1.466	84	214	0.702	1.425	1.140E-03
214950000	-0.519	0.766	2.512	26.427	26.546	1.476	85	215	0.716	1.397	1.140E-03
216300000	-0.432	0.817	2.665	30.049	30.167	1.482	85	216	0.760	1.317	1.140E-03
217650000	-0.341	0.862	2.766	33.900	34.013	1.489	85	218	0.788	1.269	1.140E-03
219000000	-0.263	0.888	3.002	37.262	37.383	1.490	85	219	0.856	1.169	1.140E-03
220350000	-0.164	0.914	3.164	41.740	41.860	1.495	86	220	0.902	1.109	1.140E-03
221700000	-0.073	0.923	3.574	46.072	46.211	1.493	86	222	1.019	0.982	1.140E-03
223050000	0.019	0.927	3.856	50.889	51.035	1.495	86	223	1.099	0.910	1.140E-03
224400000	0.117	0.920	4.296	56.599	56.761	1.495	86	224	1.224	0.817	1.140E-03
225750000	0.212	0.903	4.888	62.838	63.028	1.493	86	226	1.393	0.718	1.140E-03
227100000	0.298	0.878	5.553	69.458	69.680	1.491	85	227	1.583	0.632	1.140E-03
228450000	0.385	0.843	6.451	77.451	77.719	1.488	85	228	1.839	0.544	1.140E-03
229800000	0.465	0.801	7.679	86.344	86.685	1.482	85	230	2.189	0.457	1.140E-03
231150000	0.547	0.746	9.274	97.857	98.296	1.476	85	231	2.643	0.378	1.140E-03
232500000	0.619	0.689	11.489	111.259	111.850	1.468	84	233	3.274	0.305	1.140E-03
233850000	0.681	0.627	14.364	126.716	127.527	1.458	84	234	4.094	0.244	1.140E-03
235200000	0.746	0.553	18.584	149.162	150.316	1.447	83	235	5.296	0.189	1.140E-03
236550000	0.798	0.473	26.335	178.728	180.657	1.425	82	237	7.506	0.133	1.140E-03
237900000	0.837	0.398	38.070	214.875	218.221	1.395	80	238	10.850	0.092	1.140E-03
239250000	0.877	0.306	62.819	281.712	288.632	1.351	77	239	17.904	0.056	1.140E-03
240600000	0.902	0.224	114.423	374.049	391.159	1.274	73	241	32.611	0.031	1.140E-03
241950000	0.919	0.126	302.533	557.469	634.270	1.074	62	242	86.222	0.012	1.140E-03
243300000	0.928	0.036	1067.614	559.109	1205.157	0.482	28	243	304.270	0.003	1.140E-03
244650000	0.928	-0.055	823.500	-687.930	1080.322	-0.681	-39	245	234.698	0.004	1.140E-03
246000000	0.919	-0.151	226.675	-514.275	562.015	-1.156	-66	246	64.602	0.015	1.140E-03
247350000	0.897	-0.251	90.321	-340.553	352.327	-1.312	-75	247	25.741	0.039	1.140E-03
248700000	0.874	-0.325	54.135	-267.353	272.779	-1.371	-79	249	15.428	0.065	1.140E-03
250050000	0.835	-0.414	33.056	-208.165	210.773	-1.413	-81	250	9.421	0.106	1.140E-03
251400000	0.788	-0.496	22.751	-170.514	172.025	-1.438	-82	251	6.484	0.154	1.140E-03
252750000	0.733	-0.575	16.524	-143.048	144.006	-1.456	-83	253	4.709	0.212	1.140E-03
254100000	0.679	-0.639	12.793	-124.859	125.513	-1.469	-84	254	3.646	0.274	1.140E-03
255450000	0.611	-0.706	9.944	-108.637	109.091	-1.480	-85	255	2.834	0.353	1.140E-03
256800000	0.540	-0.762	8.102	-96.170	96.510	-1.487	-85	257	2.309	0.433	1.140E-03
258150000	0.453	-0.816	6.627	-84.552	84.812	-1.493	-86	258	1.889	0.529	1.140E-03
259500000	0.372	-0.853	5.948	-76.003	76.236	-1.493	-86	260	1.695	0.590	1.140E-03
260850000	0.284	-0.887	5.096	-68.232	68.427	-1.496	-86	261	1.452	0.689	1.140E-03
262200000	0.194	-0.913	4.370	-61.575	61.730	-1.500	-86	262	1.245	0.803	1.140E-03
263550000	0.097	-0.926	3.992	-55.383	55.526	-1.499	-86	264	1.138	0.879	1.140E-03
264900000	0.019	-0.929	3.751	-50.895	51.033	-1.497	-86	265	1.069	0.936	1.140E-03
266250000	-0.085	-0.929	3.168	-45.555	45.665	-1.501	-86	266	0.903	1.108	1.140E-03
267600000	-0.178	-0.913	3.030	-41.113	41.225	-1.497	-86	268	0.864	1.158	1.140E-03
268950000	-0.266	-0.894	2.724	-37.232	37.331	-1.498	-86	269	0.776	1.288	1.140E-03
270300000	-0.351	-0.863	2.581	-33.564	33.663	-1.494	-86	270	0.735	1.360	1.140E-03
271650000	-0.440	-0.820	2.454	-29.872	29.973	-1.489	-85	272	0.699	1.430	1.140E-03
273000000	-0.520	-0.772	2.301	-26.573	26.672	-1.484	-85	273	0.656	1.525	1.140E-03
274350000	-0.592	-0.719	2.175	-23.560	23.661	-1.479	-85	274	0.620	1.613	1.140E-03
275700000	-0.663	-0.654	2.067	-20.489	20.593	-1.470	-84	276	0.589	1.698	1.140E-03
277050000	-0.726	-0.582	2.037	-17.543	17.661	-1.455	-83	277	0.580	1.723	1.140E-03
278400000	-0.776	-0.509	1.980	-14.890	15.021	-1.439	-82	278	0.564	1.772	1.140E-03
279750000	-0.829	-0.422	1.916	-11.969	12.121	-1.412	-81	280	0.546	1.832	1.140E-03
281100000	-0.861	-0.344	1.944	-9.609	9.804	-1.371	-79	281	0.554	1.805	1.140E-03
282450000	-0.890	-0.255	1.960	-6.999	7.268	-1.298	-74	282	0.558	1.791	1.140E-03
283800000	-0.916	-0.148	1.839	-3.991	4.394	-1.139	-65	284	0.524	1.908	1.140E-03
285150000	-0.926	-0.065	1.854	-1.759	2.556	-0.759	-43	285	0.529	1.892	1.140E-03
286500000	-0.926	0.020	1.914	0.547	1.991	0.278	16	287	0.546	1.833	1.140E-03
287850000	-0.921	0.122	1.851	3.289	3.774	1.058	61	288	0.528	1.895	1.140E-03
289200000	-0.901	0.210	1.976	5.738	6.069	1.239	71	289	0.563	1.776	1.140E-03
290550000	-0.876	0.297	1.996	8.231	8.470	1.333	76	291	0.569	1.758	1.140E-03
291900000	-0.843	0.383	2.008	10.810	10.995	1.387	79	292	0.572	1.748	1.140E-03
293250000	-0.802	0.465	2.031	13.414	13.567	1.421	81	293	0.579	1.728	1.140E-03
294600000	-0.749	0.541	2.178	16.149	16.295	1.437	82	295	0.620	1.613	1.140E-03
295950000	-0.693	0.615	2.187	18.958	19.084	1.456	83	296	0.623	1.604	1.140E-03
297300000	-0.626	0.682	2.287	21.935	22.054	1.467	84	297	0.652	1.534	1.140E-03
298650000	-0.559	0.743	2.374	25.016	25.128	1.476	85	299	0.676	1.478	1.140E-03
300000000	-0.482	0.791	2.515	28.046	28.158	1.481	85	300	0.717	1.395	1.140E-03

ANNEXURE 8 Electrical parameters of the untreated JS3 rock sample for the VHF range

Frequency (Hertz)	VNA Real (r)	VNA imaginary (x)	Resistance (Ohm)	Reactance (Ohm)	Magnitude (Ohm)	Angle (Radians)	Angle (Degrees)	Frequency (MegaHertz)	Resistivity (Ohm-meter)	Conductivity (Siemens per meter)	Rock Area (Square Meters)	
30000000	-0.686	-0.718	0.196	-21.387	21.388	-1.562	-89	30	0.062	16.162	1.260E-03	
31350000	-0.753	-0.642	0.296	-18.406	18.411	-1.555	-89	31	0.093	10.736	1.260E-03	
32700000	-0.820	-0.554	0.287	-15.314	15.317	-1.552	-89	33	0.090	11.073	1.260E-03	
34050000	-0.887	-0.468	0.395	-12.640	12.647	-1.540	-88	34	0.124	8.039	1.260E-03	
35400000	-0.916	-0.369	0.327	-9.691	9.697	-1.537	-88	35	0.103	9.719	1.260E-03	
36750000	-0.954	-0.264	0.246	-6.798	6.802	-1.535	-88	37	0.078	12.902	1.260E-03	
38100000	-0.973	-0.170	0.306	-4.325	4.336	-1.500	-86	38	0.096	10.368	1.260E-03	
39450000	-0.983	-0.065	0.368	-1.650	1.691	-1.352	-77	39	0.116	8.635	1.260E-03	
40800000	-0.984	0.035	0.394	0.882	0.966	1.151	66	41	0.124	8.061	1.260E-03	
42150000	-0.974	0.150	0.380	3.825	3.844	1.472	84	42	0.120	8.362	1.260E-03	
43500000	-0.951	0.244	0.462	6.321	6.338	1.498	86	44	0.146	6.871	1.260E-03	
44850000	-0.921	0.344	0.435	9.042	9.053	1.523	87	45	0.137	7.302	1.260E-03	
46200000	-0.878	0.434	0.554	11.678	11.691	1.523	87	46	0.174	5.735	1.260E-03	
47550000	-0.827	0.523	0.598	14.485	14.497	1.530	88	48	0.189	5.307	1.260E-03	
48900000	-0.767	0.608	0.611	17.412	17.423	1.536	88	49	0.192	5.199	1.260E-03	
50250000	-0.687	0.696	0.666	20.880	20.900	1.539	88	50	0.210	4.770	1.260E-03	
51600000	-0.608	0.761	0.818	24.040	24.054	1.537	88	52	0.258	3.879	1.260E-03	
52950000	-0.515	0.814	1.216	27.532	27.558	1.527	87	53	0.384	2.607	1.260E-03	
54300000	-0.420	0.856	1.662	31.144	31.189	1.517	87	54	0.524	1.910	1.260E-03	
55650000	-0.341	0.871	2.459	34.054	34.143	1.499	86	56	0.775	1.291	1.260E-03	
57000000	-0.266	0.906	2.233	37.396	37.462	1.511	87	57	0.703	1.422	1.260E-03	
58350000	-0.186	0.931	2.163	40.934	40.991	1.518	87	58	0.681	1.469	1.260E-03	
59700000	-0.080	0.958	1.952	45.953	45.995	1.528	88	60	0.615	1.626	1.260E-03	
61050000	0.027	0.962	1.985	51.383	51.422	1.532	88	61	0.625	1.600	1.260E-03	
62400000	0.124	0.955	2.190	56.861	56.904	1.532	88	62	0.690	1.450	1.260E-03	
63750000	0.220	0.941	2.229	62.991	63.030	1.535	88	64	0.702	1.424	1.260E-03	
65100000	0.326	0.911	2.499	70.918	70.962	1.536	88	65	0.780	1.273	1.260E-03	
66450000	0.417	0.872	2.968	79.205	79.261	1.533	88	66	0.935	1.070	1.260E-03	
67800000	0.498	0.821	4.187	88.851	88.950	1.524	87	68	1.319	0.758	1.260E-03	
69150000	0.576	0.774	4.435	99.439	99.537	1.526	87	69	1.397	0.716	1.260E-03	
70500000	0.659	0.712	4.723	114.317	114.414	1.530	88	71	1.488	0.672	1.260E-03	
71850000	0.734	0.638	5.767	133.517	133.642	1.528	88	72	1.817	0.550	1.260E-03	
73200000	0.797	0.559	7.512	158.039	158.217	1.523	87	73	2.366	0.423	1.260E-03	
74550000	0.852	0.469	11.306	193.925	194.254	1.513	87	75	3.561	0.281	1.260E-03	
75900000	0.896	0.380	17.363	244.943	245.557	1.500	86	76	5.469	0.183	1.260E-03	
77250000	0.927	0.288	32.494	326.300	327.914	1.472	84	77	10.236	0.098	1.260E-03	
78600000	0.952	0.192	71.658	489.463	494.681	1.425	82	79	22.572	0.044	1.260E-03	
79950000	0.969	0.087	315.179	1019.106	1066.731	1.271	73	80	99.281	0.010	1.260E-03	
81300000	0.973	-0.019	2419.187	-1781.961	3004.636	-0.635	-36	81	762.044	0.001	1.260E-03	
82650000	0.969	-0.124	145.562	-758.544	772.383	-1.381	-79	83	45.849	0.022	1.260E-03	
84000000	0.950	-0.211	57.105	-448.329	451.951	-1.444	-83	84	17.988	0.056	1.260E-03	
85350000	0.921	-0.317	23.986	-297.224	298.191	-1.490	-85	85	7.556	0.132	1.260E-03	
86700000	0.884	-0.405	15.460	-228.181	228.704	-1.503	-86	87	4.870	0.205	1.260E-03	
88050000	0.836	-0.501	9.153	-180.371	180.605	-1.520	-87	88	2.883	0.346	1.260E-03	
89400000	0.778	-0.585	6.606	-149.350	149.496	-1.527	-87	89	2.081	0.481	1.260E-03	
90750000	0.712	-0.665	4.818	-126.542	126.633	-1.533	-88	91	1.517	0.659	1.260E-03	
92100000	0.642	-0.730	4.247	-110.418	110.500	-1.532	-88	92	1.338	0.747	1.260E-03	
93450000	0.561	-0.794	3.301	-96.402	96.459	-1.537	-88	93	1.040	0.962	1.260E-03	
94800000	0.473	-0.847	2.916	-85.126	85.175	-1.537	-88	95	0.918	1.089	1.260E-03	
96150000	0.384	-0.892	2.380	-75.912	75.949	-1.539	-88	96	0.750	1.334	1.260E-03	
97500000	0.293	-0.925	2.189	-68.241	68.277	-1.539	-88	98	0.689	1.451	1.260E-03	
98850000	0.186	-0.957	1.573	-60.648	60.669	-1.545	-89	99	0.495	2.018	1.260E-03	
100200000	0.091	-0.966	1.673	-54.882	54.907	-1.540	-88	100	0.527	1.897	1.260E-03	
101550000	-0.015	-0.989	1.520	-49.196	49.219	-1.540	-88	102	0.479	2.089	1.260E-03	
102900000	-0.119	-0.962	1.401	-44.182	44.204	-1.539	-88	103	0.441	2.266	1.260E-03	
104250000	-0.219	-0.947	1.153	-39.738	39.754	-1.542	-88	104	0.363	2.753	1.260E-03	
105600000	-0.311	-0.919	1.158	-35.867	35.886	-1.539	-88	106	0.365	2.741	1.260E-03	
106950000	-0.409	-0.880	1.067	-31.883	31.900	-1.537	-88	107	0.336	2.975	1.260E-03	
108300000	-0.501	-0.832	0.962	-28.232	28.249	-1.537	-88	108	0.303	3.299	1.260E-03	
109650000	-0.580	-0.776	0.985	-25.029	25.048	-1.531	-88	110	0.310	3.224	1.260E-03	
111000000	-0.662	-0.707	0.947	-21.658	21.678	-1.527	-87	111	0.298	3.353	1.260E-03	
112350000	-0.731	-0.635	0.926	-18.668	18.690	-1.521	-87	112	0.292	3.427	1.260E-03	
113700000	-0.796	-0.566	0.796	-15.726	15.746	-1.520	-87	114	0.251	3.988	1.260E-03	
115050000	-0.849	-0.469	0.817	-12.883	12.909	-1.507	-86	115	0.257	3.885	1.260E-03	
116400000	-0.893	-0.374	0.856	-10.039	10.076	-1.486	-85	116	0.270	3.710	1.260E-03	
117750000	-0.926	-0.283	0.836	-7.466	7.512	-1.459	-84	118	0.263	3.797	1.260E-03	
119100000	-0.950	-0.174	0.875	-4.544	4.628	-1.380	-79	119	0.276	3.626	1.260E-03	
120450000	-0.959	-0.089	0.954	-2.311	2.500	-1.179	-68	120	0.301	3.326	1.260E-03	
121800000	-0.962	0.015	0.989	0.391	1.045	0.383	22	122	0.305	3.276	1.260E-03	
123150000	-0.957	0.124	0.895	3.234	3.356	1.301	75	123	0.282	3.546	1.260E-03	
124500000	-0.936	0.229	0.931	6.032	6.103	1.418	81	125	0.293	3.409	1.260E-03	
125850000	-0.908	0.313	1.031	8.383	8.446	1.448	83	126	0.325	3.080	1.260E-03	
127200000	-0.889	0.408	1.063	11.147	11.197	1.476	85	127	0.335	2.985	1.260E-03	
128550000	-0.816	0.508	1.068	14.288	14.328	1.496	86	129	0.336	2.973	1.260E-03	
129900000	-0.763	0.586	1.174	16.833	16.874	1.501	86	130	0.370	2.704	1.260E-03	
131250000	-0.700	0.668	1.176	19.801	19.836	1.511	87	131	0.370	2.700	1.260E-03	
132600000	-0.627	0.725	1.278	22.846	22.883	1.515	87	133	0.402	2.485	1.260E-03	
133950000	-0.544	0.792	1.281	26.316	26.348	1.522	87	134	0.403	2.479	1.260E-03	
135300000	-0.453	0.848	1.341	29.941	29.971	1.526	87	135	0.422	2.368	1.260E-03	
136650000	-0.372	0.885	1.457	33.200	33.232	1.527	87	137	0.459	2.179	1.260E-03	
138000000	-0.274	0.921	1.567	37.255	37.288	1.529	88	138	0.494	2.026	1.260E-03	
139350000	-0.184	0.940	1.795	41.118	41.157	1.527	88	139	0.565	1.768	1.260E-03	
140700000	-0.080	0.956	1.913	45.937	45.977	1.529	88	141	0.603	1.660	1.260E-03	
142050000	0.017	0.959	2.134	50.852	50.897	1.529	88	142	0.672	1.488	1.260E-03	
143400000	0.123	0.952	2.368	56.806	56.855	1.529	88	143	0.746	1.341	1.260E-03	
144750000	0.208	0.935	2.719	62.263	62.322	1.527	87	145	0.857	1.168	1.260E-03	
146100000	0.312	0.907	3.059	70.017	70.084	1.527	87	146	0.964	1.038	1.260E-03	
147450000	0.400	0.870	3.763	77.905	77.996	1.523	87	147	1.185	0.844	1.260E-03	
148800000	0.495	0.821	4.382	88.327	88.436	1.521	87	149	1.380	0.724	1.260E-03	
150150000	0.569	0.770	5.371	98.949	99.095	1.517	87	150	1.692	0.591	1.260E-03	**Resonating frequency interpolated 1.6230E+08**
151500000	0.649	0.704	6.717	113.776	113.974	1.512	87	152	2.116	0.473	1.260E-03	
152850000	0.716	0.636	8.572	131.238	131.518	1.506	86	153	2.700	0.370	1.260E-03	
154200000	0.777	0.556	12.165	155.050	155.528	1.492	86	154	3.838	0.261	1.260E-03	
155550000	0.835	0.470	16.564	189.544	190.267	1.484	85	156	5.218	0.192	1.260E-03	
156900000	0.880	0.376	27.008	241.682	243.187	1.460	84	157	8.508	0.118	1.260E-03	
158250000	0.909	0.292	47.705	312.238	315.861	1.419	81	158	15.027	0.067	1.260E-03	**Resistance interpolated 2037.594**
159600000	0.930	0.204	101.449	438.947	450.518	1.344	77	160	31.956	0.031	1.260E-03	
160950000	0.948	0.096	386.656	801.176	889.599	1.121	64	161	121.795	0.008	1.260E-03	
162300000	0.952	0.000	2036.049	3.917	2036.053	0.002	0	162	641.356	0.002	1.260E-03	
163650000	0.949	-0.099	378.866	-775.515	863.112	-1.116	-64	164	119.343	0.008	1.260E-03	
165000000	0.929	-0.183	134.162	-474.028	492.648	-1.295	-74	165	42.261	0.024	1.260E-03	
166350000	0.902	-0.282	59.326	-316.204	321.721	-1.385	-79	166	18.688	0.054	1.260E-03	

Frequency (Hertz)	VNA Real (r)	VNA Imaginary (x)	Resistance (Ohm)	Reactance (Ohm)	Magnitude (Ohm)	Angle (Radians)	Angle (Degrees)	Frequency (MegaHertz)	Resistivity (Ohm-meter)	Conductivity (Siemens per meter)	Rock Area (Square Meters)
167700000	0.871	-0.372	33.386	-239.980	242.292	-1.433	-82	168	10.517	0.095	1.260E-03
169050000	0.823	-0.471	19.905	-186.026	187.088	-1.464	-84	169	6.270	0.159	1.260E-03
170400000	0.776	-0.542	15.262	-157.627	158.364	-1.474	-84	170	4.807	0.208	1.260E-03
171750000	0.714	-0.614	12.281	-133.868	134.428	-1.479	-85	172	3.869	0.258	1.260E-03
173100000	0.651	-0.683	9.311	-116.115	116.488	-1.491	-85	173	2.933	0.341	1.260E-03
174450000	0.567	-0.754	7.238	-99.739	100.001	-1.498	-86	174	2.280	0.439	1.260E-03
175800000	0.492	-0.801	6.446	-89.013	89.246	-1.499	-86	176	2.030	0.492	1.260E-03
177150000	0.410	-0.842	5.787	-79.597	79.807	-1.498	-86	177	1.823	0.549	1.260E-03
178500000	0.310	-0.885	4.791	-70.268	70.432	-1.503	-86	179	1.509	0.663	1.260E-03
179850000	0.224	-0.908	4.406	-63.673	63.826	-1.502	-86	180	1.388	0.721	1.260E-03
181200000	0.128	-0.925	3.946	-57.232	57.368	-1.502	-86	181	1.243	0.805	1.260E-03
182550000	0.034	-0.933	3.542	-51.748	51.869	-1.502	-86	183	1.116	0.896	1.260E-03
183900000	-0.059	-0.927	3.438	-46.782	46.908	-1.497	-86	184	1.083	0.923	1.260E-03
185250000	-0.159	-0.912	3.291	-41.932	42.061	-1.492	-86	185	1.037	0.965	1.260E-03
186600000	-0.242	-0.888	3.292	-38.071	38.214	-1.485	-85	187	1.037	0.964	1.260E-03
187950000	-0.339	-0.854	3.071	-33.861	34.000	-1.480	-85	188	0.967	1.034	1.260E-03
189300000	-0.417	-0.819	2.909	-30.556	30.694	-1.476	-85	189	0.916	1.091	1.260E-03
190650000	-0.498	-0.772	2.745	-27.204	27.342	-1.470	-84	191	0.865	1.156	1.260E-03
192000000	-0.567	-0.722	2.640	-24.254	24.397	-1.462	-84	192	0.832	1.203	1.260E-03
193350000	-0.636	-0.663	2.501	-21.277	21.423	-1.454	-83	193	0.788	1.270	1.260E-03
194700000	-0.706	-0.597	2.224	-18.290	18.425	-1.450	-83	195	0.701	1.427	1.260E-03
196050000	-0.767	-0.522	2.056	-15.369	15.506	-1.438	-82	196	0.648	1.544	1.260E-03
197400000	-0.820	-0.438	1.928	-12.506	12.654	-1.418	-81	197	0.607	1.646	1.260E-03
198750000	-0.860	-0.356	1.875	-9.917	10.093	-1.384	-79	199	0.591	1.693	1.260E-03
200100000	-0.895	-0.263	1.778	-7.180	7.397	-1.328	-76	200	0.560	1.786	1.260E-03
201450000	-0.918	-0.171	1.716	-4.600	4.910	-1.214	-70	201	0.541	1.850	1.260E-03
202800000	-0.934	-0.073	1.638	-1.960	2.554	-0.875	-50	203	0.516	1.938	1.260E-03
204150000	-0.937	0.019	1.617	0.498	1.692	0.298	17	204	0.509	1.963	1.260E-03
205500000	-0.931	0.125	1.584	3.341	3.698	1.128	65	206	0.499	2.005	1.260E-03
206850000	-0.918	0.217	1.480	5.837	6.021	1.323	76	207	0.466	2.146	1.260E-03
208200000	-0.893	0.309	1.457	8.414	8.539	1.399	80	208	0.459	2.179	1.260E-03
209550000	-0.858	0.401	1.431	11.110	11.202	1.443	83	210	0.451	2.218	1.260E-03
210900000	-0.810	0.488	1.521	13.886	13.969	1.462	84	211	0.479	2.087	1.260E-03
212250000	-0.757	0.568	1.526	16.651	16.720	1.479	85	212	0.481	2.080	1.260E-03
213600000	-0.691	0.653	1.466	19.885	19.939	1.497	86	214	0.462	2.163	1.260E-03
214950000	-0.622	0.713	1.665	22.697	22.758	1.498	86	215	0.525	1.906	1.260E-03
216300000	-0.540	0.781	1.666	26.195	26.248	1.507	86	216	0.525	1.906	1.260E-03
217650000	-0.466	0.826	1.773	29.162	29.216	1.510	87	218	0.558	1.791	1.260E-03
219000000	-0.379	0.870	1.863	32.722	32.775	1.514	87	219	0.587	1.704	1.260E-03
220350000	-0.285	0.905	2.000	36.643	36.697	1.516	87	220	0.630	1.587	1.260E-03
221700000	-0.188	0.931	2.138	40.867	40.922	1.519	87	222	0.674	1.485	1.260E-03
223050000	-0.096	0.944	2.380	45.128	45.191	1.518	87	223	0.750	1.334	1.260E-03
224400000	0.008	0.950	2.581	50.363	50.428	1.520	87	224	0.813	1.230	1.260E-03
225750000	0.103	0.945	2.821	55.687	55.758	1.520	87	226	0.889	1.125	1.260E-03
227100000	0.195	0.929	3.260	61.446	61.533	1.518	87	227	1.027	0.974	1.260E-03
228450000	0.293	0.903	3.741	68.644	68.746	1.516	87	228	1.179	0.849	1.260E-03
229800000	0.381	0.868	4.350	76.365	76.489	1.514	87	230	1.370	0.730	1.260E-03
231150000	0.461	0.827	5.351	84.883	85.051	1.508	86	231	1.686	0.593	1.260E-03
232500000	0.547	0.774	6.327	96.278	96.485	1.505	86	233	1.993	0.502	1.260E-03
233850000	0.622	0.715	7.754	109.359	109.634	1.500	86	234	2.443	0.409	1.260E-03
235200000	0.692	0.649	9.660	125.814	126.184	1.494	86	235	3.043	0.329	1.260E-03
236550000	0.761	0.568	12.823	149.532	150.080	1.485	85	237	4.039	0.248	1.260E-03
237900000	0.808	0.498	17.479	174.818	175.690	1.471	84	238	5.506	0.182	1.260E-03
239250000	0.849	0.422	25.048	210.080	211.568	1.452	83	239	7.890	0.127	1.260E-03
240600000	0.893	0.324	42.387	278.434	281.642	1.420	81	241	13.352	0.075	1.260E-03
241950000	0.920	0.241	74.515	373.455	380.817	1.374	79	242	23.472	0.043	1.260E-03
243300000	0.940	0.147	190.611	583.059	613.425	1.255	72	243	60.042	0.017	1.260E-03
244650000	0.948	0.058	848.826	957.404	1279.503	0.845	48	245	267.380	0.004	1.260E-03
246000000	0.950	-0.039	1199.869	-964.171	1539.257	-0.677	-39	246	377.959	0.003	1.260E-03
247350000	0.941	-0.146	188.069	-586.748	616.152	-1.261	-72	247	59.242	0.017	1.260E-03
248700000	0.923	-0.237	73.626	-381.293	388.336	-1.380	-79	249	23.192	0.043	1.260E-03
250050000	0.894	-0.327	39.375	-276.563	279.352	-1.429	-82	250	12.403	0.081	1.260E-03
251400000	0.860	-0.411	24.460	-218.064	219.432	-1.459	-84	251	7.705	0.130	1.260E-03
252750000	0.811	-0.495	17.141	-176.277	177.108	-1.474	-84	253	5.399	0.185	1.260E-03
254100000	0.764	-0.565	13.039	-150.607	151.170	-1.484	-85	254	4.107	0.243	1.260E-03
255450000	0.700	-0.647	9.036	-127.138	127.459	-1.500	-86	255	2.846	0.351	1.260E-03
256800000	0.629	-0.714	7.314	-110.225	110.467	-1.505	-86	257	2.304	0.434	1.260E-03
258150000	0.555	-0.773	5.949	-97.231	97.413	-1.510	-86	258	1.874	0.534	1.260E-03
259500000	0.467	-0.830	4.791	-85.300	85.434	-1.515	-87	260	1.509	0.663	1.260E-03
260850000	0.389	-0.867	4.267	-77.076	77.194	-1.515	-87	261	1.344	0.744	1.260E-03
262200000	0.300	-0.904	3.554	-69.124	69.215	-1.519	-87	262	1.120	0.893	1.260E-03
263550000	0.207	-0.927	3.312	-62.326	62.414	-1.518	-87	264	1.043	0.959	1.260E-03
264900000	0.109	-0.945	2.814	-55.992	56.063	-1.521	-87	265	0.887	1.128	1.260E-03
266250000	0.024	-0.949	2.669	-51.205	51.275	-1.519	-87	266	0.841	1.189	1.260E-03
267600000	-0.071	-0.947	2.391	-46.360	46.421	-1.519	-87	268	0.753	1.328	1.260E-03
268950000	-0.172	-0.933	2.222	-41.571	41.630	-1.517	-87	269	0.700	1.429	1.260E-03
270300000	-0.266	-0.913	1.960	-37.491	37.542	-1.519	-87	270	0.617	1.620	1.260E-03
271650000	-0.359	-0.879	1.870	-33.559	33.611	-1.515	-87	272	0.589	1.698	1.260E-03
273000000	-0.441	-0.843	1.703	-30.227	30.275	-1.515	-87	273	0.536	1.864	1.260E-03
274350000	-0.520	-0.792	1.735	-26.980	27.036	-1.507	-86	274	0.546	1.830	1.260E-03
275700000	-0.602	-0.732	1.631	-23.596	23.652	-1.502	-86	276	0.514	1.946	1.260E-03
277050000	-0.673	-0.671	1.499	-20.642	20.696	-1.498	-86	277	0.472	2.118	1.260E-03
278400000	-0.738	-0.596	1.493	-17.664	17.727	-1.486	-85	278	0.470	2.126	1.260E-03
279750000	-0.792	-0.521	1.463	-14.949	15.020	-1.473	-84	280	0.461	2.171	1.260E-03
281100000	-0.844	-0.432	1.418	-12.035	12.118	-1.454	-83	281	0.447	2.240	1.260E-03
282450000	-0.881	-0.344	1.439	-9.410	9.520	-1.419	-81	282	0.453	2.206	1.260E-03
283800000	-0.908	-0.263	1.418	-7.096	7.236	-1.374	-79	284	0.447	2.238	1.260E-03
285150000	-0.930	-0.162	1.448	-4.307	4.544	-1.247	-71	285	0.456	2.193	1.260E-03
286500000	-0.941	-0.070	1.464	-1.894	2.392	-0.903	-52	287	0.461	2.169	1.260E-03
287850000	-0.942	0.022	1.497	0.573	1.603	0.366	21	288	0.472	2.120	1.260E-03
289200000	-0.931	0.120	1.578	3.203	3.570	1.113	64	289	0.497	2.012	1.260E-03
290550000	-0.917	0.218	1.506	5.848	6.039	1.319	76	291	0.474	2.108	1.260E-03
291900000	-0.890	0.309	1.526	8.415	8.552	1.391	80	292	0.481	2.080	1.260E-03
293250000	-0.858	0.391	1.545	10.850	10.959	1.429	82	293	0.487	2.055	1.260E-03
294600000	-0.812	0.471	1.698	13.440	13.547	1.445	83	295	0.535	1.869	1.260E-03
295950000	-0.761	0.551	1.718	16.195	16.286	1.465	84	296	0.541	1.848	1.260E-03
297300000	-0.704	0.624	1.759	18.941	19.022	1.478	85	297	0.554	1.805	1.260E-03
298650000	-0.634	0.697	1.771	22.088	22.159	1.491	85	299	0.558	1.792	1.260E-03
300000000	-0.566	0.754	1.848	24.970	25.036	1.497	86	300	0.582	1.718	1.260E-03

ANNEXURE 9 Electrical parameters of the untreated JS4 rock sample for the VHF range

Frequency (Hertz)	VNA Real (r)	VNA Imaginary (x)	Resistance (Ohm)	Reactance (Ohm)	Magnitude (Ohm)	Angle (Radians)	Angle (Degrees)	Frequency (MegaHertz)	Resistivity (Ohm-meter)	Conductivity (Siemens per meter)	Rock Area (Square Meters)
30000000	-0.644	-0.764	0.246	-23.046	23.047	-1.560	-89	30	0.074	13.461	1.200E-03
31350000	-0.719	-0.679	0.316	-19.884	19.887	-1.555	-89	31	0.095	10.481	1.200E-03
32700000	-0.783	-0.605	0.298	-17.055	17.058	-1.553	-89	33	0.089	11.192	1.200E-03
34050000	-0.839	-0.525	0.275	-14.341	14.343	-1.552	-89	34	0.083	12.102	1.200E-03
35400000	-0.886	-0.431	0.386	-11.519	11.526	-1.537	-88	35	0.116	8.634	1.200E-03
36750000	-0.927	-0.341	0.312	-8.901	8.906	-1.536	-88	37	0.094	10.689	1.200E-03
38100000	-0.955	-0.244	0.353	-6.294	6.304	-1.515	-87	38	0.106	9.456	1.200E-03
39450000	-0.976	-0.135	0.379	-3.441	3.461	-1.461	-84	39	0.114	8.806	1.200E-03
40800000	-0.987	-0.021	0.326	-0.540	0.630	-1.028	-59	41	0.098	10.238	1.200E-03
42150000	-0.981	0.073	0.407	1.857	1.901	1.355	78	42	0.122	8.183	1.200E-03
43500000	-0.967	0.166	0.481	4.240	4.276	1.458	84	44	0.144	6.932	1.200E-03
44850000	-0.945	0.264	0.473	6.857	6.873	1.502	86	45	0.142	7.049	1.200E-03
46200000	-0.914	0.356	0.491	9.394	9.407	1.519	87	46	0.147	6.787	1.200E-03
47550000	-0.864	0.465	0.504	12.594	12.604	1.531	88	48	0.151	6.619	1.200E-03
48900000	-0.809	0.549	0.616	15.350	15.362	1.531	88	49	0.185	5.414	1.200E-03
50250000	-0.752	0.621	0.712	17.971	17.985	1.531	88	50	0.214	4.680	1.200E-03
51600000	-0.676	0.699	0.821	21.202	21.218	1.532	88	52	0.246	4.061	1.200E-03
52950000	-0.588	0.764	1.140	24.614	24.641	1.525	87	53	0.342	2.924	1.200E-03
54300000	-0.502	0.808	1.702	27.732	27.784	1.509	86	54	0.511	1.958	1.200E-03
55650000	-0.430	0.827	2.424	30.308	30.404	1.491	85	56	0.727	1.375	1.200E-03
57000000	-0.359	0.873	2.095	33.459	33.524	1.506	86	57	0.628	1.591	1.200E-03
58350000	-0.271	0.912	1.920	37.260	37.310	1.519	87	58	0.576	1.736	1.200E-03
59700000	-0.185	0.940	1.800	41.108	41.147	1.527	87	60	0.540	1.851	1.200E-03
61050000	-0.082	0.963	1.590	45.911	45.938	1.536	88	61	0.477	2.097	1.200E-03
62400000	0.024	0.962	1.958	51.225	51.263	1.533	88	62	0.587	1.703	1.200E-03
63750000	0.110	0.957	2.120	56.022	56.062	1.533	88	64	0.636	1.572	1.200E-03
65100000	0.213	0.944	2.096	62.597	62.643	1.537	88	65	0.629	1.591	1.200E-03
66450000	0.305	0.916	2.596	69.312	69.360	1.533	88	66	0.779	1.284	1.200E-03
67800000	0.402	0.874	3.333	77.890	77.961	1.528	88	68	1.000	1.000	1.200E-03
69150000	0.484	0.838	3.260	86.504	86.565	1.533	88	69	0.978	1.022	1.200E-03
70500000	0.563	0.792	3.412	96.860	96.920	1.536	88	71	1.024	0.977	1.200E-03
71850000	0.643	0.728	4.261	110.791	110.873	1.532	88	72	1.276	0.782	1.200E-03
73200000	0.719	0.653	5.544	129.206	129.325	1.528	88	73	1.663	0.601	1.200E-03
74550000	0.783	0.574	7.526	152.420	152.606	1.521	87	75	2.258	0.443	1.200E-03
75900000	0.840	0.492	9.929	183.754	184.022	1.517	87	76	2.979	0.336	1.200E-03
77250000	0.887	0.403	14.712	230.003	230.473	1.507	86	77	4.414	0.227	1.200E-03
78600000	0.921	0.314	24.938	299.210	300.248	1.488	85	79	7.481	0.134	1.200E-03
79950000	0.949	0.216	53.760	437.360	440.652	1.448	83	80	16.128	0.062	1.200E-03
81300000	0.966	0.119	170.426	778.696	797.126	1.355	78	81	51.128	0.020	1.200E-03
82650000	0.977	0.011	3420.094	1661.960	3802.510	0.452	26	83	1026.028	0.001	1.200E-03
84000000	0.971	-0.078	372.521	-1130.662	1190.449	-1.253	-72	84	111.756	0.009	1.200E-03
85350000	0.958	-0.179	74.488	-530.672	535.875	-1.431	-82	85	22.347	0.045	1.200E-03
86700000	0.932	-0.286	28.252	-331.312	332.514	-1.486	-85	87	8.476	0.118	1.200E-03
88050000	0.902	-0.368	18.351	-254.811	255.471	-1.499	-86	88	5.505	0.182	1.200E-03
89400000	0.857	-0.458	12.020	-198.941	199.304	-1.510	-87	89	3.606	0.277	1.200E-03
90750000	0.803	-0.548	7.757	-161.418	161.604	-1.523	-87	91	2.327	0.430	1.200E-03
92100000	0.749	-0.621	5.970	-138.290	138.419	-1.528	-88	92	1.791	0.558	1.200E-03
93450000	0.679	-0.693	4.952	-118.786	118.889	-1.529	-88	93	1.485	0.673	1.200E-03
94800000	0.597	-0.767	3.602	-102.181	102.245	-1.536	-88	95	1.081	0.925	1.200E-03
96150000	0.528	-0.813	3.359	-92.021	92.082	-1.534	-88	96	1.008	0.992	1.200E-03
97500000	0.435	-0.868	2.642	-80.949	80.992	-1.538	-88	98	0.793	1.261	1.200E-03
98850000	0.340	-0.912	2.087	-71.967	71.997	-1.542	-88	99	0.626	1.597	1.200E-03
100200000	0.249	-0.937	2.074	-64.967	65.001	-1.539	-88	100	0.622	1.607	1.200E-03
101550000	0.153	-0.958	1.800	-58.561	58.589	-1.540	-88	102	0.540	1.852	1.200E-03
102900000	0.046	-0.973	1.396	-52.411	52.429	-1.544	-88	103	0.419	2.388	1.200E-03
104250000	-0.054	-0.971	1.300	-47.259	47.277	-1.543	-88	104	0.390	2.564	1.200E-03
105600000	-0.142	-0.960	1.311	-43.119	43.138	-1.540	-88	106	0.393	2.542	1.200E-03
106950000	-0.241	-0.940	1.186	-38.786	38.804	-1.540	-88	107	0.356	2.810	1.200E-03
108300000	-0.341	-0.908	1.142	-34.624	34.642	-1.538	-88	108	0.343	2.919	1.200E-03
109650000	-0.434	-0.867	1.062	-30.891	30.909	-1.536	-88	110	0.319	3.138	1.200E-03
111000000	-0.526	-0.815	0.999	-27.237	27.256	-1.534	-88	111	0.300	3.336	1.200E-03
112350000	-0.597	-0.761	1.028	-24.316	24.338	-1.529	-88	112	0.308	3.243	1.200E-03
113700000	-0.680	-0.691	0.912	-20.931	20.951	-1.527	-88	114	0.274	3.653	1.200E-03
115050000	-0.748	-0.614	0.907	-17.888	17.911	-1.520	-87	115	0.272	3.674	1.200E-03
116400000	-0.805	-0.536	0.929	-15.115	15.143	-1.509	-86	116	0.279	3.588	1.200E-03
117750000	-0.854	-0.450	0.942	-12.381	12.397	-1.495	-86	118	0.283	3.540	1.200E-03
119100000	-0.897	-0.355	0.933	-9.528	9.573	-1.473	-84	119	0.280	3.572	1.200E-03
120450000	-0.925	-0.269	0.953	-7.111	7.174	-1.438	-82	120	0.286	3.496	1.200E-03
121800000	-0.949	-0.168	0.938	-4.391	4.490	-1.360	-78	122	0.281	3.553	1.200E-03
123150000	-0.962	-0.060	0.932	-1.561	1.818	-1.032	-59	123	0.280	3.576	1.200E-03
124500000	-0.965	0.034	0.887	0.860	1.249	0.782	45	125	0.266	3.760	1.200E-03
125850000	-0.951	0.134	1.007	3.504	3.646	1.291	74	126	0.302	3.309	1.200E-03
127200000	-0.931	0.231	1.042	6.112	6.200	1.402	80	127	0.313	3.198	1.200E-03
128550000	-0.904	0.326	1.024	8.749	8.809	1.454	83	129	0.307	3.255	1.200E-03
129900000	-0.866	0.421	1.001	11.516	11.559	1.484	85	130	0.300	3.330	1.200E-03
131250000	-0.816	0.510	1.041	14.334	14.371	1.498	86	131	0.312	3.202	1.200E-03
132600000	-0.760	0.580	1.093	17.083	17.118	1.507	86	133	0.328	3.050	1.200E-03
133950000	-0.695	0.662	1.186	19.999	20.034	1.512	87	134	0.356	2.811	1.200E-03
135300000	-0.628	0.724	1.286	22.801	22.837	1.514	87	135	0.386	2.589	1.200E-03
136650000	-0.543	0.791	1.323	26.295	26.329	1.521	87	137	0.397	2.520	1.200E-03
138000000	-0.458	0.840	1.478	29.673	29.710	1.521	87	138	0.443	2.255	1.200E-03
139350000	-0.369	0.887	1.440	33.342	33.373	1.528	88	139	0.432	2.315	1.200E-03
140700000	-0.286	0.914	1.658	36.723	36.760	1.526	87	141	0.498	2.010	1.200E-03
142050000	-0.183	0.940	1.810	41.187	41.227	1.527	87	142	0.543	1.842	1.200E-03
143400000	-0.084	0.957	1.862	45.749	45.787	1.530	88	143	0.559	1.790	1.200E-03
144750000	0.015	0.967	2.218	50.757	50.806	1.527	87	145	0.665	1.503	1.200E-03
146100000	0.115	0.951	2.432	56.352	56.404	1.528	88	146	0.730	1.371	1.200E-03
147450000	0.208	0.934	2.827	62.308	62.372	1.525	87	147	0.848	1.179	1.200E-03
148800000	0.296	0.910	3.167	68.750	68.822	1.525	87	149	0.950	1.053	1.200E-03
150150000	0.392	0.873	3.754	77.157	77.248	1.522	87	150	1.126	0.888	1.200E-03
151500000	0.481	0.826	4.512	86.817	86.934	1.519	87	152	1.354	0.739	1.200E-03
152850000	0.559	0.775	5.468	97.445	97.598	1.515	87	153	1.640	0.610	1.200E-03
154200000	0.647	0.702	7.145	113.640	113.865	1.508	86	154	2.143	0.467	1.200E-03
155550000	0.718	0.632	9.156	131.517	131.835	1.501	86	156	2.747	0.364	1.200E-03
156900000	0.765	0.565	12.662	150.919	151.449	1.487	85	157	3.799	0.263	1.200E-03
158250000	0.817	0.484	18.113	180.761	181.666	1.471	84	158	5.434	0.184	1.200E-03
159600000	0.866	0.390	29.048	229.508	231.339	1.445	83	160	8.714	0.115	1.200E-03
160950000	0.896	0.310	47.510	290.185	294.049	1.409	81	161	14.253	0.070	1.200E-03
162300000	0.922	0.214	101.235	412.470	424.712	1.330	76	162	30.370	0.033	1.200E-03
163650000	0.938	0.118	296.768	664.375	727.644	1.151	66	164	89.031	0.011	1.200E-03
165000000	0.944	0.014	1628.668	430.199	1684.527	0.258	15	165	488.600	0.002	1.200E-03
166350000	0.939	-0.067	687.434	-814.066	1065.490	-0.870	-50	166	206.230	0.005	1.200E-03

Resonating frequency interpolated 1.6514E+08

Resistance interpolated 1812.193

Frequency (Hertz)	VNA Real (r)	VNA Imaginary (x)	Resistance (Ohm)	Reactance (Ohm)	Magnitude (Ohm)	Angle (Radians)	Angle (Degrees)	Frequency (MegaHertz)	Resistivity (Ohm-meter)	Conductivity (Siemens per meter)	Rock Area (Square Meters)
167700000	0.929	-0.170	158.047	-500.433	524.797	-1.265	-72	168	47.414	0.021	1.200E-03
169050000	0.904	-0.262	73.189	-336.954	344.811	-1.357	-78	169	21.957	0.046	1.200E-03
170400000	0.870	-0.353	42.217	-249.596	253.141	-1.403	-80	170	12.665	0.079	1.200E-03
171750000	0.827	-0.439	27.493	-197.115	199.023	-1.432	-82	172	8.248	0.121	1.200E-03
173100000	0.779	-0.521	18.971	-162.504	163.607	-1.455	-83	173	5.691	0.176	1.200E-03
174450000	0.726	-0.588	15.085	-139.594	140.407	-1.463	-84	174	4.526	0.221	1.200E-03
175800000	0.657	-0.659	12.076	-119.367	119.977	-1.470	-84	176	3.623	0.276	1.200E-03
177150000	0.581	-0.720	9.596	-103.296	103.741	-1.478	-85	177	2.879	0.347	1.200E-03
178500000	0.506	-0.778	8.209	-91.592	91.959	-1.481	-85	179	2.463	0.406	1.200E-03
179850000	0.422	-0.826	6.875	-81.222	81.513	-1.486	-85	180	2.062	0.485	1.200E-03
181200000	0.335	-0.861	6.192	-72.763	73.025	-1.486	-85	181	1.858	0.538	1.200E-03
182550000	0.247	-0.886	5.683	-65.564	65.810	-1.484	-85	183	1.705	0.587	1.200E-03
183900000	0.154	-0.904	5.176	-58.984	59.210	-1.483	-85	184	1.553	0.644	1.200E-03
185250000	0.057	-0.912	4.797	-52.974	53.191	-1.480	-85	185	1.439	0.695	1.200E-03
186600000	-0.026	-0.907	4.695	-48.351	48.578	-1.474	-84	187	1.408	0.710	1.200E-03
187950000	-0.113	-0.898	4.407	-43.901	44.122	-1.471	-84	188	1.322	0.756	1.200E-03
189300000	-0.202	-0.884	3.997	-39.688	39.888	-1.470	-84	189	1.199	0.834	1.200E-03
190650000	-0.278	-0.862	3.770	-36.290	36.485	-1.467	-84	191	1.131	0.884	1.200E-03
192000000	-0.373	-0.830	3.349	-32.228	32.401	-1.467	-84	192	1.005	0.995	1.200E-03
193350000	-0.453	-0.792	3.056	-28.904	29.065	-1.465	-84	193	0.917	1.091	1.200E-03
194700000	-0.527	-0.749	2.801	-25.901	26.052	-1.463	-84	195	0.840	1.190	1.200E-03
196050000	-0.609	-0.688	2.536	-22.481	22.623	-1.458	-84	196	0.761	1.314	1.200E-03
197400000	-0.677	-0.625	2.363	-19.518	19.660	-1.450	-83	197	0.709	1.411	1.200E-03
198750000	-0.739	-0.558	2.144	-16.736	16.873	-1.443	-83	199	0.643	1.555	1.200E-03
200100000	-0.792	-0.483	2.029	-14.023	14.169	-1.427	-82	200	0.609	1.642	1.200E-03
201450000	-0.843	-0.392	1.918	-11.059	11.224	-1.399	-80	201	0.575	1.738	1.200E-03
202800000	-0.880	-0.305	1.815	-8.403	8.597	-1.358	-78	203	0.544	1.837	1.200E-03
204150000	-0.907	-0.222	1.726	-6.029	6.271	-1.292	-74	204	0.518	1.931	1.200E-03
205500000	-0.930	-0.113	1.627	-3.030	3.439	-1.078	-62	206	0.488	2.049	1.200E-03
206850000	-0.938	-0.015	1.590	-0.406	1.641	-0.250	-14	207	0.477	2.097	1.200E-03
208200000	-0.938	0.077	1.519	2.045	2.547	0.932	53	208	0.456	2.195	1.200E-03
209550000	-0.926	0.171	1.515	4.580	4.824	1.251	72	210	0.454	2.200	1.200E-03
210900000	-0.901	0.281	1.480	7.605	7.748	1.379	79	211	0.444	2.252	1.200E-03
212250000	-0.871	0.365	1.491	10.040	10.150	1.423	82	212	0.447	2.236	1.200E-03
213600000	-0.830	0.450	1.530	12.661	12.753	1.451	83	214	0.459	2.179	1.200E-03
214950000	-0.780	0.535	1.531	15.498	15.574	1.472	84	215	0.459	2.177	1.200E-03
216300000	-0.718	0.616	1.568	18.505	18.572	1.486	85	216	0.470	2.126	1.200E-03
217650000	-0.654	0.687	1.562	21.429	21.486	1.498	86	218	0.469	2.134	1.200E-03
219000000	-0.583	0.744	1.737	24.336	24.398	1.500	86	219	0.521	1.919	1.200E-03
220350000	-0.494	0.807	1.816	28.004	28.063	1.506	86	220	0.545	1.835	1.200E-03
221700000	-0.410	0.854	1.881	31.446	31.503	1.511	87	222	0.564	1.772	1.200E-03
223050000	-0.320	0.892	2.022	35.150	35.208	1.513	87	223	0.606	1.649	1.200E-03
224400000	-0.226	0.920	2.198	39.140	39.202	1.515	87	224	0.659	1.517	1.200E-03
225750000	-0.128	0.940	2.314	43.617	43.678	1.518	87	226	0.694	1.440	1.200E-03
227100000	-0.036	0.943	2.781	48.031	48.112	1.513	87	227	0.834	1.199	1.200E-03
228450000	0.062	0.944	2.963	53.288	53.369	1.515	87	228	0.889	1.125	1.200E-03
229800000	0.160	0.932	3.381	59.193	59.290	1.514	87	230	1.014	0.986	1.200E-03
231150000	0.247	0.911	3.890	65.218	65.334	1.511	87	231	1.167	0.857	1.200E-03
232500000	0.345	0.880	4.441	73.121	73.256	1.510	87	233	1.332	0.751	1.200E-03
233850000	0.430	0.842	5.150	81.414	81.576	1.508	86	234	1.545	0.647	1.200E-03
235200000	0.521	0.790	6.105	92.490	92.691	1.505	86	235	1.832	0.546	1.200E-03
236550000	0.588	0.738	7.516	103.202	103.475	1.498	86	237	2.255	0.443	1.200E-03
237900000	0.663	0.674	9.313	118.775	119.140	1.493	86	238	2.794	0.358	1.200E-03
239250000	0.726	0.608	12.011	137.018	137.543	1.483	85	239	3.603	0.278	1.200E-03
240600000	0.782	0.530	16.238	161.368	162.183	1.471	84	241	4.871	0.205	1.200E-03
241950000	0.834	0.444	23.738	197.577	198.998	1.451	83	242	7.121	0.140	1.200E-03
243300000	0.874	0.366	34.460	244.333	246.751	1.431	82	243	10.338	0.097	1.200E-03
244650000	0.908	0.270	63.308	331.979	337.962	1.382	79	245	18.992	0.053	1.200E-03
246000000	0.929	0.185	131.955	471.159	489.288	1.298	74	246	39.587	0.025	1.200E-03
247350000	0.944	0.081	525.938	837.316	988.791	1.010	58	247	157.781	0.006	1.200E-03
248700000	0.948	-0.011	1800.813	-300.189	1842.600	-0.213	-12	249	540.244	0.002	1.200E-03
250050000	0.943	-0.115	296.622	-702.233	762.309	-1.171	-67	250	88.987	0.011	1.200E-03
251400000	0.929	-0.196	113.312	-451.183	465.174	-1.325	-76	251	33.993	0.029	1.200E-03
252750000	0.903	-0.295	50.018	-305.962	310.023	-1.409	-81	253	15.005	0.067	1.200E-03
254100000	0.869	-0.378	31.983	-236.011	238.168	-1.436	-82	254	9.595	0.104	1.200E-03
255450000	0.829	-0.461	20.911	-190.587	191.731	-1.462	-84	255	6.273	0.159	1.200E-03
256800000	0.781	-0.537	15.230	-159.690	160.414	-1.476	-85	257	4.569	0.219	1.200E-03
258150000	0.713	-0.628	10.179	-131.740	132.132	-1.494	-86	258	3.054	0.327	1.200E-03
259500000	0.656	-0.685	8.578	-116.669	116.984	-1.497	-86	260	2.573	0.389	1.200E-03
260850000	0.578	-0.751	6.916	-101.220	101.456	-1.503	-86	261	2.075	0.482	1.200E-03
262200000	0.498	-0.807	5.591	-89.312	89.487	-1.508	-86	262	1.677	0.596	1.200E-03
263550000	0.412	-0.853	4.783	-79.501	79.645	-1.511	-87	264	1.435	0.697	1.200E-03
264900000	0.331	-0.889	4.010	-71.810	71.922	-1.515	-87	265	1.203	0.831	1.200E-03
266250000	0.229	-0.919	3.571	-63.862	63.962	-1.515	-87	266	1.071	0.933	1.200E-03
267600000	0.148	-0.935	3.248	-58.420	58.511	-1.515	-87	268	0.974	1.026	1.200E-03
268950000	0.049	-0.946	2.862	-52.552	52.630	-1.516	-87	269	0.859	1.165	1.200E-03
270300000	-0.053	-0.947	2.515	-47.195	47.262	-1.518	-87	270	0.755	1.325	1.200E-03
271650000	-0.144	-0.934	2.449	-42.806	42.879	-1.514	-87	272	0.735	1.361	1.200E-03
273000000	-0.236	-0.914	2.325	-38.685	38.755	-1.511	-87	273	0.698	1.434	1.200E-03
274350000	-0.330	-0.886	2.070	-34.689	34.751	-1.511	-87	274	0.621	1.610	1.200E-03
275700000	-0.410	-0.850	2.013	-31.369	31.433	-1.507	-86	276	0.604	1.656	1.200E-03
277050000	-0.504	-0.802	1.779	-27.606	27.664	-1.506	-86	277	0.534	1.874	1.200E-03
278400000	-0.579	-0.745	1.789	-24.443	24.509	-1.498	-86	278	0.537	1.863	1.200E-03
279750000	-0.657	-0.679	1.666	-21.180	21.245	-1.492	-85	280	0.499	2.002	1.200E-03
281100000	-0.719	-0.609	1.673	-18.310	18.386	-1.480	-85	281	0.502	1.993	1.200E-03
282450000	-0.782	-0.526	1.621	-15.249	15.335	-1.465	-84	282	0.486	2.056	1.200E-03
283800000	-0.826	-0.448	1.651	-12.672	12.779	-1.441	-83	284	0.495	2.019	1.200E-03
285150000	-0.861	-0.372	1.672	-10.336	10.471	-1.410	-81	285	0.502	1.994	1.200E-03
286500000	-0.899	-0.270	1.614	-7.346	7.521	-1.355	-78	287	0.484	2.065	1.200E-03
287850000	-0.920	-0.183	1.609	-4.924	5.180	-1.255	-72	288	0.483	2.072	1.200E-03
289200000	-0.934	-0.084	1.609	-2.232	2.751	-0.946	-54	289	0.483	2.072	1.200E-03
290550000	-0.939	0.007	1.585	0.192	1.597	0.121	7	291	0.476	2.103	1.200E-03
291900000	-0.930	0.101	1.668	2.702	3.175	1.018	58	292	0.500	1.999	1.200E-03
293250000	-0.916	0.186	1.706	5.024	5.306	1.243	71	293	0.512	1.954	1.200E-03
294600000	-0.890	0.289	1.699	7.894	8.075	1.359	78	295	0.510	1.962	1.200E-03
295950000	-0.854	0.381	1.755	10.633	10.777	1.407	81	296	0.526	1.900	1.200E-03
297300000	-0.818	0.455	1.776	12.947	13.068	1.435	82	297	0.533	1.877	1.200E-03
298650000	-0.783	0.541	1.837	15.905	16.011	1.456	83	299	0.551	1.814	1.200E-03
300000000	-0.709	0.608	1.922	18.483	18.583	1.467	84	300	0.577	1.734	1.200E-03

ANNEXURE 10 Electrical parameters of the untreated JS5 rock sample for the VHF range

Frequency (Hertz)	VNA Real (r)	VNA Imaginary (x)	Resistance (Ohm)	Reactance (Ohm)	Magnitude (Ohm)	Angle (Radians)	Angle (Degrees)	Frequency (MegaHertz)	Resistivity (Ohm-meter)	Conductivity (Siemens per meter)	Rock Area (Square Meters)	
30000000	-0.709	-0.691	0.289	-20.325	20.327	-1.557	-89	30	0.087	11.552	1.200E-03	
31350000	-0.781	-0.611	0.249	-17.228	17.230	-1.556	-89	31	0.075	13.403	1.200E-03	
32700000	-0.843	-0.519	0.279	-14.162	14.164	-1.551	-89	33	0.084	11.912	1.200E-03	
34050000	-0.893	-0.426	0.289	-11.312	11.316	-1.545	-89	34	0.087	11.543	1.200E-03	
35400000	-0.931	-0.333	0.298	-8.685	8.690	-1.536	-88	35	0.090	11.172	1.200E-03	
36750000	-0.961	-0.227	0.327	-5.830	5.839	-1.515	-87	37	0.098	10.204	1.200E-03	
38100000	-0.971	-0.131	0.504	-3.358	3.396	-1.422	-81	38	0.151	6.611	1.200E-03	
39450000	-0.985	-0.017	0.384	-0.431	0.577	-0.843	-48	39	0.115	8.674	1.200E-03	
40800000	-0.980	0.084	0.420	2.137	2.178	1.377	79	41	0.126	7.942	1.200E-03	
42150000	-0.962	0.196	0.471	5.042	5.064	1.478	85	42	0.141	7.080	1.200E-03	
43500000	-0.937	0.294	0.465	7.660	7.674	1.510	87	44	0.139	7.172	1.200E-03	
44850000	-0.900	0.387	0.526	10.298	10.311	1.520	87	45	0.158	6.339	1.200E-03	
46200000	-0.852	0.485	0.544	13.233	13.244	1.530	88	46	0.163	6.127	1.200E-03	
47550000	-0.792	0.578	0.542	16.297	16.306	1.538	88	48	0.163	6.155	1.200E-03	
48900000	-0.726	0.653	0.690	19.189	19.201	1.535	88	49	0.207	4.832	1.200E-03	
50250000	-0.651	0.728	0.728	22.364	22.376	1.538	88	50	0.219	4.581	1.200E-03	
51600000	-0.558	0.799	0.828	26.071	26.084	1.539	88	52	0.248	4.025	1.200E-03	
52950000	-0.458	0.848	1.257	29.802	29.829	1.529	88	53	0.377	2.653	1.200E-03	
54300000	-0.364	0.876	1.848	33.362	33.413	1.515	87	54	0.554	1.804	1.200E-03	
55650000	-0.278	0.891	2.639	36.709	36.803	1.499	86	56	0.792	1.263	1.200E-03	
57000000	-0.203	0.923	2.304	40.146	40.211	1.513	87	57	0.691	1.447	1.200E-03	
58350000	-0.114	0.946	2.164	44.267	44.320	1.522	87	58	0.649	1.541	1.200E-03	
59700000	-0.011	0.960	2.033	49.392	49.434	1.530	88	60	0.610	1.640	1.200E-03	
61050000	0.092	0.959	2.063	55.012	55.051	1.533	88	61	0.619	1.616	1.200E-03	
62400000	0.191	0.943	2.420	61.118	61.166	1.531	88	62	0.726	1.378	1.200E-03	
63750000	0.294	0.920	2.521	68.417	68.463	1.534	88	64	0.756	1.322	1.200E-03	
65100000	0.394	0.884	2.752	76.960	77.009	1.535	88	65	0.826	1.211	1.200E-03	
66450000	0.494	0.834	3.188	87.633	87.691	1.534	88	66	0.956	1.046	1.200E-03	
67800000	0.568	0.777	4.795	98.084	98.201	1.522	87	68	1.438	0.695	1.200E-03	
69150000	0.646	0.721	4.920	111.614	111.922	1.527	87	69	1.476	0.678	1.200E-03	
70500000	0.725	0.651	5.112	130.288	130.369	1.532	88	71	1.534	0.652	1.200E-03	
71850000	0.782	0.577	7.234	151.634	151.806	1.523	87	72	2.170	0.461	1.200E-03	
73200000	0.844	0.484	10.372	187.278	187.565	1.515	87	73	3.112	0.321	1.200E-03	
74550000	0.893	0.386	16.811	240.435	241.022	1.501	86	75	5.043	0.198	1.200E-03	
75900000	0.925	0.298	29.528	315.143	316.523	1.477	85	76	8.858	0.113	1.200E-03	
77250000	0.955	0.198	61.611	485.585	489.488	1.445	83	77	18.483	0.054	1.200E-03	
78600000	0.967	0.103	234.267	880.031	910.679	1.311	75	79	70.280	0.014	1.200E-03	
79950000	0.974	-0.007	3628.245	-942.656	3748.702	-0.254	-15	80	1088.474	0.001	1.200E-03	
81300000	0.968	-0.107	209.727	-858.278	883.531	-1.331	-76	81	62.918	0.016	1.200E-03	
82650000	0.952	-0.218	45.969	-438.057	440.463	-1.466	-84	83	13.791	0.073	1.200E-03	
84000000	0.922	-0.320	21.729	-295.273	296.071	-1.497	-86	84	6.519	0.153	1.200E-03	
85350000	0.884	-0.409	14.300	-226.529	226.980	-1.508	-86	85	4.290	0.233	1.200E-03	
86700000	0.836	-0.501	9.152	-180.233	180.465	-1.520	-87	87	2.746	0.364	1.200E-03	
88050000	0.780	-0.579	7.251	-150.980	151.154	-1.523	-87	88	2.175	0.460	1.200E-03	
89400000	0.715	-0.661	4.956	-127.508	127.604	-1.532	-88	89	1.487	0.673	1.200E-03	
90750000	0.638	-0.735	3.899	-109.461	109.530	-1.535	-88	91	1.170	0.855	1.200E-03	
92100000	0.550	-0.803	3.052	-94.796	94.846	-1.539	-88	92	0.916	1.092	1.200E-03	
93450000	0.464	-0.856	2.551	-83.966	84.005	-1.540	-88	93	0.765	1.307	1.200E-03	
94800000	0.379	-0.897	2.142	-75.352	75.383	-1.542	-88	95	0.643	1.556	1.200E-03	
96150000	0.279	-0.932	1.958	-67.122	67.152	-1.542	-88	96	0.587	1.703	1.200E-03	
97500000	0.184	-0.955	1.736	-60.517	60.542	-1.542	-88	98	0.521	1.920	1.200E-03	
98850000	0.082	-0.972	1.385	-54.359	54.377	-1.545	-89	99	0.416	2.409	1.200E-03	
100200000	-0.028	-0.974	1.263	-48.566	48.583	-1.545	-89	100	0.379	2.639	1.200E-03	
101550000	-0.123	-0.965	1.236	-44.021	44.038	-1.543	-88	102	0.371	2.692	1.200E-03	
102900000	-0.225	-0.945	1.184	-39.488	39.506	-1.541	-88	103	0.355	2.816	1.200E-03	
104250000	-0.321	-0.918	1.065	-35.467	35.483	-1.541	-88	104	0.320	3.130	1.200E-03	
105600000	-0.427	-0.873	0.986	-31.205	31.221	-1.539	-88	106	0.296	3.381	1.200E-03	
106950000	-0.518	-0.827	0.841	-27.732	27.745	-1.540	-88	107	0.252	3.964	1.200E-03	
108300000	-0.602	-0.762	0.900	-24.200	24.217	-1.534	-88	108	0.270	3.705	1.200E-03	
109650000	-0.669	-0.701	0.934	-21.405	21.425	-1.527	-88	110	0.280	3.569	1.200E-03	
111000000	-0.746	-0.621	0.853	-18.087	18.107	-1.524	-87	111	0.256	3.906	1.200E-03	
112350000	-0.806	-0.538	0.854	-15.157	15.181	-1.515	-87	112	0.256	3.903	1.200E-03	
113700000	-0.860	-0.450	0.787	-12.295	12.320	-1.507	-86	114	0.236	4.235	1.200E-03	
115050000	-0.900	-0.358	0.826	-9.583	9.619	-1.485	-85	115	0.248	4.036	1.200E-03	
116400000	-0.932	-0.256	0.858	-6.734	6.789	-1.444	-83	116	0.257	3.888	1.200E-03	
117750000	-0.956	-0.153	0.817	-3.971	4.054	-1.368	-78	118	0.245	4.080	1.200E-03	
119100000	-0.963	-0.064	0.886	-1.647	1.870	-1.077	-62	119	0.266	3.761	1.200E-03	
120450000	-0.964	0.046	0.879	1.179	1.470	0.930	53	120	0.264	3.792	1.200E-03	
121800000	-0.955	0.153	0.830	3.989	4.074	1.366	78	122	0.249	4.016	1.200E-03	
123150000	-0.932	0.249	0.906	6.570	6.632	1.434	82	123	0.272	3.681	1.200E-03	
124500000	-0.898	0.347	0.975	9.318	9.369	1.467	84	125	0.292	3.420	1.200E-03	
125850000	-0.857	0.448	0.900	12.280	12.313	1.498	86	126	0.270	3.702	1.200E-03	
127200000	-0.806	0.529	0.990	14.939	14.972	1.505	86	127	0.297	3.368	1.200E-03	
128550000	-0.745	0.610	1.055	17.855	17.887	1.512	87	129	0.317	3.159	1.200E-03	
129900000	-0.680	0.681	1.123	20.730	20.761	1.517	87	130	0.337	2.969	1.200E-03	
131250000	-0.596	0.754	1.220	24.193	24.224	1.520	87	131	0.366	2.732	1.200E-03	
132600000	-0.513	0.816	1.192	27.612	27.638	1.528	88	133	0.358	2.796	1.200E-03	
133950000	-0.428	0.861	1.349	30.973	31.002	1.527	88	134	0.405	2.471	1.200E-03	
135300000	-0.341	0.897	1.504	34.455	34.487	1.527	87	135	0.451	2.216	1.200E-03	
136650000	-0.246	0.928	1.617	38.461	38.495	1.529	88	137	0.485	2.061	1.200E-03	
138000000	-0.146	0.950	1.708	42.896	42.930	1.531	88	138	0.513	1.951	1.200E-03	
139350000	-0.045	0.960	1.907	47.688	47.726	1.531	88	139	0.572	1.748	1.200E-03	
140700000	0.059	0.960	2.094	53.120	53.161	1.531	88	141	0.628	1.592	1.200E-03	
142050000	0.151	0.948	2.446	58.544	58.595	1.529	88	142	0.734	1.363	1.200E-03	
143400000	0.250	0.926	2.716	65.155	65.212	1.529	88	143	0.815	1.227	1.200E-03	
144750000	0.355	0.892	3.226	73.587	73.657	1.527	87	145	0.968	1.033	1.200E-03	
146100000	0.436	0.855	3.749	81.476	81.562	1.525	87	146	1.125	0.889	1.200E-03	
147450000	0.530	0.800	4.524	92.943	93.053	1.522	87	147	1.357	0.737	1.200E-03	
148800000	0.609	0.742	5.609	105.556	105.705	1.518	87	149	1.683	0.594	1.200E-03	
150150000	0.683	0.674	7.067	121.514	121.719	1.513	87	150	2.120	0.472	1.200E-03	
151500000	0.745	0.605	9.127	140.427	140.724	1.506	86	152	2.738	0.365	1.200E-03	
152850000	0.801	0.528	12.706	165.846	166.332	1.494	86	153	3.812	0.262	1.200E-03	
154200000	0.853	0.426	18.566	235.155	235.878	1.479	85	154	5.555	[illegible]	1.200E-03	Resonating
155550000	0.895	0.343	31.701	296.695	298.372	1.465	84	156	9.510	0.105	1.200E-03	frequency
156900000	0.927	0.248	58.342	369.411	373.990	1.409	81	157	17.503	0.057	1.200E-03	interpolated
158250000	0.942	0.158	152.096	555.721	576.159	1.304	75	158	45.629	0.022	1.200E-03	1.6043E+08
159600000	0.958	0.049	977.295	[illegible]	[illegible]	0.854	49	160	[illegible]	0.003	1.200E-03	
160950000	0.955	-0.035	1205.358	-1056.735	[illegible]	-0.720	-41	161	[illegible]	0.003	1.200E-03	
162300000	0.945	-0.137	208.576	-623.467	657.415	-1.248	-72	162	62.568	0.016	1.200E-03	Resistance
163650000	0.924	-0.239	70.797	-379.111	385.665	-1.386	-79	164	21.239	0.047	1.200E-03	interpolated
165000000	0.894	-0.333	37.095	-272.446	274.954	-1.436	-82	165	11.117	0.090	1.200E-03	1339.364
166350000	0.858	-0.416	24.381	-214.500	215.882	-1.458	-84	166	7.314	0.137	1.200E-03	

Frequency (Hertz)	VNA Real (r)	VNA Imaginary (x)	Resistance (Ohm)	Reactance (Ohm)	Magnitude (Ohm)	Angle (Radians)	Angle (Degrees)	Frequency (MegaHertz)	Resistivity (Ohm-meter)	Conductivity (Siemens per meter)	Rock Area (Square Meters)
167700000	0.803	-0.511	15.479	-170.384	171.086	-1.480	-85	168	4.644	0.215	1.200E-03
169050000	0.749	-0.586	11.759	-144.307	144.785	-1.489	-85	169	3.528	0.283	1.200E-03
170400000	0.683	-0.660	9.064	-123.111	123.444	-1.497	-86	170	2.719	0.368	1.200E-03
171750000	0.616	-0.722	7.419	-107.950	108.204	-1.502	-86	172	2.226	0.449	1.200E-03
173100000	0.528	-0.789	5.843	-93.375	93.558	-1.508	-86	173	1.753	0.570	1.200E-03
174450000	0.447	-0.836	5.064	-83.246	83.400	-1.510	-87	174	1.519	0.658	1.200E-03
175800000	0.362	-0.873	4.595	-74.716	74.857	-1.509	-86	176	1.378	0.725	1.200E-03
177150000	0.265	-0.906	4.073	-66.608	66.733	-1.510	-87	177	1.222	0.818	1.200E-03
178500000	0.168	-0.930	3.430	-59.719	59.816	-1.513	-87	179	1.029	0.972	1.200E-03
179850000	0.075	-0.940	3.165	-54.030	54.123	-1.512	-87	180	0.950	1.053	1.200E-03
181200000	-0.030	-0.942	2.884	-48.357	48.443	-1.511	-87	181	0.865	1.156	1.200E-03
182550000	-0.117	-0.930	2.874	-44.010	44.104	-1.506	-86	183	0.862	1.160	1.200E-03
183900000	-0.211	-0.911	2.728	-39.675	39.769	-1.502	-86	184	0.818	1.222	1.200E-03
185250000	-0.307	-0.882	2.560	-35.487	35.579	-1.499	-86	185	0.768	1.302	1.200E-03
186600000	-0.397	-0.841	2.548	-31.644	31.746	-1.490	-85	187	0.764	1.308	1.200E-03
187950000	-0.469	-0.798	2.560	-28.555	28.670	-1.481	-85	188	0.768	1.302	1.200E-03
189300000	-0.551	-0.744	2.405	-25.146	25.261	-1.475	-85	189	0.722	1.386	1.200E-03
190650000	-0.624	-0.684	2.292	-22.032	22.151	-1.467	-84	191	0.688	1.454	1.200E-03
192000000	-0.690	-0.619	2.192	-19.107	19.233	-1.457	-83	192	0.658	1.521	1.200E-03
193350000	-0.745	-0.553	2.082	-16.508	16.639	-1.445	-83	193	0.625	1.601	1.200E-03
194700000	-0.799	-0.475	1.948	-13.720	13.857	-1.430	-82	195	0.584	1.712	1.200E-03
196050000	-0.847	-0.390	1.819	-10.938	11.089	-1.406	-81	196	0.546	1.832	1.200E-03
197400000	-0.888	-0.293	1.710	-8.028	8.208	-1.361	-78	197	0.513	1.950	1.200E-03
198750000	-0.914	-0.213	1.599	-5.736	5.954	-1.299	-74	199	0.480	2.084	1.200E-03
200100000	-0.934	-0.111	1.545	-2.961	3.340	-1.090	-62	200	0.463	2.158	1.200E-03
201450000	-0.940	-0.019	1.548	-0.509	1.630	-0.318	-18	201	0.464	2.153	1.200E-03
202800000	-0.940	0.072	1.487	1.923	2.431	0.913	52	203	0.446	2.242	1.200E-03
204150000	-0.926	0.187	1.427	4.992	5.192	1.292	74	204	0.428	2.336	1.200E-03
205500000	-0.903	0.281	1.420	7.588	7.717	1.386	79	206	0.426	2.347	1.200E-03
206850000	-0.871	0.370	1.426	10.167	10.267	1.431	82	207	0.428	2.338	1.200E-03
208200000	-0.832	0.453	1.430	12.710	12.791	1.459	84	208	0.429	2.332	1.200E-03
209550000	-0.780	0.548	1.365	15.751	15.810	1.484	85	210	0.410	2.442	1.200E-03
210900000	-0.722	0.618	1.478	18.407	18.467	1.491	85	211	0.443	2.256	1.200E-03
212250000	-0.653	0.692	1.471	21.550	21.600	1.503	86	212	0.441	2.266	1.200E-03
213600000	-0.579	0.753	1.589	24.616	24.667	1.506	86	214	0.477	2.097	1.200E-03
214950000	-0.502	0.810	1.576	27.835	27.880	1.514	87	215	0.473	2.116	1.200E-03
216300000	-0.414	0.859	1.659	31.382	31.426	1.518	87	216	0.498	2.010	1.200E-03
217650000	-0.322	0.897	1.797	35.164	35.210	1.520	87	218	0.539	1.855	1.200E-03
219000000	-0.226	0.926	1.948	39.211	39.260	1.521	87	219	0.584	1.711	1.200E-03
220350000	-0.129	0.944	2.116	43.577	43.629	1.522	87	220	0.635	1.576	1.200E-03
221700000	-0.036	0.953	2.272	48.079	48.133	1.524	87	222	0.682	1.467	1.200E-03
223050000	0.066	0.952	2.515	53.531	53.590	1.524	87	223	0.754	1.325	1.200E-03
224400000	0.158	0.941	2.839	59.003	59.072	1.523	87	224	0.852	1.174	1.200E-03
225750000	0.251	0.920	3.236	65.381	65.441	1.521	87	226	0.971	1.030	1.200E-03
227100000	0.346	0.889	3.689	72.968	73.061	1.520	87	227	1.107	0.903	1.200E-03
228450000	0.436	0.848	4.421	81.770	81.889	1.517	87	228	1.326	0.754	1.200E-03
229800000	0.521	0.798	5.317	92.108	92.261	1.513	87	230	1.595	0.627	1.200E-03
231150000	0.590	0.747	6.507	102.847	103.052	1.508	86	231	1.952	0.512	1.200E-03
232500000	0.657	0.688	7.996	116.336	116.610	1.502	86	233	2.399	0.417	1.200E-03
233850000	0.730	0.612	10.209	136.768	137.149	1.496	86	234	3.063	0.327	1.200E-03
235200000	0.793	0.530	13.840	163.815	164.399	1.487	85	235	4.152	0.241	1.200E-03
236550000	0.840	0.452	19.822	196.670	197.666	1.470	84	237	5.947	0.168	1.200E-03
237900000	0.876	0.370	30.602	243.657	245.571	1.446	83	238	9.181	0.109	1.200E-03
239250000	0.910	0.281	53.053	322.629	326.962	1.408	81	239	15.916	0.063	1.200E-03
240600000	0.937	0.185	115.774	485.105	498.729	1.337	77	241	34.732	0.029	1.200E-03
241950000	0.950	0.092	401.690	837.895	929.206	1.124	64	242	120.507	0.008	1.200E-03
243300000	0.951	0.000	2006.318	-6.517	2006.329	-0.003	0	243	601.895	0.002	1.200E-03
244650000	0.949	-0.098	367.850	-804.967	885.037	-1.142	-65	245	110.358	0.009	1.200E-03
246000000	0.936	-0.192	107.683	-469.032	481.234	-1.345	-77	246	32.305	0.031	1.200E-03
247350000	0.912	-0.282	51.567	-323.205	327.293	-1.413	-81	247	15.470	0.065	1.200E-03
248700000	0.877	-0.377	28.239	-239.404	241.063	-1.453	-83	249	8.472	0.118	1.200E-03
250050000	0.836	-0.463	18.040	-191.734	192.581	-1.477	-85	250	5.412	0.185	1.200E-03
251400000	0.790	-0.537	13.113	-161.450	161.981	-1.490	-85	251	3.934	0.254	1.200E-03
252750000	0.729	-0.618	9.577	-135.762	136.099	-1.500	-86	253	2.873	0.348	1.200E-03
254100000	0.666	-0.681	8.044	-118.409	118.682	-1.503	-86	254	2.413	0.414	1.200E-03
255450000	0.594	-0.748	5.921	-103.129	103.299	-1.513	-87	255	1.776	0.563	1.200E-03
256800000	0.508	-0.812	4.567	-90.042	90.158	-1.520	-87	257	1.370	0.730	1.200E-03
258150000	0.435	-0.853	3.970	-81.439	81.535	-1.522	-87	258	1.191	0.840	1.200E-03
259500000	0.349	-0.889	3.650	-73.200	73.291	-1.521	-87	260	1.095	0.913	1.200E-03
260850000	0.256	-0.920	3.129	-65.690	65.764	-1.523	-87	261	0.939	1.065	1.200E-03
262200000	0.167	-0.939	2.853	-59.576	59.645	-1.523	-87	262	0.856	1.168	1.200E-03
263550000	0.066	-0.951	2.541	-53.507	53.567	-1.523	-87	264	0.762	1.312	1.200E-03
264900000	-0.028	-0.952	2.356	-48.509	48.566	-1.522	-87	265	0.707	1.415	1.200E-03
266250000	-0.120	-0.945	2.160	-44.023	44.075	-1.522	-87	266	0.648	1.543	1.200E-03
267600000	-0.229	-0.926	1.902	-39.103	39.150	-1.522	-87	268	0.571	1.752	1.200E-03
268950000	-0.315	-0.899	1.821	-35.441	35.487	-1.519	-87	269	0.546	1.831	1.200E-03
270300000	-0.394	-0.866	1.758	-32.147	32.195	-1.516	-87	270	0.527	1.896	1.200E-03
271650000	-0.479	-0.822	1.636	-28.708	28.755	-1.514	-87	272	0.491	2.037	1.200E-03
273000000	-0.568	-0.763	1.551	-25.086	25.134	-1.509	-86	273	0.465	2.149	1.200E-03
274350000	-0.645	-0.699	1.495	-21.867	21.918	-1.503	-86	274	0.449	2.229	1.200E-03
275700000	-0.706	-0.640	1.393	-19.265	19.315	-1.499	-86	276	0.418	2.394	1.200E-03
277050000	-0.764	-0.567	1.375	-16.522	16.579	-1.488	-85	277	0.412	2.425	1.200E-03
278400000	-0.818	-0.482	1.386	-13.822	13.692	-1.469	-84	278	0.416	2.404	1.200E-03
279750000	-0.865	-0.394	1.334	-10.836	10.917	-1.448	-83	280	0.400	2.499	1.200E-03
281100000	-0.902	-0.304	1.255	-8.188	8.294	-1.419	-81	281	0.377	2.655	1.200E-03
282450000	-0.922	-0.221	1.363	-5.904	6.059	-1.344	-77	282	0.409	2.445	1.200E-03
283800000	-0.941	-0.125	1.315	-3.312	3.564	-1.193	-68	284	0.395	2.535	1.200E-03
285150000	-0.947	-0.026	1.353	-0.676	1.512	-0.463	-27	285	0.406	2.464	1.200E-03
286500000	-0.945	0.071	1.350	1.884	2.318	0.949	54	287	0.405	2.469	1.200E-03
287850000	-0.935	0.165	1.306	4.377	4.568	1.281	73	288	0.392	2.551	1.200E-03
289200000	-0.912	0.251	1.426	6.759	6.907	1.363	78	289	0.428	2.338	1.200E-03
290550000	-0.879	0.350	1.440	9.577	9.685	1.422	81	291	0.432	2.315	1.200E-03
291900000	-0.842	0.431	1.456	12.051	12.138	1.451	83	292	0.437	2.289	1.200E-03
293250000	-0.795	0.510	1.558	14.654	14.737	1.465	84	293	0.468	2.139	1.200E-03
294600000	-0.742	0.587	1.561	17.375	17.445	1.481	85	295	0.468	2.136	1.200E-03
295950000	-0.674	0.663	1.640	20.443	20.509	1.491	85	296	0.492	2.032	1.200E-03
297300000	-0.606	0.724	1.706	23.299	23.361	1.498	86	297	0.512	1.954	1.200E-03
298650000	-0.535	0.780	1.768	26.304	26.363	1.504	86	299	0.531	1.885	1.200E-03
300000000	-0.451	0.829	1.942	29.683	29.746	1.505	86	300	0.583	1.717	1.200E-03

ANNEXURE 11 Photographs of the rock cutting equipment

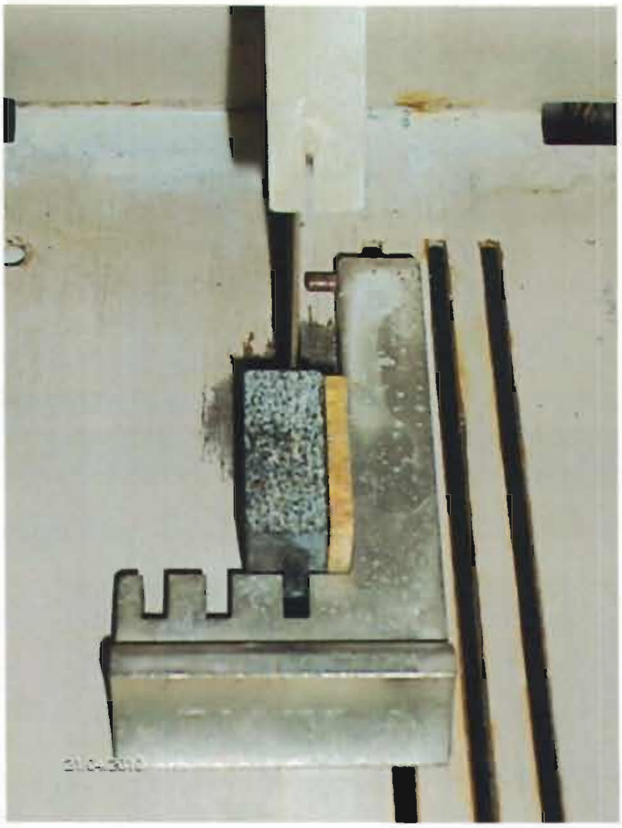

ANNEXURE 12 Photographs of PPC1 (87 x 47 mm), PPC2 (59 x 47 mm), PPC3 (28 x 47 mm) and PPC4 (18 x 33 mm)

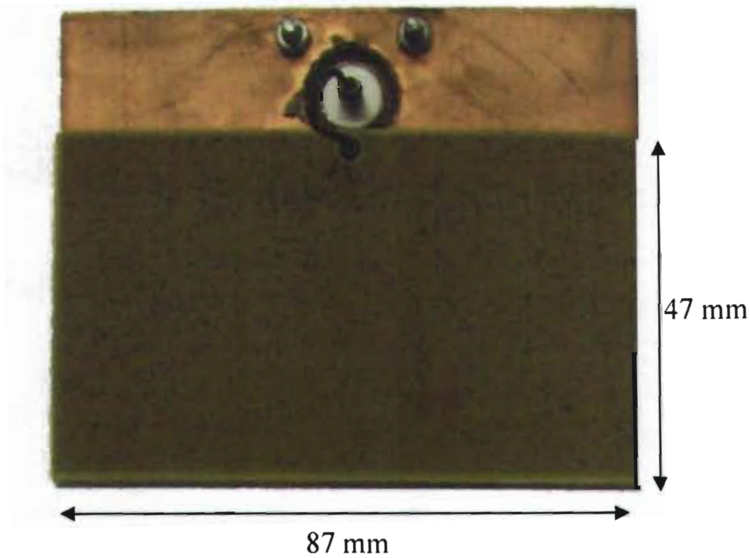

PPC1

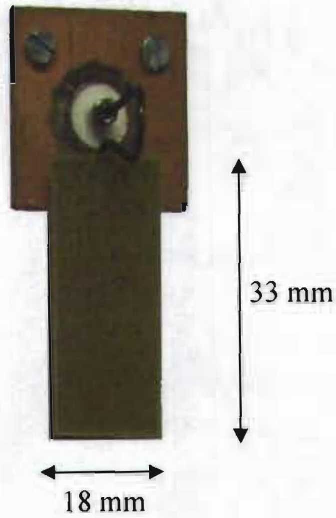

PPC4

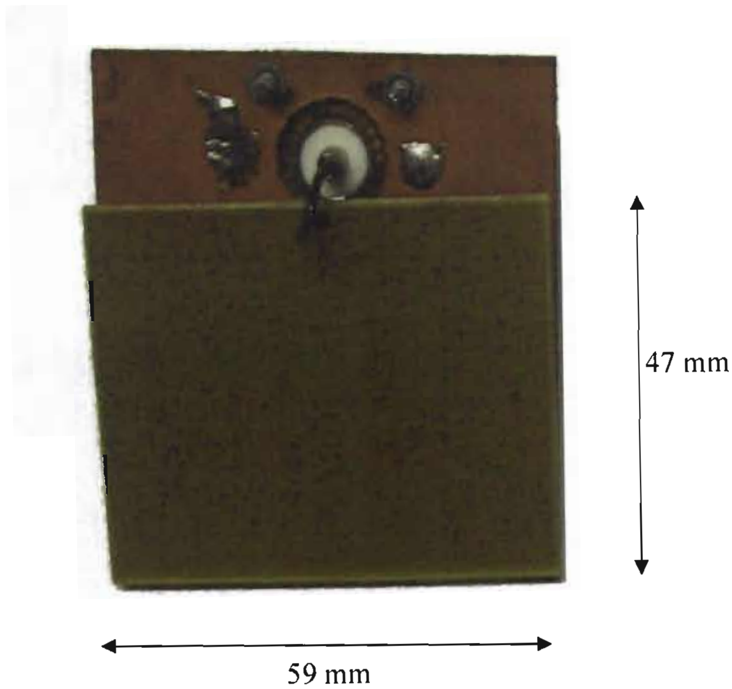

PPC2

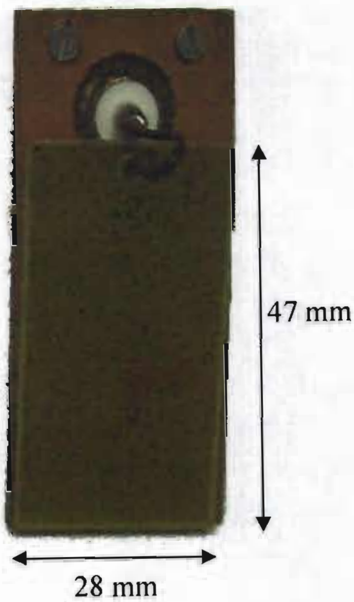

PPC3

ANNEXURE 13 Mathematical equations for resonating frequency to phase angle for the rock samples derived from the basic square waveform

Sample name	**Rock sample**	**Resonating frequency**	**Phase angle equation ϕ in radians**
JSA	Dolerite	160.14 MHz	$\phi=\sum_{n=1}^{201}[172\times\frac{\sin(n\times\frac{\pi}{2})}{n\times\frac{\pi}{2}}]\times\cos(2\times\pi\times n\times 0.012278\times(f+22.782))$
JSB	Marble	162.58 MHz	$\phi=\sum_{n=1}^{201}[172\times\frac{\sin(n\times\frac{\pi}{2})}{n\times\frac{\pi}{2}}]\times\cos(2\times\pi\times n\times 0.01225\times(f+20.471))$
JSC	Granite	167.85 MHz	$\phi=\sum_{n=1}^{201}[172\times\frac{\sin(n\times\frac{\pi}{2})}{n\times\frac{\pi}{2}}]\times\cos(2\times\pi\times n\times 0.01194\times(f+20.695))$
JSD	Sandstone	170.08 MHz	$\phi=\sum_{n=1}^{201}[172\times\frac{\sin(n\times\frac{\pi}{2})}{n\times\frac{\pi}{2}}]\times\cos(2\times\pi\times n\times 0.01109\times(f+22.709))$
JSE	Mudstone	153.15 MHz	$\phi=\sum_{n=1}^{201}[172\times\frac{\sin(n\times\frac{\pi}{2})}{n\times\frac{\pi}{2}}]\times\cos(2\times\pi\times n\times 0.01202\times(f+21.589))$
JS1	Marble	162.61 MHz	$\phi=\sum_{n=1}^{201}[172\times\frac{\sin(n\times\frac{\pi}{2})}{n\times\frac{\pi}{2}}]\times\cos(2\times\pi\times n\times 0.012232\times(f+21.452))$
JS2	Marble	159.74 MHz	$\phi=\sum_{n=1}^{201}[172\times\frac{\sin(n\times\frac{\pi}{2})}{n\times\frac{\pi}{2}}]\times\cos(2\times\pi\times n\times 0.012228\times(f+23.152))$
JS3	Marble	162.30 MHz	$\phi=\sum_{n=1}^{201}[172\times\frac{\sin(n\times\frac{\pi}{2})}{n\times\frac{\pi}{2}}]\times\cos(2\times\pi\times n\times 0.012232\times(f+21.652))$
JS4	Granite	165.14 MHz	$\phi=\sum_{n=1}^{201}[172\times\frac{\sin(n\times\frac{\pi}{2})}{n\times\frac{\pi}{2}}]\times\cos(2\times\pi\times n\times 0.01202\times(f+21.752))$
JS5	Marble	160.43 MHz	$\phi=\sum_{n=1}^{201}[172\times\frac{\sin(n\times\frac{\pi}{2})}{n\times\frac{\pi}{2}}]\times\cos(2\times\pi\times n\times 0.0123\times(f+22.252))$

ANNEXURE 14 K-Type thermocouple pressed firmly against the surface of a rock sample with the temperature meter shown below

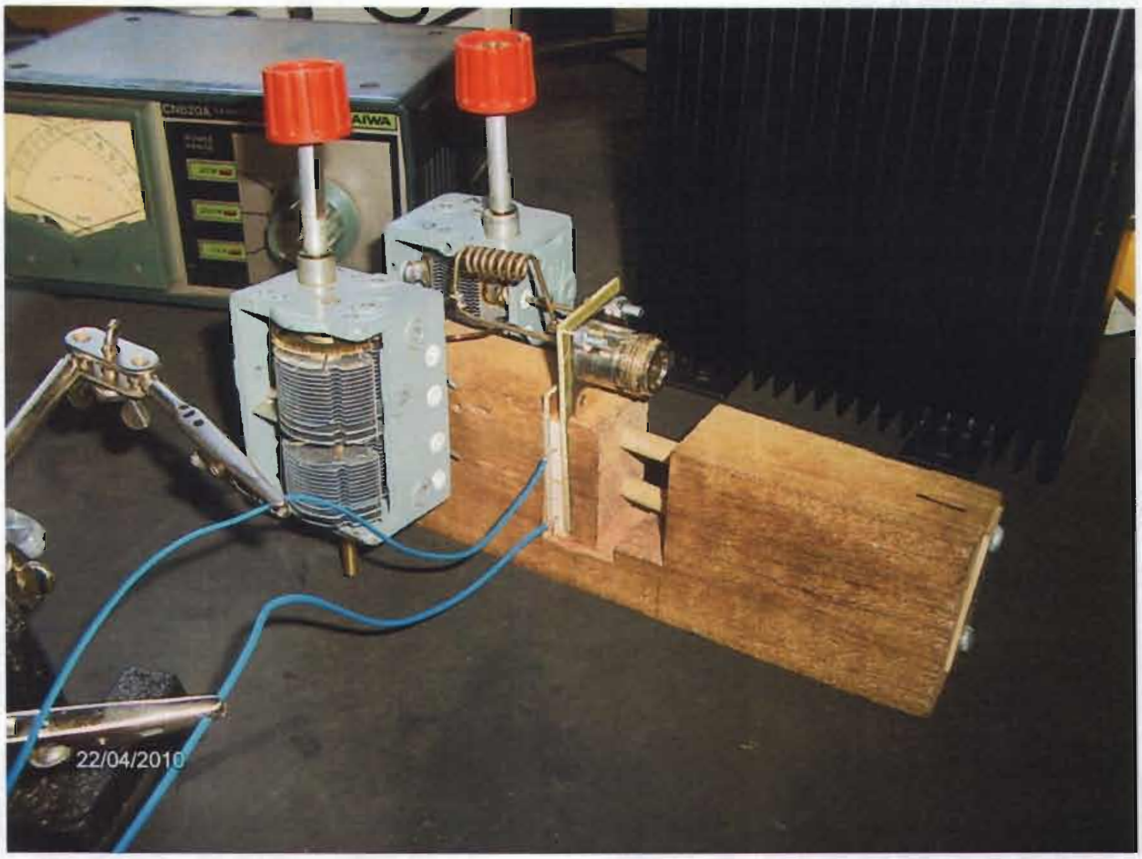

ANNEXURE 15 Temperature rise curves for the JSB and JSC rock samples

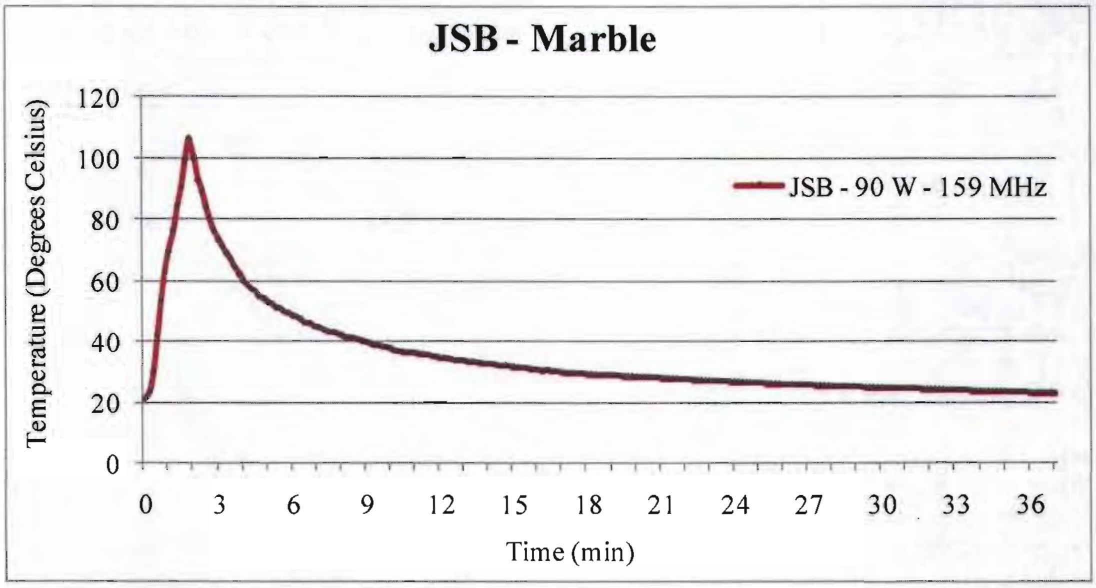

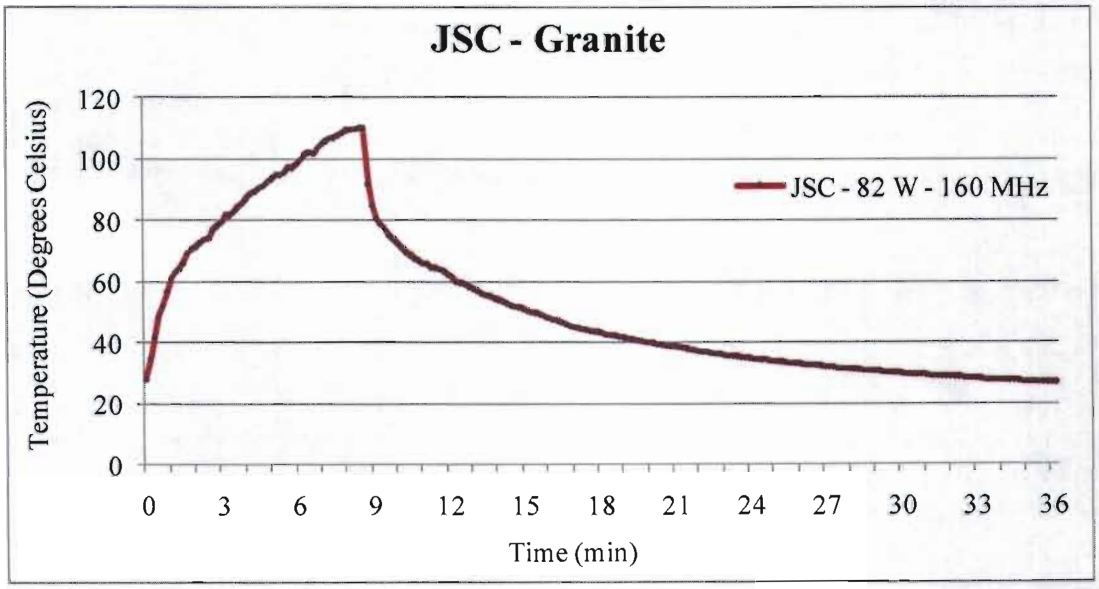

ANNEXURE 16 Temperature rise curves for the JSD and JSE rock samples

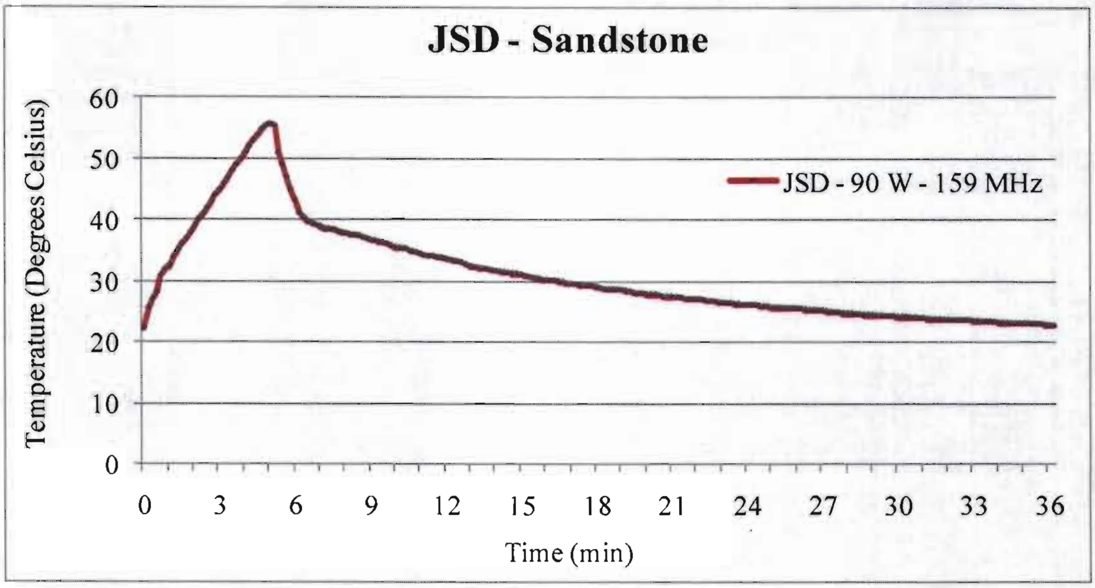

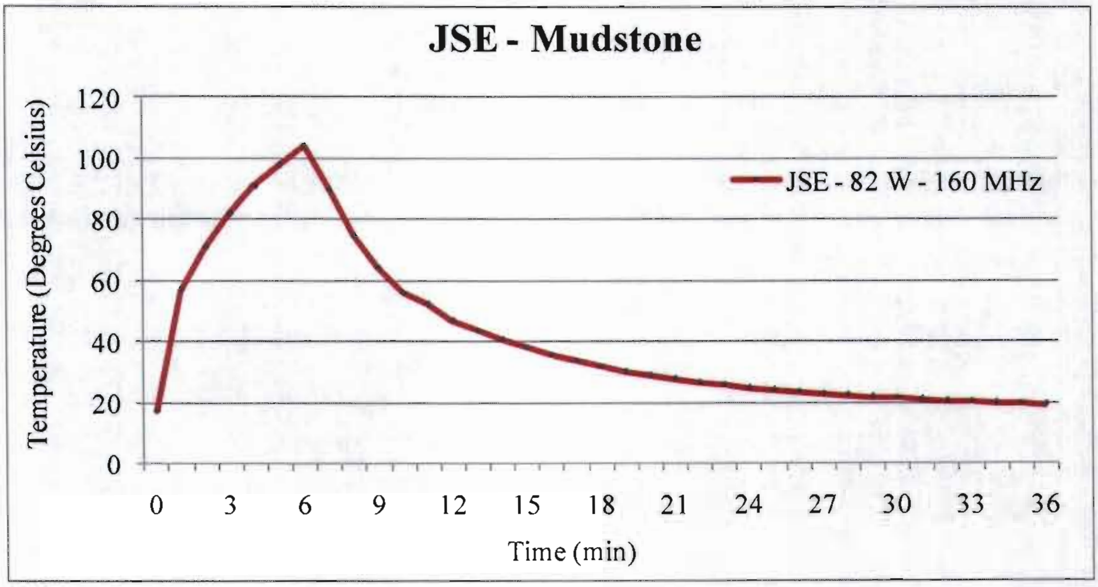

ANNEXURE 17 Temperature rise curves for the JS1 and JS3 rock samples

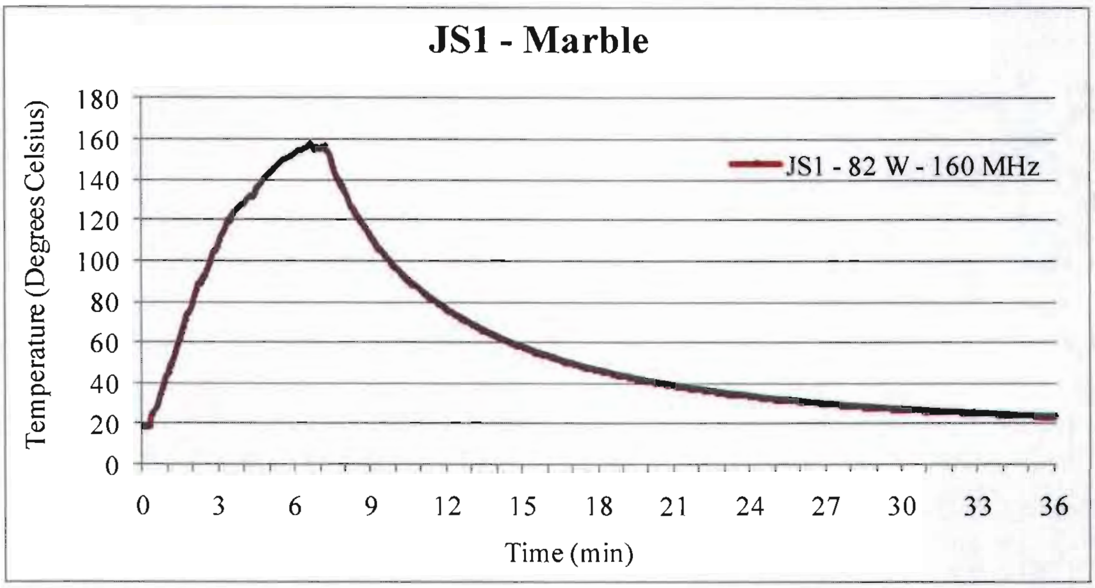

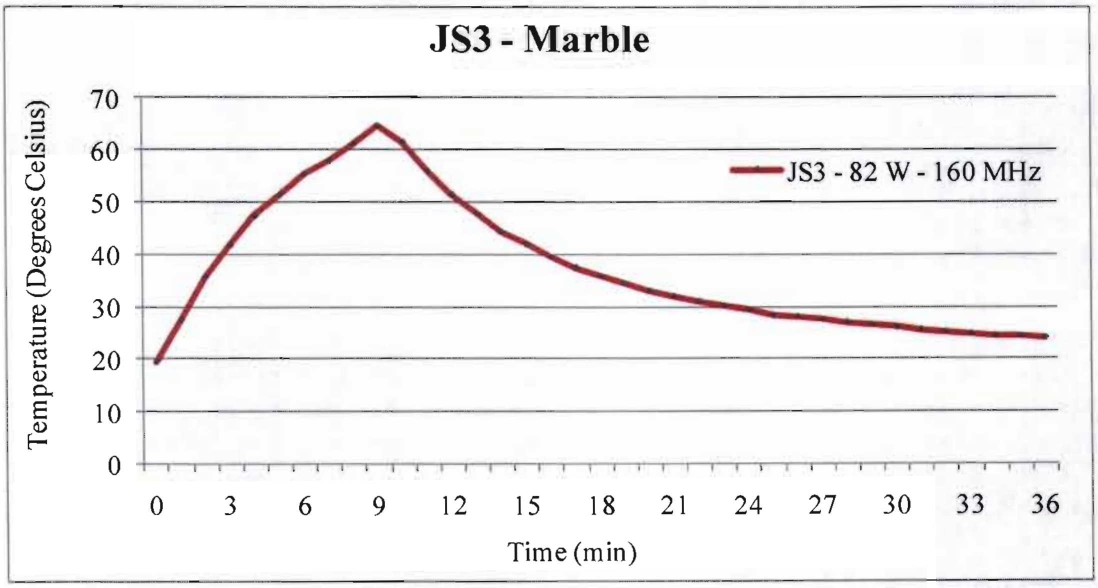

ANNEXURE 18 Temperature rise curves for the JS4 and JS5 rock samples

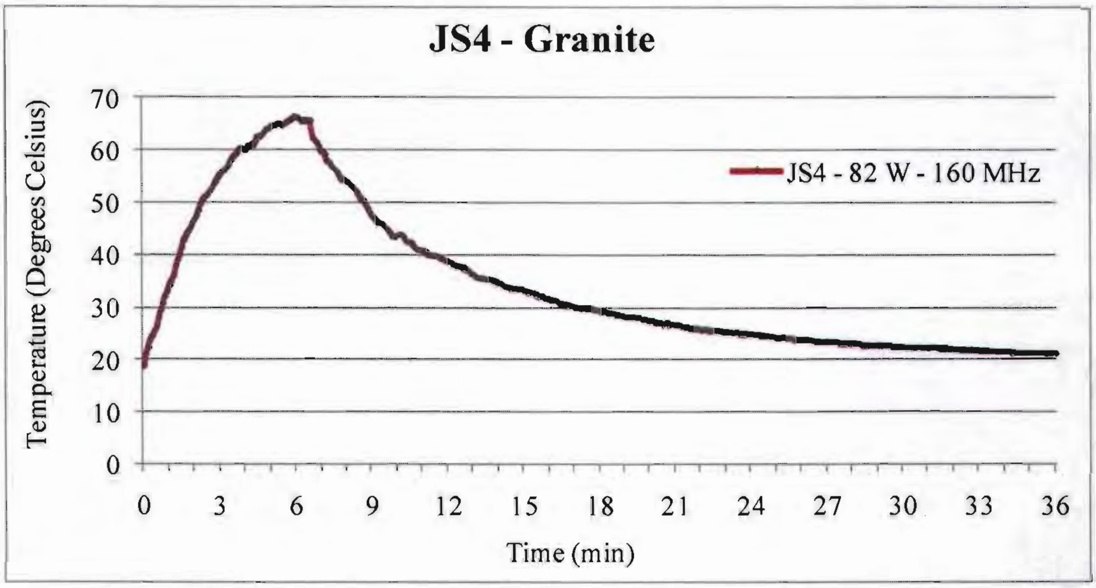

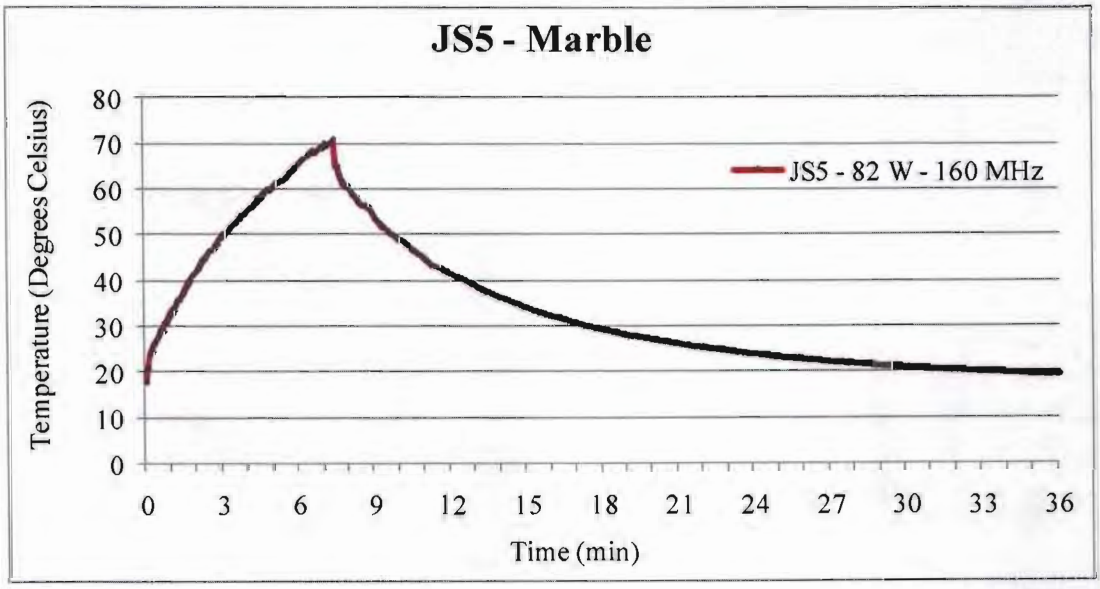

ANNEXURE 19 Photograph of the swing-pot mill and shallow cylinder (two internal rings and a heavy disc)

ANNEXURE 20 HIOKI 3286-20 clamp-on power meter used to measure the power consumption of the RF amplifiers and the swing-pot mill

ANNEXURE 21 Particle screening sieves (250 µm, 150 µm, 90 µm and 38 µm) placed on top of each other

ANNEXURE 22 Photograph of the RF amplifiers

ANNEXURE 23 Equations used to convert the Cartesian Coordinates obtained from the Vector Network Analyser (VNA) into electrical parameters

Vector Network Analyzer (VNA)	Real part	$r := -.713$
	Imaginary part	$x := -.668$

1. Calculate resistance	$R := \frac{1 - r^2 - x^2}{(1-r)^2 + x^2} \cdot 50$	$R = 0.672$	Ohm
2. Calculate reactance	$Re := 2 \cdot \frac{x}{(1-r)\cdot(1-x) + x^2} \cdot 50$	$Re = -20.221$	Ohm
3. Calculate magnitude	$Mag := \sqrt{R^2 + Re^2}$	$Mag = 20.232$	Ohm
4. Calculate angle	$Angle := atan\left(\frac{Re}{R}\right)$	$Angle = -88.098 \cdot deg$	

ANNEXURE 24 Photograph of the ten thin sections used in the SEM analysis

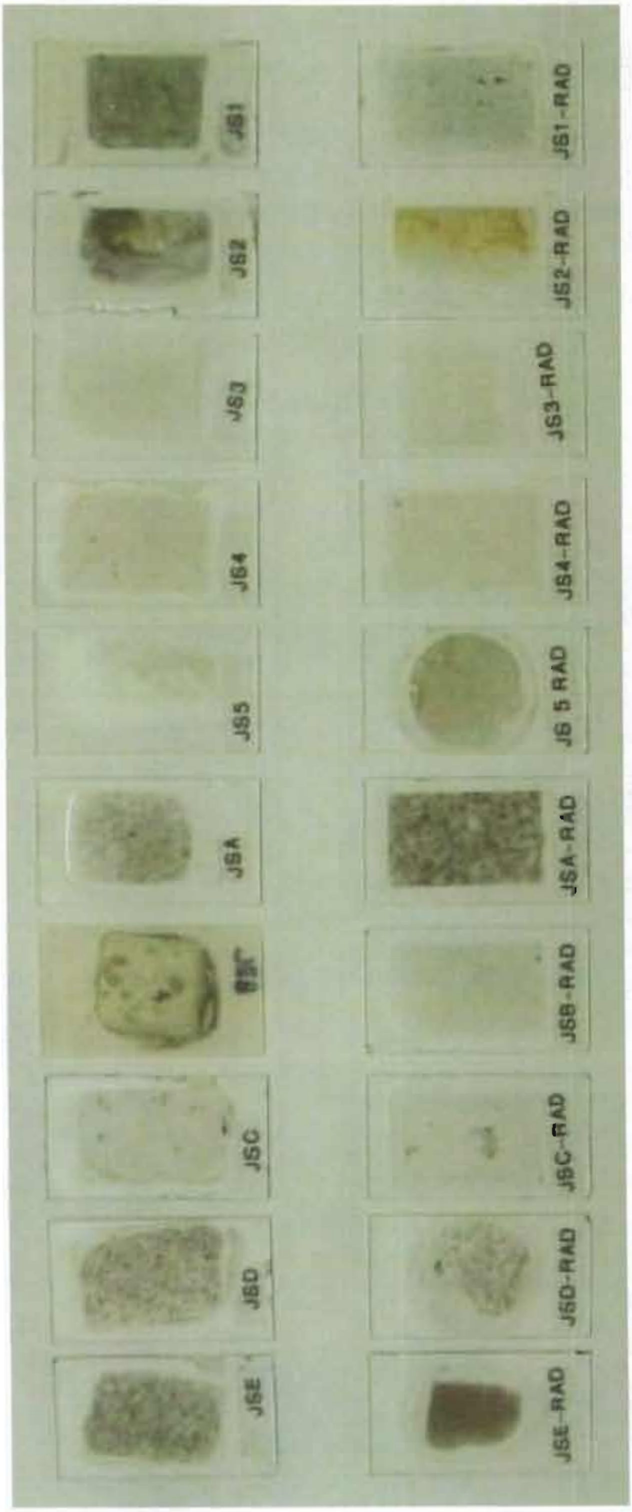

Untreated on the left and treated on the right

ANNEXURE 26 TURNITIN originality report for this thesis

Turnitin Originality Report

Evaluating the effects of radio-frequency treatment of rocks. Textural changes and implications for rock comminution by James Swart

From Thesis (DTECH)

Processed on 12-06-10 3:39 AM PST
ID: 162517762
Word Count: 34399

Similarity Index	Similarity by Source	
21%	Internet Sources:	11%
	Publications:	15%
	Student Papers:	7%

sources:

1 4% match (publications)
James Swart. "THE ELECTRICAL PROPERTIES OF CHLORITE TREMOLITE MARBLE MEASURED FOR A RANGE OF RADIO FREQUENCIES", Mineral Processing and Extractive Metallurgy Review, 10/2009

2 1% match (Internet from 4/7/10)
http://www.bsyse.wsu.edu/tang/Previouswebsite/Resources/pdfdocs/Postharvest/tang54.pdf

3 1% match (Internet from 1/13/07)
http://minerals.net/resource/property/tenacity.htm

4 1% match (publications)
Gaete-Garreton, L.. "Development of an ultrasonic high-pressure roller press", Chemical Engineering Science, 200310

5 1% match (publications)
Marc Rutschlin. "A guarded cylindrical capacitor for the non-destructive measurement of hard rock core samples", Measurement Science and Technology, 06/01/2006

6 1% match (Internet from 3/1/08)
http://individual.utoronto.ca/dr_shcho/Goldrock2006Manu-Cho.pdf

7 < 1% match (publications)
Gaete-Garreton, L.F.. "Application of ultrasound in comminution", Ultrasonics, 200003

8 < 1% match (publications)
Jones, D.A.. "Microwave heating applications in environmental engineering-a review", Resources, Conservation & Recycling, 200201

9 < 1% match (Internet from 2/21/09)
http://www.geophysics.dias.ie/mtnet/papers/EMWK5HP_ReviewVolumes/2002SantaFe/Nover_2002SantaFeReview_SG_2005.pdf

10 < 1% match (Internet)
http://thehallofmaat.com/maat/categories.php?op=newindex&catid=8

11 < 1% match (Internet from 1/30/10)
http://sbsp.jp/sbdt/cosmo/Uken02-5.pdf

12 < 1% match (student papers from 02/11/10)
Submitted to Tshwane University of Technology on 2010-02-11

13 < 1% match (Internet from 4/8/08)
http://www.equipland.com/objects/catalog/product/extras/14069_hp_8752a.pdf

14 < 1% match (publications)
Everard. "Power Amplifiers", Fundamentals of RF Circuit Design, 2001

15 < 1% match (Internet from 4/24/09)
http://www.jjcatsrocks.com/Aterminology.htm

16 < 1% match (publications)
R.J. Fontana. "Recent System Applications of Short-Pulse Ultra-Wideband (UWB) Technology", IEEE Transactions on Microwave Theory and Techniques, 9/2004

ANNEXURE 25 Photograph of the ten polished sections obtained from the grindability analysis

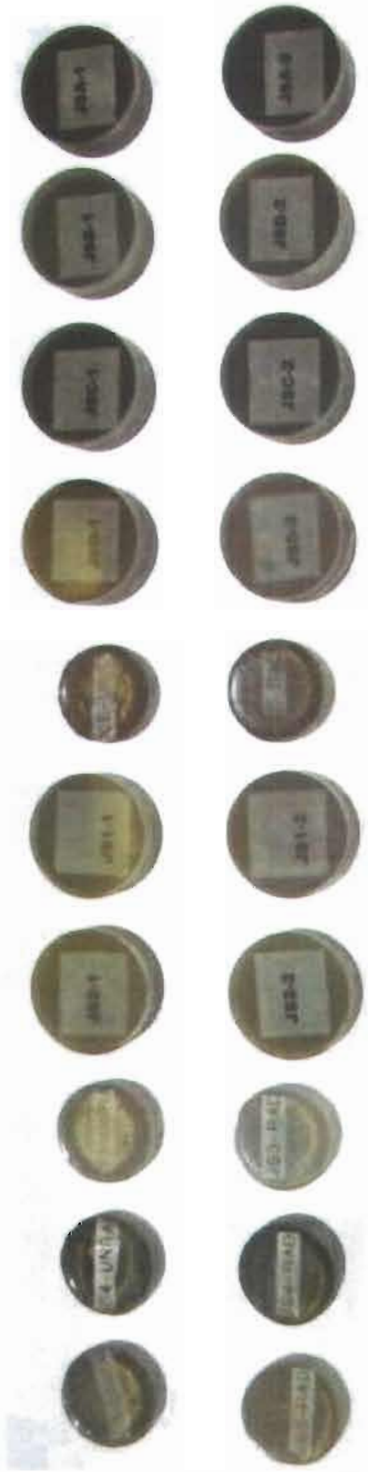

Untreated on the left and treated on the right